

1979

THE STRUCTURAL AND PHYSICAL PROPERTIES OF CRYSTALLINE ANTIBIOTIC MATERIALS

GANE, PATRICK ARTHUR CHARLES

<http://hdl.handle.net/10026.1/2046>

<http://dx.doi.org/10.24382/3828>

University of Plymouth

All content in PEARL is protected by copyright law. Author manuscripts are made available in accordance with publisher policies. Please cite only the published version using the details provided on the item record or document. In the absence of an open licence (e.g. Creative Commons), permissions for further reuse of content should be sought from the publisher or author.

THE STRUCTURAL AND PHYSICAL
PROPERTIES OF CRYSTALLINE
ANTIBIOTIC MATERIALS

BY

PATRICK ARTHUR CHARLES GANE B.Sc., A.R.C.S.

A THESIS SUBMITTED FOR THE
DEGREE OF
DOCTOR OF PHILOSOPHY
OF THE
COUNCIL FOR NATIONAL ACADEMIC AWARDS

PLYMOUTH POLYTECHNIC
SCHOOL OF
MATHEMATICAL SCIENCES

NOVEMBER 1979

PLYMOUTH POLYTECHNIC
LIBRARY

Accn.
No.

5500029

Class.
No.

T-548.83 GAW

Contl.
No.

X700154646

TABLE OF CONTENTS

	<u>Page</u>
<u>Abstract</u>	xii
<u>Chapter 1:</u> The Determination of Structure by the Scattering of X-rays from a Single Crystal	1
Introduction	1
1.1 The basis for crystal structure analysis	4
1.2 The scattering of a wave packet	4
1.3 The scattering of X-rays by atoms	10
1.4 Diffraction from a crystal	11
1.5 The reciprocal lattice	12
1.6 Intensity data collection and the Weissenberg method	13
1.7 Determination of cell dimensions	14
1.8 Determination of space group	16
1.9 Factors affecting observed intensities:	18
Absorption	18
Primary and secondary extinction	19
Atomic vibration - the temperature factor	20
Polarisation	20
The Lorentz factor	21
1.10 The structure factor	21
1.11 The Wilson Plot	23
1.12 Structure determination methods:	24
Heavy atom technique	25
Direct methods	26
Application of direct methods	29
1.13 Structure completion:	31
Fourier F_0 synthesis	31
Difference ΔF synthesis	32

		<u>Page</u>
1.14	Least-squares refinement and residual index, R	33
1.15	Accuracy of bond lengths and angles	34
<u>Chapter 2:</u>	The Crystal and Molecular Structure of 7-chloro-2-methyl-5-phenyl-3-propyl[2,3-b]-imidazolyl quinoline	37
2.1	Introduction	37
2.2	Crystal preparation	38
2.3	Space group and unit cell determination	38
2.4	Intensity data collection and preliminary treatment	39
2.5	Structure determination	39
2.6	Refinement of the structure	44
2.7	Discussion	46
<u>Chapter 3:</u>	The Crystal and Molecular Structure of the methyl ester of 5,5-dimethyl-2-(2-phenoxyethyl-5-oxo-1,3-oxazolin-4-ylidene)-1,3-thiazolidine-4-carboxylic acid	58
3.1	Introduction	58
3.2	Experimental	59
3.3	Structure determination	60
3.4	Structure refinement	61
3.5	Discussion	69
<u>Chapter 4:</u>	The Crystal and Molecular Structure of the Phenyl Ester of Carbenicillin (Carfecillin)	83
4.1	Introduction	83
4.2	Crystal preparation and preliminary X-ray studies	83
4.3	Intensity data collection and preliminary treatment	86
4.4	Structure determination	88
4.5	Structure refinement	94
4.6	Discussion	95
4.7	A comparison of the conformation of the penicillin nucleus with known penicillins and cephalosporins	101

	<u>Page</u>
<u>Chapter 5:</u> The Configuration and Conformation of the side-chain substituents in penicillin derivatives	115
5.1 Introduction	115
5.2 Side chain configuration and associated nuclear magnetic resonance	115
5.3 Relative orientations of the C(17) side-chain substituent in the phenyl ester of carbenicillin	121
(i) Relative orientation in fresh solution	127
(ii) Relative orientation after equilibration	128
5.4 Side-chain configuration and associated circular dichroism	148
5.5 Further possibilities for conformational change outside the penicillin nucleus	163
 <u>Appendices</u>	
A Computer programs for the calculation of orthorhombic Patterson function, (1), and electron density Fourier synthesis, (2), in space group $P2_12_12$	165
B List of structure factors for	181
(i) SH62 $P2(1)2(1)2$: $C_{20}H_{18}N_3C_2$	182
(ii) SNP $P2(1)/C$: $C_{17}H_{18}N_2O_5S$	194
(iii) CARF $P2(1)$: Phenyl ester of carbenicillin	204
 <u>References</u>	 211

LIST OF TABLES

<u>Table</u>	<u>Page</u>	
2.1	Co-ordinates of non-hydrogen atoms in $C_{20}H_{18}N_3Cl$	53
2.2	Bond lengths in $C_{20}H_{18}N_3Cl$	54
2.3	Bond angles in $C_{20}H_{18}N_3Cl$	55
2.4	Co-ordinates of hydrogen atoms in $C_{20}H_{18}N_3Cl$	56
2.5	Thermal parameters for $C_{20}H_{18}N_3Cl$	57
3.1	Starting set of reflexions with associated phases and equivalent sign relations	62
3.2	Co-ordinates of non-hydrogen atoms in $C_{17}H_{18}N_2O_5S$	76
3.3	Bond lengths in $C_{17}H_{18}N_2O_5S$	77
3.4	Bond angles in $C_{17}H_{18}N_2O_5S$	78
3.5	Co-ordinates of hydrogen atoms in $C_{17}H_{18}N_2O_5S$	80
3.6(a)	Thermal parameters for non-hydrogen atoms in $C_{17}H_{18}N_2O_5S$	81
(b)	Thermal parameters for hydrogen atoms in $C_{17}H_{18}N_2O_5S$	82
4.1	Co-ordinates of non-hydrogen atoms in carfecillin	108
4.2	Bond lengths in carfecillin	109
4.3	Bond lengths in carfecillin	110
4.4	Co-ordinates of hydrogen atoms in carfecillin	111
4.5	Thermal parameters for carfecillin	112/113
4.6	Planarity of the penicillin nucleus in carfecillin	114
5.1	β lactam proton magnetic resonance spin-spin splitting coupling constants, J, and chemical shifts, δ	147
5.2	Circular dichroism data for the principal Cotton Effects	162

LIST OF ILLUSTRATIONS

<u>Figure</u>	<u>Page</u>	
1.1	Path of integration in the complex k' plane	8
1.2	Oscillation geometry	14
1.3	Intensity distribution curves	18
2.1	Progress of the structure determination during electron density Fourier synthesis of $C_{20}H_{18}N_3Cl$	42/43
2.2	Sectioning of SHELX 'BLOC' refinement	45
2.3	Bond lengths in $C_{20}H_{18}N_3Cl$	47
2.4	Bond angles in $C_{20}H_{18}N_3Cl$	48
2.5	The crystal structure of $C_{20}H_{18}N_3Cl$ viewed along a	49
2.6	The crystal structure of $C_{20}H_{18}N_3Cl$ viewed along c	50
3.1	Sectioning for SHELX 'BLOC' refinement	63
3.2	Schematic labelling of the non-hydrogen atoms in $C_{17}H_{18}N_2O_5S$	64
3.3	Bond lengths in $C_{17}H_{18}N_2O_5S$	65
3.4	Bond angles in $C_{17}H_{18}N_2O_5S$	66
3.5	The crystal structure of $C_{17}H_{18}N_2O_5S$ viewed along b	67
3.6	The crystal structure of $C_{17}H_{18}N_2O_5S$ viewed along a	68
4.1	Perspective view of the twinning of carfecillin crystals	84
4.2	Twinning of crystals of carfecillin	85
4.3	Wilson Plot for carfecillin	87
4.4	Progress of electron density Fourier synthesis during the structure determination of carfecillin	92/93
4.5	SHELX 'BLOC' sectioning of carfecillin	94
4.6	Schematic labelling and inter-atomic distances in carfecillin	97
4.7	Bond angles in carfecillin	98
4.8	The crystal structure of carfecillin viewed along a	99
4.9	The crystal structure of carfecillin viewed along b	100

	<u>Page</u>	
4.10	Conformation of thiazolidine rings of known penicillin structures	104
4.11	Bonding geometry at β lactam nitrogen in some penicillins and cephalosporins	105
4.12	The comparative structural arrangements of the nuclei of penicillins, Δ^3 and Δ^2 - cephalosporins	106
5.1	Geometrical parameters used in describing the relative side-chain orientation in the phenyl ester of carbenicillin	123
5.2	Transformation of co-ordinate axes	124
5.3	Contour plot of n.m.r. shielding values for protons in the vicinity of a benzene ring	126
5.4	Distances of C(17) and its substituents from H(C(6))	129
5.5	Theoretical geometry about C(17)	132
5.6	Conformation of the C(15) = O(16) chromophore with respect to C(17) substituents in amoxicillin and ampicillin	151

PROTON MAGNETIC RESONANCE SPECTRA:

<u>Trace</u>	<u>Page</u>
1 (a) Methyl ester of carbenicillin in fresh solution] 135
(b) Methyl ester of carbenicillin after equilibration	
2 (a) Ethyl ester of carbenicillin in fresh solution] 136
(b) Ethyl ester of carbenicillin after equilibration	
3 (a) Methyl ester of carbenicillin, β lactam H^1 resonance in solution after time 't'] 137
(b) Ethyl ester of carbenicillin, β lactam H^1 resonance in solution after time 't'	
4 (a) Phenyl ester of carbenicillin after equilibration] 138
(b) Phenyl ester of carbenicillin, β lactam H^1 resonance in solution after time 't'	
5 (a) D-Amino-phenylacetamido penicillanic acid (ampicillin)] 139
(b) D-Amino-phenylacetamido penicillanic acid (ampicillin), β lactam H^1 resonance at varying sample concentration 'c'	
6 (a) D- Amino-hydroxybenzyl penicillin (amoxycillin)] 140
(b) D- Amino-hydroxybenzyl penicillin (amoxycillin), β lactam H^1 resonance at varying sample concentration 'c'	
7 (a) D-Tyrosyl penicillin] 141
(b) D-Tyrosyl penicillin, β lactam H^1 resonance at varying sample concentration 'c'	
8 (a) L-Amino-phenylacetamido penicillanic acid] 142
(b) L-Amino-hydroxybenzyl penicillin	
9 (a) L-Amino-hydroxybenzyl penicillin and L-amino- phenylacetamido penicillanic acid, β lactam H^1 resonances] 143
(b) L-Tyrosyl penicillin and D-tyrosyl penicillin, β lactam H^1 resonances	
10 (a) L-Tyrosyl penicillin] 144
(b) L-Tyrosyl penicillin, β lactam H^1 resonance at varying sample concentration 'c'	

CIRCULAR DICHROISM SPECTRA

	<u>Page</u>
CD	
(1) Phenethicillin Potassium	154
(2) Predicted CD spectrum of 6-APA	155
(3) Amino-phenylacetamido penicillanic acid	156
(4) Amino-hydroxybenzyl penicillin	157
(5) Tyrosyl penicillin	158
(6) Methyl ester of carbenicillin	159
(7) Ethyl ester of carbenicillin	160
(8) Phenyl ester of carbenicillin	161

ACKNOWLEDGEMENTS

I wish to convey my thanks to the Governors of the Polytechnic and to Dr. C.M. Gillett for providing the facilities and ancillary services for this work, and to express my deep gratitude to Dr. M.O. Boles for his patience, humour and helpful supervision and to Dr. R.J. Girven for his sage advice in the early stages of this work.

The support and advice, provided by Beecham Pharmaceuticals, are gratefully acknowledged and I am indebted to Mr. A.E. Bird and his colleagues at the Chemotherapeutic Research Centre, Brockham Park, for supplies of purified compounds.

My thanks are also extended to Dr. G. Kirk of the Chelsea School of Pharmacy, for supplies of novel heterocyclic compounds and to Dr. L. Re and co-workers at Snamprogetti Società per Azioni for supply of their suspected novel class of unsaturated penicillins.

The structure determinations bear witness to the excellent service and useful advice of Drs. M. Elder and M. Pickering, and Miss P. Machin of the Science Research Council Microdensitometer Service at Daresbury.

I wish to thank also Dr. K. Bancroft of the School of Environmental Sciences, Plymouth Polytechnic, for assistance and guidance in the collection of n.m.r. spectra and Westfield College, University of London, for chiroptical facilities, particularly Dr. P.M. Scopes of the Department of Chemistry.

I have appreciated the assistance of the departmental technicians and workshop staff and the services provided by the Learning Resources Centre and Reprographic Department.

I wish to extend my thanks to Mr. R. Srodzinski for his unstinting determination to provide photographic excellence during the preparation of this thesis and to Mrs. S. Tolan and Miss G. Stock for undertaking to demonstrate their 'code-breaking' talents in typing.

My greatest appreciation must be for those forbearing friends who remained such throughout, and for the devoted support given by my Mother during this work.

DECLARATION

The work described in this thesis was carried out in the School of Mathematical Sciences, Plymouth Polytechnic, under the supervision of Dr. M.O. Boles.

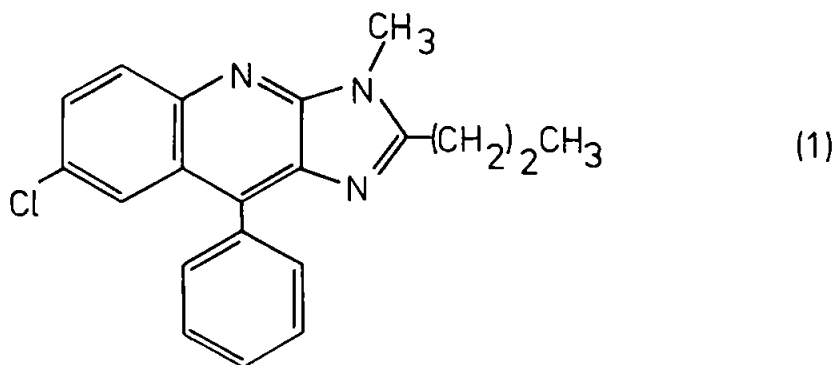
This is to certify that the work described in this thesis has been performed by Mr. P.A.C. Gane under my supervision during the years 1976-1979.

M. O. Boles.

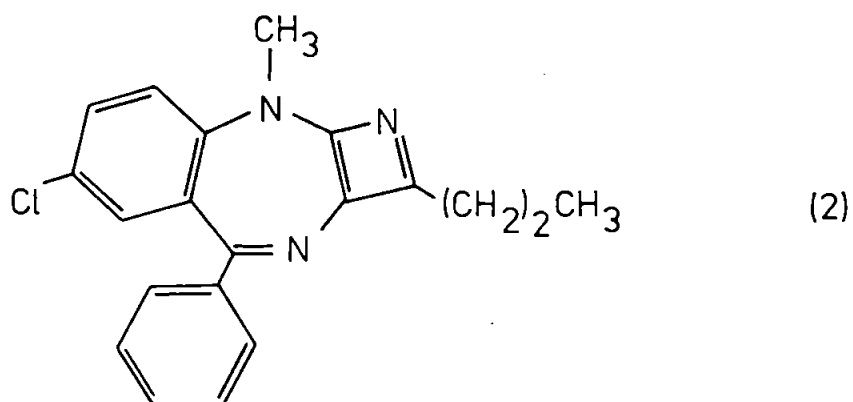
Dr. M.O. Boles,
Senior Lecturer,
School of Mathematical Sciences,
Plymouth Polytechnic,
Plymouth.

ABSTRACT

Effectiveness in biological chemical environments virtually defines the term 'drug' when applied to any attempt to modify that environment by the introduction of an influence in terms of a specific compound or group of compounds. Interest in the configuration of the molecules involved in such modifications led to the X-ray structure determinations, discussed in the thesis, of the following three compounds; (i) 7-chloro-2-methyl-5-phenyl-3-propyl[2,3-b]-imidazolyl quinoline.

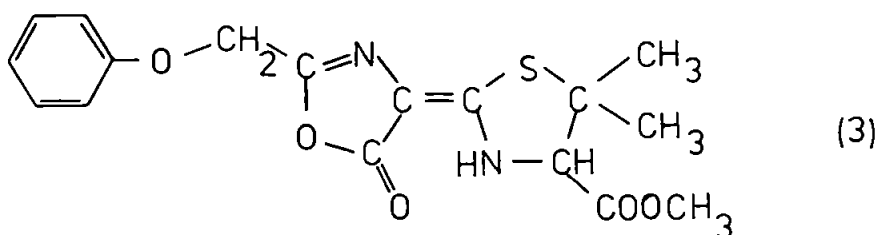


Derived from the psychoactive drug Librium, it was thought to conform to the structure,

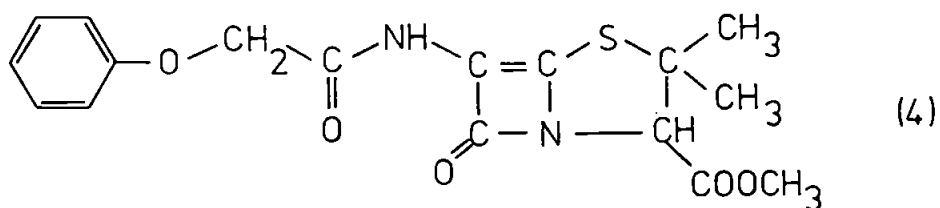


containing the highly strained 4-membered monocyclic azete system (Shenoy, a thesis submitted for the degree of Doctor of Philosophy, University of London, 1975), and suggested as one of the first examples of possible stable 4-membered azacyclobutadiene rings.

(ii) The methyl ester of 5,5-dimethyl-2-(2-phenoxyethyl-5-oxo-1,3-oxazolin-4-ylidene)-1,3-thiazolidine-4-carboxylic acid.



$C_{17}H_{18}N_2O_5S$ was first reported by Brandt, Bassignani and Re, (1976, Tetrahedron Letters No. 44, pp 3979-3982), to have configuration (4),

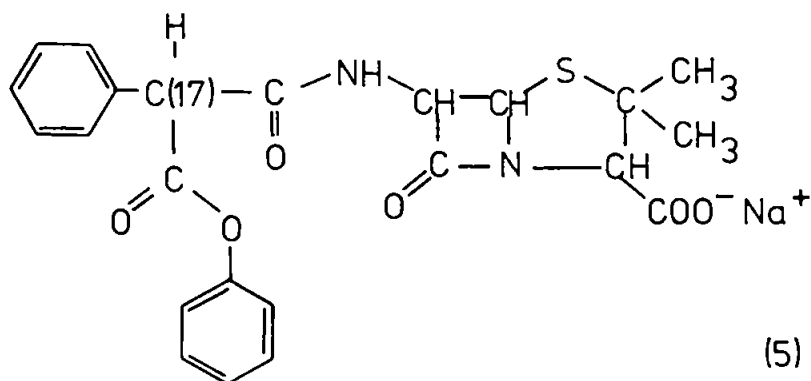


i.e. that of a novel class of DL-5,6-didehydropenicillins. Its reported weak antibacterial activity, thought to be associated with the unsaturated nature of the penicillin nucleus promoted its X-ray structure analysis.

Subsequently, Bachi and Vaya, (1977, Tetrahedron Letters No. 25, pp 2209-2212), suggested the configuration (3) which has been confirmed by the structure determination.

A comparison of the proposed derivations of (3) and (4) is made, and the conformation of the unconstrained thiazolidine ring is discussed in comparison with the constraining effect of adjacent β lactams in the nuclei of known penicillin structures.

(iii) The phenyl ester of carbenicillin (carfecillin).



The crystal structure is used to facilitate a comparison of the configurations of both the penicillin nucleus and the side-chain substituents of C(17) with other penicillin derivatives of known crystal structure.

The conformation in aqueous solution about C(17) is reflected in the modification of H^1 n.m.r. signals from the β lactam protons for the methyl and ethyl esters of carbenicillin between the two epimers. A

similar effect is noted for the two diastereoisomers of amino-hydroxybenzyl penicillin, amino-phenylacetamido penicillanic acid and a tyrosyl penicillin.

To evaluate a correlation between the absolute configuration and n.m.r. studies, circular dichroism spectra from penicillin compounds have been characterised and the mutarotation exhibited by the esters of carbenicillin used to describe configurational equilibria about C(17) in terms of their characteristic n.m.r. spectra.

CHAPTER 1

The Determination of Structure by the Scattering of X-Rays from a Single Crystal

INTRODUCTION

The bioactivity of organic compounds may depend upon numerous factors such as the reactivity and relative orientation of constituent functional groups. Overall molecular size and shape often results in preferential receptor site occupation in certain 'lock-and-key' mechanisms. The crystalline solid state consists of a regular array of molecules with relative orientations which minimise the potential energy associated with both inter-molecular and inter-atomic interactions. Crystal structure analysis reveals the molecular geometry associated with the crystalline state, and a study of structures within a group of similar compounds, provides the possibility of distinguishing these geometrical features which play an important part in biological activity.

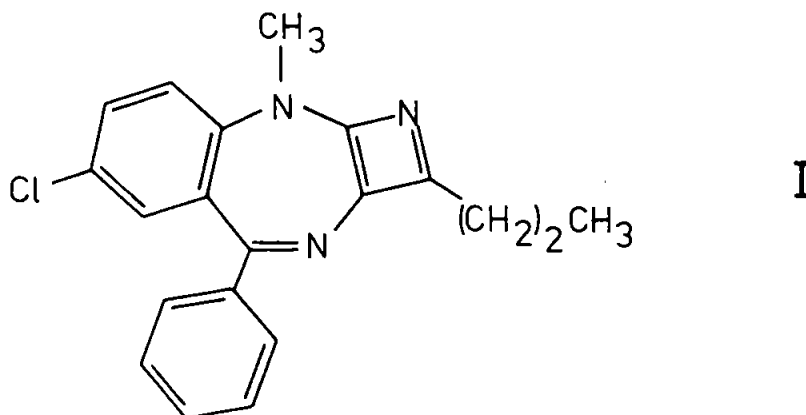
Assignment of molecular structure can be achieved without the analysis of the crystalline state by techniques which provide limited information by their use alone, but in conjunction, provide a means whereby the most probable structure may be derived. Constituent atoms are analysed by mass spectrometry, and molecular weight analysis results in determination of the number of each elemental atoms in the molecule. Nuclear magnetic resonance methods, provide a description of the chemical environment about some constituent atomic sites, enabling a possible ordering of particular groups to be achieved. Further analysis by optical methods can be made to study the relative configuration of certain optically active groups. However, the structure solution satisfying the results obtained by these

methods is often not unique and only limited information regarding the geometrical features of the molecule is obtained.

The techniques of single crystal analysis discussed in this chapter, bear a particular emphasis upon those used in the determination of the crystal structures described in the following chapters, and are progressively developed from the more general aspects of the scattering of radiation and regarded as a particular solution to the scattering process. The various analyses of X-ray diffraction data centre upon the determination of diffracted intensity, and associated phase angle, and the Fourier synthesis of the model structure with its subsequent least-squares refinement.

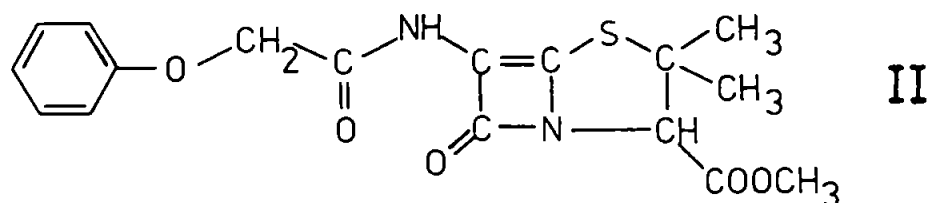
This thesis describes the use of the methods of X-ray crystallography to assign the structures of three compounds in the crystalline state, which were considered of interest either by virtue of their proposed novel structures or to further the comparison of known groups of biologically active compounds.

The novel pharmacologically active azete, I, is of interest because it is derived from the psychoactive drug Librium, and contains the highly strained azete system. Only a few azete compounds have been reported, and the stability of monocyclic azetes is very low.



Structure determination of the dehydropenicillin, II, was carried out as a preliminary to the investigation of the reported weak

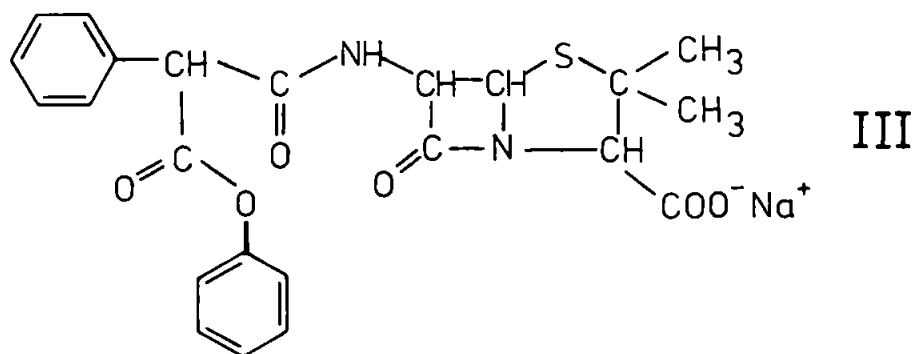
antibacterial activity, suggested to result from the "unsaturated"



nature of the penicillin nucleus.

Chapters 2 and 3 describe the eventual reassignment of structure to both compounds I and II.

The esters of carbenicillin are shown to undergo change of the side-chain substituents in solution, (ref Ch. 5); investigation of the nature of the processes involved was facilitated by the X-ray structural investigations of the phenyl ester of carbenicillin, III, described in Chapter 4.



The configuration and conformation of the side-chain substituents in some penicillin derivatives of known structure is discussed in Chapter 5 and compared with that of three esters of carbenicillin, including III, using distinguishing features arising from H^1 nuclear magnetic resonance spectra and circular dichroism measurements.

1.1 The basis for crystal structure analysis

The laws of diffraction alone can provide the basis for crystal structure analysis; however, such laws result from the observations made from a particular state of matter ie. the crystalline state, whereas the techniques of analysis stem from the combination of fundamental aspects of matter, relating more to the scattering process itself. Diffraction can therefore be considered to emerge as a direct result of constraints applied to the scattering process by the spatial geometry within the crystal. Thus, a complete description of the basic scattering process, and its particular solution under certain constraining conditions for X-ray diffraction, such as elastic wave/matter interactions and subsequent interference phenomena, is used to form a basis for the development of the mathematical models used in the structure analyses discussed later.

The field of X-ray crystallography is well served by many standard texts; particular use has been made of the works of M.J. Buerger,¹ E. W. Nuffield², M.F. C. Ladd and R.A. Palmer³, M.M. Woolfson⁴, G.H. Stout and L.H. Jensen⁵, and International Tables for X-ray Crystallography⁶.

1.2 The scattering of a wave packet

The wave-particle description of matter, developed largely from an understanding of energy/matter interactions and their eventual equivalency, has resulted in considerable information concerning the nature of energy scattering processes, in particular, those associated with the atom and its constituents.

The crystalline state provides a unique interaction with incident radiation which is described by the modification of a wave packet under the influence of a potential^{7,8}.

Motion under the influence of a potential V , which is appreciably

different from zero only within a sphere surrounding the origin of radius 'a', may be described by the Schrödinger equation

$$\left(-\frac{\hbar^2}{2\mu} \nabla^2 + V \right) \psi = E\psi \quad \dots \text{Eqn 1.1}$$

where ψ describes a wave packet, E the energy eigenvalue associated with it and μ the reduced mass.

Simplification of Eqn. 1.1 is achieved using the substitutions

$$k^2 = \frac{2\mu E}{\hbar^2} \quad \text{and} \quad U = \frac{2\mu V}{\hbar^2} \quad \text{to become}$$

$$(\nabla^2 + k^2) \psi = U\psi \quad \dots \text{Eqn 1.2}$$

Considering $U\psi$ as a temporary inhomogeneity, Eqn. 1.2

can be solved by the superposition of a particular solution and complementary function. Formally, a particular solution can be constructed in terms of the Green's function $G(\underline{r}, \underline{r}')$ which is a solution of the equation

$$(\nabla^2 + k^2) G(\underline{r}, \underline{r}') = -4\pi \delta(\underline{r} - \underline{r}') \quad \dots \text{Eqn 1.3}$$

where the Dirac delta function has the property

$$\int \delta(\underline{r} - \underline{r}') d^3r' = 1 \quad \dots \text{Eqn 1.4}$$

provided the region of integration includes $\underline{r}' = \underline{r}$.

Hence, by Eqn. 1.4

$$\begin{aligned} \int U(\underline{r}') \psi(\underline{r}') \delta(\underline{r} - \underline{r}') d^3r' \\ = U(\underline{r}) \psi(\underline{r}) \end{aligned} \quad \dots \text{Eqn 1.5}$$

and provides the inhomogeneity $U\psi$ as required.

Thus, the expression

$$\frac{-1}{4\pi} \int G(\underline{r}, \underline{r}') U(\underline{r}') \psi(\underline{r}') d^3r' \quad \dots \text{Eqn 1.6}$$

solves Eqn. 1.2 adequately.

The complementary function is found as an arbitrary solution of the homogeneous equation

$$(\nabla^2 + k^2) \psi = 0 \quad \dots \text{Eqn 1.7}$$

which is the Schrödinger equation for a free particle (no scattering) and has the solution corresponding to a plane wave. Choosing a suitable normalisation factor establishes the integral equation.

$$\psi_{\underline{k}}(\underline{r}) = \frac{1}{(2\pi)^{3/2}} e^{j\underline{k} \cdot \underline{r}} - \frac{1}{4\pi} \int G(\underline{r}, \underline{r}') U(\underline{r}') \psi_{\underline{k}}(\underline{r}') d^3r'$$

... Eqn 1.8

as a particular set of solutions of the Schrödinger equation.

The magnitude of the wave vector \underline{k} has a definite value, fixed by the energy eigenvalue, but its direction is determined physically by the direction of incidence. A complete knowledge of \underline{k} , however, does not completely define $\psi_{\underline{k}}(\underline{r})$ in Eqn. 1.8, for there remains an infinite choice of Green's function $G(\underline{r}, \underline{r}')$. To determine suitable Green's functions, the solution to Eqn. 1.3 must be found.

$$(\nabla^2 + k^2) G(\underline{r}) = -4\pi \delta(\underline{r}) \quad \dots \text{Eqn 1.9}$$

describes a simplified expression of Eqn. 1.3

Defining $\delta(\underline{r})$ by

$$\delta(\underline{r}) = \frac{1}{(2\pi)^3} \int e^{j\underline{k}' \cdot \underline{r}} d^3k' \quad \dots \text{Eqn 1.10}$$

suggests the application of the Fourier transform description of $G(\underline{r})$, well known in diffraction processes, giving

$$G(\underline{r}) = \int g(\underline{k}') e^{j\underline{k}' \cdot \underline{r}} d^3k' \quad \dots \text{Eqn 1.11}$$

Substitution in Eqn 1.9 gives

$$(\nabla^2 + k^2) \int g(\underline{k}') e^{j\underline{k}' \cdot \underline{r}} d^3k' = -\frac{1}{2\pi^2} \int e^{j\underline{k}' \cdot \underline{r}} d^3k' \quad \dots \text{Eqn 1.12}$$

and hence,

$$\int g(\underline{k}') (-k'^2 + k^2) e^{j\underline{k}' \cdot \underline{r}} d^3k' = -\frac{1}{2\pi^2} \int e^{j\underline{k}' \cdot \underline{r}} d^3k' \quad \dots \text{Eqn 1.13}$$

which in turn gives

$$g(\underline{k}') = \frac{1}{2\pi^2} \left(\frac{1}{k'^2 - k^2} \right) \quad \dots \text{Eqn 1.14}$$

furnishing the Fourier representation in reciprocal k-space, (ref § 1.5),

$$G(\underline{r}) = \frac{1}{2\pi^2} \int \frac{e^{j\underline{k}' \cdot \underline{r}}}{k'^2 - k^2} d^3k' \quad \dots \text{Eqn 1.15}$$

Evaluation of this integral over all space is conveniently carried out by expressing in terms of polar co-ordinates, letting the colatitude θ coincide with the angle between the vectors \underline{k}' and \underline{r} . Thus, Eqn. 1.15 becomes

$$G(\underline{r}) = \frac{1}{2\pi^2} \int_{-\infty}^{+\infty} \int_0^{2\pi} \int_0^{\pi} \frac{e^{jk'r \cos \theta}}{k'^2 - k^2} k'^2 \sin\theta \, d\theta \, d\phi \, dk' \quad \dots \text{Eqn 1.16}$$

which may more conveniently be rewritten to give

$$G(\underline{r}) = -\frac{1}{\pi r} \frac{d}{dr} \int_{-\infty}^{+\infty} \frac{e^{jk'r}}{k'^2 - k^2} dk' \quad \dots \text{Eqn 1.17}$$

following the integration over θ and ϕ .

The resulting integrand has simple poles on the real axis in the complex k' plane at $k' = \pm k$ and a solution may be found by using an integration path such as in Fig. 1.1, avoiding the poles.

Since r is taken to be positive, a closed contour produced by a semicircle, in the upper half plane, joining the path of integration along the real axis from $-\infty$ to $+\infty$ will suffice.

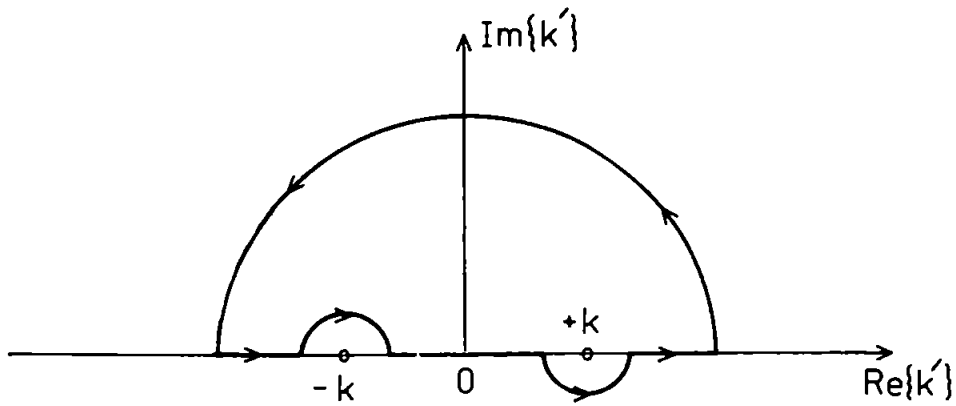


Fig. 1.1. Path of integration in the complex k' plane

Thus, Eqn. 1.17 becomes

$$G(r) = -\frac{1}{\pi r} \frac{d}{dr} \oint \frac{e^{jk'r}}{k'^2 - k^2} dk' \quad \dots \text{Eqn 1.18}$$

in which, by the use of the residue theorem

$$\oint \frac{e^{jk'r}}{k'^2 - k^2} dk' = 2\pi j \left(\frac{e^{jkr}}{2k} - \frac{e^{-jkr}}{2k} \right) \quad \dots \text{Eqn 1.19}$$

Hence,

$$G(r) = \frac{e^{jkr}}{r} + \frac{e^{-jkr}}{r} \quad \dots \text{Eqn 1.20a}$$

which can be expressed as

$$G(r) = G_+(r) + G_-(r) \quad \dots \text{Eqn 1.20b}$$

where $G_+(r)$ and $G_-(r)$ are both Green's functions, each satisfying Eqn. 1.9.

Thus, the Green's functions required as solutions to Eqn. 1.3 are

$$G_{\pm}(r, r') = \frac{\exp(\pm jk|r - r'|)}{|r - r'|} \quad \dots \text{Eqn 1.21}$$

and substitution in the integral equation, Eqn. 1. 8, results in two distinct eigensolutions, denoted by $\psi^{(+)}$ and $\psi^{(-)}$ given by

$$\psi_{\underline{k}}^{(+)}(\underline{r}) = \frac{1}{(2\pi)^{3/2}} e^{j\underline{k}\cdot\underline{r}} - \frac{1}{4\pi} \int \frac{\exp(+j\underline{k}\cdot|\underline{r}-\underline{r}'|)}{|\underline{r}-\underline{r}'|} U(\underline{r}') \psi_{\underline{k}}^{(+)}(\underline{r}') d^3r'$$

... Eqn. 1.22

In view of the fact that U exists only for values of $r' < a$, the integrand can be closely approximated. If r is chosen so large that the quadratic term can be neglected, and if, further, r' in the denominator of the integrand is neglected, as is the case in all macroscopic measurement techniques, then

$$\psi_{\underline{k}}^{(+)}(\underline{r}) \sim \frac{1}{(2\pi)^{3/2}} e^{j\underline{k}\cdot\underline{r}} - \frac{e^{+j\underline{k}\cdot\underline{r}}}{4\pi r} \int e^{+j\underline{k}'\cdot\underline{r}'} U(\underline{r}') \psi_{\underline{k}}^{(+)}(\underline{r}') d^3r'$$

... Eqn 1.23

where $\underline{k}' = \hat{\underline{r}} \underline{k}$.

This asymptotic expression can be written as

$$\psi_{\underline{k}}^{(+)}(\underline{r}) \sim \frac{1}{(2\pi)^{3/2}} \left(e^{j\underline{k}\cdot\underline{r}} + \frac{e^{+j\underline{k}\cdot\underline{r}}}{r} f_{\underline{k}}^{(+)}(\hat{\underline{r}}) \right) \quad (r \text{ large}) \quad \dots \text{Eqn. 1.24}$$

where

$$f_{\underline{k}}^{(+)}(\hat{\underline{r}}) = - \frac{(2\pi)^{3/2}}{4\pi} \int e^{+j\underline{k}'\cdot\underline{r}'} U(\underline{r}') \psi_{\underline{k}}^{(+)}(\underline{r}') d^3r'$$

... Eqn. 1.25

Physically, $\psi^{(+)}$, when modified by $\exp\left(-j\frac{Et}{\hbar}\right)$,

represents the outgoing solution of the Schrödinger equation.

Thus, Eqn. 1.24, describes the wave function $\psi^{(+)}$ in terms of an incident plane wave, of energy and direction governed by the wave vector \underline{k} , and a scattered outgoing radial wave falling in amplitude

as the inverse of the distance from the scatterer and with a modified amplitude, defined as the scattering amplitude, $f_{\vec{k}}^{\Lambda}(\vec{r})$. The term $f_{\vec{k}}^{\Lambda}(\vec{r})$, in turn, is dependent upon the scattering potential and whether the process is elastic, (Thomson scattering), or inelastic, (Compton scattering), determines the energy of the radial wave and thus, the wave vector \vec{k}' . It is therefore, the scattering amplitude and its associated phase which furnishes the means by which the properties of the process can be determined. The effective measurement of $f_{\vec{k}}^{\Lambda}(\vec{r})$ forms the basis for the methods of structure analysis considered in the following discussion.

1.3 The scattering of X-rays by atoms

Section 1.2 adequately described the interaction of a wave packet, for example on X-ray photon, with a central potential such as that of a free electron. However, the electrons surrounding atoms are not free but bound into definite energy states. Thus, Thomson scattering corresponds to the electron remaining in the same energy state after scattering, whereas Compton scattering will involve the transition of the electron between energy states with the absorption or emission of discrete energy quanta.

The coherently scattered component will suffer from ordered interference and provides a systematic means of analysing the scattering centres involved. Hence, the observationally valuable part of the scattering amplitude is related to an outgoing wave of energy unchanged from that of the incident wave i.e. $k' = k$. The ratio of the amplitude of the coherently scattered component from an atomic electron, contributing an idealised spherically symmetric charge distribution to that from an electron situated at the origin is defined as the scattering factor for that electron, f_e . If an atom contains Z electrons then the total ratio of amplitudes will be the sum of the individual ratios, $(f_e)_i$,

for each electron and is defined as the atomic scattering factor, f_a , given by

$$f_a = \sum_{i=1}^Z (f_e)_i \quad \dots \text{Eqn. 1.26}$$

Scattering factors used in this work were taken from International Tables for X-ray Crystallography, Vol III, or Acta. Cryst., A24 (1968) 321.

The scattering factor describes a reduction in amplitude of the scattered wave with increase of scattering angle: at zero scattering angle $f_a = Z$.

1.4 Diffraction from a crystal

Section 1.2 discussed the scattering of a photon of wave vector $\vec{k} = \frac{2\pi}{\lambda} \vec{k}$ from a single scattering centre. The condition that all atoms in a three dimensional array (crystal lattice) should scatter in phase in some direction can be fulfilled by three conditions.

Defining a scattering vector \vec{s} , such that

$$\vec{s} = \frac{n}{2\pi} \vec{k} = \frac{n}{\lambda} \vec{k}, \quad (n \text{ integer}) \quad \dots \text{Eqn. 1.27}$$

the three conditions that atoms separated by \vec{a} , \vec{b} or \vec{c} should scatter in phase, where the vectors \vec{a} , \vec{b} and \vec{c} are the three vectors which define the array, are

$$\begin{aligned} \vec{a} \cdot \vec{s} &= h \\ \vec{b} \cdot \vec{s} &= k \\ \vec{c} \cdot \vec{s} &= \ell \end{aligned} \quad \dots \text{Eqns 1.28}$$

where h , k and ℓ are integers. Eqns. 1.28 are the Laue equations, so called, after the first demonstration of diffraction of X-rays from a regular crystal lattice by von Laue in 1912.

The three integers h , k and ℓ can be chosen to uniquely define

a given interference maximum, (known as the X-ray reflexion), and are the Miller indices of that reflexion. Eqns. 1.28 also describe a family of planes in the crystal space and so, therefore, do the Miller indices.

1.5 The Reciprocal Lattice

To examine the scattering vector \underline{s} , and hence the crystal structure, it is necessary to describe \underline{s} in terms of three basis vectors, which themselves relate to the vectors \underline{a} , \underline{b} and \underline{c} which in turn define the unit cell of the crystal ie, that parallelepiped which, reproduced by close packing in three dimensions, gives the whole crystal.

The three vectors \underline{a}^* , \underline{b}^* and \underline{c}^* are used to define the reciprocal lattice where \underline{a}^* , \underline{b}^* and \underline{c}^* satisfy the complete set of relationships.

$$\begin{array}{lll} \underline{a} \cdot \underline{a}^* = 1 & \underline{a} \cdot \underline{b}^* = 0 & \underline{a} \cdot \underline{c}^* = 0 \\ \underline{b} \cdot \underline{a}^* = 0 & \underline{b} \cdot \underline{b}^* = 1 & \underline{b} \cdot \underline{c}^* = 0 \\ \underline{c} \cdot \underline{a}^* = 0 & \underline{c} \cdot \underline{b}^* = 0 & \underline{c} \cdot \underline{c}^* = 1 \end{array} \quad \dots \text{Eqns. 1.29}$$

which uniquely define \underline{a}^* , \underline{b}^* and \underline{c}^* in terms of the real space vectors \underline{a} , \underline{b} and \underline{c} such that

$$\underline{a}^* = \frac{\underline{b} \wedge \underline{c}}{\underline{a} \cdot (\underline{b} \wedge \underline{c})}$$

$$\underline{b}^* = \frac{\underline{c} \wedge \underline{a}}{\underline{a} \cdot (\underline{b} \wedge \underline{c})} \quad \dots \text{Eqns. 1.30}$$

$$\underline{c}^* = \frac{\underline{a} \wedge \underline{b}}{\underline{a} \cdot (\underline{b} \wedge \underline{c})}$$

Thus, using Eqns. 1.29, the scattering vector, \underline{s} , can be

defined, such that it satisfies Eqns. 1.28, by

$$\vec{s} = h\vec{a}^* + k\vec{b}^* + l\vec{c}^* \quad \dots \text{Eqn. 1.31}$$

Thus, each set of Miller indices is related to a particular scattering vector \vec{s}_{hkl} . The spacing between the real space planes defined by (hkl) is given by

$$d_{hkl} = \frac{1}{|\vec{s}_{hkl}|} \quad \dots \text{Eqn. 1.32}$$

Bragg⁹ showed that an X-ray beam incident at an angle θ_{hkl} to the family of planes (hkl) was diffracted such that the diffraction maximum occurred along a path also at angle θ to the same planes, given that θ_{hkl} satisfied the relation

$$2d_{hkl} \sin \theta_{hkl} = \lambda \quad \dots \text{Eqn. 1.32}$$

Hence, the scattering vector \vec{s}_{hkl} determines the unique Bragg angle θ_{hkl} .

1.6 Intensity data collection and the Weissenberg method

The photographic density produced by the impingement of an X-ray photon on a film is related to the square of the amplitude of the oscillation associated with the wave packet, and thus, provides the means by which the intensity of each reflexion can be measured. The range of intensity that can be measured by a single film is limited by the saturation response of the emulsion. An increase in the available measurement range was achieved using the multiple film technique, so that each reflexion intensity was measured within the linear optical density response, given by the relation $\log_{10} \left(\frac{I}{I_0} \right)$ where the logarithmic argument recorded the fraction of total possible measurable intensity. Photographic densities were measured by the Science Research Council microdensitometer service at Daresbury, consisting of an Optronics International System P-1000 Photoscan interfaced to a Computer Automation ALPHA -16 mini-computer with 16K

of 16-bit words of core store.

A Philips PW 10/10 X-ray generator operating at 34kV, 20mA using a Cu tube and Ni filter was used to generate nearly monochromatic $\text{CuK}\alpha$ X-radiation ($\lambda = 1.5418\text{\AA}$). All X-ray measurements were obtained using either Stoe or Nonius Weissenberg cameras. Application of the Weissenberg camera to data collection is described in refs. 3, 4 and 5. Zero layer Weissenberg photographs were obtained by the normal beam method and upper layers by the equi-inclination method. Similar exposure times were used for each layer and the inter-layer scale factors were set initially at 1; they were subsequently refined during the least-squares refinement, (§ 1.14).

1.7 Determination of Cell Dimensions

Fig 1.2 shows a greatly magnified crystal, mounted to rotate about an axis corresponding to a unit cell edge. The family of planes perpendicular to this axis will diffract to the n^{th} order maximum at an angle Ω_n to the zero order maximum if

$$r \sin \Omega_n = n\lambda \quad \dots \text{Eqn.1.34}$$

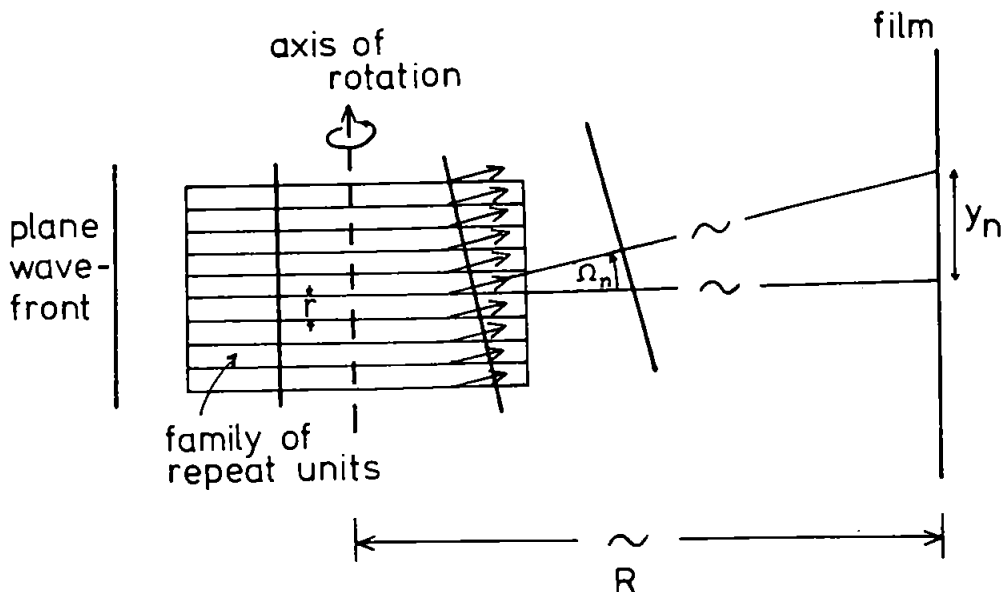


Fig.1.2 Oscillation geometry.

is satisfied, where r is the repeat distance along the rotation axis. Thus, a measurement of the separation of the zero layer and n^{th} lines, y_n , from the resulting oscillation photograph, is related to Ω_n by

$$\tan \Omega_n = \frac{y_n}{R} \quad \dots \text{Eqn. 1.35}$$

Hence, r is obtained from Eqn. 1.34 as

$$r = \frac{n\lambda}{\sin \left(\tan^{-1} \frac{y_n}{R} \right)} \quad \text{Eqn. 1.36}$$

where R is the true film radius.

The lengths of the two remaining unit cell axes were obtained from zero layer Weissenberg photographs, by measuring the perpendicular distance between equivalent axial reflexions on opposite halves of the film.

The angles between the unit cell axes, defined by

$$\begin{aligned} \alpha &= \cos^{-1} \left(\frac{\hat{b} \cdot \hat{c}}{bc} \right) \\ \beta &= \cos^{-1} \left(\frac{\hat{a} \cdot \hat{c}}{ac} \right) \\ \gamma &= \cos^{-1} \left(\frac{\hat{a} \cdot \hat{b}}{ab} \right) \end{aligned} \quad \dots \text{Eqns. 1.37}$$

were determined from the separation of the axial lines on zero level Weissenberg photographs.

Accurate cell dimensions were obtained from zero level Weissenberg photographs, calibrated using an annealed gold wire, taken about two axial directions. The separation between pairs of equivalent high angle reflexions on either half of the film was measured and the corresponding value of θ subsequently calculated gave a small statistical spread for d by Eqn. 1.32, of standard deviation $\sim 0.03\text{\AA}$.

1.8 Determination of Space Group

The fundamental repetition characteristics within a crystal can be expressed in terms of one of the 14 Bravais lattices. All the possible unique combinations of symmetry elements, or point groups, places the unit cell within one of 32 crystal classes. Consideration of both the Bravais lattice and crystal class together with any translation operators describes the unit cell in terms of one of the 230 space groups.

Since X-ray diffraction is dependent upon the spatial array of atoms within a crystal, then any operation relating equivalent parts of that array will be displayed in the resulting symmetry of oscillation and Weissenberg photographs. Thus, space group determination requires knowledge of the number of molecules within the unit cell and the identification of any symmetry elements by which they are related.

The number of molecules, N , per unit cell was obtained from the measured density of the crystal using the relation

$$N = \frac{V \rho N_o}{M} \quad \dots \text{Eqn. 1.38}$$

where

V = volume of unit cell, in m^3

ρ = measured density, kgm^{-3}

N_o (Avogadro's number) = 6.023×10^{26} molecules/kilo-gramme
molecular weight

M = molecular weight.

Symmetry elements involving translation operators result in extinction of certain families of reflexions by destructive interference. Such symmetry elements encountered in the non-centrosymmetric space groups $P2_12_12$ and $P2_1$, and the centrosymmetric space group $P2_1/c$ discussed later include 2-fold screw axes

and glide planes.

A 2-fold screw axis (2_1) effectively halves the separation between planes normal to the axis and the reciprocal nature of the diffraction array results in doubling of the separation of interference maxima, or equivalently, causing phase cancellation of all odd-order reflexions from these planes. The 2_1 axis, however, has no simple ordered effect on the spacing of other planes and thus, only axial reflexions of order $2n + 1$, (n integer), suffer regular extinction.

The effect upon the diffraction array of a glide plane is very similar to that of a 2_1 axis. Upper level Weissenberg photographs were used to distinguish between axial absences caused by a 2_1 axis, and those which resulted from rotation of the crystal about an axis in the glide plane normal to the translation vector of the glide (ref. 3 - Chapter 2).

A combination of symmetry elements within a space group results in a linear superposition of the systematic absences derived from the individual elements.

Consideration of the systematic absences alone does not uniquely define all space groups for they provide no information regarding the presence or otherwise of a centre of symmetry. A test which may be used to detect a centre of symmetry is the $N(z)$ test, suggested by Howells, Phillips and Rogers (1950)¹⁰, and considers a cumulative distribution curve for intensities. $N(z)$ is the fraction of reflexions with intensities less than or equal to z times the mean intensity. Fig. 1.3 shows a theoretical plot of $N(z)$ against z for centric and acentric distributions. The consistently lower values of $N(z)$ in the case of the acentric, compared with those for the centric distributions, modelled the tendency for the intensity of reflexions from the noncentrosymmetric space group crystals, ($P2_1 2_1 2$) (ref Chapter 2)

and $P2_1$ (ref. Chapter 4)), to be more closely distributed about their mean than were those from the centrosymmetric crystals, ($P2_1/c$ (ref. Chapter 3)), discussed in this thesis.

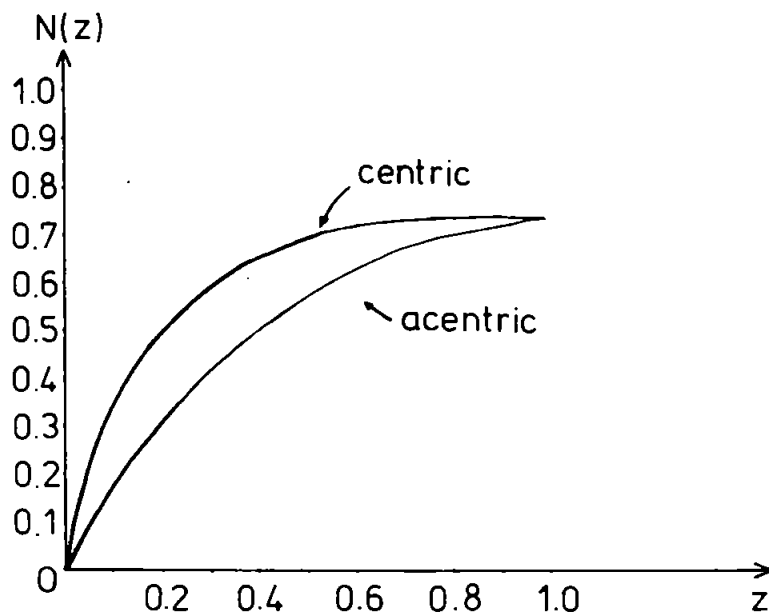


Fig. 1.3 Intensity distribution curves.

1.9 Factors affecting observed intensities

Absorption

Attenuation of the X-ray beam whilst passing through a crystal of thickness t is given by

$$I = I_0 e^{-\mu_\lambda t} \quad \dots \text{Eqn. 1.39}$$

where I_0 is the intensity of the incident beam and I that of the emergent beam. μ_λ , the linear absorption coefficient, is expressed in terms of the mass absorption coefficient $\left(\frac{\mu}{\rho}\right)_{\lambda, E_i}$ for a

given wavelength λ and element E_i by

$$\mu_\lambda = \rho \sum_i \frac{P_i}{100} \left(\frac{\mu}{\rho}\right)_{\lambda, E_i} \quad \dots \text{Eqn. 1.40}$$

where ρ is the density of the compound composed of $P_i\%$ of each element E_i .

Correction factors are integral parts of many crystallographic programs provided the crystal shape is known. Numerical approximations are used to provide a value for the average length of the X-ray beam in the crystal for given reflexions. Interpolation of intra-crystal path lengths between fixed 'grid' points, separated by known path lengths within the crystal, was used to provide an absorption correction from the SHELX²¹ 'ABSC' routine (ref. Chapter 4).

Primary and Secondary Extinction

Whilst the orientation of the crystal is such as to meet the Bragg condition, every point in the crystal is exposed to both the incident beam and part of the diffracted beam. Any systematic effect by crystal interaction with a diffracted beam, results in primary extinction, and assumes a perfectly regular geometry within the crystal, which in practice is confined only to microscopic regions of the crystal known as mosaic blocks. The mosaic structure of such ideally imperfect crystals, introduced by kinetic/thermal energy during crystallisation, is such that effects due to primary extinction can be considered random and therefore, neglected.

Observations relating the intensities of reflexions relies upon the assumption that all planes contributing to a reflexion receive the same incident intensity. However, in the case of the most intense reflexions, transmission of the incident intensity through the crystal is attenuated by reflexion from those planes first encountered by the beam, thus, planes deeper in the crystal receive less radiation and contribute a reduced intensity to the diffracted beam, such that the reflexion suffers from secondary extinction. A compromise was therefore made between a reduction in crystal size and the resulting lowering of diffraction intensity such that only a few very strong reflexions were affected, and these were omitted at the final stage of refinement.

Atomic Vibration - the temperature factor

Atoms, bound within a crystal structure, are consequently at a potential energy minimum related to the bonding processes within the molecule. Thus, any additional random energy, for example, a rise in temperature, will result in vibrational motion of the atoms. The electron cloud is, therefore, spread over a larger region than if the atom were totally at rest, resulting in a faster fall off of scattering amplitude with increasing Bragg angle. The effective atomic scattering factor, $(f_a)_T$, for an atom undergoing isotropic vibration may be expressed in terms of that for the stationary atom, f_a , by

$$(f_a)_T = f_a e^{-\frac{B(\sin^2 \theta)}{\lambda^2}} \quad \dots \text{Eqn. 1.41}$$

where the exponential term is known as the Debye-Waller factor^{11,12}.

The isotropic temperature factor, B, is related to the mean square displacement, $\overline{U^2}$, of the atom, normal to the reflecting plane by

$$B = 8\pi^2 \overline{U^2} \quad \dots \text{Eqn. 1.42}$$

Anisotropic vibration is described in terms of a symmetric 3 x 3 matrix of the mean-square amplitudes of vibration U_{ij} , such that Eqn. 1.41 becomes

$$\begin{aligned} (f_a)_T = f_a \exp [& -2\pi^2 (U_{11} h^2 a^{*2} + U_{22} k^2 b^{*2} \\ & + U_{33} l^2 c^{*2} + 2U_{12} hka^*b^* \\ & + 2U_{13} hl a^* c^* + 2U_{23} klb^* c^*)] \end{aligned} \quad \dots \text{Eqn. 1.43}$$

Polarisation

X-ray reflexion by a crystal plane is more efficient for that component of the incident beam which is parallel to the plane than that which is perpendicular to it. Thus, an unpolarised incident X-ray beam becomes partially polarised upon diffraction. For such an unpolarised incident beam, the measured intensity must be corrected by a factor $\frac{1}{p}$, where

$$p = \frac{1 + \cos^2 2\theta}{2} \quad \dots \text{Eqn. 1.44}$$

defines the polarisation, p , in terms of the Bragg angle.

The Lorentz-factor

Methods of collecting intensity data, in general, involve the rotation of the crystal in the X-ray beam such that each reciprocal lattice point passes through the sphere of reflexion, satisfying a given Bragg condition. Thus, the time taken for the reciprocal lattice point to pass through the sphere varies with its position in reciprocal space and its direction of approach. For a Weissenberg equi-inclination setting angle of μ , the measured intensity is corrected by the application of a factor $\frac{1}{L}$, where

$$L = \frac{\sin \theta}{\sin 2\theta \sqrt{(\sin^2 \theta - \sin^2 \mu)}} \quad \dots \text{Eqn. 1.45}$$

is the Lorentz factor.

Thus, the corrected intensity of a given reflexion $I(hk\ell)$ is obtained from the measured intensity by

$$I(hk\ell) = \frac{I(hk\ell)}{Lp} \text{ (measured)} \quad \dots \text{Eqn. 1.46}$$

1.10 The Structure Factor

In section 1.2, the solution of the scattering process, expressed in terms of the Green's function given by the Fourier transform in Eqn. 1.11, describes the diffraction pattern in terms of the scattering object. In the case of X-ray diffraction, the scattering object is the electron density $\rho(\underline{r})$ and the diffraction pattern $F(\underline{k})$ of the unit cell is therefore the Fourier transform of the electron density within that cell of Volume V .

Hence,

$$F(\underline{k}) = \int_V \rho(\underline{r}) e^{j\underline{k} \cdot \underline{r}} d^3r \quad \dots \text{Eqn. 1.47}$$

and

$$\rho(\underline{r}) = \int_{V^*} F(\underline{k}) e^{-j\underline{k} \cdot \underline{r}} d^3k \quad \dots \text{Eqn. 1.48}$$

where $V^* = \frac{1}{V}$ is the reciprocal lattice unit cell volume.

A crystal is defined by the convolution of the unit cell with the crystal lattice, thus the Fourier transform (F T) of the crystal i.e. the complete X-ray diffraction pattern, by the convolution theorem can be expressed as $\sum_{hkl} F(\underline{s}_{hkl}) = \text{FT} \{ \text{unit cell} * \text{reciprocal lattice} \}$

$$= F(\underline{k}) \times \text{reciprocal lattice} \quad \dots \text{Eqn. 1.49}$$

Thus, $F(\underline{s}_{hkl})$, where \underline{s}_{hkl} are the scattering vectors given by Eqn. 1.31, exists only at the discrete reciprocal lattice points.

Hence, Eqns. 1.47 and 1.48 reduce to

$$F(\underline{s}_{hkl}) = \int_V \rho(\underline{r}) e^{j2\pi \underline{s}_{hkl} \cdot \underline{r}} d^3r \quad \dots \text{Eqn. 1.50}$$

$$\rho(\underline{r}) = \frac{1}{V} \sum_{(hkl)} F(\underline{s}_{hkl}) e^{-j2\pi \underline{s}_{hkl} \cdot \underline{r}} \quad \dots \text{Eqn. 1.51}$$

The vectors \underline{s}_{hkl} are described by Miller indices h, k and l, and so, therefore, $F(\underline{s}_{hkl})$ can be written as the familiar structure factor $F(hkl)$. Splitting the electron density in Eqn. 1.50 into the individual electron densities, $\rho_n(\underline{r}')$ for each of the N atoms making up the unit cell, $F(hkl)$ becomes

$$\begin{aligned} F(hkl) &= \sum_{n=1}^N \int_V \rho_n(\underline{r}') e^{j2\pi \underline{s}_{hkl} \cdot (\underline{r}_n + \underline{r}')} d^3r' \\ &= \sum_{n=1}^N (f_a)_n e^{j2\pi \underline{s}_{hkl} \cdot \underline{r}_n} \quad \dots \text{Eqn. 1.52} \end{aligned}$$

where \underline{r}_n is the vector position of the nth atom and $(f_a)_n$ is the atomic scattering factor given in Eqn. 1.26.

The structure factor is therefore complex and may be expressed as

$$F(hkl) = \left| F(hkl) \right| e^{j\phi_{hkl}} \quad \dots \text{Eqn. 1.53}$$

where $\left| F(hkl) \right|$ is the ratio of the scattering amplitude from the unit cell to that from a point electron and ϕ_{hkl} gives the phase relative to that of a point electron situated at the unit cell origin. Calculation of the structure factor is facilitated by symmetry reduction of Eqn. 1.52 specific to each space group (the programs in Appendix A use the symmetry reduced expressions for $F(hkl)$ given in International Tables for X-ray Crystallography, Vol. 1)⁸.

1.11 The Wilson Plot

Assuming that the temperature factor, B , is the same for each atom and is isotropic, the structure factor modulus $\left| F(hkl)_R \right|$, for atoms at rest, is related to the measured intensity by

$$I(hkl) = K \left| F(hkl)_R \right|^2 \exp \left(-2B \left(\frac{\sin^2 \theta}{\lambda^2} \right) \right) \quad \dots \text{Eqn. 1.54}$$

where K is a scale factor. To place the relative intensities $I(hkl)$, and thus $\left| F(hkl) \right|^2$, on an approximately absolute basis, K and B must be determined.

The theoretical average absolute intensity, $\langle I_{abs} \rangle$, is given by

$$\langle I_{abs} \rangle = \sum_{i=1}^N (f_{a_i})^2 \quad \dots \text{Eqn. 1.55}$$

for N atoms in the unit cell.

Thus, since B is assumed constant, by Eqn. 1.41 and 1.55

$$\begin{aligned} \langle I_{abs} \rangle &= \exp \left(-2B \left(\frac{\sin^2 \theta}{\lambda^2} \right) \right) \sum_{i=1}^N f_{a_i}^2 \\ &= \exp \left(-2B \left(\frac{\sin^2 \theta}{\lambda^2} \right) \right) \left\langle \left| F(hkl)_R \right|^2 \right\rangle \quad \dots \text{Eqn. 1.56} \end{aligned}$$

Hence, by Eqn. 1.54

$$\frac{\langle I(hkl) \rangle}{N \sum_{i=1} f_a^2} = K \exp \left(- 2B \frac{(\sin^2 \theta)}{\lambda^2} \right) \dots \text{Eqn. 1.57}$$

To form a linear relation, Eqn. 1.57 becomes

$$\ln \left(\frac{\langle I(hkl) \rangle}{N \sum_{i=1} f_a^2} \right) = \ln K - 2B \frac{(\sin^2 \theta)}{\lambda^2} \dots \text{Eqn. 1.58}$$

However, the f_a 's are not constant, but vary with scattering angle as $\frac{\sin \theta}{\lambda}$. Division of reciprocal space into thin concentric shells minimises the effect of this variation.

Thus, $\langle I(hkl) \rangle_{\theta}$, is taken as the average value of the relative intensities within each shell and the f_a 's are chosen suitably for that shell.

From Eqn. 1.58, a plot of $\ln \left(\frac{\langle I(hkl) \rangle}{N \sum_{i=1} f_a^2} \right)_{\theta}$

against $\frac{\sin^2 \theta}{\lambda^2}$ is a straight line of slope $- 2B$ and co-ordinate intercept $\ln K$. The graph is termed a Wilson plot (A. J. C. Wilson¹³).

The theory, Eqn. 1.54, assumes a random distribution of identical atoms throughout the unit cell, in practice it is found that the Wilson plot can be used to determined values of K and B adequate for preliminary data analysis without this restriction (ref. Ch. 4).

1.12 Structure determination methods

The intensity of an X-ray reflexion from a crystal is proportional to $|F(hkl)|^2$ and thus only the moduli of the structure factors are directly obtainable from the diffraction data. The solution of a structure rests with the computation of the electron density from Eqn. 1.51 which requires the determination of the phases of a large number of reflexions.

There are two major techniques which can lead to a full structure determination; the heavy atom method and direct methods. These techniques are particularly relevant to the present work and their application is discussed in detail.

Heavy Atom Technique

A. L. Patterson¹⁴ defined the centrosymmetric function $P(\underline{r})$ in terms of the autocorrelation of the electron density $\rho(\underline{r})$ as

$$\begin{aligned}
 P(\underline{r}) &= P(-\underline{r}) = V(\rho(\underline{r}) * \rho(\underline{r})) \\
 &= V \int_V \rho(\underline{r}') \rho(\underline{r}' + \underline{r}) d^3r' \quad \dots \text{Eqn. 1.59}
 \end{aligned}$$

and by Eqn. 1.51 this becomes

$$P(\underline{r}) = \frac{1}{V} \sum_{(hkl)} |F(hkl)|^2 e^{-j2\pi s_{hkl} \cdot \underline{r}} \quad \dots \text{Eqn. 1.60}$$

Since $\rho(\underline{r})$ depends upon the number of electrons in the atom, Z , $P(\underline{r})$ has peaks of weight $Z_i Z_j$ at $\underline{r}_i - \underline{r}_j$ where i, j take all values from 1 to N , the number of atoms in the unit cell. Computation of $P(\underline{r})$ requires no knowledge of the phases, ϕ_{hkl} , of the structure factors, $F(hkl)$. Thus, provided the atomic number of an atom is sufficiently large, (\sim twice that of the average of the remaining atoms for structures of the size discussed later) the vector between it and its symmetry related atoms may be found, which, with a suitable choice of origin, gives the position of that 'heavy' atom within the unit cell.

If the electron density $\rho(\underline{r}')$ for each atom were concentrated at the atom origin ($\underline{r}' = 0$), then Eqn. 1.59 would result in more discernable peaks. Such a process is equivalent to considering a point atom at rest. By a rearrangement of Eqn. 1.41, the scattering factor for an atom at rest is given by

$$f_a = (f_a)_T \exp\left(B \left(\frac{\sin^2 \theta}{\lambda^2} \right) \right) \quad \dots \text{Eqn. 1.61}$$

A point atom at rest has a scattering factor equal to its

atomic number, thus, by simple identity

$$Z = \frac{Z}{f_a} (f_a)_T \exp \left(B \frac{(\sin^2 \theta)}{\lambda^2} \right) \quad \dots \text{Eqn. 1.62}$$

and since

$$\left| F(hk\ell) \right| = \sum_{i=1}^N (f_{a_i})_T e^{j2\pi \mathbf{s}_{hk\ell} \cdot \mathbf{r}_i} \quad \dots \text{Eqn. 1.63}$$

then the modulus of the structure factor for point atoms at rest is

$$\begin{aligned} \left| F(hk\ell) \right|_{\text{point}} &= \sum_{i=1}^N Z_i e^{j2\pi \mathbf{s}_{hk\ell} \cdot \mathbf{r}_i} \\ &= \sum_{i=1}^N Z_i \left| F(hk\ell) \right| \exp \left(B \frac{(\sin^2 \theta)}{\lambda^2} \right) \quad \dots \text{Eqn. 1.64} \\ &= \sum_{i=1}^n f_{a_i} \end{aligned}$$

Use of $\left| F(hk\ell) \right|_{\text{point}}^2$ in Eqn. 1.60 results in a sharpened Patterson function with the advantage of more localised peaks with consequently less overlap.

Oversharpener can introduce peaks due to diffraction ripples, which, together with series termination effects caused by the finite range of h , k and ℓ used in the summation can lead to spurious results. Use of both the Patterson and sharpened Patterson functions together gave the most reliable heavy atom positions. The particular crystal system and its space group symmetry enables Eqn. 1.60 to be reduced to its simplest form, as expressed, for example, in the computation for space group $P2_1 2_1 2$ in Appendix A.

Direct Methods

The determination of relationships between the structure factors can lead to sufficient information about their phases to obtain the electron density directly from Eqn. 1.51.

For any complex numbers a_i , b_i , the Cauchy inequality is given by

$$\left| \sum_{i=1}^N a_i b_i \right|^2 \leq \sum_{i=1}^N |a_i|^2 \sum_{i=1}^N |b_i|^2$$

... Eqn. 1.65

Harker and Kasper (1948)¹⁵ applied this relation to structure factors. In order to consider relating structure factors for any h, k and ℓ, it is necessary to normalise all F(hkℓ) to remove that affect due to sin θ fall off of the scattering factors. Such normalised structure factors are often defined by

$$|E(hk\ell)| = \frac{|F(hk\ell)|}{\sqrt{\left(\sum_{i=1}^N (f_{a_i})^2 \right)^{\frac{1}{2}}}} \quad \dots \text{Eqn. 1.66}$$

and can be written

$$E(hk\ell) = \sum_{i=1}^N n_i e^{j2\pi s_{hk\ell} \cdot r_i} \quad \dots \text{Eqn. 1.67}$$

where $n_i = \frac{(f_{a_i})}{\sqrt{\left(\sum_{i=1}^N (f_{a_i})^2 \right)^{\frac{1}{2}}}}$... Eqn. 1.68

$$\sqrt{\left(\sum_{i=1}^N (f_{a_i})^2 \right)^{\frac{1}{2}}}$$

In the case of a centrosymmetric structure, the phase $\phi_{hk\ell}$ is given by 0 or π and so only the real part of E(hkℓ) need be considered ie, from Eqn. 1.67

$$E(hk\ell) = \sum_{i=1}^n n_i \cos 2\pi s_{hk\ell} \cdot r_i \quad \dots \text{Eqn. 1.69}$$

Letting $a_i = \sqrt{n_i}$ and $b_i = \sqrt{(n_i) \cos 2\pi s_{hk\ell} \cdot r_i}$ the Cauchy inequality, Eqn. 1.65, becomes

$$E(hk\ell)^2 \leq \sum_{i=1}^N n_i \sum_{i=1}^N n_i \cos^2 2\pi s_{hk\ell} \cdot r_i \quad \dots \text{Eqn. 1.70}$$

which reduces to

$$E(hk\ell)^2 \leq \sum_{i=1}^N n_i \left(\frac{1}{2} \sum_{i=1}^N n_i + \frac{1}{2} \sum_{i=1}^N n_i \cos 2\pi s_{hk\ell} \cdot r_i \right)$$

... Eqn. 1.71

by a trigonometrical identity.

Defining a unitary structure factor

$$|U(hk\ell)|^2 = \frac{|E(hk\ell)|^2}{\left(\sum_{i=1}^N n_i\right)^2} \quad \dots \text{Eqn. 1.72}$$

Eqn. 1.71 becomes

$$U(hk\ell)^2 \leq \frac{1}{2} + \frac{1}{2} U(2h \ 2k \ 2\ell) \quad \dots \text{Eqn. 1.73}$$

which written as

$$U(2h \ 2k \ 2\ell) \geq 2U(hk\ell)^2 - 1 \quad \dots \text{Eqn. 1.74}$$

enables the sign of $U(2h \ 2k \ 2\ell)$, and hence $E(2h \ 2k \ 2\ell)$, to be determined from the magnitude of $E(hk\ell)$, provided the magnitude of $U(hk\ell)$ is sufficiently large.

Many such inequalities may be found by suitable partitioning of $E(hk\ell)$ taking into account any possible symmetry reduction within the space group concerned.

If inequalities are produced by taking the sum and difference of $E(hk\ell)$ and $E(h' \ k' \ \ell')$, then, assuming that $|E(hk\ell)|$ and $|E(h'k'\ell')|$ are both large enough,

$$s(hk\ell) s(h' \ k' \ \ell') s(h-h', k-k', \ell-\ell') = 1 \quad \dots \text{Eqn. 1.75}$$

where $s(hk\ell)$ refers to the sign of $E(hk\ell)$. Sayre¹⁶, Cochran¹⁷ and Zachariasen¹⁸ (1952) separately showed that Eqn. 1.75 is approximately true even for $|E|$'s smaller than was necessary to satisfy the inequality relations. Eqn. 1.75 provides the means of computing a sign - relation expansion pathway for all E 's considered large enough to satisfy or nearly satisfy the inequality relations.

For non-centrosymmetric structures, $\phi_{hk\ell}$ must be determined by the use of general phase relations. From Sayre¹⁶ it was suggested that if the phases of a few reflexions are known, then

an expectation value for others may be estimated by

$$\langle \phi_{hkl} \rangle = \phi_{h'k'l'} + \phi_{h-h', k-k', l-l'} \quad \dots \text{Eqn. 1.76}$$

Further expectation values may be found by the tangent expression

$$\langle \tan \phi_{hkl} \rangle = \frac{\sum_{(h'k'l')} |E(h'k'l')| |E(h-h', k-k', l-l')| \sin(\phi_{h'k'l'} + \phi_{h-h', k-k', l-l'})}{\sum_{(h'k'l')} |E(h'k'l')| |E(h-h', k-k', l-l')| \cos(\phi_{h'k'l'} + \phi_{h-h', k-k', l-l'})} \quad \dots \text{Eqn. 1.77}$$

derived by Karle and Hauptman (1956)²³.

Cochran¹⁹ (1955) investigated the general form of the probability distribution of $\langle \phi_{hkl} \rangle$ and showed that the probability of ϕ_{hkl} being within 20° of $\langle \phi_{hkl} \rangle$ is 0.31 and the probability that it is within 40° is 0.57.

Application of Direct Methods

The sign relations and the tangent formula predict structure factor phases from a starting set of predetermined phases. In the structures under consideration, three of the starting set phases must be chosen so as to fix the origin of the unit cell on each of its three axes. Since, three linearly independent vectors are necessary to define any Euclidean space uniquely, then the three starting set phases must be those of reflexions whose associated scattering vectors \underline{s}_{hkl} are linearly independent. Using the three reciprocal axis vectors \underline{a}^* , \underline{b}^* and \underline{c}^* as a set of basis vectors then by the definition of \underline{s}_{hkl} (Eqn. 1.31),

$$\underline{s}_{hkl} = \begin{pmatrix} h \\ k \\ l \end{pmatrix} = \underline{h} \quad \dots \text{Eqn. 1.78}$$

A set of n vectors are said to be linearly dependent if there exists a set of n integers a_1, \dots, a_n , not all zero such that

$$\sum_{i=1}^n a_i \underline{h}_i = 0 \quad \dots \text{Eqn. 1.79}$$

Since the starting set must be those phases of some of the most intense reflexions, Eqn. 1.79, alone, would restrict the possibility of even finding a starting set. However, symmetry within each space group allows one of a number of permissible origins to be chosen so that certain linear combinations of phases whose values are independent of the choice of permissible origin remain unchanged. Such linear combinations are structure seminvariants. Eqn. 1.79 can thus be modified to become

$$\sum_{i=1}^n a_i h_i = 0 \pmod{\omega_s} \quad \dots \text{Eqn. 1.80}$$

ie, for the vectors h_i to be linearly independent modulo ω_s , there must not exist any set of n integers $a_1 \dots a_n$, at least one of which being incongruent to zero modulo ω_i , for some i , such that Eqn. 1.80 holds, where ω_s is defined as the seminvariant modulus, having components ω_i , and is defined by the space group.

Thus the three origin determining reflexions must be chosen such that the triple h_1, h_2 and h_3 is linearly independent modulo ω_s ie. such that the vectors $h_1, h_2, h_3, h_1+h_2, h_2+h_3, h_3+h_1$ and $h_1+h_2+h_3$ are each linearly independent modulo ω_s .^{22,23}

In non-centrosymmetric space groups, the phase of a further reflexion must be fixed in order to define the enantiomorph. The enantiomer of a structure gives rise to a change of sign of ϕ_{hkl} . The enantiomorph determining reflexion must be chosen with phase other than 0 or π (since these are not affected by change of $+\phi$ to $-\phi$) and must be a structure seminvariant. The phase of the enantiomorph reflexion is thus chosen to lie within the range 0 to π or π to 2π . Certain space groups restrict the choice to $\frac{\pi}{2}$ by their inherent symmetry. Otherwise, a choice of $\frac{\pi}{4}$ or $\frac{3\pi}{4}$ will give a maximum

error of $\frac{+\pi}{4}$.

The use of a starting set, found by the above rules, may be sufficient to determine the phases of a large number of reflexions of high E. If the number of reliably estimated phases is not large enough, then many trials using less reliable estimation of phase may be carried out using different starting sets, known as the multiresolution method, (MULTAN²⁰, SHELX²¹).

Further relations between E(hkl)'s have been developed by Karle and Karle (1964, 1966)^{24,25}, using a symbolic addition method in which a limited number of reflexions with high |E(hkl)| and many interactions are given symbols to represent their phases and solutions evaluating these symbols are subsequently related to the auxiliary phase determining relations, already described, to form a reliability check and the possibility of a multiresolution approach within the expansion pathway.

1.13 Structure Completion

The previous sections described methods of obtaining the phase of those reflexions either associated with the position of a heavy atom, or which take part in more general phase relationships. In the first case, the structure has to be extended to determine the remaining atomic positions, whereas, in the second case, often only a partial structure can be determined and the structure remains to be completed.

Fourier F_o-Synthesis

The electron density synthesis Eqn. 1.51 is calculated using as Fourier coefficients the observed structure factor amplitudes combined with calculated phases, based on atomic positions included in the model. Atoms included in the model appear with increased peak height together with the appearance of smaller peaks suggesting

positions of further atoms in the structure.

If phases used in the synthesis are computed by direct methods then their associated $|E(hk\ell)|$'s can be used to produce an 'E-map'. Atomic positions are indicated by the higher peaks in the map. Further atomic positions may be found by the Fourier method using phase angles calculated from the accepted atomic positions and measured $|F(hk\ell)|$'s.

Syntheses used in the early stages of structure determination often suffer from series termination effects that cause spurious rippling in the map especially if a restricted set of amplitudes is used; (this caused particular problems in the structure determination described in Ch. 4).

Difference ΔF -Synthesis

The difference, $\Delta\rho(\mathbf{r})$, between the observed electron density, as given by F_o synthesis, and the calculated electron density from the structure model is defined as

$$\Delta\rho(\mathbf{r}) = \frac{1}{V} \sum_{(hk\ell)} (|F_o(hk\ell)| - |F_c(hk\ell)|) e^{j\alpha_c} e^{-j2\pi s_{hk\ell} \cdot \mathbf{r}}$$

... Eqn. 1.81

where α_c is the phase of $F_c(hk\ell)$.

Atoms which are correctly placed do not give rise to peaks on this map, but missing atoms are shown by distinct positive peaks and incorrectly placed atoms by negative 'holes'. Careful use of difference syntheses can result in information concerning assignment of atom type due to the difference in electron density between alternatives. Anisotropic thermal vibration may also be distinguished from the appearance of asymmetrically placed peaks and 'holes' surrounding given atom positions.

Optimisation of the information obtained from the ΔF synthesis

was used to check the placing of hydrogen atoms within the structure model following geometrical calculation of their positions.

1.14 Least-Squares Refinement and Residual Index, R

The structure factor $F(hkl)$, as described by

$$F(hkl) = \sum_{i=1}^n f_{a_i} e^{-B_i \frac{\sin^2 \theta}{\lambda^2}} \cdot e^{j2\pi s_{hkl} \cdot r_i} \quad \dots \text{Eqn. 1.82}$$

is a function of the position vector r_i of each atom and of the temperature factor B_i (or U_{ij}).

For small errors in these parameters, an extension of the total differential gives

$$\Delta F(hkl) - \sum_{i=1}^N \left(\frac{\partial F(hkl)}{\partial B_i} \cdot \Delta B_i + \frac{\partial F(hkl)}{\partial r_i} \cdot \Delta r_i \right) = 0 \quad \dots \text{Eqn. 1.83}$$

If, however, $\Delta F(hkl)$ is given by the difference between the observed and calculated structure factor, ($F_o(hkl) - F_c(hkl)$) and $F(hkl)$ is substituted by $F_c(hkl)$ within the summation, Eqn. 1.83 is usually not identically zero. A revised calculated structure factor $F'_c(hkl)$, may therefore be obtained by

$$F'_c(hkl) = F_c(hkl) + \sum_{i=1}^N \left(\frac{\partial F_c(hkl)}{\partial B_i} \cdot \Delta B_i + \frac{\partial F_c(hkl)}{\partial r_i} \cdot \Delta r_i \right) \quad \dots \text{Eqn. 1.84}$$

and thus,

$$F_o(hkl) - F'_c(hkl) = \Delta F(hkl) - \sum_{i=1}^N \left(\frac{\partial F_c(hkl)}{\partial B_i} \cdot \Delta B_i + \frac{\partial F_c(hkl)}{\partial r_i} \cdot \Delta r_i \right) \quad \dots \text{Eqn. 1.85}$$

The range of (hkl) provides a set of equations of

the form 1.85 and a least-squares solution for the error in the parameters is calculated which minimises

$$D = \sum_{(h \ k \ \ell)} (F_o(hk\ell) - F_c'(hk\ell))^2 \quad \dots \text{Eqn. 1.86}$$

Convergence to the best set of values is indicated by the minimised static value of the residual index, R, after successive cycles of refinement where

$$R = \frac{\sum_{(h \ k \ \ell)} \left| |F_o(hk\ell)| - |F_c'(hk\ell)| \right|}{\sum_{(h \ k \ \ell)} |F_o(hk\ell)|} \quad \dots \text{Eqn. 1.87}$$

1.15 Accuracy of Bond Lengths and Angles

Bond lengths and angles are functions of the atomic position vectors r_i which are parameters of the least-squares refinement. The error, in terms of standard deviation, of a function f related to n independent variables x_i ($i = 1$ to n) is given by

$$\sigma_f = \sqrt{\sum_{i=1}^n \left[\frac{\partial f}{\partial x_i} \right]^2 \sigma_i^2} \quad \dots \text{Eqn. 1.88}$$

where σ_i^2 is the variance of variable x_i .

The bond length, as a function of the position vectors r_1 and r_2 between atoms 1 and 2 is given by

$$\ell_{12} = |r_2 - r_1| = |r_{12}| \quad \dots \text{Eqn. 1.89}$$

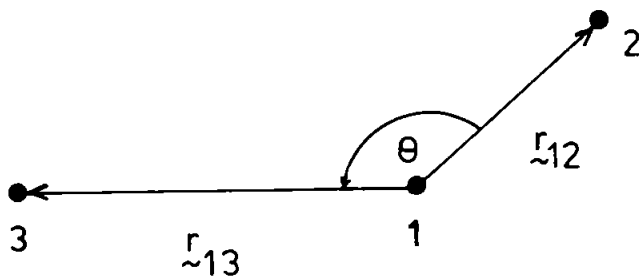
which reduces to

$$\ell_{12} = \sqrt{(x_{12}^2 a^2 + y_{12}^2 b^2 + z_{12}^2 c^2)} \quad \dots \text{Eqn. 1.90}$$

where x , y and z are the components of r related to orthogonal axes of units a, b and c respectively.

Thus, if the atoms are uncorrelated, the standard deviation in ℓ is given by Eqn. 1.88 as

$$\sigma_\ell = \sqrt{\left((\sigma_{x_1}^2 + \sigma_{x_2}^2) \left(\frac{x_{12} a}{\ell} \right)^2 + (\sigma_{y_1}^2 + \sigma_{y_2}^2) \left(\frac{y_{12} b}{\ell} \right)^2 + (\sigma_{z_1}^2 + \sigma_{z_2}^2) \left(\frac{z_{12} c}{\ell} \right)^2 \right)} \quad \dots \text{Eqn. 1.91}$$



Similarly, the bond angle, θ , between bonds 1-2 and 1-3 may be obtained by the scalar product of the interatomic vectors ie.

$$\underline{r}_{12} \cdot \underline{r}_{13} = l_{12} l_{13} \cos \theta \quad \dots \text{Eqn. 1.92}$$

which when related to orthogonal axes gives

$$\theta = \cos^{-1} \frac{(x_{12} x_{13} + y_{12} y_{13} + z_{12} z_{13})}{l_{12} l_{13}} \quad \dots \text{Eqn. 1.93}$$

and therefore by equation 1.88

$$\sigma_{\theta} = \left(\frac{\sigma_{r_1}^2}{l_{12}^2} + \frac{\sigma_{r_2}^2}{l_{12}^2} + \frac{\sigma_{r_3}^2}{l_{13}^2} \right)^{\frac{1}{2}} \quad \dots \text{Eqn. 1.94}$$

where $\sigma_{r_1}^2$, $\sigma_{r_2}^2$ and $\sigma_{r_3}^2$ are the variance in positions of the atoms 1, 2 and 3 respectively, (ref. 7, Ch 17).

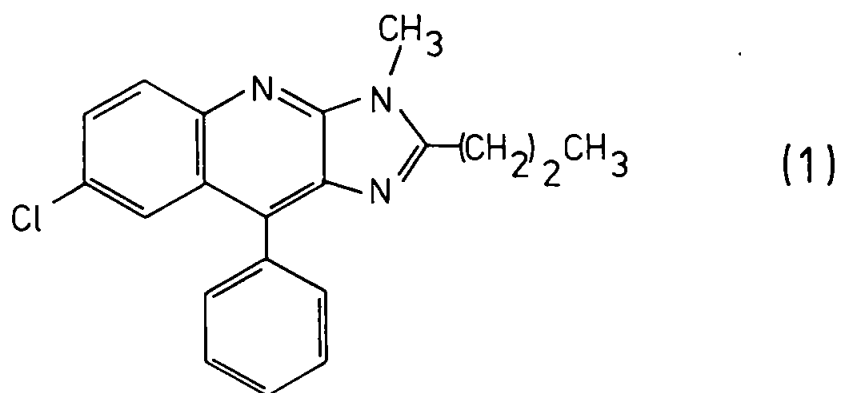
The deviations calculated using the relations described take no account of errors such as errors in data collection, unit cell parameters etc. Thus, such a treatment of errors should be viewed as a measure of accuracy with respect to self-consistent parametrical errors.

Sections 1.6 to 1.15 have discussed the major crystallographic

measurements and computations required to carry out a single crystal structure analysis. These are developed further in the following chapters and applied to the structures referred to in the Introduction.

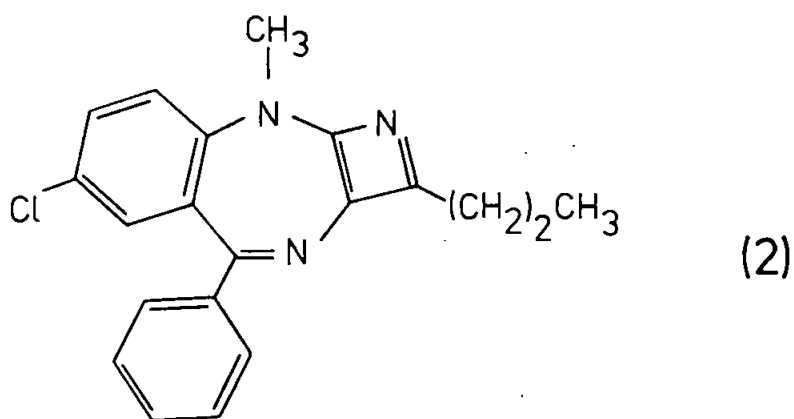
CHAPTER TWO

The Crystal and Molecular Structure of
7-Chloro-2-Methyl-5-Phenyl-3-Propyl [2,3 -b] -
Imidazolyl Quinoline.



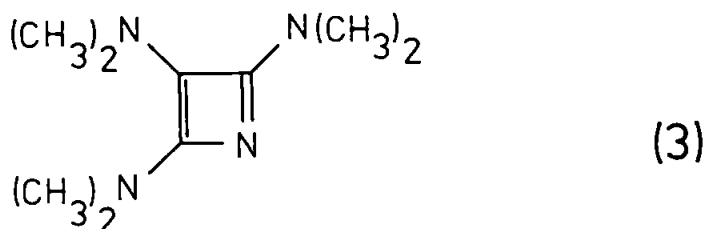
2.1 Introduction

The title compound (1) $C_{20}H_{18}N_3Cl$, provided by Dr G. Kirk, Department of Pharmacy of Chelsea College, University of London, was considered of interest because it is derived from the psychoactive drug Librium, and was thought to conform to the structure,



i.e., that of a 7-chloro-1-methyl-5-phenyl-3-propyl-azeto - [2,3 -b] [1,4] benzodiazepine containing the highly strained 4-membered azete system.

Shenoy, (1975)²⁶, assigned the structure (2) on the basis of C^{13} , H^1 n.m.r., U.V. and mass spectroscopy data. No examples of stable 4-membered azacyclobutadiene rings had previously been reported, though Seybold et al, (1973)²⁷, inferred that they had prepared tris (dimethylamino) azacyclobutadiene (3),



though the stability of the monocyclic azete is very low.

2.2 Crystal Preparation

R.J. Girven, (1977)²⁸, prepared crystals of the compound in order that configuration (2) could be confirmed by structure determination. The best crystallisation solvent was found to be acetone; using, as solution, 104 mg of starting material in 5 cm³ acetone and heating to 45°C followed by cooling to room temperature over two hours, colourless rod shaped crystals were obtained, up to 1 cm in length.

2.3 Space Group and Unit Cell Determination

Preliminary X-ray investigations showed the crystals to belong to the orthorhombic system, and to have unit cell dimensions, $a = 7.43$ (3), $b = 21.56$ (3) and $c = 10.69$ (3) Å, $V = 1712.44$ Å³, with

elongation of the crystal along the a^* reciprocal crystallographic axis.

Weissenberg photographs revealed systematic absences $0k0$, $k = 2n + 1$ and $h00$, $h = 2n + 1$, (n integer). The density was determined by flotation in potassium iodide solution to be 1293 kgm^{-3} . For a structure having $Z = 4$ molecules per unit cell, the calculated density was found to be 1303 kgm^{-3} using Eqn. 138. It was thus concluded that the crystal symmetry must be that of the space group $P2_12_12$.

2.4 Intensity Data Collection and Preliminary Treatment

Equi-inclination Weissenberg techniques were employed using the multifilm method of data collection. The Stoe camera was used throughout with $\text{CuK}\alpha$ radiation. Crystals were rotated about the a^* reciprocal axis and intensity data collected for the zero layer and five upper layers, using exposure periods of 5 days. Additional data was collected for each level using 12 hours exposure, in order to bring the most intense reflexions within the measurable range.

Intensity measurements were carried out at the SRC Microdensitometer Service, Daresbury. 2222 reflexions were of measurable intensity.* L_p corrections and conversion to F_o values were carried out by the HKLF and MERG routines of the SHELX program, resulting in an overall isotropic temperature factor, of estimated value $U = 0.074 \text{ \AA}^2$ from a modified K-curve⁶⁰ and linear absorption coefficient $\mu (\text{CuK}\alpha) = 1898 \text{ m}^{-1}$.

2.5 Structure Determination

The presence of a chlorine atom in the molecule enabled the structure to be solved by the heavy atom method.

The space group $P2_12_12$ has equivalent positions in the unit cell given by

*A possible 3869 reflexions are contained within the experimental Cu sphere.

$$\left. \begin{array}{l} x, y, z \\ \bar{x}, \bar{y}, z \\ \frac{1}{2} + x, \frac{1}{2} - y, \bar{z} \\ \frac{1}{2} - x, \frac{1}{2} + y, \bar{z} \end{array} \right\}$$

for the corresponding atoms in each of the four molecules within the unit cell.

The Patterson function, given in Eqn. 1.60, reduces to the form

$$P(u,v,w) = \frac{8}{V} \sum_{hkl} |F(hkl)|^2 \cos 2\pi hu \cos 2\pi kv \cos 2\pi lw \quad \dots \text{Eqn. 2.1}$$

in the orthorhombic system, where the multiplying constant $\frac{8}{V}$, normalises spatially (V) and symmetrically (8).

A peak at the point (u,v,w) in the Patterson map indicates that there exist, within the unit cell, atoms at (x_1, y_1, z_1) and (x_2, y_2, z_2) , such that

$$\left. \begin{array}{l} u = x_1 - x_2 \\ v = y_1 - y_2 \\ w = z_1 - z_2 \end{array} \right\} \quad \dots \text{Eqns. 2.2}$$

Thus, the equivalent positions in $P2_12_12$ correspond to Patterson peaks at

$$\left. \begin{array}{l} (u_1, v_1, w_1) = (2x, 2y, 0) \\ (u_2, v_2, w_2) = (\frac{1}{2}, \frac{1}{2} - 2y, 2z) \\ (u_3, v_3, w_3) = (\frac{1}{2} - 2x, \frac{1}{2}, 2z) \end{array} \right\} \quad \dots \text{Eqn. 2.3}$$

ie.

$$\begin{array}{ll} (2x, 2y) & \text{on the } w = 0 \text{ section,} \\ (\frac{1}{2} - 2y, 2z) & \text{" " } u = \frac{1}{2} \text{ " ,} \\ \text{and } (\frac{1}{2} - 2x, 2z) & \text{" " } v = \frac{1}{2} \text{ " .} \end{array}$$

Computation of P(u,v,w) was performed in both the unsharpened form (Eqn. 2.1) and the sharpened form using the sharpening function

given in Eqn. 1.64, by the use of program (1) given in Appendix A.

Peaks consistent with Eqns. 2.3 gave a solution for the chlorine atomic position at

$$\left. \begin{array}{l} x = 0.091 \\ y = 0.198 \\ z = 0.225 \end{array} \right\} \dots \text{Eqns. 2.4}$$

Further synthesis of the electron density (Eqn. 1.51) can be expressed in terms of the spatial co-ordinates (X, Y, Z) within the $P2_12_12_1$ unit cell by

$$\rho(X, Y, Z) = \frac{8}{V} \left\{ \begin{array}{l} \sum_{\substack{hkl \\ (h+k = 2n)}} |F(hkl)| [\cos 2\pi hX \cos 2\pi kY \cos 2\pi lZ \cos \alpha(hkl)] \\ - \sin 2\pi hX \sin 2\pi kY \sin 2\pi lZ \sin \alpha(hkl)] \\ - \sum_{\substack{hkl \\ (h+k = 2n+1)}} |F(hkl)| [\sin 2\pi hX \sin 2\pi kY \cos 2\pi lZ \cos \alpha(hkl) \\ - \cos 2\pi hX \cos 2\pi kY \sin 2\pi lZ \sin \alpha(hkl)] \end{array} \right\} \dots \text{Eqn. 2.5}$$

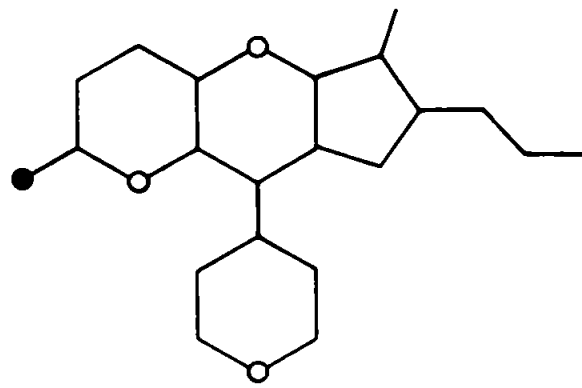
where

$$\alpha(hkl) = \tan^{-1} \left\{ \frac{-\sin 2\pi \left(hx + \frac{h+k}{4} \right) \sin 2\pi \left(ky - \frac{h+k}{4} \right) \sin 2\pi lz}{\cos 2\pi \left(hx + \frac{h+k}{4} \right) \cos 2\pi \left(ky - \frac{h+k}{4} \right) \cos 2\pi lz} \right\} \dots \text{Eqn. 2.6}$$

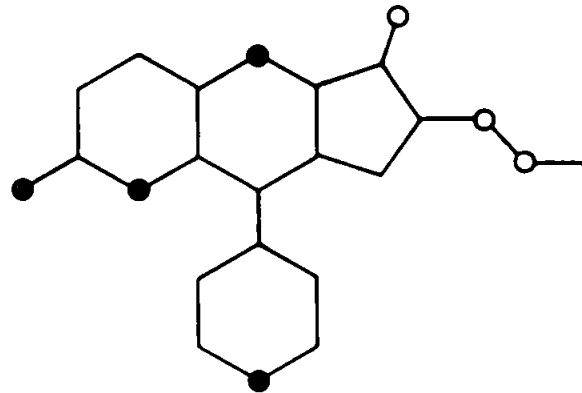
is the phase of reflexion (hkl) contributed by an atom at (x,y,z). The program written to compute this function is given in Appendix A (2).

Fig 2.1 shows the progress of the Fourier syntheses in the structure determination process; where the symbols ● and o describe respectively those atoms used in the synthesis and those derived from it.

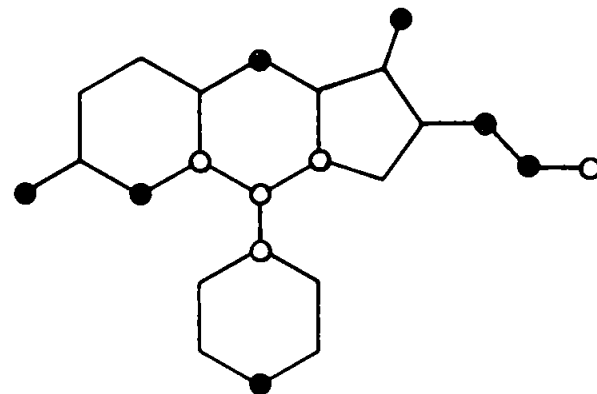
Initial phasing of Eqn. 2.5 was carried out using those observed reflexions $F_o(hkl)$ thought to have a significant scattering contribution from the chlorine atom already found by the Patterson



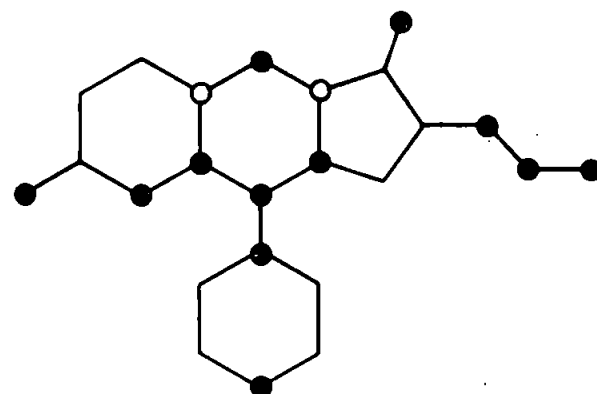
A.



B.

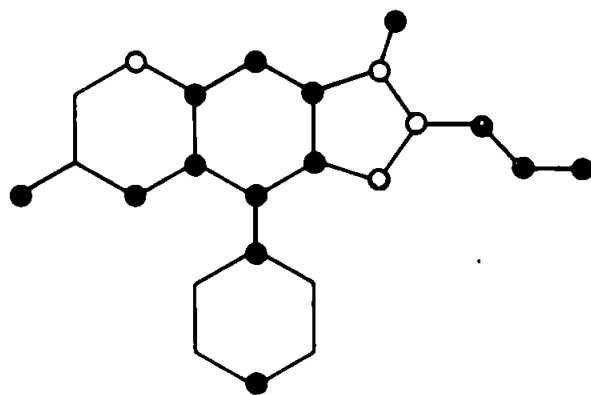


C.

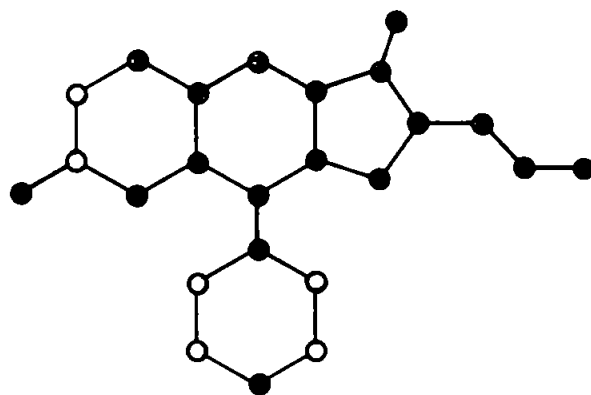


D.

Fig 2.1. Progress of the structure determination during electron density Fourier Synthesis.



E.



F.

Fig 2.1 (contd.)

method. The criterion used for selection of reflexions in this initial phasing was

$$|F_c(hkl)|_{Cl} > 0.3|F_o(hkl)| \quad \dots \text{Eqn. 2.7}$$

where $|F_c(hkl)|_{Cl}$ is the calculated structure factor modulus for the chlorine atom alone. The resultant synthesis, using 668 reflexions produced three further peaks thought to be consistent with new atomic positions. The newly found interatomic vectors were calculated, and corresponding Patterson peaks used to verify the new positions as C(3), N(11) and C(18), Fig. 2.1 (A).

Further use of Eqn. 2.5 was made to produce subsequent syntheses using those observed reflexions satisfying the inequality

$$|F_c(hkl)| > 0.3 |F_o(hkl)| \quad \dots \text{Eqn. 2.8}$$

where $|F_c(hkl)|$ is the calculated structure factor modulus for all derived atoms, and corresponding values of $\alpha(hkl)$, calculated by Eqn. 2.6, for all derived atomic positions.

The six-membered ring containing N(11) was quickly recognised to show a departure from the expected structure (2), as early as synthesis (D) and the spatial relation with the derived positions of C(21) confirmed the attachment of C(21) to an alternative conjugation. The side chain C(22), C(23), and C(24) had also therefore to branch from the same ring system as C(21) which proved inconsistent with the existence of a four-membered azete ring. Subsequent synthesis revealed the existence of a five-membered ring which when used in the phase calculation allowed the determination of the two remaining six-membered rings in the final synthesis.

2.6 Refinement of the Structure

Six cycles of unweighted full matrix least-squares isotropic refinement resulted in an unweighted R factor of 0.1498 excluding

H atoms from the refinement.

Anisotropic refinement was carried out using SHELX 'BLOC' sectioning, partitioning the structure into 6 sections, Fig. 2.2, to maintain the number of parameters refined in any one cycle within the maximum of 112, compatible with the limited storage capacity of the ICL 1903A machine used.

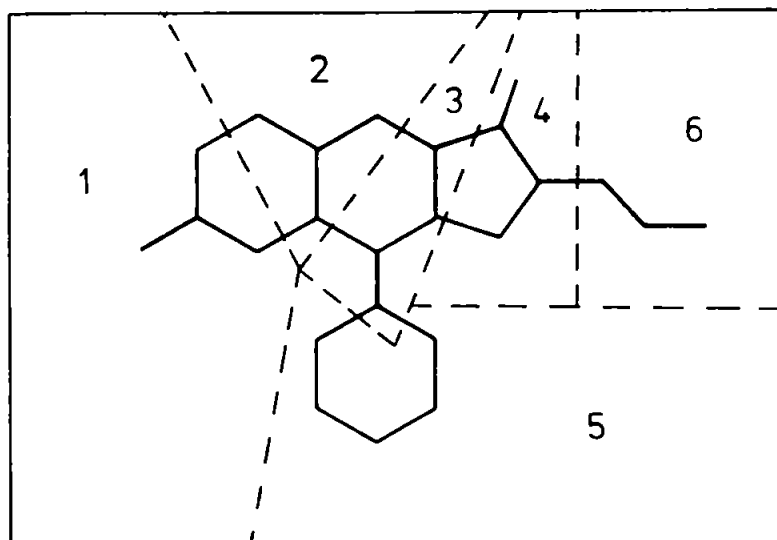


Fig. 2.2 Sectioning for SHELX 'BLOC' refinement. These sections were refined in pairs, to provide the following overlap.

<u>Cycle</u>	<u>Sections</u>	<u>Refined</u>
1	1	2
2	2	3
3	3	4
4	4	5
5	5	6
6	6	1

H atoms were included in the anisotropic refinement with temperature factors fixed at the values of the isotropic temperature factor of the carrier atom, obtained at the isotropic refinement stage, the bond length being fixed at 1.08\AA , resulting initially in $R = 0.1121$. Final anisotropic refinement was carried out with the omission of nine low order reflexions showing severe intensity reduction by secondary extinction.

The final value of the unweighted R factor for the refined structure was 0.0821. Structure factors are listed in Appendix B (ref. SH62 P2₁2₁2).

2.7 Discussion

The final co-ordinates of the non-hydrogen atoms are given in Table 2.1. The bond distances and angles are listed with their standard deviations in Tables 2.2 and 2.3, and are illustrated in Figs. 2.3 and 2.4. The H atom co-ordinates are given in Table 2.4. Thermal parameters are listed with their standard deviations in Table 2.5. Fig 2.5 gives a view of the complete unit cell contents along a and Fig 2.6 shows the complete unit cell contents viewed along c .

The structure exists with the whole of the conjugated ring system and linear side chains virtually coplanar; the separation between the planes of adjacent parallel molecules $\sim 3.6\text{\AA}$. However, the side chain phenyl group is constrained such that the plane of the ring makes an angle of $\sim 65^\circ$ to the plane of the remaining molecule effected by rotation about C(8) - C(15); a feature which maintains a parallel relationship with the plane of the same group in the adjacent molecule with a perpendicular interplanar separation $\sim 1.8\text{\AA}$ as shown in Fig 2.6.

Synthesis of the compound, (Shenoy, 1975)²⁶, was an indirect

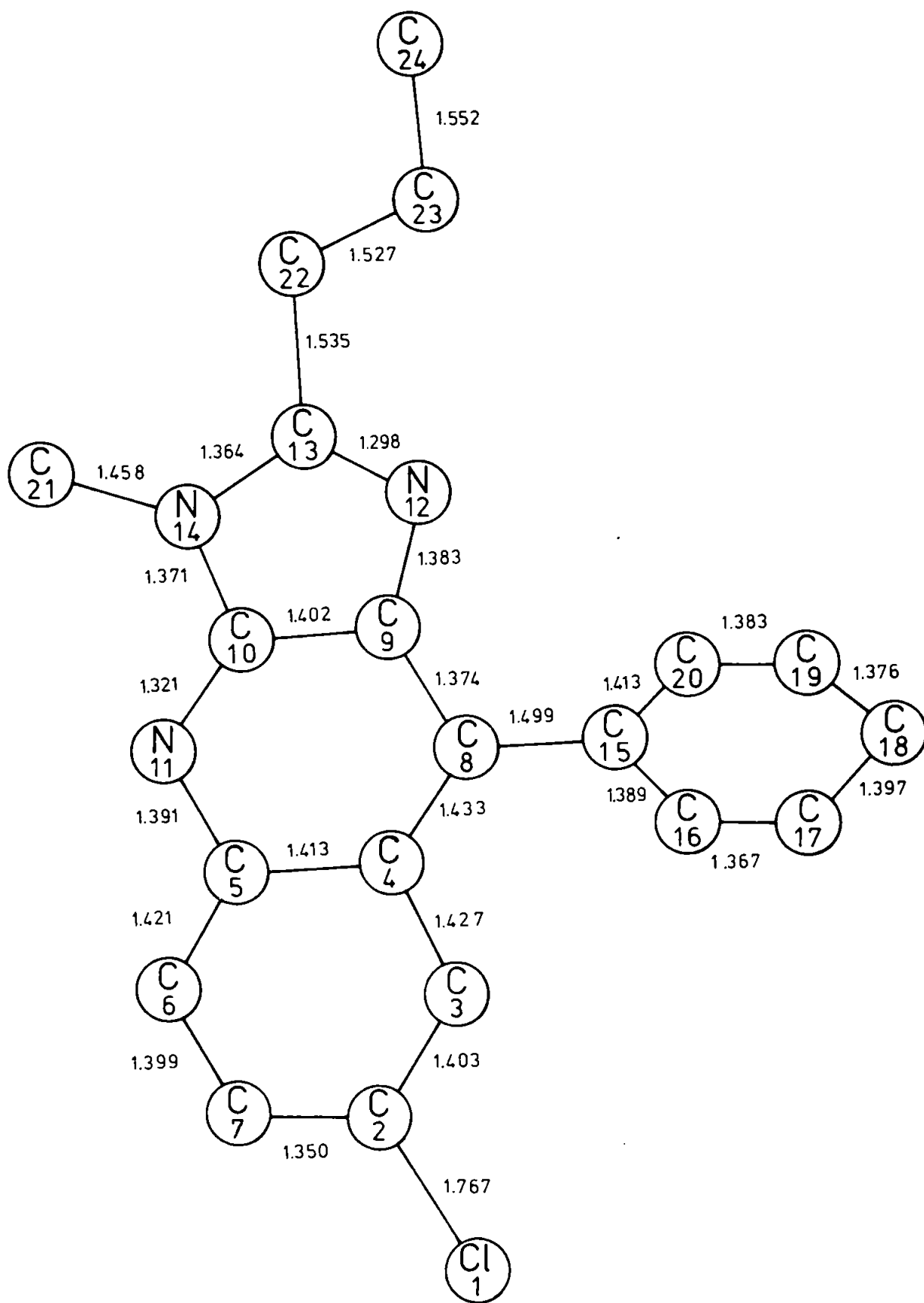


Figure 2.3 Bond lengths in $C_{20}H_{18}N_3Cl$

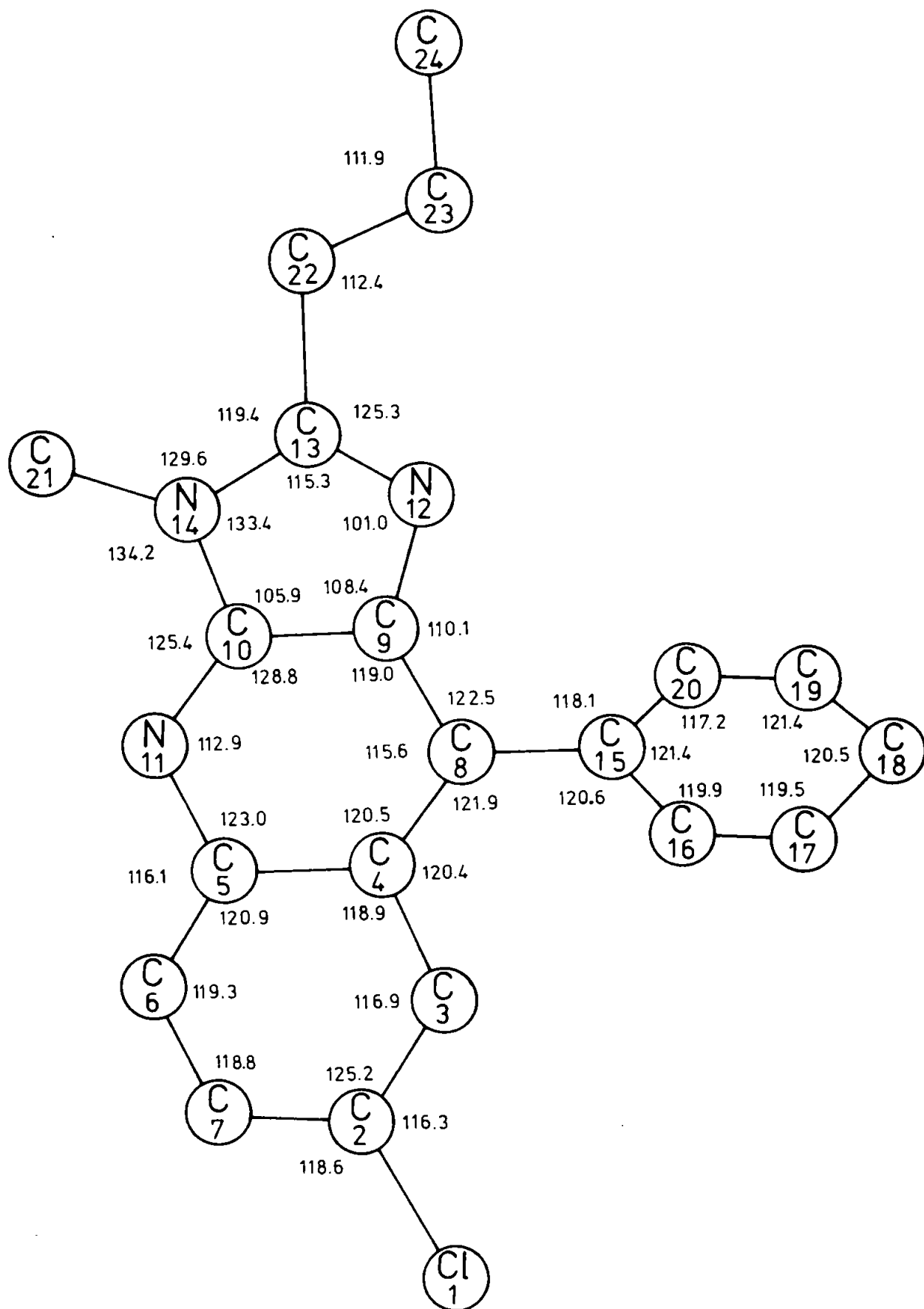


Figure 2.4 Bond angles in $C_{20}H_{18}N_3Cl$

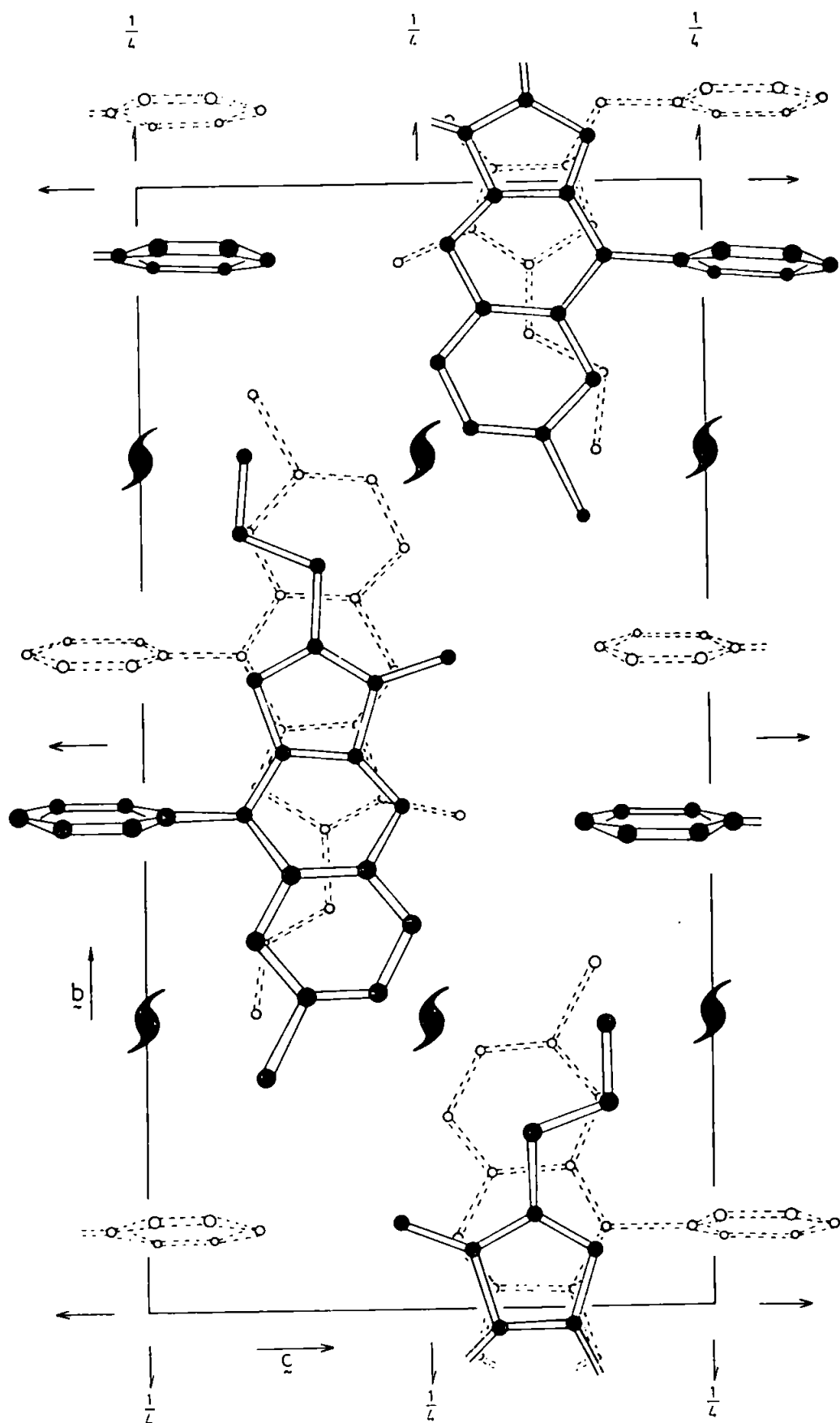


Figure 2.5 The Crystal structure of $C_{20}H_{18}N_3Cl$ viewed along a .

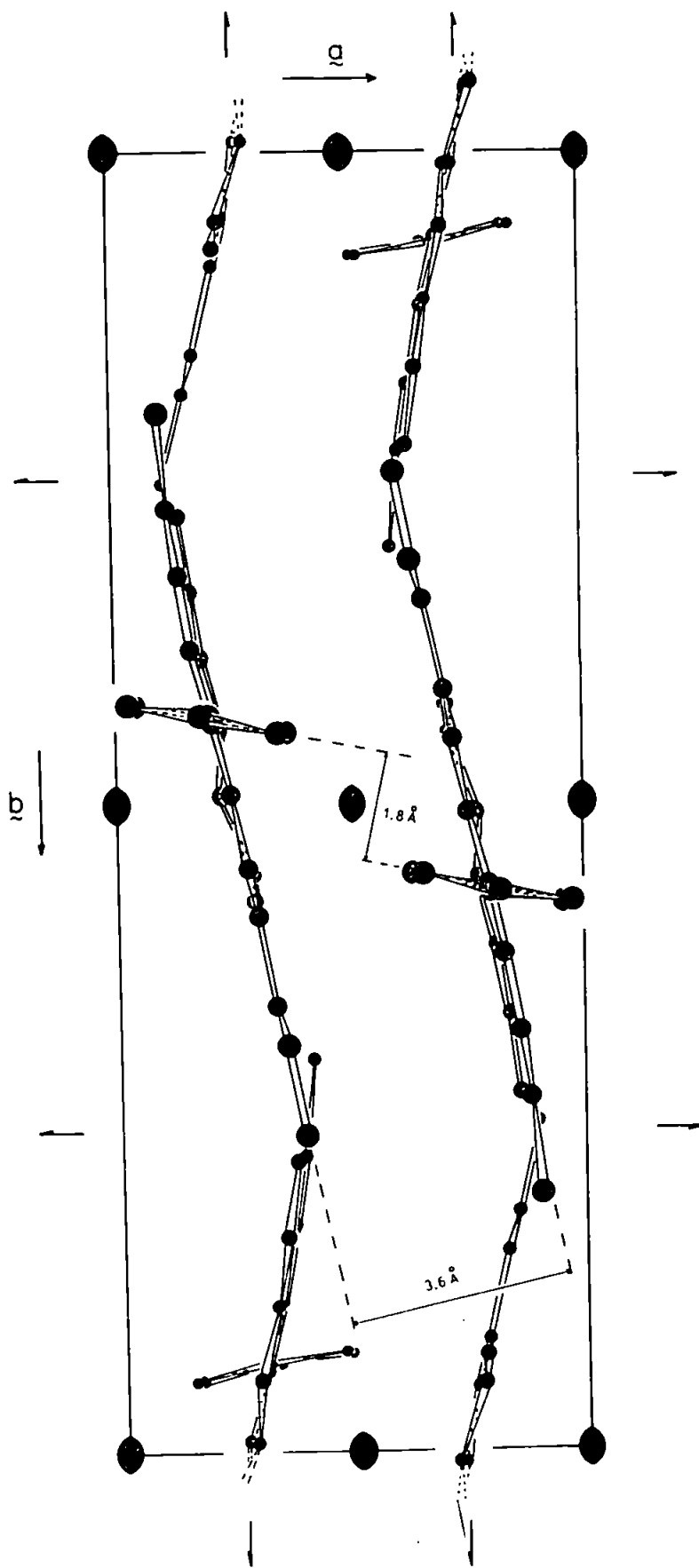
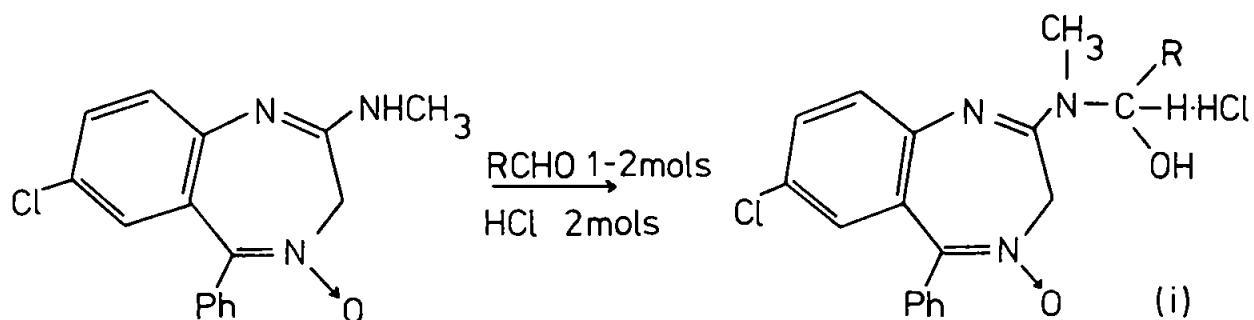
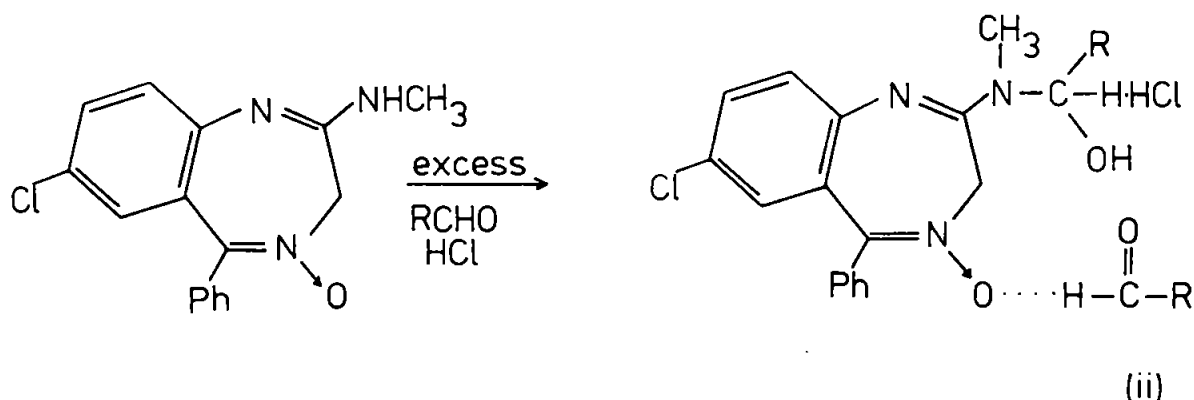


Figure 2.6 The Crystal structure of $C_{20}H_{18}N_3Cl$ viewed along c .

result of an attempt to react aldehydes with chlordiazepoxide under acidic conditions.

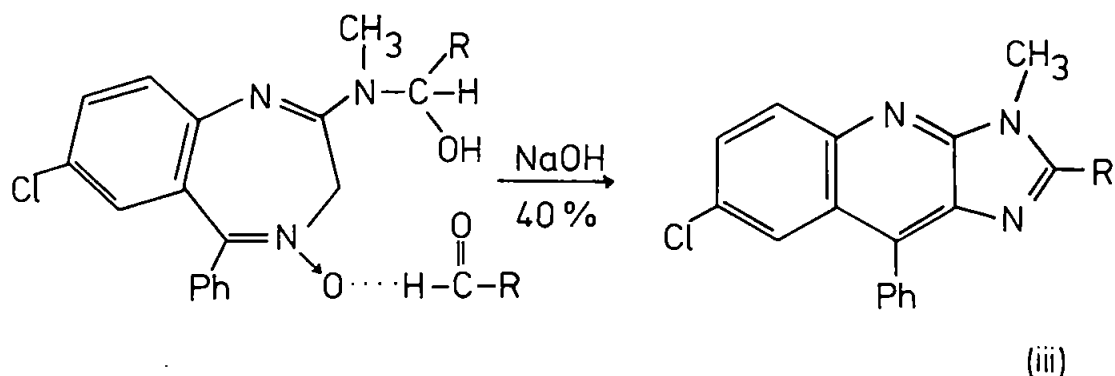


The reaction was repeated using forced conditions (excess aldehyde) resulting in an adduct



Treatment of methanolic solutions of the adduct with 40% aqueous NaOH, gave products which analysed for C, H, N and Cl only. Carboxylic acid was shown to be present in the mother liquor after acidification, indicating the removal of the O from the N-oxide function. In the case of butyraldehyde used in reaction (ii), the H^1 n.m.r. spectrum of the product after treatment with 40% NaOH showed peaks for: a n-propyl side chain, a deshielded N-methyl group and only eight aromatic protons; features fully consistent with both the proposed azete structure, (2), and that found by the X-ray structure analysis described here, to correspond to structure (1).

It is therefore concluded that the reaction formalism,



involving the cleavage of the seven-membered ring, becomes the only interpretation consistent with the evidence provided by structure determination.

The activity of the parent chlordiazepoxide as an antianxiety agent is greatly dependent upon the existence of the $(C = \overset{\text{O}}{\underset{\text{O}}{\text{N}}})$ system, though removal of the O from the N-oxide function is not critical for retention of activity (F. J. Patracek, Chemistry of Psychopharmacological Agents)²⁹. It might be expected therefore, that breaking of the C = N bond would result in a diminishing of the typical anticonvulsant activity. However, the structure of the resultant compound is more akin to that of a tricyclic antidepressant though retaining the unsaturated nature within the central ring system similar to that of the parent compound.

TABLE 2.1. Final co-ordinates obtained from least-squares refinement. Co-ordinates are given as fractions of cell edges $\times 10^4$. Standard deviations in parentheses are with respect to the last figures given .

	x	y	z
C ^l (1)	913(4)	1966(1)	2172(3)
C(2)	1217(13)	2702(3)	2869(9)
C(3)	1441(10)	3203(3)	2046(8)
C(4)	1734(10)	3797(3)	2594(6)
C(5)	1802(10)	3847(4)	3912(7)
C(6)	1547(13)	3319(4)	4685(8)
C(7)	1257(14)	2740(4)	4129(10)
C(8)	2062(9)	4328(3)	1820(6)
C(9)	2449(9)	4869(3)	2444(6)
C(10)	2433(10)	4870(4)	3756(6)
N(11)	2142(9)	4403(3)	4529(5)
N(12)	2189(7)	459(2)	7992(5)
C(13)	2002(9)	787(3)	6987(6)
N(14)	2196(8)	468(3)	5893(5)
C(15)	1961(10)	4294(3)	421(6)
C(16)	325(10)	4195(3)	9826(6)
C(17)	246(14)	4180(4)	8549(7)
C(18)	1818(17)	4266(3)	7853(7)
C(19)	3439(13)	4366(4)	8443(8)
C(20)	3568(10)	4376(3)	9734(7)
C(21)	2088(14)	689(4)	4607(7)
C(22)	1603(9)	1485(3)	6947(7)
C(23)	1413(11)	1766(3)	8252(8)
C(24)	1025(14)	2473(3)	8200(10)

TABLE 2.2. Bond lengths and their standard deviations (\AA) after final least-squares refinement

C(1) - C(2)	1.767(8)
C(2) - C(3)	1.403(11)
C(2) - C(7)	1.350(14)
C(3) - C(4)	1.427(10)
C(4) - C(5)	1.413(10)
C(4) - C(8)	1.433(9)
C(5) - C(6)	1.421(12)
C(5) - N(11)	1.391(10)
C(6) - C(7)	1.399(13)
C(8) - C(9)	1.374(9)
C(8) - C(15)	1.499(9)
C(9) - C(10)	1.402(9)
C(9) - N(12)	1.383(10)
C(10) - N(14)	1.371(10)
C(10) - N(11)	1.321(10)
N(12) - C(13)	1.298(9)
C(13) - N(14)	1.364(9)
C(13) - C(22)	1.535(9)
N(14) - C(21)	1.458(9)
C(15) - C(16)	1.389(10)
C(15) - C(20)	1.413(10)
C(16) - C(17)	1.367(10)
C(17) - C(18)	1.397(15)
C(18) - C(19)	1.376(15)
C(19) - C(20)	1.383(11)
C(22) - C(23)	1.527(11)
C(23) - C(24)	1.552(10)

TABLE 2.3. Bond angles ($^{\circ}$) and their standard deviations

C(3) - C(2) - C2(1)	116.3 (0.7)
C(7) - C(2) - C2(1)	118.6 (0.6)
C(7) - C(2) - C(3)	125.2 (0.7)
C(4) - C(3) - C(2)	116.9 (0.7)
C(5) - C(4) - C(3)	118.9 (0.7)
C(8) - C(4) - C(3)	120.4 (0.6)
C(8) - C(4) - C(5)	120.5 (0.6)
C(6) - C(5) - C(4)	120.9 (0.7)
N(11) - C(5) - C(4)	123.0 (0.7)
N(11) - C(5) - C(6)	116.1 (0.7)
C(5) - C(6) - C(7)	119.3 (0.8)
C(6) - C(7) - C(2)	118.8 (0.8)
C(15) - C(8) - C(4)	121.9 (0.6)
C(15) - C(8) - C(9)	122.5 (0.6)
C(9) - C(8) - C(4)	115.6 (0.6)
C(10) - C(9) - C(8)	119.0 (0.6)
N(12) - C(9) - C(8)	110.1 (0.3)
C(10) - C(9) - N(12)	108.4 (0.3)
C(9) - C(10) - N(11)	128.8 (0.7)
N(14) - C(10) - N(11)	125.4 (0.6)
N(14) - C(10) - C(9)	105.9 (0.3)
C(10) - N(11) - C(5)	112.9 (0.6)
C(9) - N(12) - C(13)	101.0 (0.2)
N(14) - C(13) - N(12)	115.3 (0.6)
C(22) - C(13) - N(12)	125.3 (0.6)
C(22) - C(13) - N(14)	119.4 (0.6)
C(21) - N(14) - C(13)	129.6 (0.6)
C(21) - N(14) - C(10)	134.2 (0.7)
C(13) - N(14) - C(10)	133.4 (0.7)
C(16) - C(15) - C(8)	120.6 (0.6)
C(20) - C(15) - C(8)	118.1 (0.6)
C(20) - C(15) - C(16)	121.4 (0.6)
C(17) - C(16) - C(15)	119.9 (0.7)
C(18) - C(17) - C(16)	119.5 (0.9)
C(19) - C(18) - C(17)	120.5 (0.8)
C(20) - C(19) - C(18)	121.4 (0.8)
C(19) - C(20) - C(15)	117.2 (0.7)
C(23) - C(22) - C(13)	112.4 (0.6)
C(24) - C(23) - C(22)	111.9 (0.7)

TABLE 2.4. Co-ordinates of hydrogen atoms.

Co-ordinates are given as fractions of cell edges $\times 10^4$.

The heavy atom associated with each hydrogen atom is also given.

Standard deviations in parentheses are with respect to the last figures given. (e.s.d.'s quoted refer to those of the parent atom).

	x	y	z
H(C3)	1385(10)	3147(3)	1042(8)
H(C6)	1554(13)	3370(4)	5690(8)
H(C7)	1091(14)	2330(4)	4698(10)
H(C16)	14(10)	4186(3)	812(6)
H(C17)	- 1024(14)	4095(4)	8088(7)
H(C18)	1749(17)	4273(3)	6844(7)
H(C19)	4648(13)	4420(4)	7893(8)
H(C20)	4020(10)	4400(3)	693(7)
H(C21) (1)	2322(14)	305(4)	3980(7)
H(C21) (2)	3092(14)	1043(4)	4448(7)
H(C21) (3)	766(14)	880(4)	4435(7)
H(C22) (1)	2682(9)	1716(3)	6455(7)
H(C22) (2)	355(9)	1555(3)	6448(7)
H(C23) (1)	2655(11)	1690(3)	8754(8)
H(C23) (2)	323(11)	1539(3)	8738(8)
H(C24) (1)	912(14)	2655(3)	9138(10)
H(C24) (2)	- 219(14)	2552(3)	7702(10)
H(C24) (3)	2114(14)	2703(3)	7718(10)

TABLE 2.5. Anisotropic temperature factors are expressed as

$\exp[-2\pi^2(U_{11}h^2a^{*2} + U_{22}k^2b^{*2} + U_{33}l^2c^{*2} + 2U_{12}hka^*b^* + 2U_{13}hl a^* c^* + 2U_{23}k\ell b^*c^*)]$. Isotropic temperature factors are expressed as

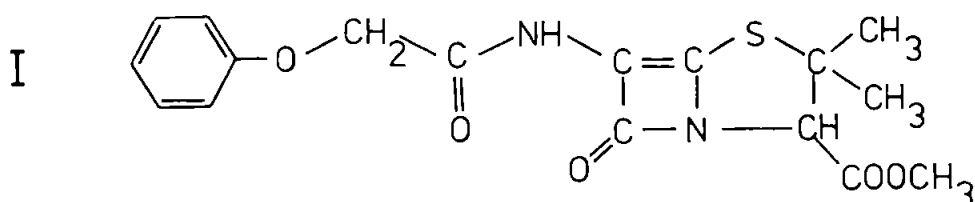
$\exp[-2\pi^2U(h^2a^{*2}+k^2b^{*2}+\ell^2c^{*2})]$. The unit of U_{ij} is $\text{\AA}^2 \times 10^4$. Standard deviations in parentheses are with respect to the last figures given.

	U or U_{11}	U_{22}	U_{33}	U_{23}	U_{13}	U_{12}
C(1)	586(22)	344(10)	921(21)	64(13)	-75(14)	-54(12)
C(2)	281(37)	281(37)	584(61)	102(39)	-83(44)	23(36)
C(3)	53(52)	422(41)	361(44)	40(35)	-22(33)	8(30)
H(C3)	239(32)					
C(4)	1(46)	407(38)	259(37)	32(30)	15(29)	19(30)
C(5)	1(47)	506(46)	315(41)	53(35)	-23(31)	50(33)
C(6)	443(68)	620(55)	353(48)	165(42)	33(43)	-11(44)
H(C6)	459(62)					
C(7)	269(66)	492(52)	642(65)	218(47)	41(48)	-34(44)
H(C7)	417(41)					
C(8)	1(38)	351(36)	222(33)	51(28)	60(28)	27(26)
C(9)	1(43)	351(37)	213(33)	8(26)	16(26)	19(27)
C(10)	1(47)	520(47)	273(37)	-14(31)	17(28)	29(33)
N(11)	218(46)	491(41)	257(32)	-3(28)	4(28)	37(33)
N(12)	6(33)	321(28)	278(27)	22(25)	-16(24)	43(22)
C(13)	1(39)	460(39)	296(35)	46(33)	-54(30)	-61(29)
N(14)	124(37)	417(34)	248(29)	103(26)	-16(25)	4(27)
C(15)	88(43)	256(34)	251(36)	-17(27)	-26(28)	2(28)
C(16)	301(53)	354(37)	227(37)	31(30)	-67(30)	-36(33)
H(C16)	278(32)					
C(17)	669(75)	439(45)	347(48)	-9(36)	-109(42)	-138(45)
H(C17)	386(38)					
C(18)	1127(99)	336(39)	263(41)	-24(34)	27(50)	-12(47)
H(C18)	464(40)					
C(19)	508(77)	562(51)	438(51)	-16(38)	301(43)	-5(44)
H(C19)	422(41)					
C(20)	215(51)	375(39)	372(40)	-3(31)	163(31)	22(32)
H(C20)	256(32)					
C(21)	555(66)	591(56)	321(42)	110(38)	15(41)	-26(49)
H(C21)(1)	472(41)					
H(C21)(2)	472(41)					
H(C21)(3)	472(41)					
C(22)	128(44)	361(33)	446(41)	165(33)	-56(32)	37(27)
H(C22)(1)	296(32)					
H(C22)(2)	296(32)					
C(23)	273(55)	324(35)	703(58)	45(36)	-19(42)	34(30)
H(C23)(1)	383(40)					
H(C23)(2)	383(40)					
C(24)	615(64)	336(37)	969(76)	-19(45)	38(62)	67(41)
H(C24)(1)	573(47)					
H(C24)(2)	573(47)					
H(C24)(3)	573(47)					

The Crystal and Molecular Structure of the Methyl Ester of 5, 5-Dimethyl-2-(2-Phenoxyethyl-5-Oxo-1, 3-Oxazolin-4-ylidene) -1, 3-Thiazolidine-4-Carboxylic Acid

3.1 Introduction

$C_{17}H_{18}N_2O_5S$ was first reported by Brandt, Bassignani and Re (1976)^{30,31} to have the configuration I,

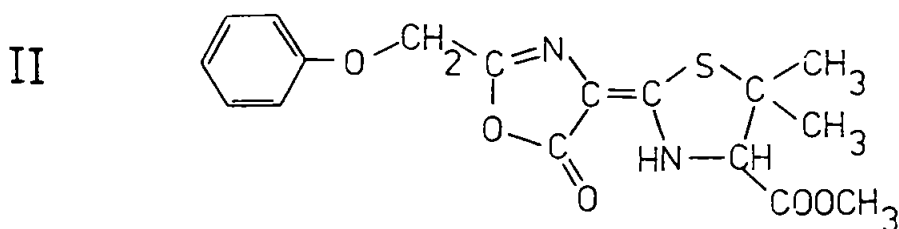


i.e. that of a DL-5, 6-didehydropenicillin, afforded on the basis of spectroscopic data (I.R., H^1 and C^{13} n.m.r., mass spectrometry).

X-ray structure analysis was undertaken as a preliminary to investigation of the reported weak antibacterial activity of the dehydropenicillin and to establish a possible correlation with the "unsaturated" nature of the penicillin nucleus.

Subsequently, Bachi and Vaya (1977)³² suggested the configuration II on the basis of a comparative study of U.V. and I.R.

spectra.



3.2 Experimental

The compound was obtained from Snamprogetti Società per Azioni, Monterotondo; Rome. Single crystals were prepared in the following manner: 30 mg starting material was dissolved in 2 cm³ ethyl acetate and to this solution 1 cm³ cyclohexane was added slowly to prevent clouding. The solution was placed in a water bath warmed to not more than 40°C and protected from light and rapid evaporation. The compound crystallised as clear needle-shaped single crystals on slowly cooling the solution.

The unit cell dimensions were determined from zero level equi-inclination Weissenberg photographs, the camera radius was determined from high-angle reflexions from an annealed gold wire. Systematic absences $h0l$, $l = 2n + 1$ and $0k0$, $k = 2n + 1$ (n integer), indicated space group $P2_1/c$ in the monoclinic system, with $a = 10.60$ (3) $b = 15.53$ (3), $c = 12.63$ (3) Å, $\beta = 61.97^\circ$, $v = 1835.25$ Å³, and linear absorption coefficient μ (CuK α) = 1714m⁻¹.

Data for intensity measurement were obtained by the equi-inclination method on Stoe and Nonius Weissenberg cameras using Ni-filtered $\text{CuK}\alpha$ radiation ($\lambda = 1.5418 \text{ \AA}$) and the multiple film technique. The crystals used for these measurements were rotated about the \tilde{c} crystallographic axis with the long edge of the crystal parallel to the rotation axis. The X-ray films showed severe reduction in intensity of reflexion at high $\sin \theta$ after crystals had prolonged exposure to X-rays; 4 different crystals were used for collection of intensity data. The intensities of the X-ray reflexions were measured by the Science Research Council microdensitometer at Daresbury. A total of 1738 reflexions were of measurable intensity. L_p corrections and conversion to F_o values were carried out by the HKLF and MERG routines of the SHELX program, resulting in an overall isotropic temperature factor, of estimated value $U = 0.066 \text{ \AA}^2$.

3.3 Structure Determination

The structure was solved by direct methods, (Germain, Main and Woolfson (1970, 1971), and Germain and Woolfson (1968)²⁰, Hauptman and Karle (1956)²², Karle and Hauptman (1956)²³, using the starting set given in Table 3.1 with the three origin determining reflexions marked ORIG and the multiresolution phase assignments marked MULT. Expansion was carried out with reflexions, having $|E(hkl)| > 1.2$, to 290 signs using 2395 relations with 4096 permutations and 116 quartets. The choice of the three origin determining reflexions was governed by Eqn. 1.80 such that the triple h_1, h_2, h_3 was linearly independent modulo ω_s . The seminvariant modulus ω_s in the case of space group $P2_1/c$ is given by Hauptman (1974)³³ as

$$\omega_s = \begin{pmatrix} 2 \\ 2 \\ 2 \end{pmatrix} \quad \dots \text{Eqn. 3.1}$$

Thus, for the three origin determining reflexions,

$$\underline{h}_1 = \begin{pmatrix} 5 \\ 2 \\ 1 \end{pmatrix} = \begin{pmatrix} 1 \\ 0 \\ 1 \end{pmatrix},$$

$$\underline{h}_2 = \begin{pmatrix} -5 \\ 7 \\ 1 \end{pmatrix} = \begin{pmatrix} -1 \\ 1 \\ 1 \end{pmatrix}$$

and $\underline{h}_3 = \begin{pmatrix} 4 \\ 5 \\ 1 \end{pmatrix} = \begin{pmatrix} 0 \\ 1 \\ 1 \end{pmatrix} \text{ modulo } \begin{pmatrix} 2 \\ 2 \\ 2 \end{pmatrix} \dots \text{ Eqns. 3.2}$

combination gives

$$\underline{h}_1 + \underline{h}_2 = \begin{pmatrix} 0 \\ 9 \\ 2 \end{pmatrix} = \begin{pmatrix} 0 \\ 1 \\ 0 \end{pmatrix},$$

$$\underline{h}_2 + \underline{h}_3 = \begin{pmatrix} -1 \\ 12 \\ 2 \end{pmatrix} = \begin{pmatrix} -1 \\ 0 \\ 0 \end{pmatrix}$$

and $\underline{h}_3 + \underline{h}_1 = \begin{pmatrix} 9 \\ 7 \\ 2 \end{pmatrix} = \begin{pmatrix} 1 \\ 1 \\ 0 \end{pmatrix} \text{ modulo } \begin{pmatrix} 2 \\ 2 \\ 2 \end{pmatrix} \dots \text{ Eqns. 3.3}$

together with

$$\underline{h}_1 + \underline{h}_2 + \underline{h}_3 = \begin{pmatrix} 4 \\ 14 \\ 3 \end{pmatrix} = \begin{pmatrix} 0 \\ 0 \\ 1 \end{pmatrix} \text{ modulo } \begin{pmatrix} 2 \\ 2 \\ 2 \end{pmatrix} \dots \text{ Eqn. 3.4}$$

such that the triple $\underline{h}_1, \underline{h}_2, \underline{h}_3$ is linearly independent modulo ω_s as required.

All the 25 non hydrogen atoms were obtained from the E map produced from an expansion pathway using the permutation of sign relations ++++----- (Table 3.1) such that the configuration II, (\neq 3.1), suggested by Bachi and Vaya (1977)³², was subsequently recognised and confirmed.

3.4 Structure Refinement

Four cycles of unweighted full matrix least-squares isotropic

TABLE 3.1 Starting set of reflexions with associated phases and equivalent sign relations.

h	k	l	E	Phase °	Sign Relations
5	2	1	3.540	0	ORIG +
-5	7	1	2.615	0	ORIG +
4	5	1	1.945	0	ORIG +
-1	4	1	3.396	0, 180	MULT + -
0	8	2	2.274	0, 180	MULT + -
0	3	2	2.896	0, 180	MULT + -
-2	7	1	2.297	0, 180	MULT + -
4	7	9	1.975	0, 180	MULT + -
-1	1	5	1.800	0, 180	MULT + -
3	6	4	1.305	0, 180	MULT + -
6	3	6	2.113	0, 180	MULT + -
-2	8	5	2.468	0, 180	MULT + -
4	7	1	1.869	0, 180	MULT + -
-2	5	1	1.950	0, 180	MULT + -
-6	3	2	2.557	0, 180	MULT + -

refinement including interlayer and overall scale factor refinement produced $R = 0.175$. Anisotropic refinement initially resulted in $R = 0.106$ with hydrogen atoms included in the refinement. The hydrogen atoms were given isotropic temperature factors fixed at the values of the isotropic temperature factor of the atom to which they are bonded, obtained at the isotropic refinement stage, the bond length being fixed at 1.08 \AA .

An $F_o - F_c$ synthesis revealed a significant positive peak adjacent to O(19) which could not be removed during refinement. Further refinement was carried out with O(19) replaced by O(19(2)) in the position indicated by the $F_o - F_c$ peak. A further $F_o - F_c$ synthesis showed a positive peak at the previous O(19) position, (O(19(1))). The ratio of the peak heights in both syntheses ($\sim 2:1$) was taken as an indication of alternative site occupation, in part confirmed by the departure from the expected benzene C-C bond length (1.39 \AA) in the phenyl group attached to O(19) illustrated in particular by the bond C(22) - C(23), (1.36 \AA). Anisotropic refinement of the O(19(1)), O(19(2)) positions, performed using site occupation factors of 0.7 and 0.3 respectively, finally resulted in $R = 0.096$.

Refinement at the anisotropic stage was carried out using SHELX 'BLOC' sectioning, with the structure partitioned into 6 sections, Fig. 3.1., to keep the number of independent variables refined in any one cycle within the maximum of 112.

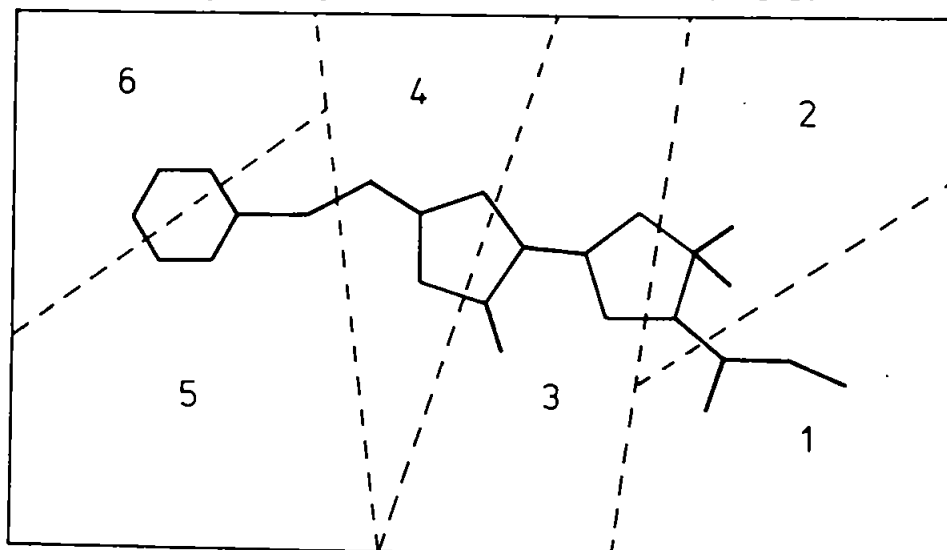


Fig. 3.1 Sectioning for SHELX 'BLOC' refinement

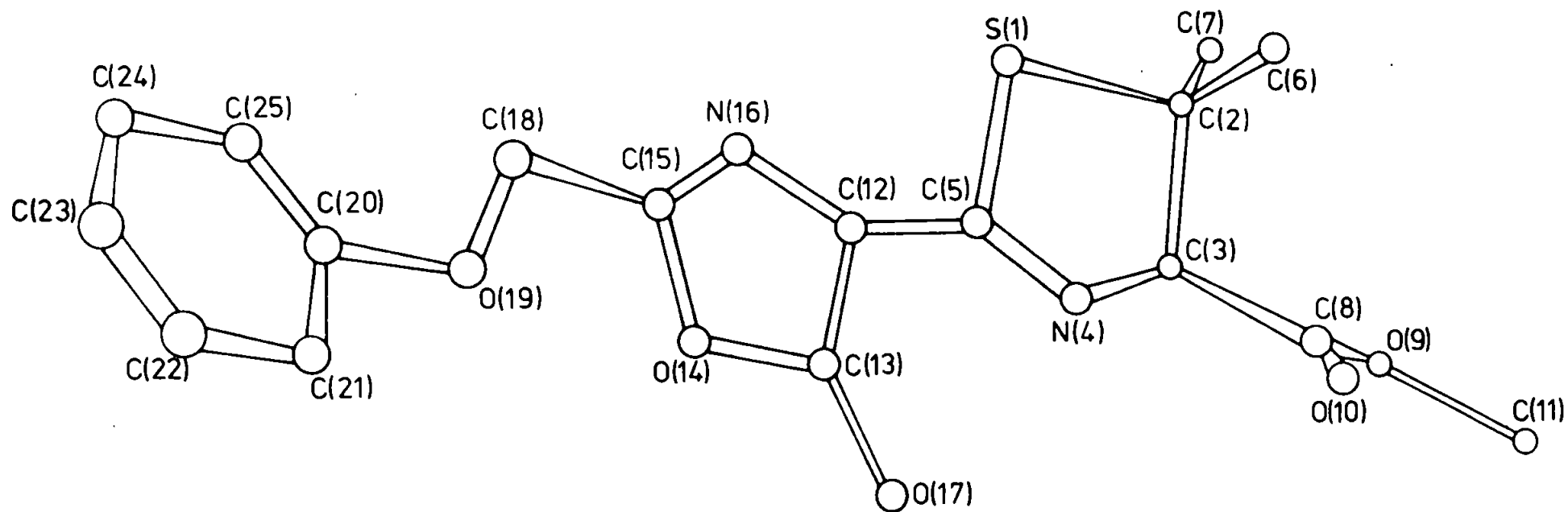


Fig.3.2 Schematic labelling of the non hydrogen atoms in the title compound, $(C_{17}H_{18}N_2O_5S)$

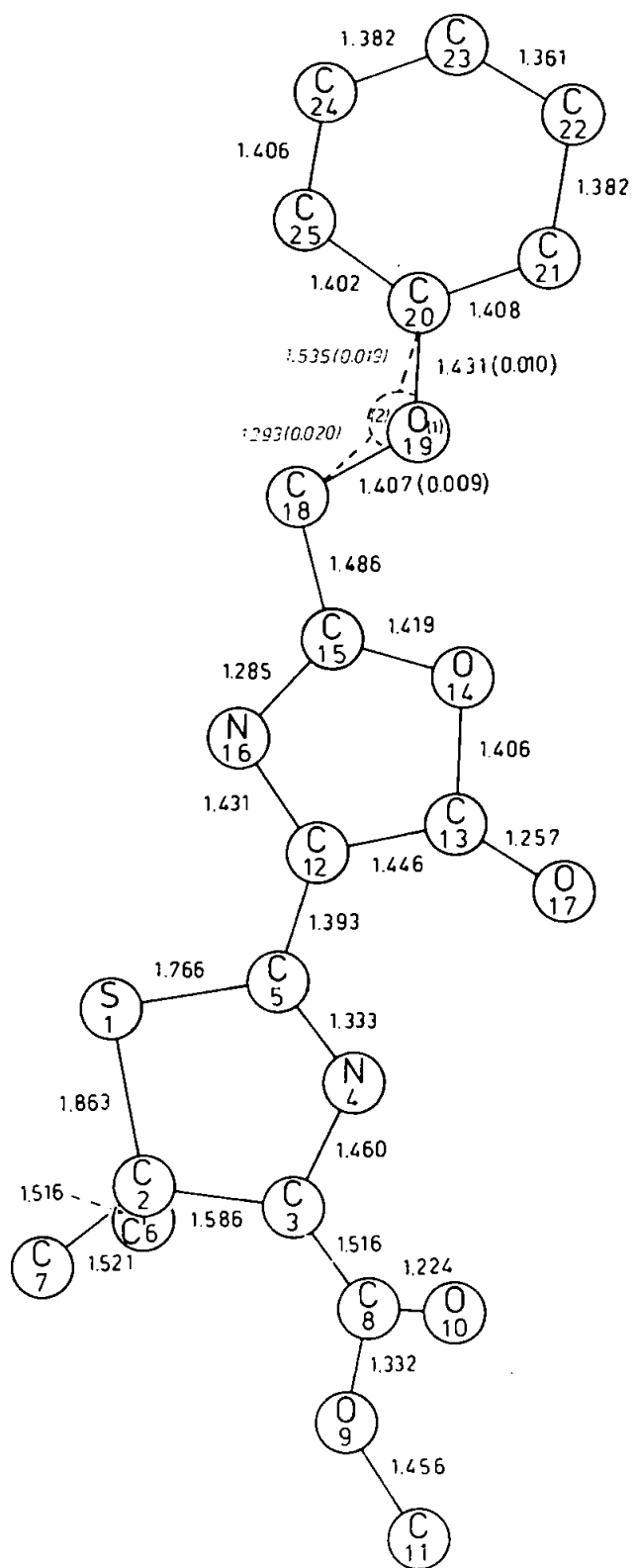


Figure 3.3 Bond lengths in $C_{17}H_{18}N_2O_5S$

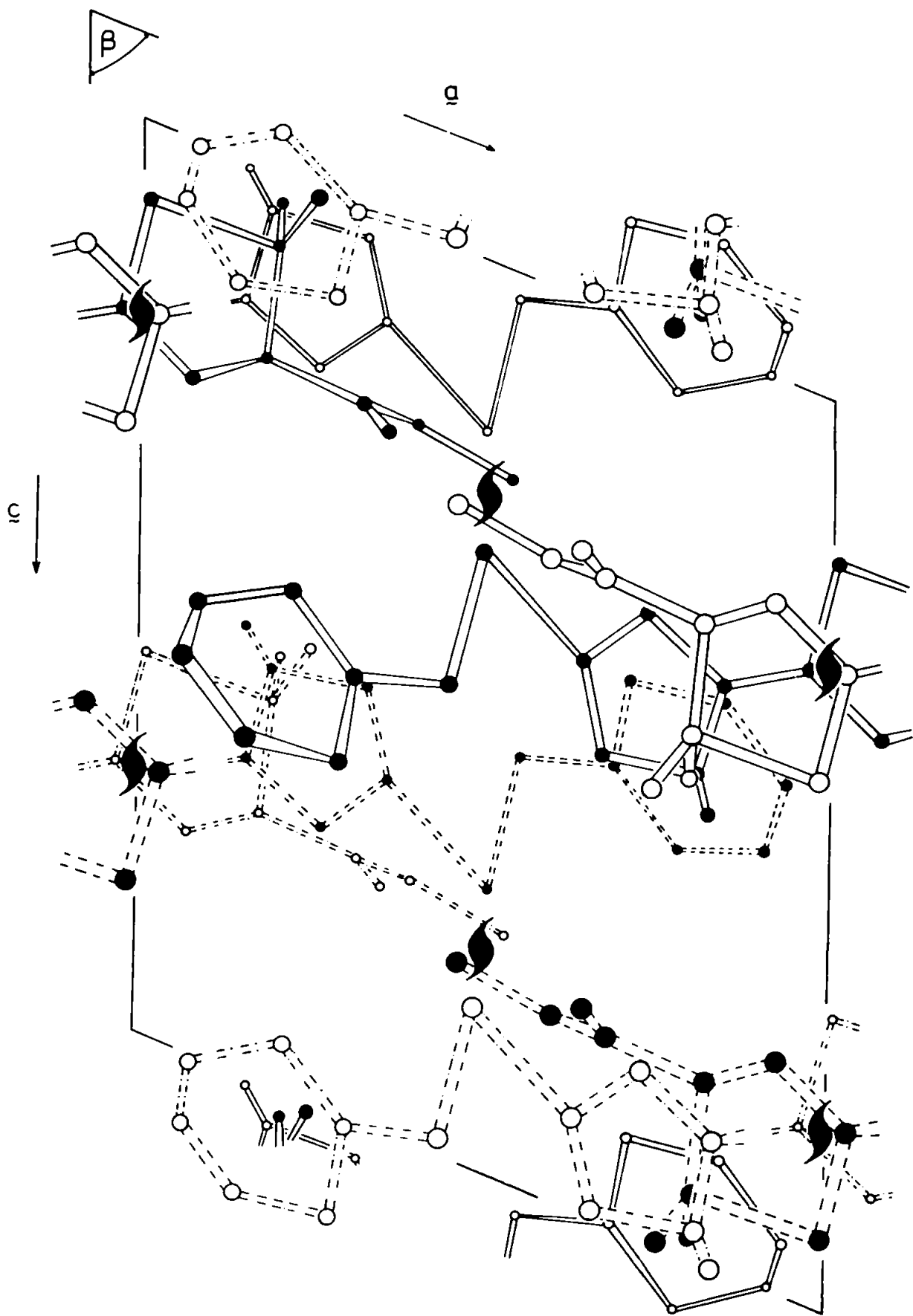


Fig.3.5 The crystal structure viewed along b , ($C_{17}H_{18}N_2O_5S$)

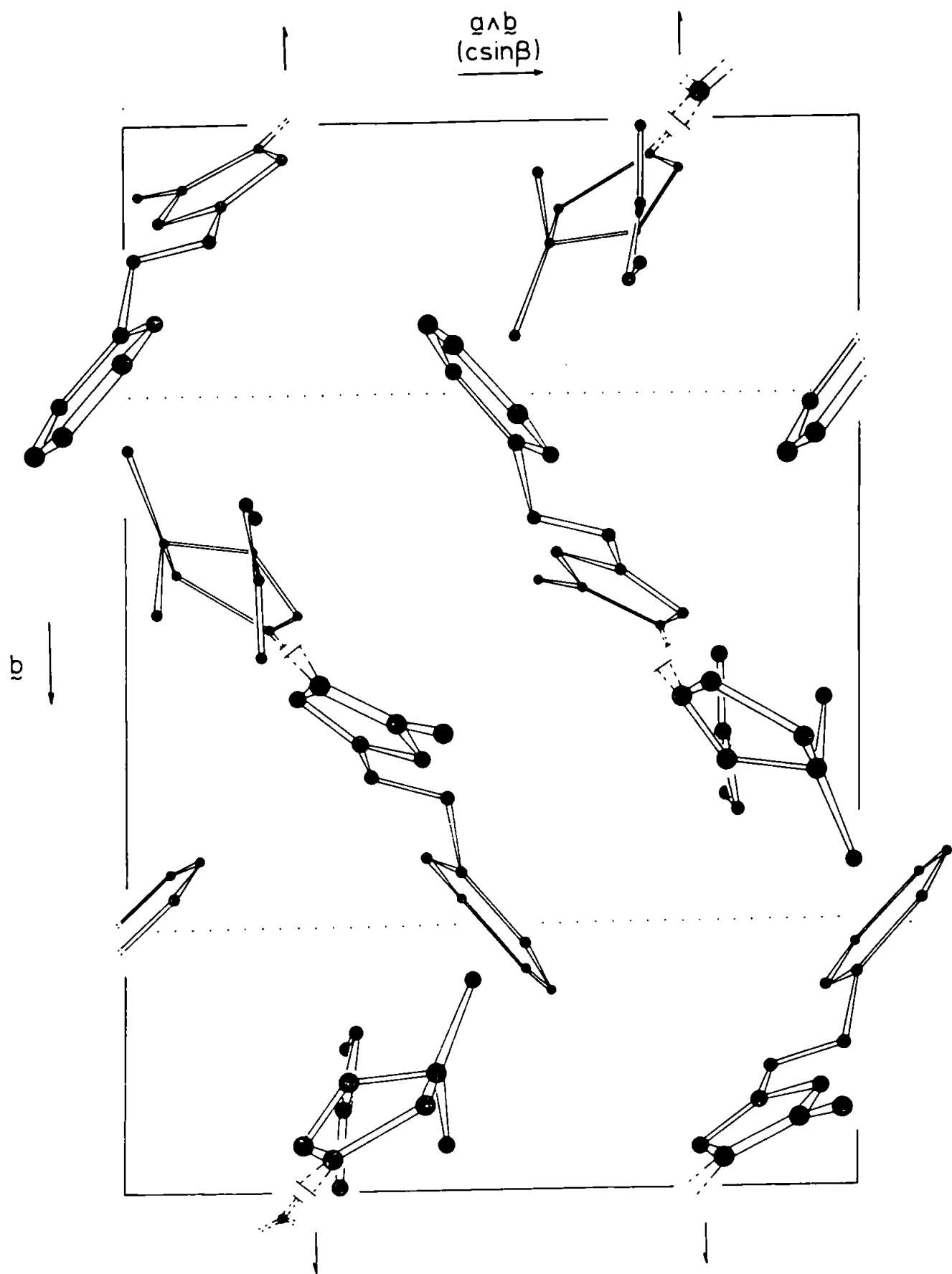


Fig.3.6 The crystal structure viewed along a , ($C_{17}H_{18}N_2O_5S$)

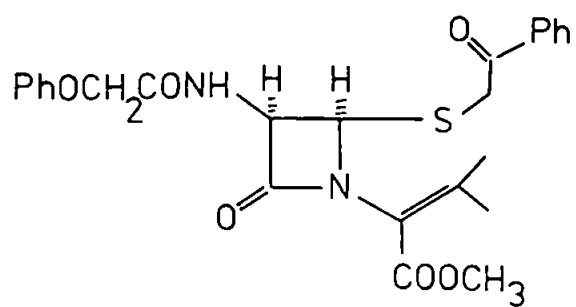
Sections were paired during refinement to provide overlap and overall refinement in 6 cycles.

The residual electron density in the final difference map was within -0.39 and $0.42 \text{ e}\text{\AA}^{-3}$. No further improvement could be made in F_o/F_c correlation probably due to the deterioration of the crystals during prolonged X-ray exposure. Structure factors are listed in Appendix B (ref. SNP P2(1)/C).

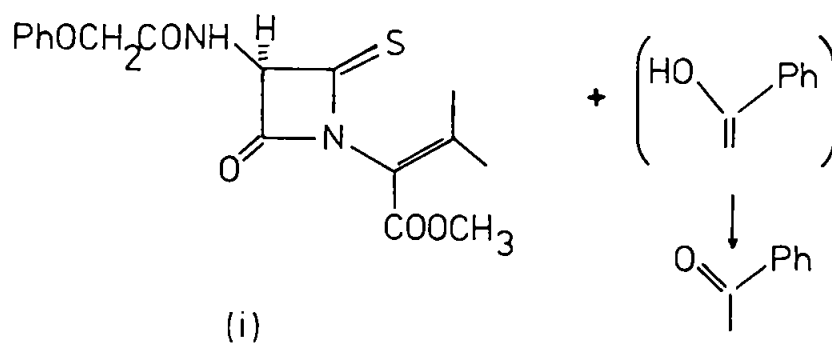
3.5 Discussion

The final co-ordinates of the non-hydrogen atoms are given in Table 3.2 with their schematic labelling illustrated in Fig. 3.2. The bond distances and angles are listed with their standard deviations in Tables 3.3 and 3.4 and illustrated in Figs. 3.3 and 3.4. The H atom co-ordinates are given in Table 3.5. Thermal parameters are listed with their standard deviations in Table 3.6(a) and (b). Fig. 3.5 gives a view of the complete unit cell contents along b and Fig. 3.6 shows the complete unit cell contents viewed along a .

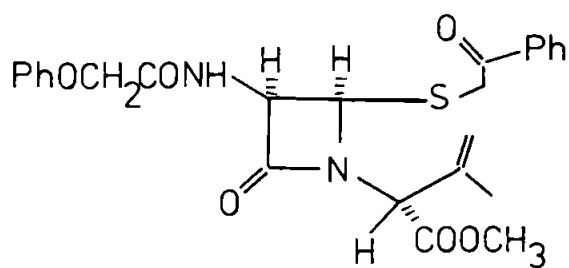
Synthesis of the DL-5, 6-dehydropenicillins was reported by Brandt, Bassignani and Re (1976b)³¹ to result from an intramolecular alkylation of a novel class of 2-azetidinones when treated with Et_3N alone. The 4-thioxo-2-azetidinones (i) and (ii); amongst the first examples of 2-azetidinones carrying a 4-thioxo group; formed the direct synthetic precursor of the 'dehydropenicillins', and were obtained, by a Norrish type II photoelimination reaction, on irradiation of the corresponding 4-acylmethylthio -2-azetidinones with U.V. light³⁰.



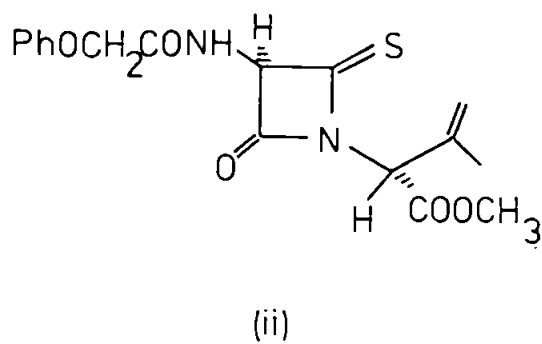
$h\nu$



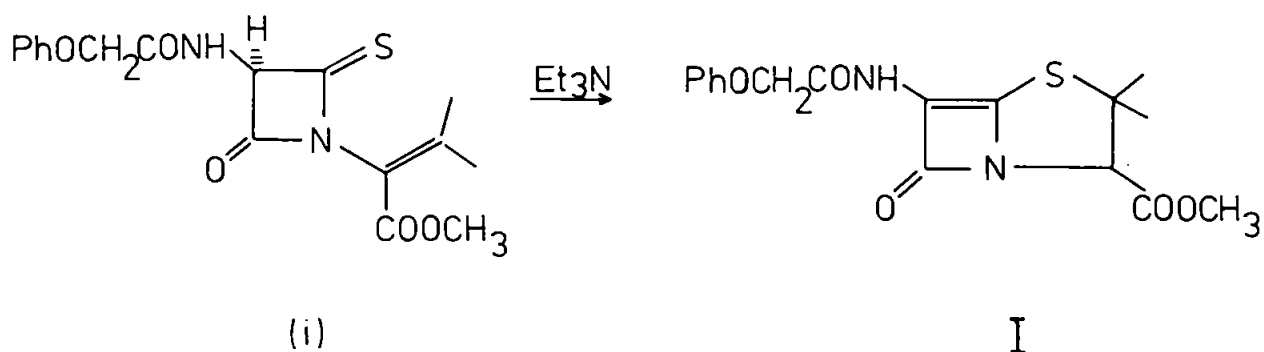
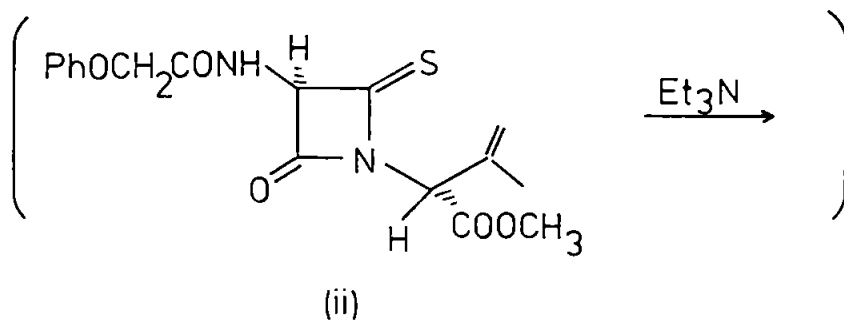
and



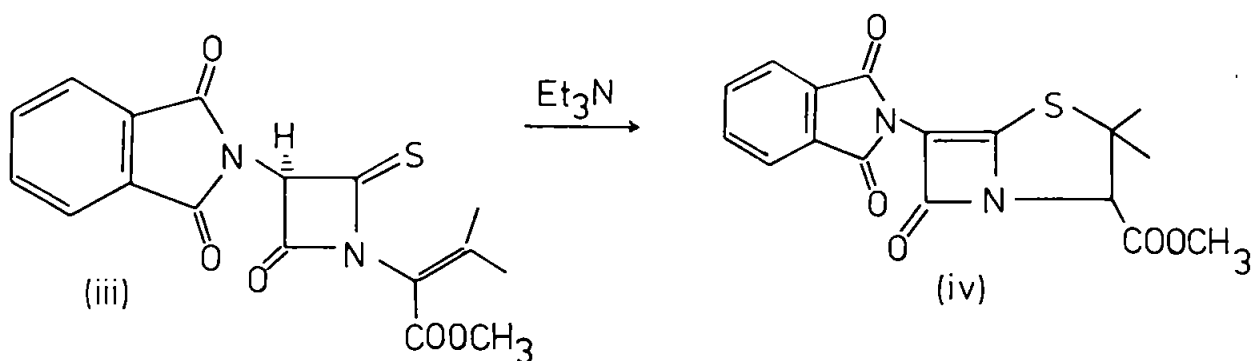
$h\nu$
(-CH₂COPh)



The suggested intramolecular alkylation, proceeding to the 'dehydropenicillin', I, was then represented by

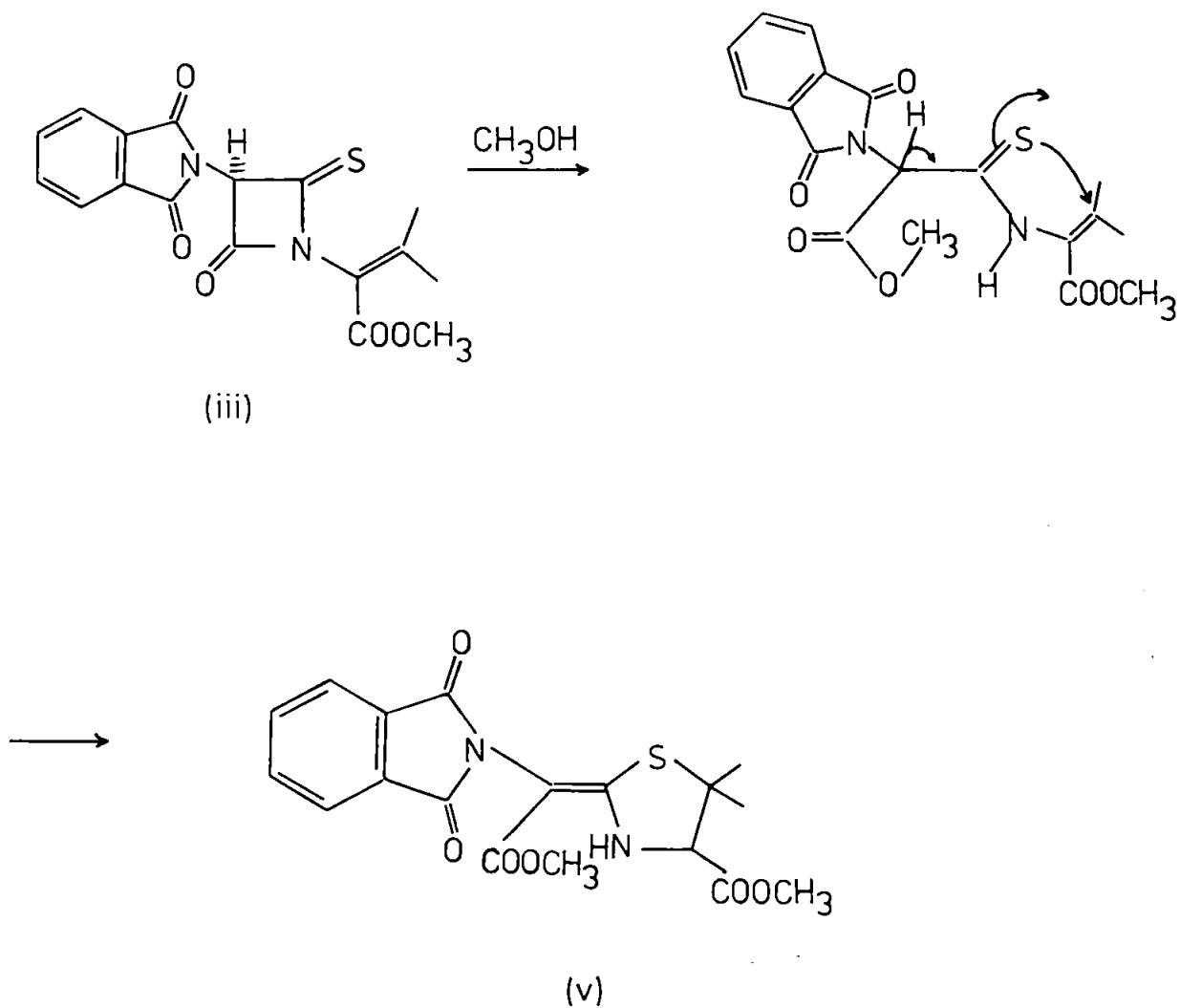


By analogy, Bachi and Vaya (1977)³² expected the conversion of the thiomalonimide, (iii), by treatment with silica gel or Et_3N , into the corresponding 'dehydropenicillin', (iv), thus,

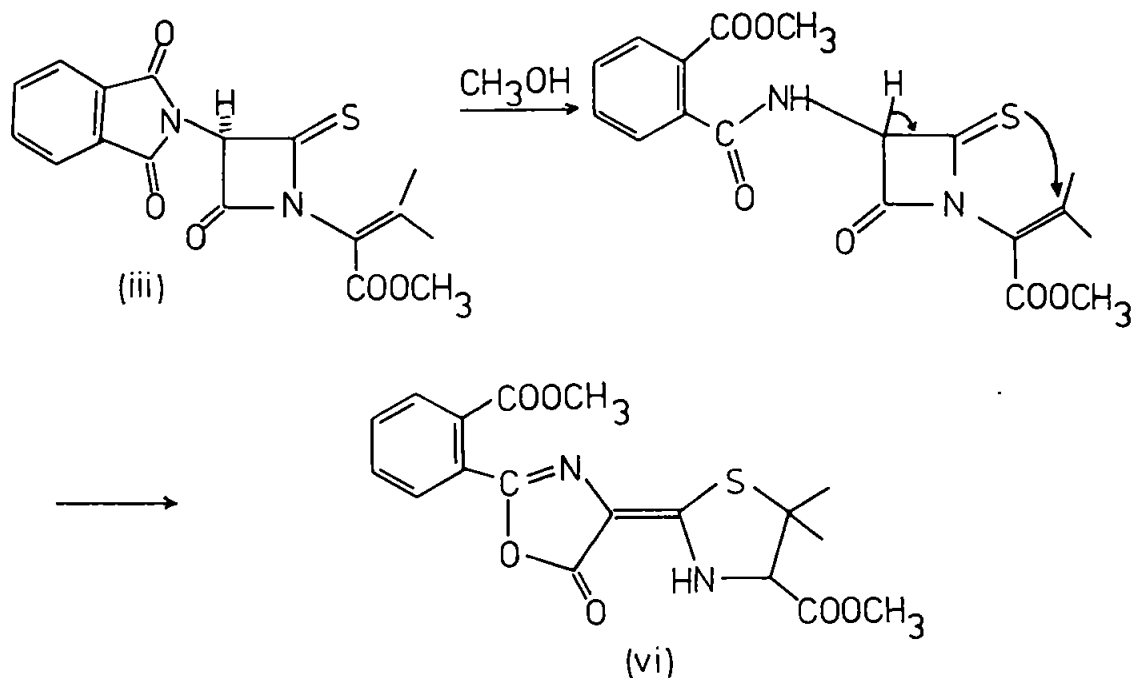


- in their hands, however, this transformation did not occur.

Treatment of the thiomalonimide, (iii), with Et_3N in absolute methanol for 5 min., afforded, after preparative t.l.c., two compounds of the same molecular weight. Structure (v) was assigned to the less polar compound and structure (vi) to the more polar compound. The major product, (v), was obtained by a nucleophilic attack of methanol at C-2 followed by a spontaneous ring closure to the thiazolidine.

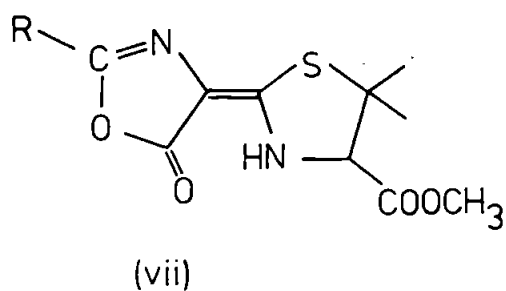


The formation of (vi) required a competitive methanolysis of the phthalamido group in (iii) to the phthaleamic ester which rearranged to the thiazolidylideneoxazolone.



A similar intramolecular rearrangement in which the azetidinone ring is cleaved by a neighbouring acylamino group occurs in many penicillins⁵⁸.

The assignment of structure (vi) to the more polar compound was corroborated by comparison of its U.V. spectrum with the spectra of other thiazolidylideneoxazolones of structure (vii) prepared by a different route,



and with those of 4-(1-thioalkylidene) - and 4 -(1-aminoalkylidene) - oxazolones⁵⁹.

The similarity between the spectral data of (vi), and that of the 'dehydropenicillin' suggested by Brandt et al³¹, together with the apparent inability to produce compound (iv), led Bachi and Vaya³² to propose the alternative structure, II.

The compound was claimed by Brandt, Bassignani and Re (1976b)³¹ to show only a very weak antibacterial activity when tested against *B. subtilis* and *Staph. aureus* by the agar diffusion disc assay. It is therefore of interest to compare the conformation of the part of the molecule in common with that of penicillins, the thiazolidine ring. Boles and Girven (1976a and b)^{34,35} compare the conformation of thiazolidine rings of known penicillin structures. The ring exists with four of its five atoms nearly coplanar and with the remaining atom out of this plane.

In this structure, the plane containing the atoms S(1), C(2) and C(5) is defined by

$$-0.2073x - 2.4491y + z = -0.8991 \quad \dots \text{Eqn. 3.5}$$

where x,y and z are measured in fractions of cell edges \underline{a} , \underline{b} and \underline{c} respectively. N(4) is 0.19 Å out of this plane, and may be considered, as in comparable structures, to be the fourth atom in the plane, though showing rather more distortion about the plane than is the case in penicillins. C(3) is 0.6 Å out of the plane defined above. The structure of the thiazolidine ring is therefore similar to that in phenoxymethylpenicillin³⁶, p-bromopenicillin³⁷ and potassium benzyl penicillin^{38,39}, (ref Chap. 4, §4.7).

The N(4) - C(5) bond length of 1.333 Å in the present compound is significantly less than the equivalent bond length in penicillin nuclei where the thiazolidine ring is constrained by the adjacent β lactam eg. in amoxycillin trihydrate⁴⁰,

ampicillin anhydrate³⁴ and ampicillin trihydrate⁴¹, the N(4) - C(5) bond lengths are 1.49, 1.45, and 1.47 Å respectively. This feature results in a marked difference in the bond angle S(1) - C(5) - N(4) between the thiazolidine ring of the title compound, (115.0°) and that of constrained penicillin nuclei of typical value ~105.5°.

O(19(1)) and O(19(2)) have positions almost symmetrical about the expected O(19) - C(20) bond with bond angles O(19(1)) - C(20) - C(21) and O(19(2)) - C(20) - C(25) being 109.1° and 106.6°, and bond angles O(19(2)) - C(20) - C(21) and O(19(1)) - C(20) - C(25) being 125.4° and 124.9° respectively, compared with the expected values of 120°. This suggests that the co-ordinates of the atoms in the benzene ring attached to O(19) have refined to the values of the weighted mean of the alternative configurations.

Table 3.2. Final coordinates obtained from least-squares refinement. Coordinates are given as fractions of cell edges $\times 10^4$. Standard deviations in parentheses are with respect to the last figures given.

	x	y	z
S(1)	95(3)	4164(2)	1227(3)
C(2)	1928(13)	3912(8)	990(12)
C(3)	1831(12)	3999(7)	2277(11)
N(4)	738(9)	4650(6)	2906(7)
C(5)	- 255(11)	4733(6)	2548(9)
C(6)	2938(17)	4553(10)	83(13)
C(7)	2297(17)	3003(9)	489(14)
C(8)	3215(13)	4248(8)	2275(11)
O(9)	4011(10)	3558(6)	2172(9)
O(10)	3581(10)	4975(6)	2388(10)
C(11)	5365(13)	3650(11)	2194(14)
C(12)	-1502(10)	5204(6)	3204(8)
C(13)	-1837(10)	5604(6)	4340(9)
O(14)	-3196(6)	5966(4)	4710(6)
C(15)	-3549(9)	5775(6)	3782(8)
N(16)	-2609(8)	5353(5)	2881(7)
O(17)	-1238(8)	5685(5)	4989(7)
C(18)	-4939(11)	6082(7)	3904(11)
O(19(1))	-5397(11)	6750(6)	4755(11)
O(19(2))	-5858(20)	6238(14)	5007(18)
C(20)	-6858(11)	7007(7)	5220(9)
C(21)	-7166(13)	7653(8)	6090(10)
C(22)	-8453(14)	8077(7)	6469(11)
C(23)	-9336(12)	7895(7)	5991(10)
C(24)	-9031(10)	7251(7)	5150(11)
C(25)	-7744(11)	6787(6)	4716(10)

Table 3.3 Bond lengths and their standard deviations (Å) after final least-squares refinement

S(1)	- C(2)	1.863(15)
S(1)	- C(5)	1.766(11)
C(2)	- C(3)	1.586(22)
C(2)	- C(6)	1.515(18)
C(2)	- C(7)	1.521(19)
C(3)	- C(8)	1.516(21)
C(3)	- N(4)	1.459(13)
N(4)	- C(5)	1.333(17)
C(5)	- C(12)	1.392(13)
C(8)	- O(9)	1.331(17)
C(8)	- O(10)	1.224(17)
O(9)	- C(11)	1.456(20)
C(12)	- C(13)	1.446(15)
C(12)	- N(16)	1.432(16)
C(13)	- O(17)	1.256(17)
C(13)	- O(14)	1.407(12)
O(14)	- C(15)	1.419(15)
C(15)	- N(16)	1.285(11)
C(15)	- C(18)	1.486(17)
C(18)	- O(19(1))	1.407(9)
C(18)	- O(19(2))	1.293(20)
O(19(1))	- C(20)	1.431(10)
O(19(2))	- C(20)	1.535(19)
C(20)	- C(21)	1.408(16)
C(20)	- C(25)	1.403(19)
C(21)	- C(22)	1.381(19)
C(22)	- C(23)	1.361(23)
C(23)	- C(24)	1.383(16)
C(24)	- C(25)	1.407(14)

Table 3.4 Bond angles ($^{\circ}$) and their standard deviations

C(5)	- S(1)	- C(2)	89.8 (0.6)
C(3)	- C(2)	- S(1)	104.9 (0.7)
C(6)	- C(2)	- S(1)	107.2 (1.1)
C(6)	- C(2)	- C(3)	113.7 (1.3)
C(7)	- C(2)	- S(1)	107.9 (1.1)
C(7)	- C(2)	- C(3)	112.7 (1.2)
C(7)	- C(2)	- C(6)	110.1 (1.0)
N(4)	- C(3)	- C(2)	105.6 (1.1)
C(8)	- C(3)	- C(2)	115.1 (0.9)
C(8)	- C(3)	- N(4)	110.1 (1.0)
C(5)	- N(4)	- C(3)	115.7 (1.0)
N(4)	- C(5)	- S(1)	115.0 (0.7)
C(12)	- C(5)	- N(4)	121.9 (1.0)
C(12)	- C(5)	- S(1)	123.0 (1.1)
O(9)	- C(8)	- C(3)	111.3 (1.1)
O(10)	- C(8)	- C(3)	126.5 (1.2)
O(10)	- C(8)	- O(9)	122.2 (1.4)
C(11)	- O(9)	- C(8)	120.3 (1.1)
C(13)	- C(12)	- C(5)	122.5 (1.2)
N(16)	- C(12)	- C(5)	126.3 (1.0)
N(16)	- C(12)	- C(13)	111.2 (0.8)
O(14)	- C(13)	- C(12)	103.7 (1.0)
O(17)	- C(13)	- C(12)	136.6 (0.9)
O(17)	- C(13)	- O(14)	119.7 (0.8)
C(15)	- O(14)	- C(13)	105.6 (0.7)
N(16)	- C(15)	- O(14)	116.2 (0.9)
C(18)	- C(15)	- O(14)	118.7 (0.8)
C(18)	- C(15)	- N(16)	125.0 (1.1)
C(15)	- N(16)	- C(12)	103.2 (0.9)
O(19(1))	- C(18)	- C(15)	106.6 (0.4)
O(19(2))	- C(18)	- C(15)	112.3 (0.9)
C(20)	- O(19(1))	- C(18)	115.9 (0.7)
C(20)	- O(19(2))	- C(18)	116.3 (1.3)
C(21)	- C(20)	- O(19(1))	109.1 (0.4)

Table 3.4 (continued)

C(21)	- C(20)	- O(19(2))	125.4 (0.9)
C(25)	- C(20)	- O(19(1))	124.9 (0.4)
C(25)	- C(20)	- O(19(2))	106.6 (0.9)
C(25)	- C(20)	- C(21)	124.7 (1.1)
C(22)	- C(21)	- C(20)	116.0 (1.4)
C(23)	- C(22)	- C(21)	121.3 (1.1)
C(24)	- C(23)	- C(22)	122.0 (1.1)
C(25)	- C(24)	- C(23)	120.3 (1.3)
C(24)	- C(25)	- C(20)	115.6 (1.0)

Table 3.5 Coordinates of hydrogen atoms.

Coordinates are given as fractions of cell edges $\times 10^4$. The heavy atom associated with each hydrogen atom is also given. Standard deviations in parentheses are with respect to the last figures given

	x	y	z
H(C3)	1542(12)	3378(7)	2711(11)
H(N4)	962(9)	4869(6)	3228(7)
H(C6)(1)	2689(17)	5197(10)	442(13)
H(C6)(2)	2823(17)	4514(10)	-722(13)
H(C6)(3)	4024(17)	4397(10)	-128(13)
H(C7)(1)	1566(17)	2561(9)	1155(14)
H(C7)(2)	3380(17)	2841(9)	280(14)
H(C7)(3)	2180(17)	2959(9)	-313(14)
H(C11)(1)	5851(13)	3024(11)	2100(14)
H(C11)(2)	5164(13)	3930(11)	3042(14)
H(C11)(3)	6077(13)	4063(11)	1471(14)
H(C18)(1)	-5673(11)	5548(7)	4137(11)
H(C18)(2)	-4799(11)	6369(7)	3077(11)
H(C21)	-6405(13)	7797(8)	6407(10)
H(C22)	-8777(14)	8553(7)	7173(11)
H(C23)	-292(12)	8273(7)	6248(10)
H(C24)	-9806(10)	7092(7)	4853(11)
H(C25)	-7436(11)	6305(6)	4022(10)

Table 3.6(a) Thermal parameters for non hydrogen atoms

Anisotropic temperature factors are expressed as

$$\exp[-2\pi^2(U_{11}h^2a^{*2} + U_{22}k^2b^{*2} + U_{33}l^2c^{*2} + 2U_{12}hka^{*b^{*}} + 2U_{13}hla^{*c^{*}} + 2U_{23}k\lb^{*c^{*}})].$$

The units of U_{ij} are $\text{\AA}^2 \times 10^4$. Standard deviations in parentheses are with respect to the last figures given.

	U_{11}	U_{22}	U_{33}	U_{23}	U_{13}	U_{12}
S(1)	612(19)	658(20)	543(25)	-326(15)	-379(15)	243(16)
C(2)	457(76)	367(73)	524(93)	-249(61)	-246(65)	110(56)
C(3)	407(70)	327(65)	392(81)	-35(51)	-168(57)	80(50)
N(4)	441(51)	435(52)	264(53)	-65(38)	-216(38)	45(41)
C(5)	491(65)	290(54)	242(59)	-29(42)	-222(49)	-33(47)
C(6)	806(112)	741(107)	396(96)	-48(79)	-232(82)	-96(88)
C(7)	717(104)	500(90)	759(110)	-368(80)	-351(84)	159(76)
C(8)	368(71)	402(76)	461(81)	-54(60)	-172(57)	87(60)
O(9)	568(60)	436(55)	759(71)	-143(48)	-344(52)	170(47)
O(10)	503(60)	341(49)	866(78)	-124(48)	-267(54)	27(42)
C(11)	341(79)	773(109)	750(114)	-190(85)	-227(74)	120(71)
C(12)	423(57)	280(54)	272(59)	-18(41)	-155(44)	-12(43)
C(13)	429(58)	333(55)	351(65)	-145(43)	-218(48)	97(41)
O(14)	374(36)	471(41)	442(43)	-169(33)	-205(31)	125(32)
C(15)	339(51)	354(54)	377(63)	-23(44)	-250(44)	7(42)
N(16)	421(48)	426(47)	394(53)	-67(40)	-230(39)	83(39)
O(17)	559(50)	817(61)	474(53)	-250(42)	-293(41)	183(42)
C(18)	608(72)	458(60)	717(80)	-266(56)	-398(61)	234(53)
O(19(1))	590(67)	566(65)	1036(88)	-365(63)	-454(62)	169(51)
O(19(2))	267(107)	633(144)	559(123)	194(114)	-83(86)	176(97)
C(20)	612(67)	673(68)	497(64)	-142(53)	-287(52)	293(54)
C(21)	807(85)	884(86)	678(78)	-244(67)	-409(64)	256(68)
C(22)	944(88)	633(75)	574(77)	-166(59)	-335(68)	285(66)
C(23)	628(68)	556(65)	638(77)	34(55)	-149(59)	200(52)
C(24)	452(55)	518(69)	944(89)	51(62)	-336(55)	12(50)
C(25)	570(62)	367(55)	584(70)	77(49)	-259(54)	18(46)

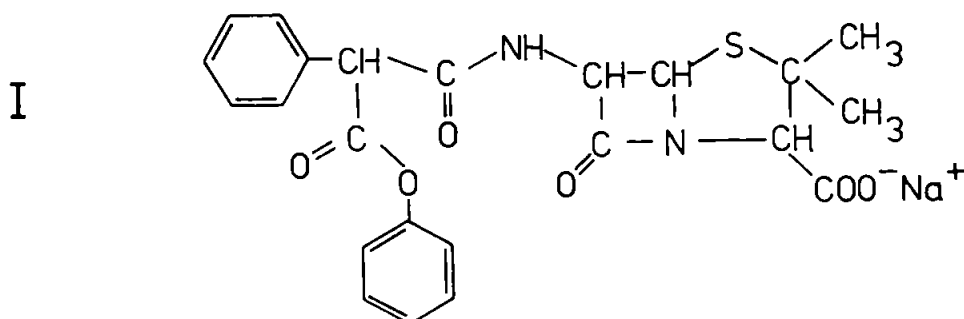
Table 3.6(b) Thermal parameters for H atoms. Isotropic temperature factors are expressed as $\exp [-2\pi^2 U(h^2 a^{*2} + k^2 b^{*2} + l^2 c^{*2})]$. The units of U are $\text{\AA}^2 \times 10^4$. Standard deviations in parentheses are with respect to the last figures given.

	U
H(C3)	390(46)
H(N4)	322(34)
H(C6)(1)	681(66)
H(C6)(2)	681(66)
H(C6)(3)	681(66)
H(C7)(1)	619(63)
H(C7)(2)	619(63)
H(C7)(3)	619(63)
H(C11)(1)	616(62)
H(C11)(2)	616(62)
H(C11)(3)	616(62)
H(C18)(1)	512(41)
H(C18)(2)	512(41)
H(C21)	717(49)
H(C22)	661(46)
H(C23)	660(47)
H(C24)	609(45)
H(C25)	494(37)

The Crystal and Molecular Structure of the
Phenyl Ester of Carbenicillin (Carfecillin).

4.1 Introduction

Esters of carbenicillin have been shown by optical rotatory measurements to undergo side-chain configurational modification in solution (ref. Ch. 5). To facilitate a study of the mechanism by which such modification takes place within the side-chain of penicillin compounds, the crystal structure of the phenyl ester of carbenicillin, I, has been determined.



Experimental

4.2 Crystal Preparation and Preliminary X-ray Studies

The compound was obtained from Beecham Research Laboratories. Preparation of suitable crystalline material was performed in the following manner: 2 g starting material was dissolved in 7 cm³ distilled water at 48°C and to this solution 18 cm³ of ethanol and 18 cm³ isopropanol was added slowly to prevent clouding. The solution was maintained at 4°C and protected from light for 7 days. After filtering and drying, flat plate-like crystals were obtained.

Preliminary X-ray investigations of these crystals revealed a doubling of the reflexions indicating that the crystals were themselves twinned. All reflexions other than the $Ok\ell$'s were doublets, showing that the ab and ac planes of the twin forms are parallel. Investigation under the microscope of each crystal used, revealed a system of twinning, common to them all, where the coincidence of the ab planes occurred between the flat plate-like faces of the constituent crystals as shown, in perspective, in Fig. 4.1. Fig. 4.2, I and II shows

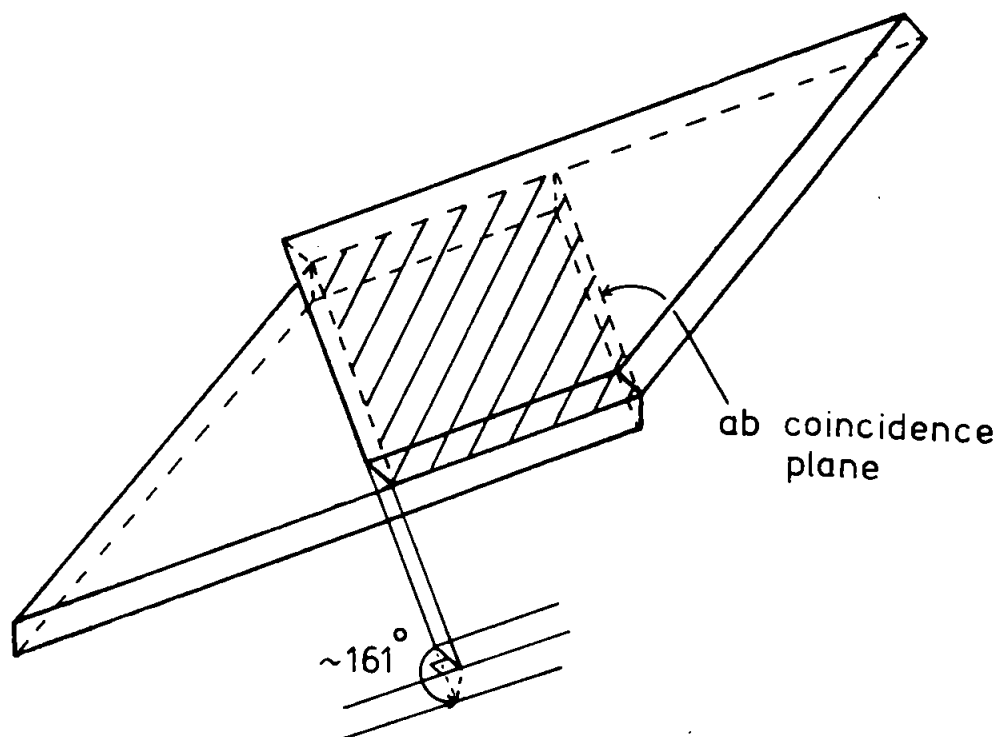
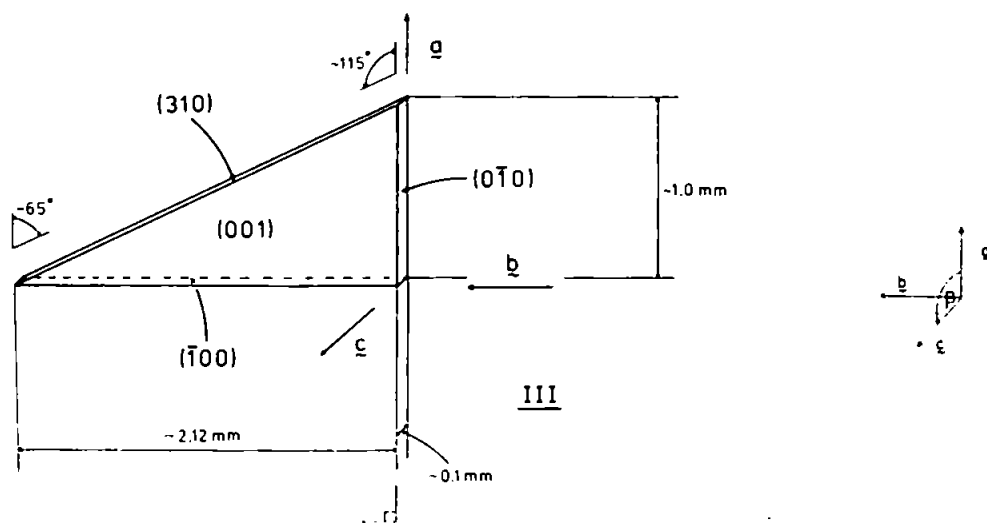
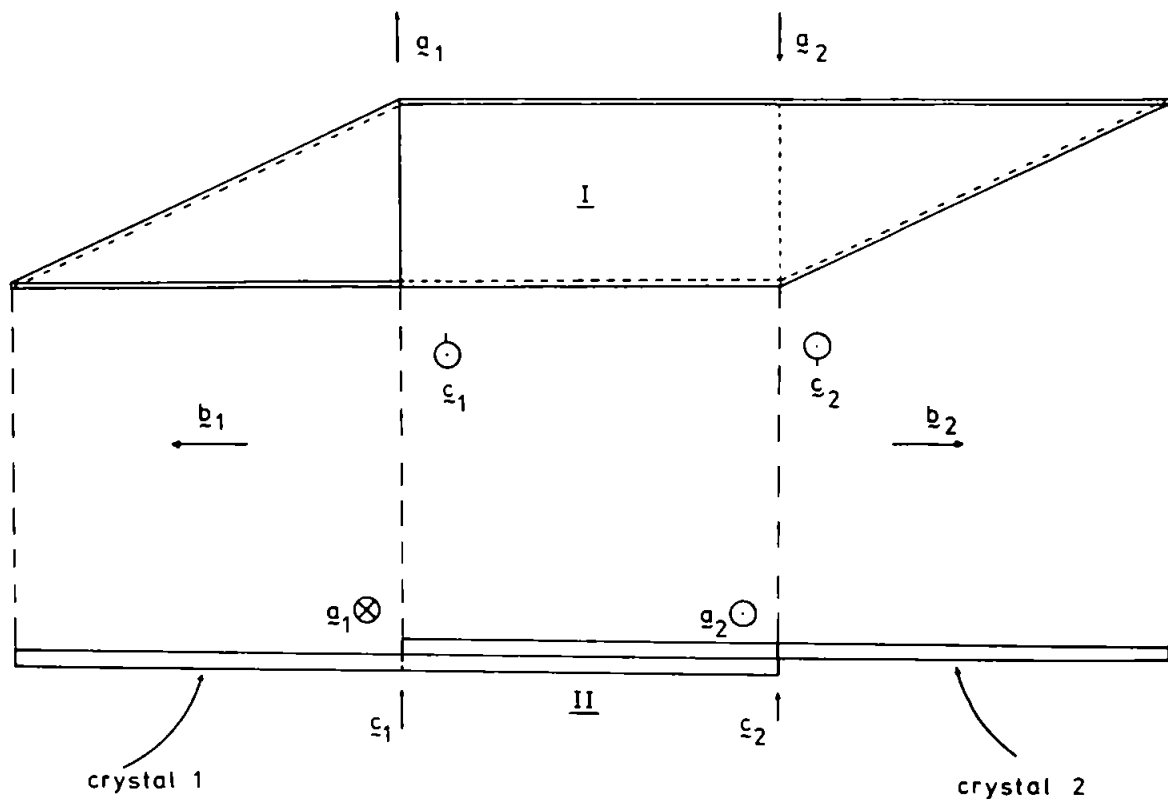


Fig.4.1 Perspective view of the twinning of Carfecillin crystals.



Twinning of crystals of Carfecillin

Fig.4.2

two aspects of one of the twin crystals. The overlapping coincidence plane proved impossible to cleave and it was found necessary to remove the triangular 'tail' of one twin for single crystal X-ray analysis, Fig. 4.2, III.

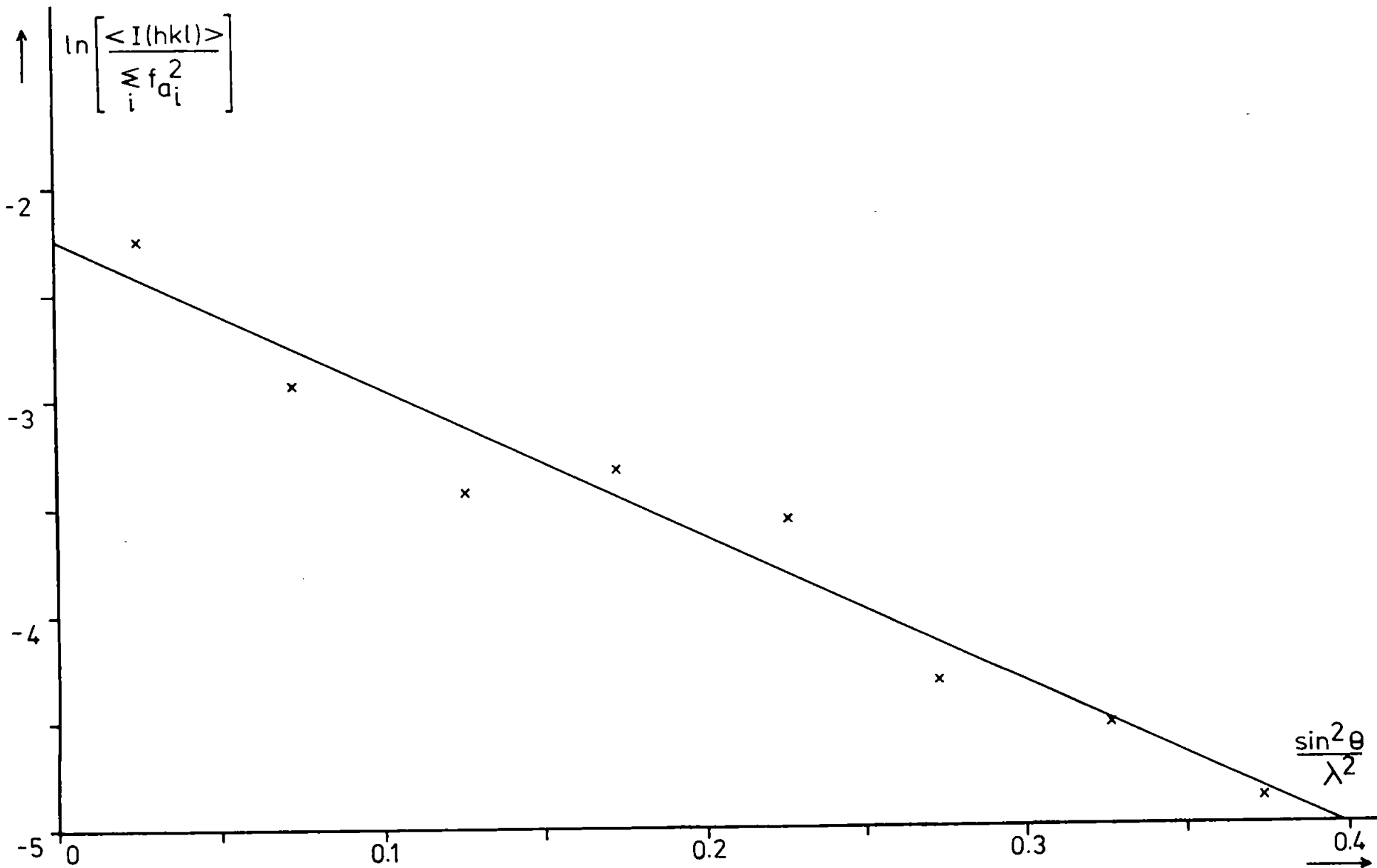
The unit-cell dimensions were determined from zero level equi-inclination Weissenberg photographs, the camera radius was determined from high-angle reflexions from an annealed gold wire. Systematic absences $0k0$, $k = 2n + 1$, (n integer), together with there being two molecules per unit cell, indicated space group $P2_1$ in the monoclinic system, with $a = 8.77(3)$, $b = 6.20(3)$, $c = 21.40(3)$ Å, $\beta = 99.5^\circ$, $V = 1147.65$ Å³, $\mu(\text{CuK}\alpha) = 1476$ m⁻¹.

4.3 Intensity Data Collection and Preliminary Treatment

Data for intensity measurement were obtained by the equi-inclination method on Stoe and Nonius Weissenberg cameras using Ni-filtered CuK α radiation ($\lambda = 1.5418$ Å) and the multiple film technique. The crystals for these measurements were rotated about the b^* reciprocal crystallographic axis with the $(\bar{1} 0 0)$ face of the crystal parallel to the rotation axis. The x-ray films showed some reduction in intensity of reflexion at high $\sin \theta$ after crystals had prolonged exposure to X-rays, 5 different crystals of very similar dimensions were used for collection of intensity data. The intensities of the X-ray reflexions were measured by the Science Research Council microdensitometer at Daresbury. A total of 1208 reflexions were of measurable intensity.

A Wilson Plot (ref Ch.1, §1.11) was used to estimate an overall scale factor and isotropic temperature factor to place the $|F_o(hkl)|$ data on an absolute scale. Groups of reflexions, within a shell of the reciprocal reflexion sphere containing ~100 reflexions were chosen omitting those with Miller indices containing only 0's or 1's, since they are close to the reciprocal origin, and thus

Fig. 4.3 Wilson Plot for Carfecillin



affected by the physical constraints of intensity measurement related to the proximity of the reciprocal origin, extinction and camera back stop interference. Such shells were described by radii lying between ha^* values. Computation of $(\sin^2\theta)/\lambda^2$ for each reflexion resulted in the following distribution of reflexions within each shell;

$(\sin^2\theta)/\lambda^2$	No. of reflexions with h, k or l \neq 0 or 1	$\langle I(hkl) \rangle$
0 - 0.05	111	357.2
0.05 - 0.10	198	179.2
0.10 - 0.15	237	108.7
0.15 - 0.20	251	121.1
0.20 - 0.25	177	96.5
0.25 - 0.30	110	44.8
0.30 - 0.35	68	36.3
0.35 - 0.40	26	25.8

A plot of $\ln \left(\frac{\langle I(hkl) \rangle}{N \sum_{i=1} f_{a_i}^2} \right)$ against

$(\sin^2\theta)/\lambda^2$ is given in Fig. 4.3, where f_{a_i} is the atomic scattering factor for the i^{th} atom at rest in the unit cell containing N atoms. The measured gradient (-6.875 = -2B) resulted in an estimated isotropic temperature factor $B = 3.5 \text{ \AA}^2$ and an overall scale factor of 0.325, given by $\sqrt{e^{-2.25}}$, where the exponent is the intercept when $(\sin^2\theta)/\lambda^2 = 0$.

4.4 Structure Determination

The major computations were carried out with the SHELX program. Initial determination of the sulphur atom position was by means of a Patterson function of the form given in Eqn. 1.60, which, upon symmetry reduction in the monoclinic system, becomes

$$P(u,v,w) = \frac{4}{V} \sum_{(hkl)} [|F(hkl)|^2 \cos 2\pi (hu + \ell w) + |F(\bar{h}k\ell)|^2 \cos 2\pi (hu - \ell w)] \cos 2\pi kv \quad \dots \text{Eqn. 4.1}$$

The equivalent positions in the space group $P2_1$ are (x,y,z) and $(-x, \frac{1}{2}+y, -z)$, resulting in expected Patterson peaks at

$$\text{and } \left. \begin{aligned} (u_1, v_1, w_1) &= (2x, \frac{1}{2}, 2z) \\ (u_2, v_2, w_2) &= (-2x, \frac{1}{2}, -2z) \end{aligned} \right\} \dots \text{Eqns. 4.2}$$

ie. peaks at $(2x, 2z)$ and $(1-2x, 1-2z)$ on the $v = \frac{1}{2}$ section, corresponding to the centrosymmetric nature of the Patterson function.

A sharpened Patterson function; in this instance performed by replacing the coefficient $|F(hkl)|^2$ in Eqn. 4.1 by $|E(hkl)| \cdot |F(hkl)|$, where $E(hkl)$ is the normalised structure factor given by Eqn. 1.66; resulted in values for x and z , consistent with Eqns. 4.2, of,

$$\left. \begin{aligned} x &= 0.2648 \\ z &= 0.1501 \end{aligned} \right\} \dots \text{Eqns. 4.3}$$

with the y value chosen as zero for convenience.

Electron density Fourier synthesis was carried out using reflexions initially phased upon the sulphur atom alone using the expression

$$\rho(x,y,z) = \frac{4}{V} \left\{ \begin{aligned} &\sum_{\substack{hkl \\ (k=2n)}} [|F(hkl)| \cos 2\pi (hX + \ell Z) \cos (2\pi kY - \alpha(hkl)) \\ &+ |F(\bar{h}k\ell)| \cos 2\pi (-hX + \ell Z) \cos (2\pi kY - \alpha(\bar{h}k\ell))] \\ &- \sum_{\substack{hkl \\ (k=2n+1)}} [|F(hkl)| \sin 2\pi (hX + \ell Z) \sin (2\pi kY - \alpha(hkl)) \\ &+ |F(\bar{h}k\ell)| \sin 2\pi (-hX + \ell Z) \sin (2\pi kY - \alpha(\bar{h}k\ell))] \end{aligned} \right\} \dots \text{Eqn. 4.4}$$

where $\alpha(hkl)$ is the phase of $F(hkl)$ given by

$$\alpha(hkl) = \tan^{-1} \left(\frac{B}{A} \right) \dots \text{Eqn. 4.5}$$

where

$$\text{and } \left. \begin{aligned} A &= 2 \cos 2\pi \left(hx + lz + \frac{k}{4} \right) \cos 2\pi \left(ky - \frac{k}{4} \right) \\ B &= 2 \cos 2\pi \left(hx + lz + \frac{k}{4} \right) \sin 2\pi \left(ky - \frac{k}{4} \right) \end{aligned} \right\} \dots \text{ Eqns. 4.6}$$

and x , y and z are the phasing atom co-ordinates. However, interpretation of the resultant map proved difficult on two accounts.

Firstly, by the nature of Eqns. 4.6, phasing on an atom placed on $y = 0$, results in the calculated phase, $\alpha(hk\ell)$, having a value of $-\frac{k\pi}{2}$. Any arbitrary value given to y , results in the same effective value of $\alpha(hk\ell)$, since a change in y represents a shift of origin along the y axis; the origin itself being arbitrary and fixed only by choice. Thus, Eqn. 4.4 reduces in the case of one atom on $y = 0$ to the form

$$\rho(XYZ) = \frac{4}{v} \left\{ \begin{aligned} &\sum_{\substack{hk\ell \\ (k=2n)}} [|F(hk\ell)| \cos 2\pi(hX + \ell Z) \\ &+ |F(\bar{h}k\ell)| \cos 2\pi(-hX + \ell Z)] \cos 2\pi kY \cos n\pi \\ &- \sum_{\substack{hk\ell \\ (k=2n+1)}} [|F(hk\ell)| \sin 2\pi(hX + \ell Z) + |F(\bar{h}k\ell)| \sin 2\pi(-hX + \ell Z)] \\ &\cos 2\pi kY \cos n\pi \end{aligned} \right\} \dots \text{ Eqn. 4.7}$$

from which it can be seen that the Y Fourier component follows a cosine variation and is therefore symmetrical about $Y = 0$, resulting in a mirror plane on $Y = 0$, and thus increasing the symmetry such that it belongs to space group $P2_1/m$. Hence, an atom derived from the first Fourier synthesis appears at x, y, z and $x, -y, z$; choosing one of these positions only, breaks the mirror symmetry and weights any subsequent syntheses toward the reduced $P2_1$ symmetry.

Secondly, due to the plate-like shape of the crystal, early attempts at Fourier synthesis using phases calculated from deduced atomic positions (x, y, z) yielded satellite positions $(-x, \frac{1}{2}-y, -z)$ caused initially by the above centrosymmetric effect. This was enhanced by absorption of diffracted intensity in passing

through extended intra-crystal path lengths for reflexions (hkℓ) with ℓ large compared with h, in contrast with relatively shorter intra-crystal path lengths for h large compared with ℓ: similarly, layers with k large, for all h and ℓ, suffer relatively large absorption, which confined early Fourier syntheses to a dominance of low order k reflexions with the result that the pseudo mirror symmetry was not easily removed. The anomalous behaviour was overcome by the application of the numerical absorption correction, based on the SHELX 'ABSC' routine, to the observed data.

Fig. 4.4 shows the progress of the electron density synthesis using absorption corrected data; where the symbols ● and ○ describe respectively those atoms used in the synthesis and those derived from it. C(2) derived from synthesis A appeared as two identical strong peaks directly above and below S(1) when viewed along the \underline{b} axis at $y \approx \pm \frac{1}{4}$, however, the nature of the Y component in Eqn. 4.7 together with a predominance of low order k values at this early stage led to doubt concerning the validity of this peak. Indeed a trial synthesis using C(2) on $y = -\frac{1}{4}$ proved intractable when compared with inter-atomic vector peaks in the Patterson map. The Patterson map, however, revealed a peak at (0, 0.3, 0) ie. directly above S(1), as in the case of synthesis A, but indicating a y co-ordinate of ± 0.3 . Choosing $y = -0.3$, successfully broke the mirror symmetry in A and produced synthesis B, from which, part of the β lactam could be derived. Completion of the penicillin nucleus was achieved by synthesis E and the side-chain determination proceeded rapidly, though the benzene rings appeared as unresolved electron density distributions defining the planes of the rings only until the final synthesis using the completed remaining molecule, defined the individual atoms satisfactorily.

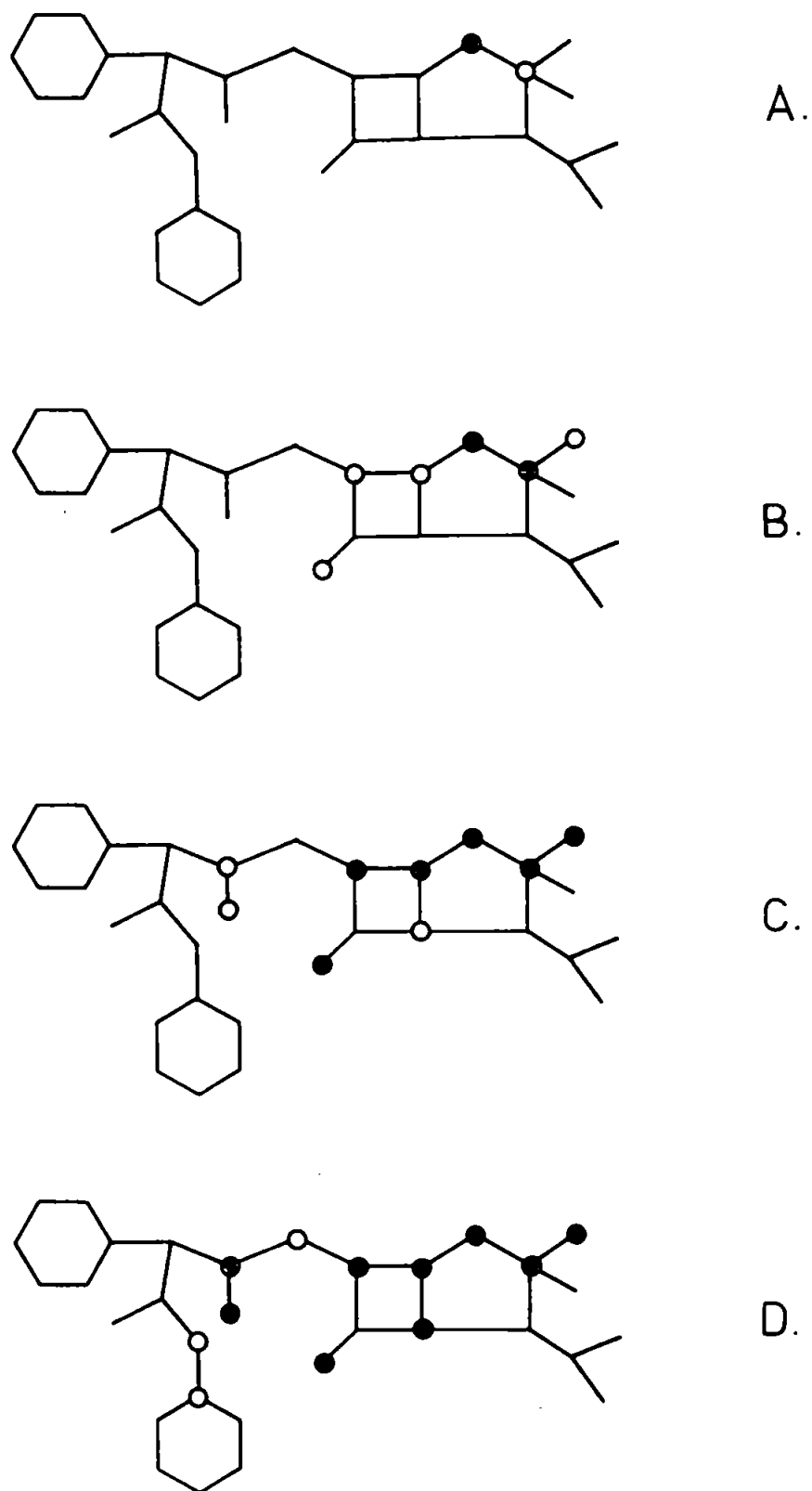
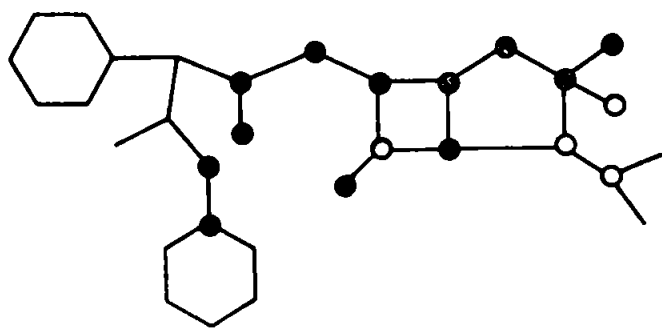
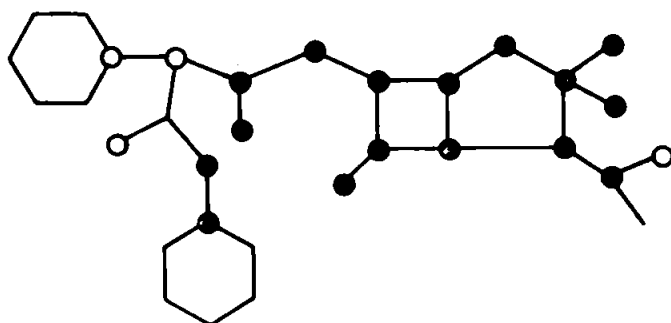


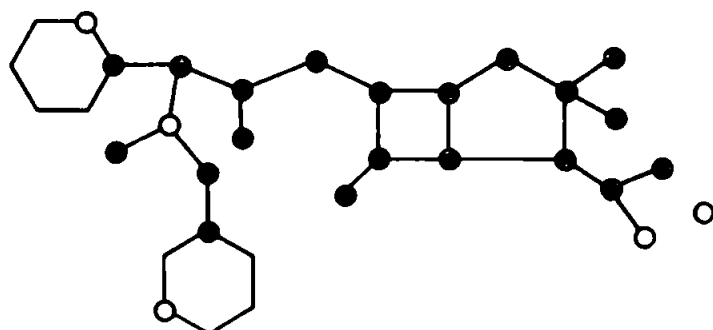
Fig. 4.4. Progress of Electron Density Fourier Synthesis during the Structure determination of Carfecillin



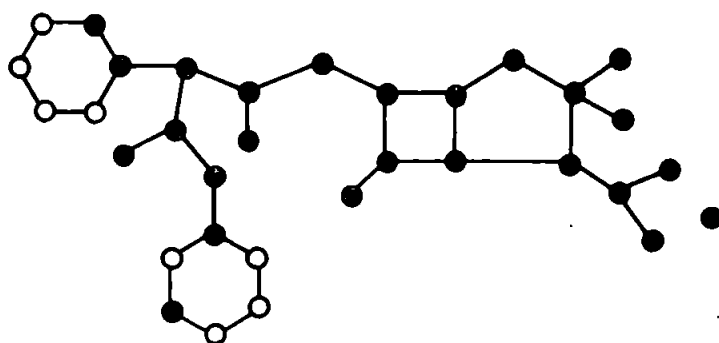
E.



F.



G.



H.

Fig. 4.4 (Continued)

4.5 Structure Refinement

Three cycles of unweighted full matrix least-squares refinement with individual isotropic temperature factors and refinement of scale factors resulted in $R = 0.120$. An $F_o - F_c$ Fourier synthesis showed considerable anisotropic thermal vibrations, associated particularly with the sulphur atom. Anisotropic refinement using the SHELX 'BLOC' to section the structure, (Fig. 4.5), with hydrogen atoms included in the refinement, resulted in $R = 0.095$ after omitting ten low order reflexions suffering from severe extinction. The hydrogen atoms were given isotropic temperature factors fixed at the values of the isotropic temperature factor of the atom to which they are bonded, obtained at the isotropic refinement stage, the bond length being fixed at 1.08 \AA . The benzene rings were refined as rigid hexagons with bond lengths fixed at 1.395 \AA . No further improvement could be made in F_o/F_c correlation probably due to the deterioration of the crystals during prolonged X-ray exposure and the possible inaccuracy inherent in the use of an absorption correction applied to the intensity data based on the assumption that all the crystals used during data collection were of the same dimensions. The observed and calculated structure factors are given in Appendix B (ref. CARF P2(1)).

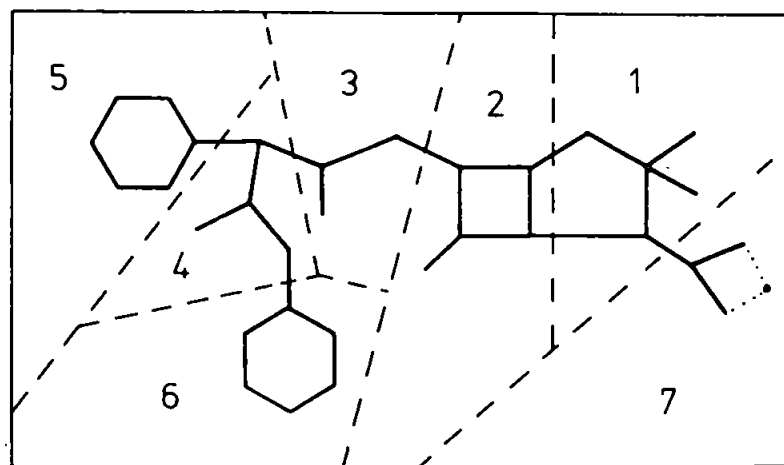
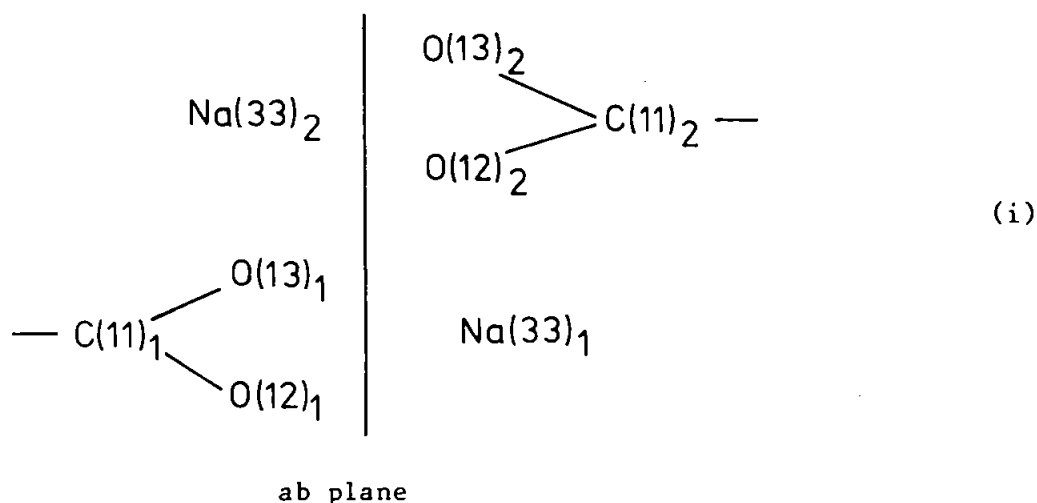


Fig. 4.5 SHELX 'BLOC' sectioning of Carfecillin.

4.6 Discussion

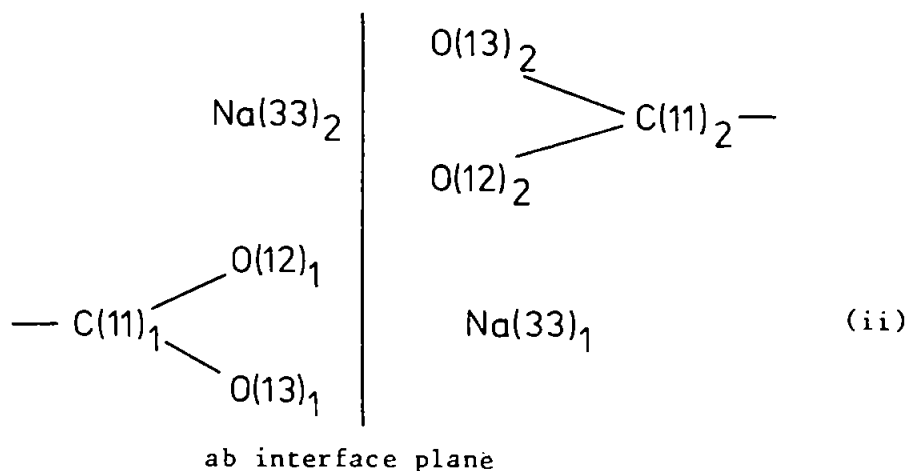
The final co-ordinates of the non-hydrogen atoms are given in Table 4.1. The bond distances and angles are listed with their standard deviations in Tables 4.2 and 4.3. The H atom co-ordinates are given in Table 4.4. Thermal parameters for all atoms are listed in Table 4.5. Fig. 4.6 shows the schematic labelling of the non hydrogen atoms together with inter-atomic distances: Fig. 4.7 shows bond angles. Fig. 4.8 gives a view of the complete unit cell contents along a and Fig. 4.9 shows the structure viewed along b .

With reference to Fig. 4.8, it can be seen that the coincidence ab plane (in the twinned crystal) passes through the ionic O^-Na^+ system where Na(33) lies almost equidistant from $O^-(12)$ and $O(13)$. Upon crystallisation from solution, two molecules could combine in one of two ways, depending on the charge distribution within the carboxylic radical. Each single crystal in the twin has an atomic arrangement thus

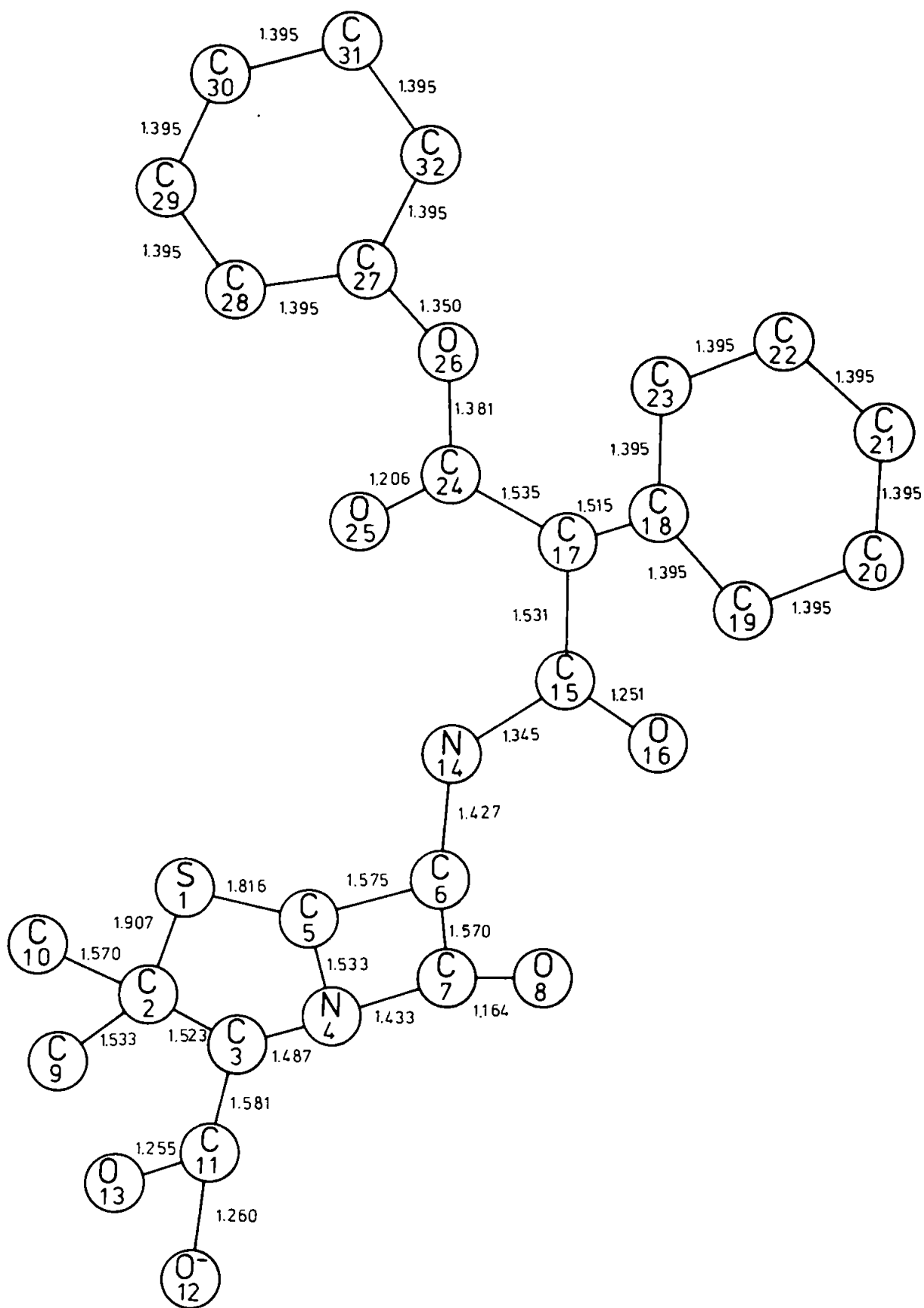


whereas at the crystal interface, the following atom arrangement

provides another orientation for similar crystal growth of the twin.

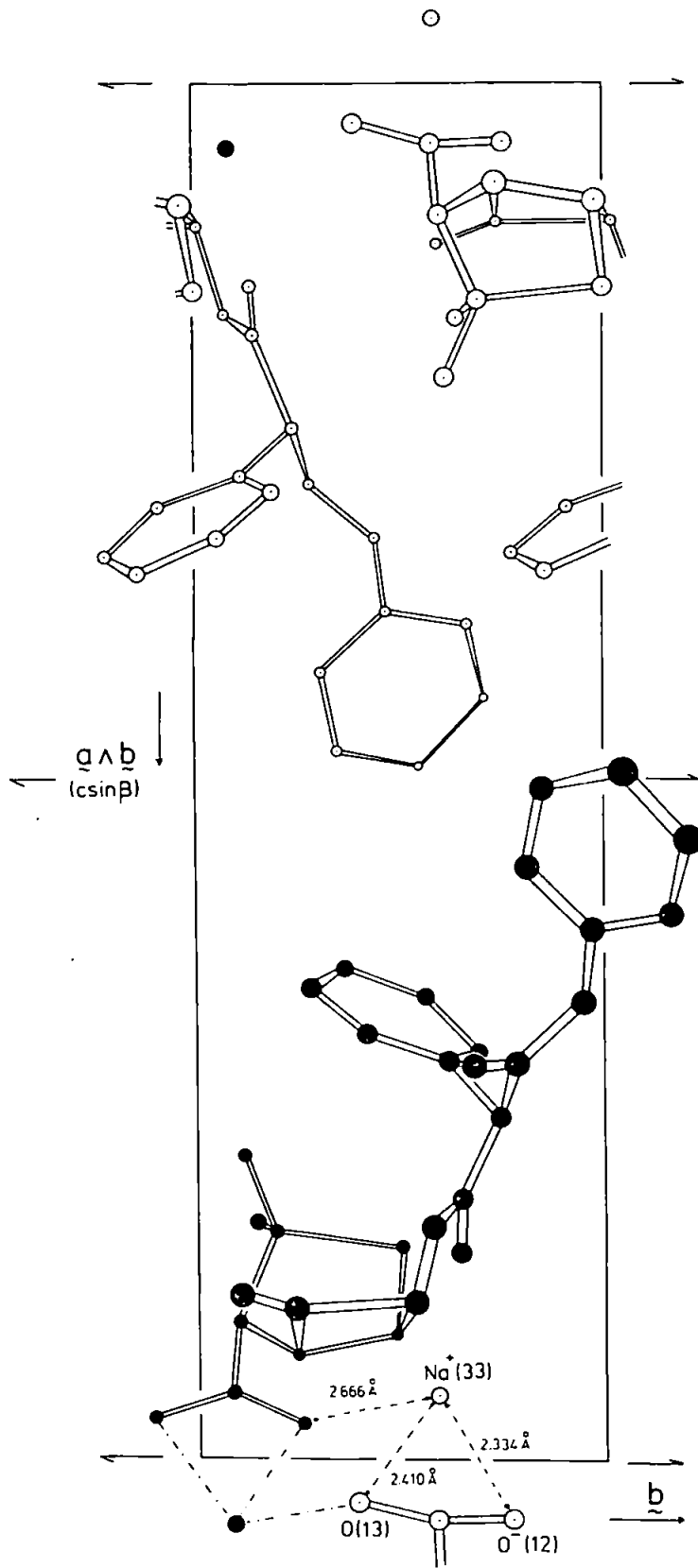


Given the interface arrangement (ii) in the twinned crystal, growth from solution can take place as in Fig. 4.8. Thus, a macro-crystal is seen to develop containing two single crystals oriented 180° with respect to each other about an axis perpendicular to the flat ab face. The nature of this twinning could explain the difficulty encountered when attempting cleavage of the twin along the coincident plane.

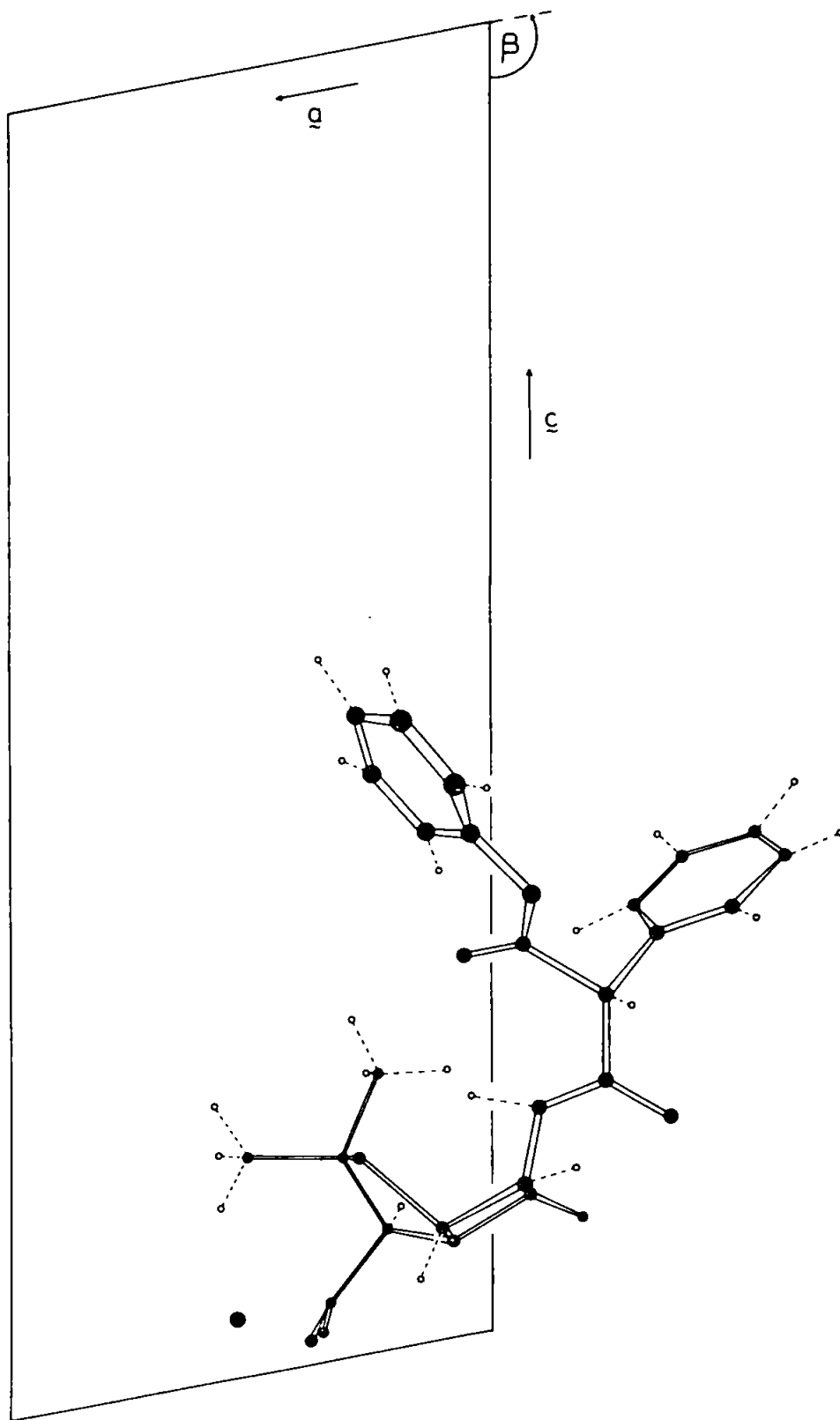


Schematic labelling and inter-atomic distances in Carfecillin

Fig. 4.6



The crystal structure of Carfecillin viewed along a
 Fig. 4.8



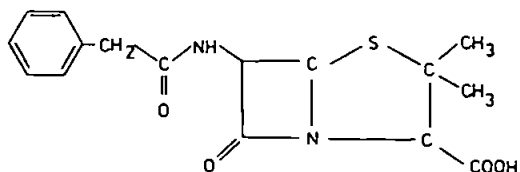
The crystal structure of Carfecillin viewed along b

Fig. 4.9

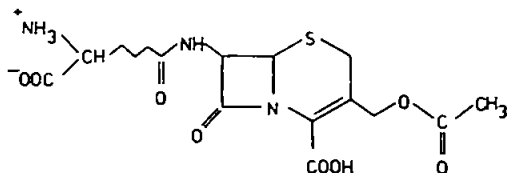
4.7 A comparison of the conformation of the penicillin nucleus
with known penicillins and cephalosporins

Some penicillins and cephalosporins, which have been the subject of detailed and accurate X-ray crystal structural studies, are listed together with their structural formulae.

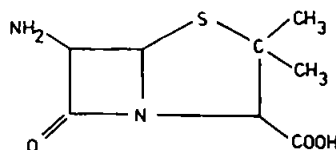
Potassium benzyl penicillin (pen. G)
 (Crowfoot et al 1949, Pitt 1952)
 (ref. no.) **38** , **39**



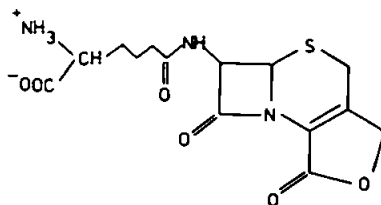
Cephalosporin C
 (Hodgkin, Maslen 1961)
42



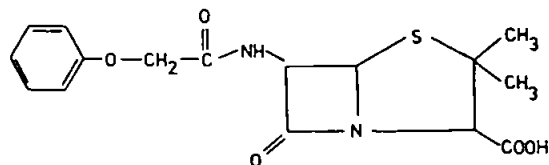
6 - amino - penicillanic acid (6-APA)
 (Diamond 1963)
43



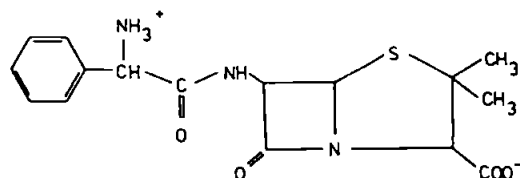
Cephalosporin C₆ (ceph C₆)
 (Diamond 1963)
43



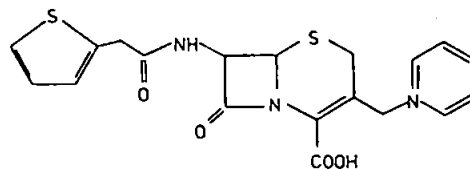
Phenoxyacetylpenicillin (pen-V)
 (Abrahamsson et al 1963)
36



Ampicillin
 (trihydrate James et al 1968)
 (anhydrate Boles, Girven 1976)
41 , **34**

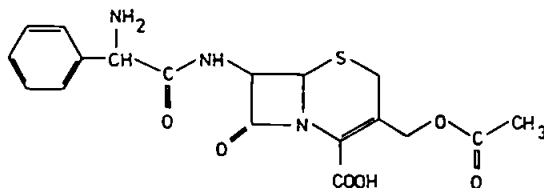


Cephaloridine hydrochloride monohydrate
 (Sweet and Dahl, 1970)
44



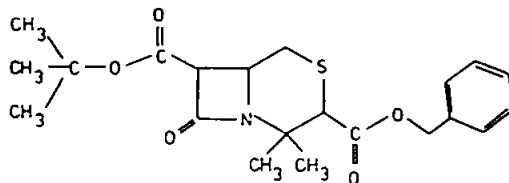
Cephaloglycin
(Sweet and Dahl 1970)

44



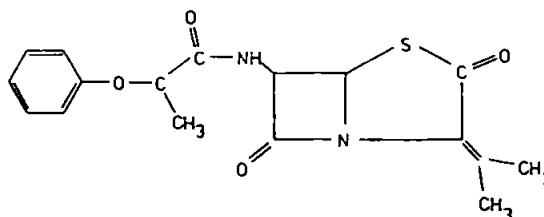
Synthetic β -lactam syn-ceph
(Kalyani and Hodgkin 1970)

45



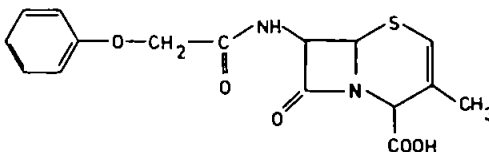
Anhydro - α - phenoxyethyl penicillin (an - pen)
(Simon and Dahl 1970)

46



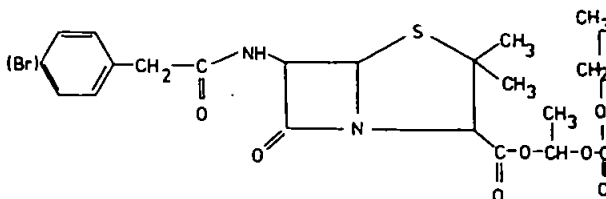
Phenoxyethyl - Δ^2 - deacetoxycephalosporin (2-cephan)
(Sweet and Dahl 1970)

44



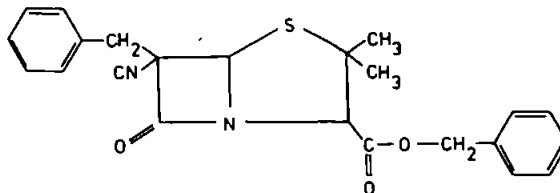
(pBr) benzyl pen. 1'
diethyl carbonate ester
(Cooregh, Palm 1976)

47



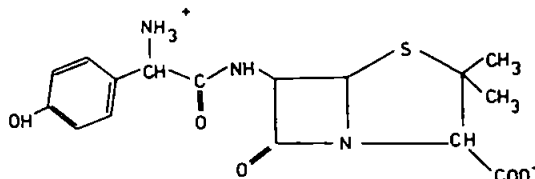
Benzyl 6 α - benzyl 6 β - isocyano - penicillanate
(Girven 1977)

28



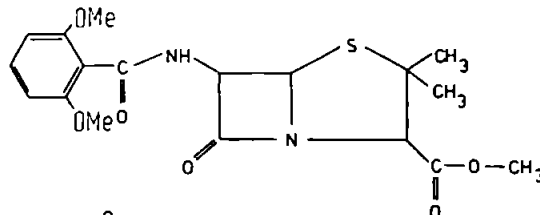
Amoxicillin trihydrate
(Boles, Girven, Gane 1977)

48



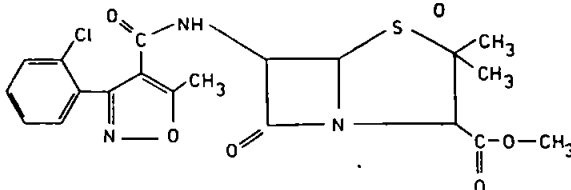
Methicillin methyl ester
(Blanpain, Melebeck, Durant 1977)

49



Cloxacillin Methyl Ester
(Blanpain, Durant 1976)

50



Contrasts between the very different molecular forms of molecules known to inhibit activity amongst bacterial enzymes, indicates that requirements for activity may not be very conformationally restrictive. Penicillin and cephalosporin antibiotics are similar stereo-chemically, not in their detailed dimensions or conformation, but because each, in its β lactam ring, contains a N-CO bond with characteristics differing from the usual amide or unstrained β lactam.

The decrease in amide character and the peculiarly distinctive behaviour of the fused β lactam, would appear to be necessary for any bactericidal action.

It is possible to facilitate a comparison amongst the reported structures by considering the molecular conformation within the penicillin nucleus. Two distinctive features are illustrated in Figs. 4.10 and 4.11.

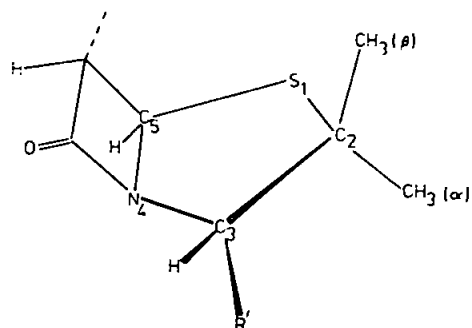
The effect of the constraining power enforced by the β lactam upon the adjoining thiazolidine ring, consisting of five atoms, maintains four of them almost coplanar, with the remaining atom removed from this plane. The non-coplanar atom differs in both Type A and B (Fig 4.10). Particular thiazolidine ring conformations appropriate to the known penicillin structures are shown. In carfecillin, C(3) is 0.42 Å out of the plane defined by S(1), C(5), N(4) and C(2) (Table 4.6). The thiazolidine ring in carfecillin is therefore very similar to that of the thiazolidine ring in phenoxymethyl penicillin, p-bromopenicillin and potassium benzyl penicillin, characterised by C(3) out of the common plane, and thus belongs to type A.

The significance of the chemical and biological activity of β lactam compounds is perhaps centered on the relative geometry of the β lactam nitrogen atom with its three substituents. The perpendicular distances of N(4) from the plane containing its neighbouring atoms appropriate to the known structures are shown in Fig. 4.11. Inclusion

CONFORMATION OF THIAZOLIDINE RINGS OF KNOWN

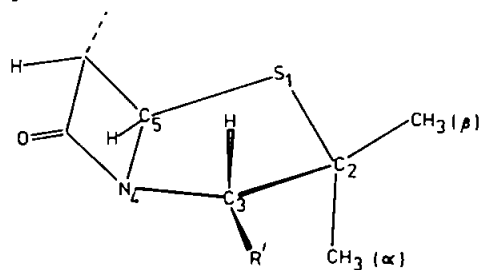
PENICILLIN STRUCTURES

TYPE A



PHENOXYMETHYL - PENICILLIN penicillin V	C ₃ down	0.51 Å
6-AMINO-PENICILLANIC ACID	N ₄ up	0.4 Å
p-BROMOPENICILLIN V	C ₃ down	0.4 Å
POTASSIUM BENZYL PENICILLIN penicillin G	C ₃ down	0.5 Å
(pBr) benzyl pen. 1' diethyl carbonate ester	C ₃ down	0.51 Å

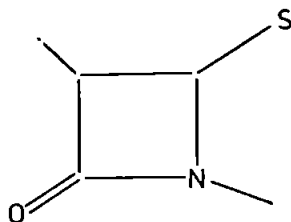
TYPE B



AMPICILLIN ANHYDRATE	C ₂ down	0.71 Å
AMPICILLIN TRIHYDRATE	S ₁ up	0.84 Å
PENICILLIN V SULPHOXIDE	S ₁ up	?
AMOXYCILLIN TRIHYDRATE	S ₁ up	0.83 Å
METHICILLIN METHYL ESTER	S ₁ up	?
CLOXACILLIN METHYL. ESTER	S ₁ up	?

Fig. 4.10

BONDING GEOMETRY AT β -LACTAM NITROGEN IN SOME
PENICILLINS AND CEPHALOSPORINS

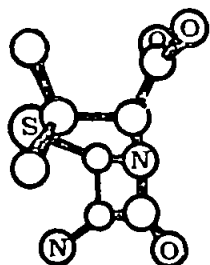


<u>COMPOUND</u>	<u>DISTANCE OF N ATOM FROM PLANE OF 3 SUBSTITUENTS (Å)</u>
METHICILLIN METHYL ESTER	0.44
PEN G	0.40
PEN V	0.40
CLOXACILLIN METHYL ESTER	0.39
(pBr) benzyl pen. 1' diethyl carbonate ester	0.38
AMOXYCILLIN TRIHYDRATE	0.38
AMPICILLIN TRIHYDRATE	0.38
AMPICILLIN ANHYDRATE	0.35
6-APA	0.32
CEPH C _c	0.32
CEPHALORIDINE	0.24
CEPHALOGLYCINE	0.22
AN-PEN	0.42
2-CEPHEM	0.06
SYN-CEPH	0.10

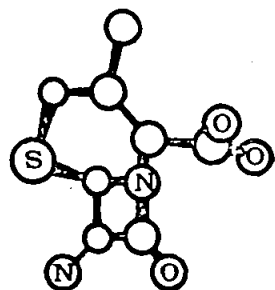
} Inactive

Fig. 4.11

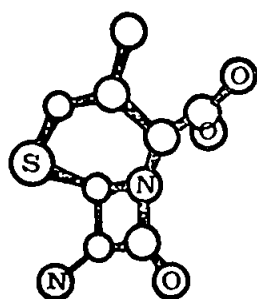
of the 'inactive' compounds must be borrowed with reference to significant differences from the antibiotics. The comparative structural arrangements of the nuclei of penicillins, Δ^3 -cephalosporins and Δ^2 -cephalosporins are given in Fig. 4.12 (a), (b) and (c) respectively.



(a) penicillins



(b) Δ^3 -cephalosporins



(c) Δ^2 -cephalosporins

Fig. 4.12 The comparative structural arrangements of the nuclei of penicillins, Δ^3 & Δ^2 -cephalosporins.

The pyramidal nature of N(4) is described by the deviation of N(4) from the plane defined by C(3), C(5) and C(7). In carfecillin, N(4) is 0.47 Å out of this plane; a similar value to that for methicillin methyl ester (0.44 Å), but somewhat greater than a typical distance of 0.35 Å for reported bactericidally active β lactam antibiotics. N(4) is also significantly out of the plane of the remaining β lactam constituents C(5), C(6) and C(7) being 0.28 Å distant , (Table 4.6).

The following chapter discusses the side-chain configuration in carfecillin, both in the crystalline state and in solution, forming a correlation between side-chain configurations of penicillin derivatives of known structure and observed H^1 n.m.r. and circular dichroism characteristics associated with those configurations.

Table 4.1 Final co-ordinates obtained from least-squares refinement .

Co-ordinates are given as fractions of cell edges $\times 10^4$. Standard deviations in parentheses are with respect to the last figures given.

	x	y	z
S(1)	2614(6)	0(0)	1492(3)
C(2)	2842(23)	-3049(42)	1580(10)
C(3)	2004(22)	-3992(37)	960(9)
N(4)	670(17)	-2555(26)	733(7)
C(5)	958(22)	-143(47)	860(9)
C(6)	-712(23)	100(40)	1032(10)
C(7)	-712(28)	-2592(43)	1009(11)
O(8)	-1514(18)	-3948(33)	1146(9)
C(9)	2097(23)	-3847(38)	2137(8)
C(10)	4622(21)	-3547(33)	1695(9)
C(11)	3078(22)	-4157(40)	437(8)
O(12)	3325(18)	-6048(24)	263(6)
O(13)	3440(15)	-2410(22)	204(6)
N(14)	-799(17)	771(27)	1663(7)
C(15)	-2133(20)	1481(37)	1822(8)
O(16)	-3398(14)	1419(22)	1454(6)
C(17)	-2141(21)	2461(35)	2478(8)
C(18)	-3141(13)	1142(24)	2848(7)
C(19)	-2605(13)	-878(24)	3073(7)
C(20)	-3491(13)	-2141(24)	3416(7)
C(21)	-4913(13)	-1383(24)	3536(7)
C(22)	-5448(13)	638(24)	3311(7)
C(23)	-4562(13)	1900(24)	2968(7)
C(24)	-575(25)	2783(45)	2908(9)
O(25)	565(15)	1680(26)	2930(6)
O(26)	-654(16)	4472(25)	3322(7)
C(27)	441(17)	4721(25)	3840(6)
C(28)	1219(17)	6686(25)	3936(6)
C(29)	2253(17)	7048(25)	4495(6)
C(30)	2509(17)	5445(25)	4958(6)
C(31)	1730(17)	3480(25)	4862(6)
C(32)	696(17)	3118(25)	4303(6)
Na(33)	4871(8)	881(13)	457(3)

Table 4.2 Bond lengths and their standard deviations (Å) after final least-squares refinement.

S(1) -	C(2)	1.907(26)
S(1) -	C(5)	1.816(19)
C(2) -	C(3)	1.523(28)
C(2) -	C(9)	1.533(31)
C(2) -	C(10)	1.570(27)
C(3) -	N(4)	1.487(25)
C(3) -	C(11)	1.580(29)
N(4) -	C(5)	1.533(33)
N(4) -	C(7)	1.434(30)
C(5) -	C(6)	1.576(30)
C(6) -	C(7)	1.570(36)
C(6) -	N(14)	1.427(26)
C(7) -	O(8)	1.164(32)
C(11) -	O(12)	1.260(29)
C(11) -	O(13)	1.255(28)
N(14) -	C(15)	1.345(24)
C(15) -	O(16)	1.251(19)
C(15) -	C(17)	1.530(26)
C(17) -	C(24)	1.535(26)
C(17) -	C(18)	1.515(24)
C(18) -	C(19)	1.395(20)
C(18) -	C(23)	1.395(18)
C(19) -	C(20)	1.395(20)
C(20) -	C(21)	1.395(18)
C(21) -	C(22)	1.395(20)
C(22) -	C(23)	1.395(20)
C(24) -	O(25)	1.206(28)
C(24) -	O(26)	1.381(29)
O(26) -	C(27)	1.350(18)
C(27) -	C(28)	1.395(21)
C(27) -	C(32)	1.395(19)
C(28) -	C(29)	1.395(17)
C(29) -	C(30)	1.395(19)
C(30) -	C(31)	1.395(21)
C(31) -	C(32)	1.395(17)
Na(33)....	O(12)	2.334
Na(33)....	O(13)	2.410

Table 4.3 Bond angles ($^{\circ}$) and their standard deviations.

C(5)	-	S(1)	-	C(2)	94.8(1.1)
C(3)	-	C(2)	-	S(1)	105.4(1.5)
C(9)	-	C(2)	-	S(1)	110.3(1.6)
C(9)	-	C(2)	-	C(3)	110.3(1.8)
C(10)	-	C(2)	-	S(1)	107.2(1.5)
C(10)	-	C(2)	-	C(3)	112.7(1.8)
C(10)	-	C(2)	-	C(9)	110.8(1.6)
N(4)	-	C(3)	-	C(2)	107.2(1.7)
C(11)	-	C(3)	-	C(2)	112.5(1.6)
C(11)	-	C(3)	-	N(4)	109.6(1.5)
C(5)	-	N(4)	-	C(3)	115.4(1.4)
C(7)	-	N(4)	-	C(3)	121.9(1.7)
C(7)	-	N(4)	-	C(5)	94.0(1.6)
N(4)	-	C(5)	-	S(1)	105.5(1.4)
C(6)	-	C(5)	-	S(1)	118.7(1.4)
C(6)	-	C(5)	-	N(4)	90.1(1.6)
C(7)	-	C(6)	-	C(5)	83.9(1.8)
N(14)	-	C(6)	-	C(5)	116.6(1.6)
N(14)	-	C(6)	-	C(7)	108.6(1.8)
C(6)	-	C(7)	-	N(4)	90.0(1.7)
O(8)	-	C(7)	-	N(4)	134.6(2.5)
O(8)	-	C(7)	-	C(6)	135.4(2.3)
O(12)	-	C(11)	-	C(3)	115.0(1.9)
O(13)	-	C(11)	-	C(3)	116.5(2.0)
O(13)	-	C(11)	-	O(12)	128.1(1.9)
C(15)	-	N(14)	-	C(6)	121.3(1.4)
O(16)	-	C(15)	-	N(14)	123.3(1.6)
C(17)	-	C(15)	-	N(14)	119.8(1.4)
C(17)	-	C(15)	-	O(16)	116.9(1.6)
C(24)	-	C(17)	-	C(15)	117.6(1.6)
C(18)	-	C(17)	-	C(15)	110.9(1.6)
C(18)	-	C(17)	-	C(24)	107.1(1.4)
C(19)	-	C(18)	-	C(17)	118.3(1.3)
C(23)	-	C(18)	-	C(17)	121.7(1.4)
C(23)	-	C(18)	-	C(19)	120.0(1.3)
C(18)	-	C(19)	-	C(20)	120.0(1.2)
C(21)	-	C(20)	-	C(19)	120.0(1.3)
C(22)	-	C(21)	-	C(20)	120.0(1.3)
C(23)	-	C(22)	-	C(21)	120.0(1.2)
C(18)	-	C(23)	-	C(22)	120.0(1.3)
O(25)	-	C(24)	-	C(17)	127.1(2.1)
O(26)	-	C(24)	-	C(17)	110.4(1.8)
O(26)	-	C(24)	-	O(25)	122.3(1.8)
C(27)	-	O(26)	-	C(24)	120.6(1.5)
C(28)	-	C(27)	-	O(26)	119.0(1.3)
C(32)	-	C(27)	-	O(26)	120.7(1.4)
C(32)	-	C(27)	-	C(28)	120.0(1.1)
C(27)	-	C(28)	-	C(29)	120.0(1.3)
C(30)	-	C(29)	-	C(28)	120.0(1.4)
C(31)	-	C(30)	-	C(29)	120.0(1.1)
C(32)	-	C(31)	-	C(30)	120.0(1.3)
C(27)	-	C(32)	-	C(31)	120.0(1.4)

Table 4.4 Co-ordinates of hydrogen atoms. Co-ordinates are given as fractions of cell edges $\times 10^4$. The heavy atom associated with each hydrogen atom is also given. Standard deviations in parentheses are with respect to the last figures given.

	x	y	z
H(C3)	1664(22)	-5618(37)	1055(9)
H(C5)	1248(22)	1067(47)	536(9)
H(C6)	-1616(23)	1097(40)	777(10)
H(C9)(1)	2666(23)	-3143(38)	2576(8)
H(C9)(2)	2251(23)	-5576(38)	2155(8)
H(C9)(3)	878(23)	-3474(38)	2071(8)
H(C10)(1)	5164(21)	-2925(33)	1315(9)
H(C10)(2)	4733(21)	-5282(33)	1713(9)
H(C10)(3)	5178(21)	-2866(33)	2139(9)
H(N14)	386(17)	623(27)	1896(7)
H(C17)	-2552(21)	4065(35)	2345(8)
H(C19)	-1504(13)	-1465(24)	2980(7)
H(C20)	-3076(13)	-3705(24)	3590(7)
H(C21)	-5599(13)	-2360(24)	3802(7)
H(C22)	-6549(13)	1224(24)	3404(7)
H(C23)	-4977(13)	3464(24)	2794(7)
H(C28)	1021(17)	7927(25)	3578(6)
H(C29)	2855(17)	8569(25)	4570(6)
H(C30)	3309(17)	5725(25)	5391(6)
H(C31)	1928(17)	2239(25)	5220(6)
H(C32)	94(17)	1597(25)	4228(6)

Table 4.5 Anisotropic temperature factors are expressed as $\exp [-2\pi^2(U_{11}h^2a^{*2} + U_{22}k^2b^{*2} + U_{33}l^2c^{*2} + 2U_{12}hka^*b^* + 2U_{13}hla^*c^* + 2U_{23}k\ell b^*c^*)]$. Isotropic temperature factors are expressed as $\exp [-2\pi^2U(h^2a^{*2} + k^2b^{*2} + l^2c^{*2})]$. The units of U_{ij} are $\text{\AA}^2 \times 10^4$. Standard deviations in parentheses are with respect to the last figures given.

	U or U_{11}	U_{22}	U_{33}	U_{23}	U_{13}	U_{12}
S(1)	201(24)	137(43)	268(30)	-39(28)	4(20)	37(27)
C(2)	182(109)	55(169)	268(127)	-78(102)	-28(90)	-68(98)
C(3)	361(114)	1(116)	293(117)	16(102)	-62(95)	-39(102)
H(C3)	164(99)					
N(4)	135(82)	10(103)	171(82)	-51(69)	-65(65)	31(68)
C(5)	203(102)	506(167)	187(116)	216(126)	-51(85)	69(126)
H(C5)	287(118)					
C(6)	260(107)	260(142)	326(136)	-62(117)	120(92)	202(113)
H(C6)	249(111)					
C(7)	308(131)	376(177)	357(141)	-148(119)	-44(106)	-149(125)
O(8)	467(102)	431(124)	904(134)	0(112)	252(95)	-194(103)
C(9)	443(128)	140(127)	181(104)	93(102)	187(94)	-112(114)
H(C9)(1)	270(109)					
H(C9)(2)	270(109)					
H(C9)(3)	270(109)					
C(10)	301(112)	1(133)	339(117)	-50(97)	-6(90)	54(97)
H(C10)(1)	253(126)					
H(C10)(2)	253(126)					
H(C10)(3)	253(126)					
C(11)	387(111)	182(150)	221(99)	20(107)	81(86)	-137(106)
O(12)	624(105)	119(104)	298(85)	21(70)	188(73)	120(76)
O(13)	355(83)	117(92)	212(83)	26(64)	134(66)	-71(65)
N(14)	278(82)	130(108)	211(81)	-45(73)	34(66)	141(73)
H(N14)	215(48)					
C(15)	135(91)	450(155)	131(95)	112(99)	68(74)	89(99)
O(16)	223(64)	78(87)	344(71)	-118(66)	-13(55)	107(63)
C(17)	226(103)	201(139)	180(99)	-152(93)	-28(80)	121(95)
H(C17)	203(57)					
C(18)	142(91)	450(157)	257(106)	-109(117)	63(80)	-42(110)
C(19)	312(117)	318(165)	327(126)	144(109)	102(100)	-36(106)
H(C19)	393(88)					
C(20)	552(161)	484(184)	386(138)	85(128)	-101(117)	-129(137)
H(C20)	393(88)					
C(21)	449(159)	963(245)	390(133)	-151(164)	168(121)	-197(177)
H(C21)	393(88)					
C(22)	292(110)	1073(265)	582(159)	-24(169)	165(112)	49(145)
H(C22)	393(88)					
C(23)	264(116)	436(158)	497(144)	12(125)	94(104)	145(115)
H(C23)	393(88)					
C(24)	294(122)	628(197)	265(116)	-196(126)	38(96)	-43(128)
O(25)	258(75)	510(114)	231(75)	-157(73)	-51(59)	-4(77)
O(26)	370(83)	316(119)	433(93)	-118(79)	-144(70)	13(72)
C(27)	422(131)	697(187)	281(118)	-77(136)	-4(96)	-231(141)
C(28)	467(143)	942(227)	236(117)	-128(127)	-78(100)	-20(148)
H(C28)	452(65)					

(continued)

Table 4.5. (continued)

	U or U ₁₁	U ₂₂	U ₃₃	U ₂₃	U ₁₃	U ₁₂
C(29)	572(155)	798(214)	400(135)	-408(145)	4(116)	-175(152)
H(C29)	452(65)					
C(30)	898(202)	1080(339)	565(192)	120(207)	-207(153)	-425(226)
H(C30)	452(65)					
C(31)	1213(245)	1324(315)	58(116)	294(159)	-126(127)	-382(250)
H(C31)	452(65)					
C(32)	815(204)	464(189)	509(151)	-90(141)	101(133)	-43(154)
H(C32)	452(65)					
Na(33)	336(38)	65(48)	364(43)	-79(36)	133(31)	-9(34)

Table 4.6. Planarity of the penicillin nucleus in carfecillin.

Equations expressed as $Px + Qy + Rz = S$ in direct space; with x , y and z given as fractions of cell edges a , b and c respectively.

	P	Q	R	S	Deviations (Å) of atoms from planes	
(a)	Planarity of the thiazolidine ring					
	-0.3810	-0.0072	1	0.0496	S(1)	0.00
					C*(2)	0.06
					C*(3)	0.42
					N(4)	0.00
					C(5)	0.00
(b)	Pyramidal nature of N(4)					
	0.0365	0.0359	1	0.0890	C(3)	0.00
					N*(4)	0.47
					C(5)	0.00
					C(7)	0.00
(c)	Deviation of N(4) and O(8) from the plane of the remaining β lactam constituents					
	0.1018	-0.0085	1	0.0958	N*(4)	0.28
					C(5)	0.00
					C(6)	0.00
					C(7)	0.00
					O*(8)	0.14

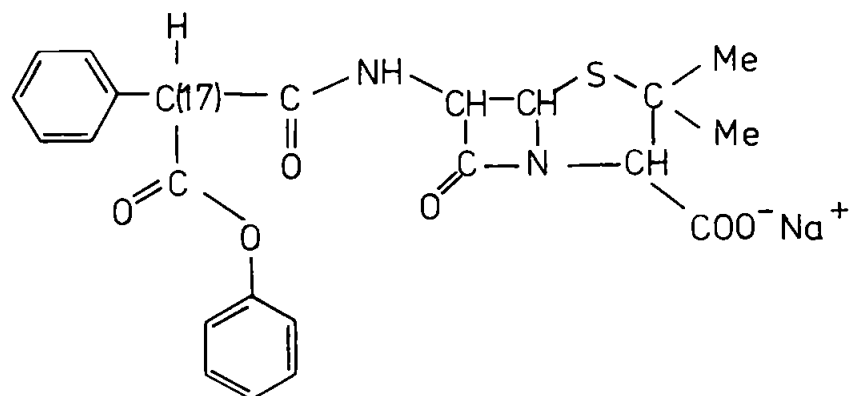
* Atoms not used to define the planes.

CHAPTER 5

The Configuration and Conformation of the side-chain substituents in Penicillin Derivatives

5.1 Introduction

The crystal structure of the phenyl ester of carbenicillin, discussed in Chapter 4, is used to facilitate a comparison of the configuration about C(17) with other penicillin derivatives of known crystal structure to form a characterisation and evaluation of the spectroscopic differences evident in the H^1 nuclear magnetic resonance and circular dichroism spectra of the respective side-chain diastereoisomeric configurations.



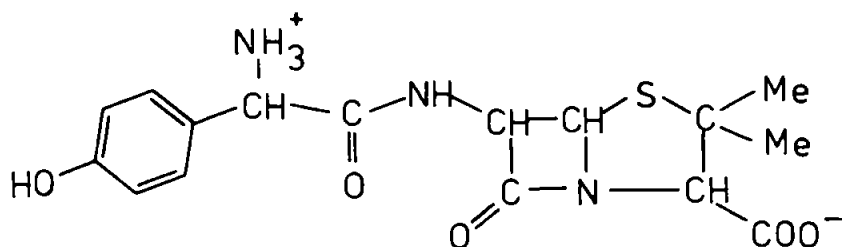
5.2 Side Chain Configuration and Associated Nuclear Magnetic Resonance

Configuration of the side chain about C(17) is shown to notably affect the H^1 n.m.r. resonance from the β lactam protons $H(C(5))$ and $H(C(6))$. In the crystalline solid state, the configuration of the

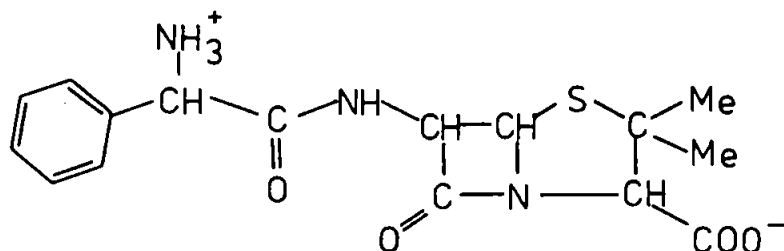
methyl and ethyl esters of carbenicillin, as in the structure of the phenyl ester of carbenicillin (ref. Ch.4), when examined by n.m.r. in fresh solution, ($t = 0$), is characterised by a singlet β lactam proton peak (Traces 1(a) and 2(a)). However, after about 30 minutes a steady state is reached (at 35°C) in D_2O solution, characterised by four β lactam proton peaks superimposed upon the singlet which in turn suffers a reduction in intensity, for the methyl and ethyl esters, (Traces 1(b), 2(b), 3(a) and 3(b)), but this effect is not apparent in the case of the phenyl ester (Traces 4(a) and 4(b)). To investigate the cause of this effect; its association with configuration about C(17): and the apparently anomalous behaviour of the phenyl ester, H^1 n.m.r. studies of the two diastereoisomers of amino-hydroxybenzyl penicillin⁴⁰, amino-phenylacetamido penicillanic acid³⁴ and a tyrosyl penicillin have been made.

The three penicillin derivatives amino-hydroxybenzyl penicillin (i), amino-phenylacetamido penicillanic acid (ii), and the tyrosyl penicillin (iii) are known to crystallise, under different conditions,

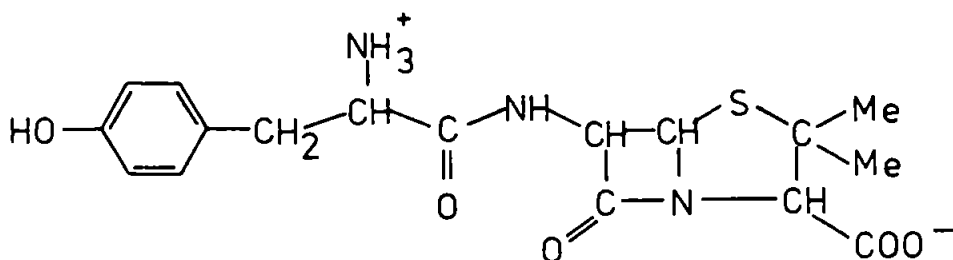
(i) Amino-hydroxybenzyl penicillin



(ii) Amino-phenylacetamido penicillanic acid



(iii) the tyrosyl penicillin



to accommodate the side chain in either the D or L forms, (N.B. D and L being assigned by optical measurements from the two C(17) configurational epimers, the penicillin nuclei remaining unchanged). These configurations are stable in solution at room temperature and no epimerisation of the two diastereoisomers takes place. Thus, the H^1 n.m.r. spectra of these compounds in the side chain D and L forms have been used to assert that the feature distinguishing the diastereoisomers of each compound is the association of a single β lactam proton peak with the side chain D form and a system of four peaks with the side chain L form (Traces 5(a), 6(a), 7(a), 8(a), 8(b), 9(a), 9(b), 10(a)). This characteristic phenomenon was demonstrated to be purely intra-molecular by determining that there was no dependence of the β lactam proton resonance upon concentration (Traces 5(b), 6(b), 7(b), 10(b), (1), (2), (3) & (4) [each Trace is shown with a scale expansion illustrating no observed change in the resonance feature at very low concentration]).

The spectra were obtained by using a Perkin-Elmer R12b nuclear magnetic resonance spectrometer with D_2O as solvent, and $NaOD/D_2O$ to form the sodium salt of the amino compounds. The spectrum produced by n.m.r. due to the β lactam protons, is conventionally described as an AB system:^{51, 52} one in which two protons are coupled together, having a coupling constant J comparable to the chemical shift δ which could be introduced by the comparative shielding of one proton by environmental effects imposed by chemical groups and their position relative to the proton within the molecular configuration.

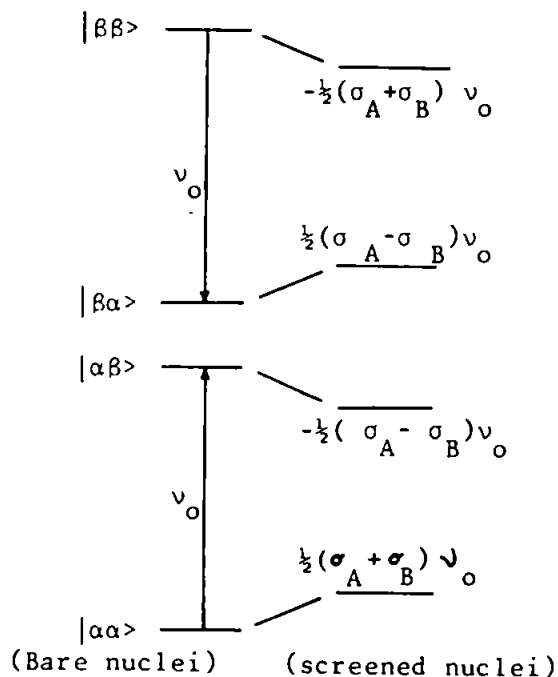
The spin Hamiltonian for the AB spectrum is given by:-

$$H = -\nu_0 (1 - \sigma_A) I_{ZA} - \nu_0 (1 - \sigma_B) I_{ZB} + J I_A \cdot I_B \quad \dots \text{Eqn. 5.a}$$

where ν_0 is the frequency at which resonance takes place for the bare proton above; σ is the screening constant which is isotropic due to the exclusive use of liquids for the purpose of n.m.r. measurements; I is the nuclear spin with I_Z as its Z component. The Hamiltonian describes the two Zeeman energies for the protons A and B in the molecular environment, combined with the spin-spin coupling. Each proton can have two spin states $|\alpha\rangle$ and $|\beta\rangle$; the combined system can be described using the set of basis functions,

$$\phi_1 = |\alpha\alpha\rangle, \phi_2 = |\alpha\beta\rangle, \phi_3 = |\beta\alpha\rangle \text{ and } \phi_4 = |\beta\beta\rangle.$$

The term $\nu_0 (1 - \sigma) I_Z$ describes the chemical shift δI_Z , where $\delta_A I_{ZA}$, splits ϕ_1 from ϕ_3 and ϕ_4 , and $\delta_B I_{ZB}$ splits ϕ_1 from ϕ_2 and ϕ_4 in terms of frequency units.



The operator $I_A \cdot I_B$ can be split into two parts

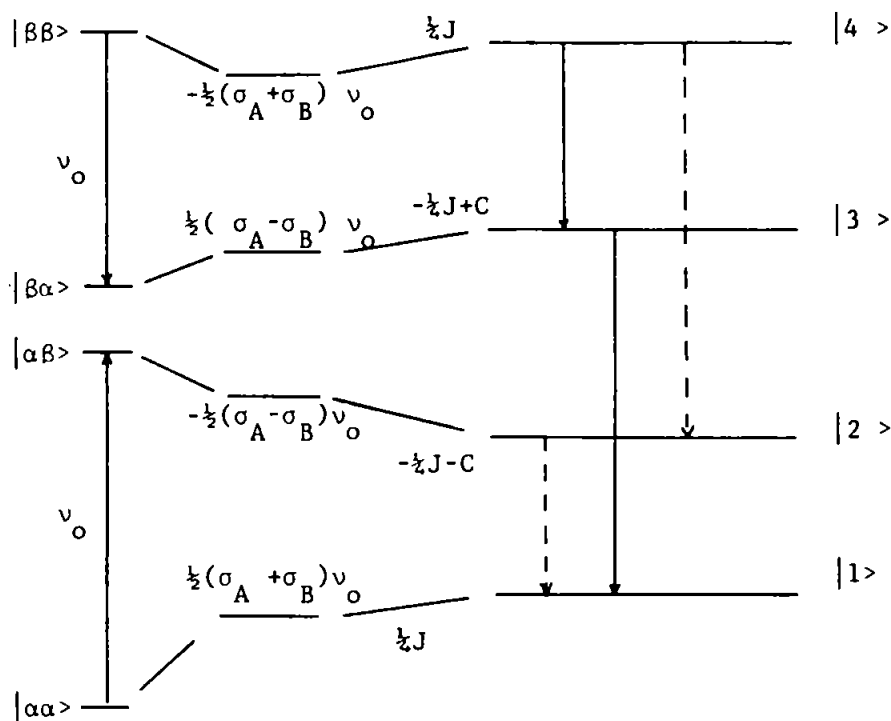
$$I_A \cdot I_B = I_{ZA} I_{ZB} + \frac{1}{2} (I_A^+ I_B^- + I_A^- I_B^+) \quad \dots \text{Eqn. 5.b}$$

where

$$I^+ |\alpha\rangle = 0, \quad I^+ |\beta\rangle = |\alpha\rangle$$

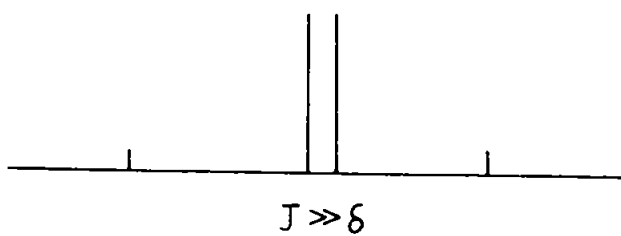
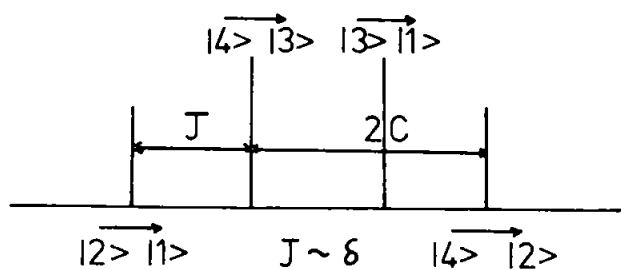
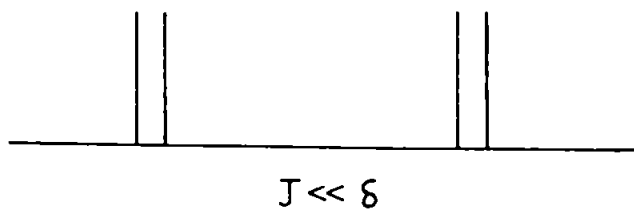
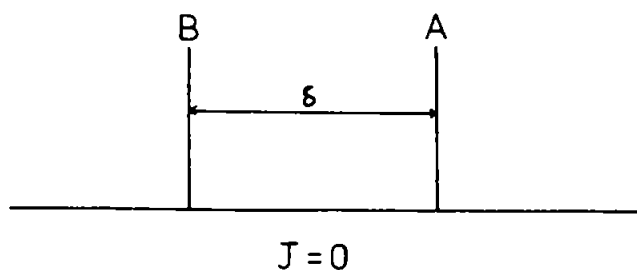
$$I^- |\alpha\rangle = |\beta\rangle \text{ and } I^- |\beta\rangle = 0. \quad \dots \text{Eqns. 5.c}$$

The effect of $\frac{1}{2} (I_A^+ I_B^- + I_A^- I_B^+)$ is to mix ϕ_2 with ϕ_3 and produces a further change of frequency of these states by, $\pm C$ respectively where $C = \frac{1}{2} \sqrt{(J^2 + \delta^2)}$. The term $I_{ZA} I_{ZB}$ shifts the levels of all states (in frequency units) by $\pm \frac{1}{4} J$ depending on each $I_Z = \pm \frac{1}{2}$ where $|\alpha\rangle$ has $I_Z = \frac{1}{2}$ and $|\beta\rangle$ has $I_Z = -\frac{1}{2}$.



(Spin-spin coupling)

For varying coupling J , relative to the difference in chemical environment for each proton δ , the spectra appear thus, in which the intensity of each resonance is related to the transition probability.



From this analysis, it can be seen that the spectra of the D forms of the penicillin derivatives correspond to $\delta = 0$, i.e. no difference in the screening tensor σ between the β lactam protons. However, the L forms have spectra corresponding to a chemical shift between the proton resonances of the same order of magnitude as the coupling, or less. The single β lactam proton peak of the fresh solution of methyl and ethyl carbenicillin esters indicates that the compounds crystallise in the configuration corresponding to the D diastereoisomer of other penicillin derivatives. Equilibrium between the two configurations is reached in solution and the mixture of the two gives rise to a superposition of the singlet upon the spin-spin split spectrum.

The phenyl ester of carbenicillin, however, is known from optical measurements, (p. 5.4), to reach equilibrium more rapidly than either the methyl or ethyl esters, yet its n.m.r. spectrum shows no shielding of the β lactam protons with time i.e. the resonance remains a singlet. An explanation of the anomaly is afforded by the consideration of the relative orientation of the phenyl group C(27) C(28) C(29) C(30) C(31) C(32), with respect to the β lactam protons, (H(C(5)) and H(C(6))), Fig. 4.6. Coupling constants and chemical shifts for those compounds showing spin-spin splitting of the β lactam proton resonance are given in Table 5.1

5.3 Relative orientations of the C(17) side-chain substituent in the phenyl ester of carbenicillin

Benzene rings can affect H^1 n.m.r. signals by introducing ring current shifts. When an aromatic ring is within a magnetic field, a current is induced which arises from the circulation of the delocalised π - electrons. This ring current produces a local magnetic field which opposes the externally applied field in the area above and below the plane of the aromatic ring, but reinforces it otherwise. The ring current effect, therefore, can produce magnetic shielding, or

deshielding, of a proton depending upon the aspect of the aromatic ring that is presented to the proton. The geometric form of the region of influence of ring current shifts corresponds to cones whose axes coincide with the direction of the principal symmetry axis. The special case of axial symmetry, in benzene, results in a spherical cone with half-angle $54^{\circ}44'$. The model described is useful for semi-quantitative estimations of the shielding effect due to the phenyl group (C(27), C(28), C(29), C(30), C(31), C(32)) of the β lactam protons (H(C(5)), H(C(6))) in carfecillin, during equilibration.

Relative orientations of the benzene ring with respect to H(C(6)), (the β lactam proton nearest the ring and hence, most likely to suffer shielding), have been calculated for all the substituent positions possible at C(17).

Inter-atomic vectors may be described by a basis set of three orthogonal unit vectors $\hat{\rho}$, $\hat{\mu}$ and \hat{n} as shown in Fig. 5.1, where $\hat{\rho}$, $\hat{\mu}$ lie in the plane of the benzene ring and \hat{n} , ($= \hat{\mu} \wedge \hat{\rho}$), perpendicular to the plane. Determination of the basis set relied on the definition of the plane in terms of the scalar product.

$$\underline{r} \cdot \underline{n} = 0 \quad \dots \text{Eqn. 5.1}$$

where \underline{r} describes any vector in the plane and \underline{n} , ($= \underline{\hat{\mu}} \wedge \underline{\hat{\rho}}$) a vector normal to the plane.

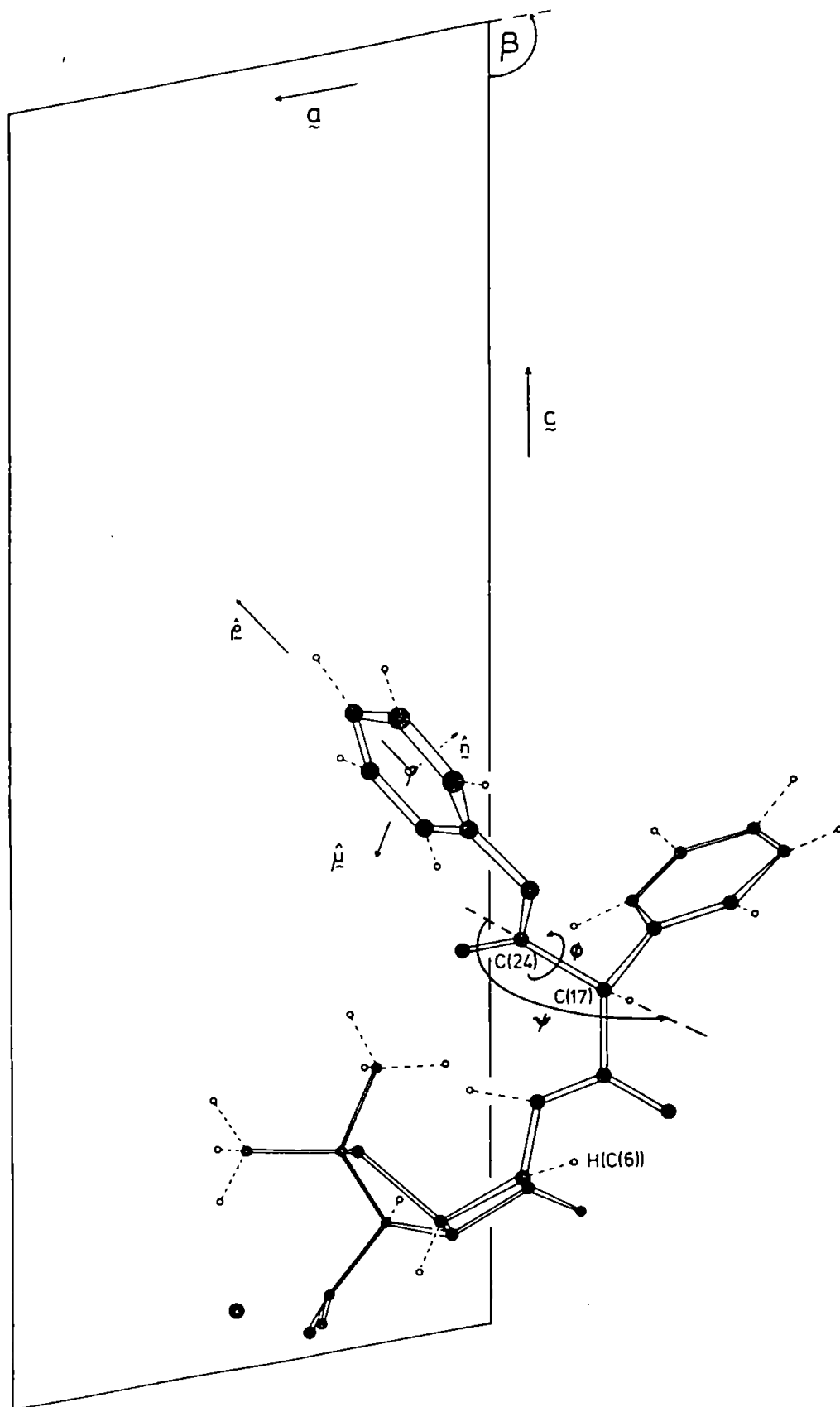
Two vectors in the plane of the benzene ring are the inter-atomic vectors

$$\underline{C(27) C(28)} \sim \begin{pmatrix} 0.0778 \\ 0.1965 \\ 0.0096 \end{pmatrix} \quad \dots \text{Eqn. 5.2}$$

and

$$\underline{C(27) C(32)} \sim \begin{pmatrix} 0.0255 \\ -0.1603 \\ 0.0463 \end{pmatrix} \quad \dots \text{Eqn. 5.3}$$

with components expressed as fractions of the unit cell vectors \underline{a} , \underline{b} and \underline{c} respectively. These vectors can be used in Eqn. 5.1 to determine the



Geometrical parameters used in describing the relative side-chain orientation of the phenyl ester of carbenicillin

Fig. 5.1

direction of \underline{n} as,

$$\underline{n} = \begin{pmatrix} -0.6082 \\ 0.1919 \\ 1 \end{pmatrix} \quad \dots \text{Eqn. 5.4}$$

(there being no necessity to uniquely define its magnitude).

$\underline{\rho}$ is conveniently defined with respect to the unit cell vectors \underline{a} , \underline{b} and \underline{c} as the interatomic vector $C(27) \sim C(30)$, such that

$$\underline{\rho} = \begin{pmatrix} 0.2068 \\ 0.0724 \\ 0.1118 \end{pmatrix} \quad \dots \text{Eqn. 5.5}$$

Thus, satisfying the definition of the plane,

$$\underline{\rho} \cdot \underline{n} \approx 0 \quad \dots \text{Eqn. 5.6}$$

is found to be true.

The two vectors $\underline{\rho}$ and \underline{n} are referred to the unit cell vectors \underline{a} , \underline{b} and \underline{c} which are not orthogonal ($\beta = 99.5^\circ$). To produce an orthogonal basis, it is necessary to transform $\underline{\rho}$ and \underline{n} to refer to orthogonalised unit basis vectors $\hat{\delta}\underline{a}$, $\hat{\delta}\underline{b}$ and $\hat{\delta}\underline{c}$, as shown in Fig. 5.2, where

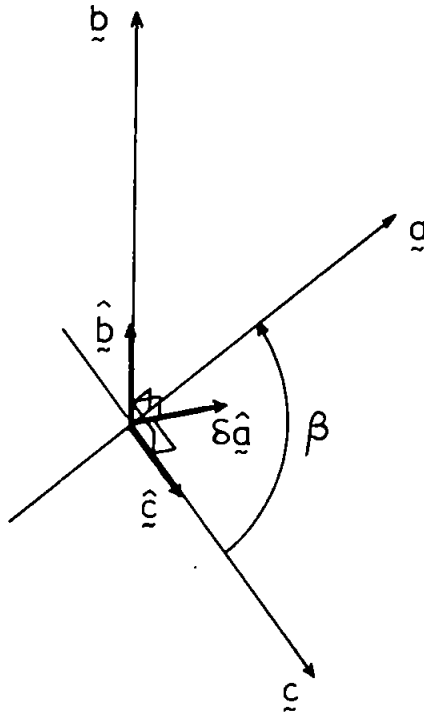


Fig. 5.2 Transformation of co-ordinate axes.

the operation δ satisfies the reorientation of \underline{a} such that

$$\text{and } \left. \begin{array}{l} \delta \underline{a} \cdot \underline{c} = 0 \\ \delta \underline{a} \cdot \underline{b} = 0 \end{array} \right\} \dots \text{Eqns. 5.7}$$

and premultiplies the magnitude of \underline{a} by $\sin \beta$.

Thus, expressed in terms of the basis $\hat{\underline{a}}$, $\hat{\underline{b}}$ and $\hat{\underline{c}}$,

$$\underline{\rho} = \begin{pmatrix} \rho_1 & \delta a \\ \rho_2 & b \\ \rho_3 & c \end{pmatrix} = \begin{pmatrix} 1.7888 \\ 0.4489 \\ 2.3925 \end{pmatrix} \dots \text{Eqn. 5.8}$$

and

$$\underline{n} = \begin{pmatrix} n_{1/\delta a} \\ n_{2/b} \\ n_{3/c} \end{pmatrix} = \begin{pmatrix} -0.0703 \\ 0.0310 \\ 0.0467 \end{pmatrix} \dots \text{Eqn. 5.9}$$

where $\underline{\rho}$ and \underline{n} still satisfy Eqn. 5.6.

Conversion to unit vectors results in

$$\hat{\underline{\rho}} = \begin{pmatrix} 0.5922 \\ 0.1486 \\ 0.7920 \end{pmatrix} \dots \text{Eqn. 5.10}$$

and

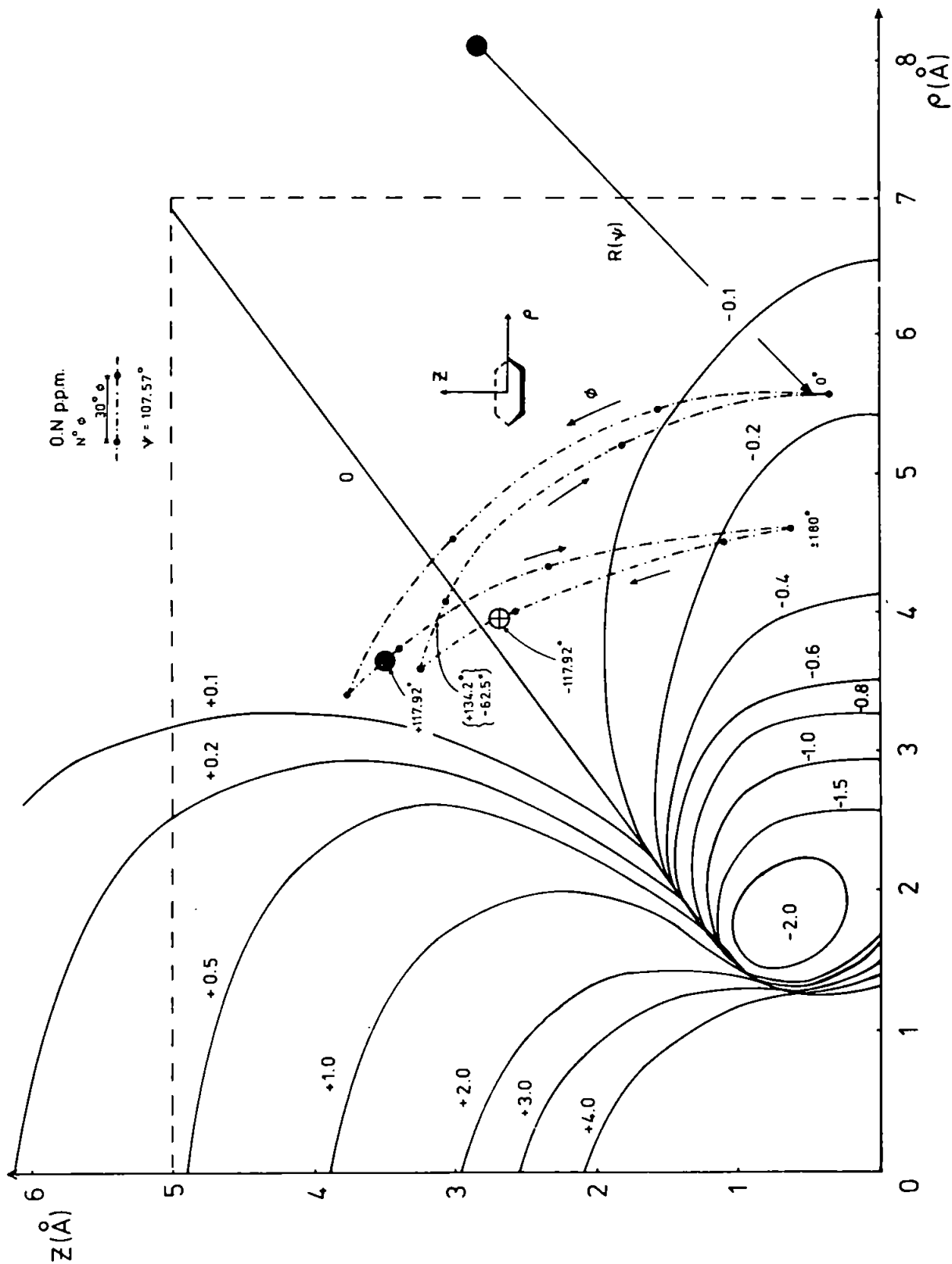
$$\hat{\underline{n}} = \begin{pmatrix} -0.7819 \\ 0.3448 \\ 0.5194 \end{pmatrix} \dots \text{Eqn. 5.11}$$

Definition of the remaining vector, $\hat{\underline{\mu}}$, in the plane of the ring is given by the vector product

$$\hat{\underline{\mu}} = \hat{\underline{\rho}} \wedge \hat{\underline{n}} \dots \text{Eqn. 5.12}$$

such that

$$\hat{\underline{\mu}} = \begin{pmatrix} -0.1959 \\ -0.9269 \\ 0.3204 \end{pmatrix} \dots \text{Eqn. 5.13}$$



Contour plot of n.m.r. shielding values for protons in the vicinity of a benzene ring

Fig.5.3

Fig. 5.3 is a contour plot of shift in n.m.r. shielding values in p.p.m., which will be experienced by hydrogen atoms as a result of the ring currents associated with the benzene ring, (from Johnson and Bovey, 1958)⁵³. The \hat{z} direction is along \hat{n} ie, the hexagonal axis of the benzene ring while ρ is the direction in the plane of the carbon atoms, ie, the $\hat{\rho}, \hat{\mu}$ plane.

(i) Relative orientation in fresh solution

In the crystalline solid state the orientation of the ester substituent benzene ring with respect to H(C(6)) is described by the vector between H(C(6)) and the centre of the benzene ring, \underline{v}_1 , expressed in terms of the newly found basis set $\hat{\rho}, \hat{\mu}$ and \hat{n} . The vector \underline{v}_1 may be conveniently obtained by considering the vector sum

$$\underline{v}_1 = \text{H(C(6))} \underset{\sim}{\text{C(17)}} + \underset{\sim}{\text{C(17)}} \underset{\sim}{\text{C(27)}} + \frac{1}{2}\underline{e} \quad \dots \text{Eqn. 5.14}$$

which gives

$$\underline{v}_1 = \begin{pmatrix} 2.6737 \\ 2.4722 \\ 7.7512 \end{pmatrix} \quad \dots \text{Eqn. 5.15}$$

expressed in terms of \hat{a}, \hat{b} and \hat{c} .

By letting

$$\underline{v}_1 = l\hat{\rho} + m\hat{\mu} + p\hat{n} \quad \dots \text{Eqn. 5.16}$$

l, m and n are given by

$$\left. \begin{aligned} l &= \underline{v}_1 \cdot \hat{\rho} \\ m &= \underline{v}_1 \cdot \hat{\mu} \\ p &= \underline{v}_1 \cdot \hat{n} \end{aligned} \right\} \quad \dots \text{Eqns. 5.17}$$

and describe the components of \underline{v}_1 in terms of the basis set $\hat{\rho}, \hat{\mu}$ and \hat{n} such that

$$\underline{v}_1 = \begin{pmatrix} 8.0897 \\ -0.3318 \\ 2.7878 \end{pmatrix} \quad \dots \text{Eqns. 5.18}$$

The distance from H(C(6)) to the centre of the ring is thus given by the two components

$$\rho = \sqrt{l^2 + m^2}$$

$$\approx 8.1 \text{ \AA} \text{ parallel to the plane of ring}$$

... Eqn. 5.19

and $z = p \approx 2.8 \text{ \AA}$ perpendicular to the plane of ring

... Eqn. 5.20

It can be seen from Fig. 5.3 that these co-ordinates lie outside the region of influence, (indicated by the 'dashed' rectangle), considered sufficient to effect any shielding of H(C(6)). Thus, the configuration of the phenyl ester of carbenicillin in fresh solution, assumed to be the configuration described above, i.e. that of the crystalline state, is such that no shielding of the β lactam protons would be expected; as evidenced by the singlet H^1 n.m.r. peak in Trace 4(b). Comparable distances between H(C(6)) and the ester substituents in the cases of the methyl and ethyl esters of carbenicillin could also be expected to result in the β lactam singlet in fresh solution.

(ii) Relative orientation after equilibration

During equilibration, a change of the ester substituent position at C(17) is described either by the replacement of the benzene substituent C(18) C(19) C(20) C(21) C(22) C(23) or of H(C(17)) by the ester. Hence, if the phenyl ester is to effect shielding of the β lactam proton H(C(6)) it must result in a closer approach between the ester and H(C(6)) than that described in the crystalline state.

To study the closeness of approach of any C(17) substituent position to H(C(6)) the unit interatomic vectors $C(17) \overset{\wedge}{\curvearrowright} C(24)$, $C(17) \overset{\wedge}{\curvearrowright} H(C(17))$ and $C(17) \overset{\wedge}{\curvearrowright} C(18)$ were determined. The distance from H(C(6)) to the end of each unit vector was given by 4.32, 3.89 and 4.33 \AA respectively as shown in Fig. 5.4.

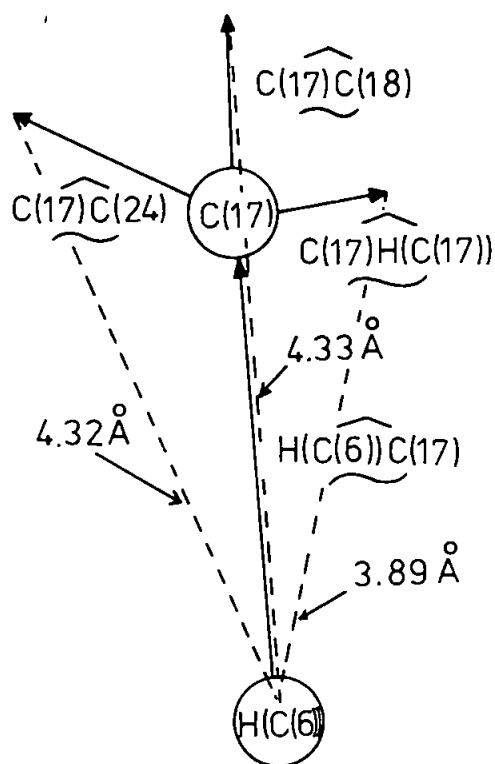


Fig. 5.4 Distances of C(17) & its substituents from H(C(6)).

Hence, substitution of the ester at H(C(17)) provides the closest approach to H(C(6)). This change of orientation can be effected by a rotation of the bond C(17) - C(24) to C(17) - H(C(17)) through the bond angle C(24) - C(17) - H(C(17)) given by

$$\cos \psi = \underbrace{C(17) \hat{C}(24)} \cdot \underbrace{C(17) \hat{H}(C(17))} \quad \dots \text{Eqn. 5.21}$$

which upon substitution gives

$$\psi = 107.57^\circ \quad \dots \text{Eqn. 5.22}$$

A general rotation of a co-ordinate system through an angle ψ about an axis inclined to the $(\hat{\rho}, \hat{\mu}, \hat{n})$ axes with direction cosines l, m and n respectively is represented by the matrix

$$R(\psi) = \begin{pmatrix} \cos \psi + l^2 (1 - \cos \psi) & lm(1 - \cos \psi) + n \sin \psi & ln(1 - \cos \psi) - m \sin \psi \\ lm(1 - \cos \psi) - n \sin \psi & \cos \psi + m^2 (1 - \cos \psi) & mn(1 - \cos \psi) + l \sin \psi \\ ln(1 - \cos \psi) + m \sin \psi & mn(1 - \cos \psi) - l \sin \psi & \cos \psi + n^2 (1 - \cos \psi) \end{pmatrix}$$

... Eqn. 5.23

The axis of rotation is the vector perpendicular to $C(17) \hat{C}(24)$ and $C(17) \hat{H}(C(17))$, ie. given by their vector product. The direction cosines are therefore found to be

$$\left. \begin{array}{l} l = 0.5651 \\ m = -0.0341 \\ n = -0.8244 \end{array} \right\} \quad \dots \text{Eqns. 5.24}$$

Hence, the matrix operator for the rotation of the ester substituent is given by

$$R(107.57^\circ) = \begin{pmatrix} 0.1139 & -0.8110 & -0.5740 \\ 0.7608 & -0.3004 & 0.6053 \\ -0.6390 & -0.5021 & 0.5829 \end{pmatrix}$$

... Eqn. 5.25

Since this operates upon $\hat{\rho}, \hat{\mu}$ and \hat{n} , the vector from $C(17)$ to the centre of the benzene ring ($= C(17) \hat{C}(27) + \frac{1}{2}\hat{\rho}$) remains unchanged when substituted at $H(C(17))$, but $H(C(6)) \hat{C}(17)$ is operated on by R . such that

$$R(107.57^\circ) [H(C(6)) \hat{C}(17)] = \begin{pmatrix} -1.5267 \\ 3.4786 \\ -0.5084 \end{pmatrix} \quad \dots \text{Eqn. 5.26}$$

expressed in terms of the basis $\hat{\rho}, \hat{\mu}$ and \hat{n} .

Rotation about the $C(17) - C(24)$ bond must now be considered to allow for conformational change about this bond.

As an approximation it is assumed that $\hat{\rho}$ is parallel to $C(17) \hat{C}(24)$; this is verified by taking the scalar product between $\hat{\rho}$

and $\hat{C}(17) \hat{C}(24)$ resulting in

$$\hat{\rho} \cdot \hat{C}(17) \hat{C}(24) = 0.95 \approx 1 \text{ as required} \quad \dots \text{Eqn. 5.27}$$

Hence, rotation about C(17) - C(24) is in the $\hat{\mu}, \hat{n}$ plane and the rotation matrix R, (Eqn. 5.23), reduces to

$$R'(\phi) = \begin{pmatrix} 1 & 0 & 0 \\ 0 & \cos\phi & -\sin\phi \\ 0 & \sin\phi & \cos\phi \end{pmatrix} \dots \text{Eqn. 5.28}$$

where ϕ is the angle of rotation.

Thus, a rotation ψ associated with a change in configuration about C(17) is accompanied by a rotation ϕ about C(17) - C(24) associated with a change in conformation.

Severe constraint upon the rotation ϕ is expected due to the vicinity of the two carbonyl groups C(15) = O(16) and C(24) = O(25). The relative orientation of the carbonyl groups in the crystalline state was assumed in some measure to represent the most probable and energetically favourable conformation, and indeed, in solution, conformation of such groups is strongly localised such that the mutually repellant nature of the carbonyls is accommodated within the constraints of the surrounding groups^{54,55}. Thus, to maintain the same relative orientation between the carbonyls, ϕ is given by

$$\begin{aligned} \phi &= \pm \frac{\psi}{109.47} \times \frac{(360)}{3} \\ &= \pm 117.92^\circ \quad \dots \text{Eqn. 5.29} \end{aligned}$$

where 109.47° is the theoretical tetrahedral bond angle as illustrated in Fig. 5.5. However, orientation with respect to the benzene ring

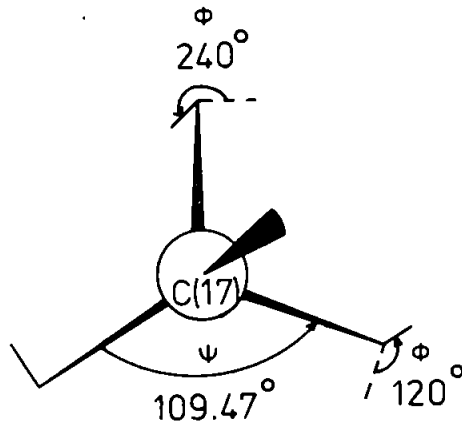


Fig. 55 Theoretical geometry about C(17).

C(18) C(19) C(20) C(21) C(22) and C(23) constrains ϕ to take the value -117.92° .

The transformed vector $H(C(6)) \widetilde{C(17)}$ therefore becomes

$$R' (-117.92^\circ) \left(R (107.57^\circ) [H(C(6)) \widetilde{C(17)}] \right) = \begin{pmatrix} -1.5267 \\ -2.0779 \\ -2.8357 \end{pmatrix}$$

... Eqn. 5.30

and the vector from $H(C(6))$ to the centre of the ring, v_2 , is given by

$$\begin{aligned}
 \underline{v}_2 &= \begin{pmatrix} -1.5267 \\ -2.0779 \\ -2.8357 \end{pmatrix} + \underbrace{C(17) C(27)} + \frac{1}{2} \underline{\rho} \\
 &= \begin{pmatrix} 3.8232 \\ -1.2748 \\ -2.5852 \end{pmatrix} \quad \dots \text{Eqn. 5.31}
 \end{aligned}$$

expressed in terms of the basis set $\hat{\underline{\rho}}$, $\hat{\underline{\mu}}$ and $\hat{\underline{n}}$.

Since the operators $R(\psi)$ and $R'(\phi)$ rotate the co-ordinate axes $(\hat{\underline{\rho}}, \hat{\underline{\mu}}, \hat{\underline{n}})$ by the same transformation as that experienced by the ester side chain, the vectors $\underbrace{C(17) C(27)}$ and $\frac{1}{2} \underline{\rho}$ remain rotationally invariant under $R(\psi)$ and $R'(\phi)$, then it is only the vector $\underbrace{H(C(6)) C(17)}$ that undergoes transformation.

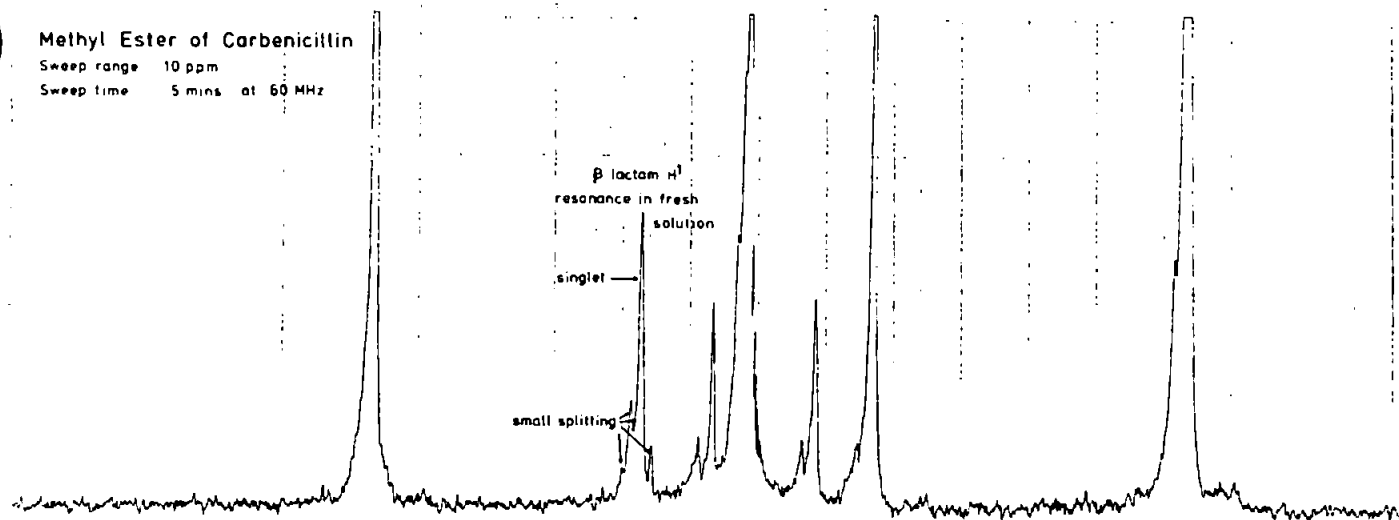
The vector \underline{v}_2 can be reduced to components parallel and perpendicular to the plane of the ring by Eqns. 5.19 and 5.20, such that

$$\begin{aligned}
 \rho &\approx 4.03 \text{ \AA} \\
 \text{and} & \\
 z &\approx 2.59 \text{ \AA}
 \end{aligned} \quad \left. \vphantom{\begin{aligned} \rho \\ \text{and} \\ z \end{aligned}} \right\} \dots \text{Eqns. 5.32}$$

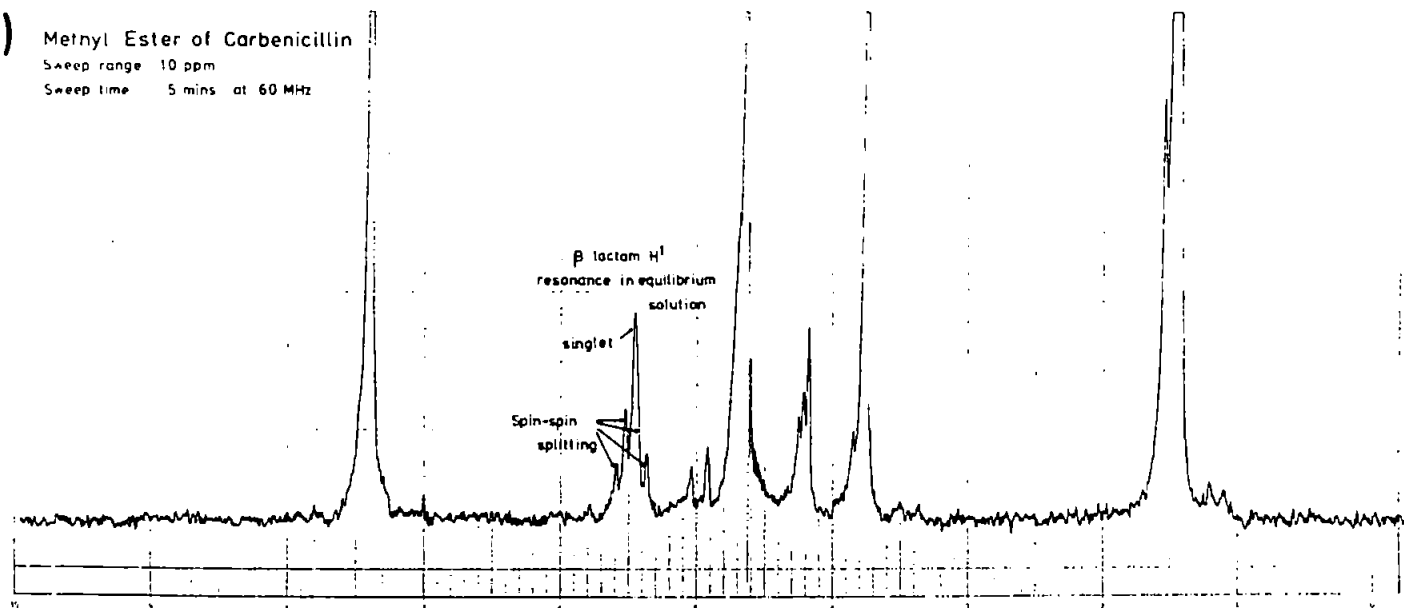
Fig. 5.3 illustrates that these co-ordinates result in an aspect of the ester substituent benzene ring, at position \otimes , lying close to the zero shielding contour, thus, no change in the β lactam proton n.m.r. signal during equilibration is to be expected for the phenyl ester of carbenicillin. The trajectory followed by the ring under arbitrary rotation ϕ , ie. conformational change, is also plotted at 30° intervals from which it can be seen that for approximately 75% of the period time, the ring orientation is such that the magnitude of the n.m.r. shielding is between ± 0.1 p.p.m. The n.m.r. spectra of the β lactam protons in the methyl and ethyl esters of carbenicillin show a splitting during equilibration, with the coupling J (in frequency units) of the order of the chemical shift δ . J was found to be 4.0Hz and 2C to be 9.0Hz; using a 60MHz oscillator, δ was estimated to be ± 0.13 p.p.m. ie. of comparable

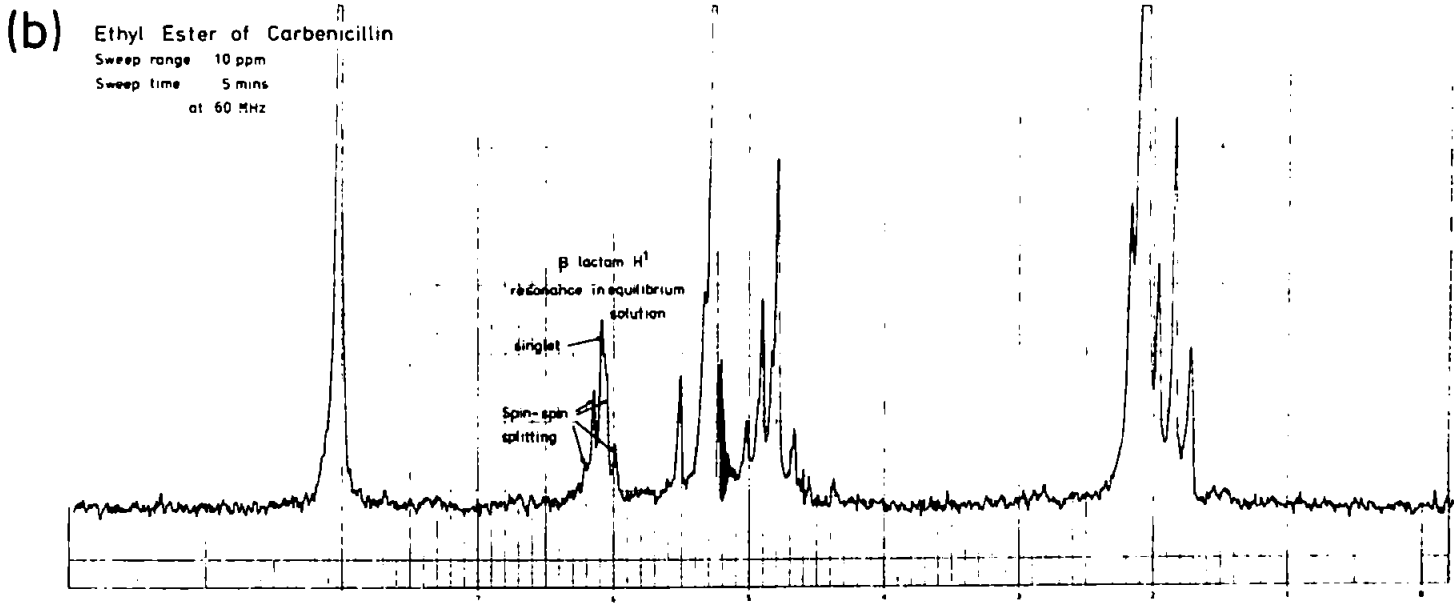
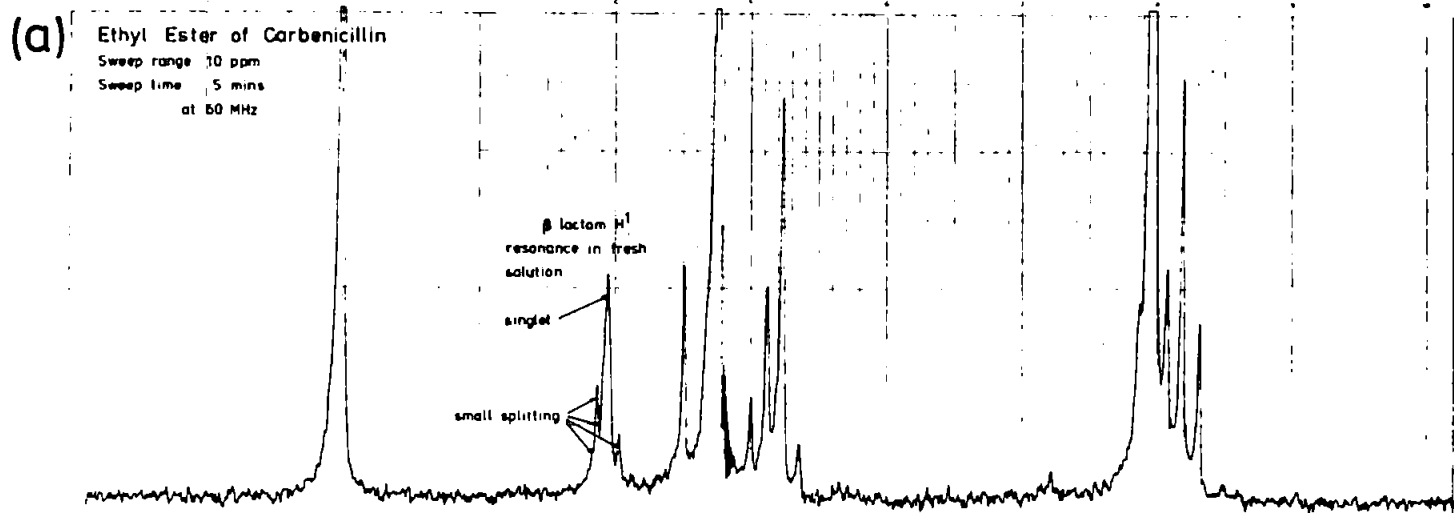
magnitude to that expected above.

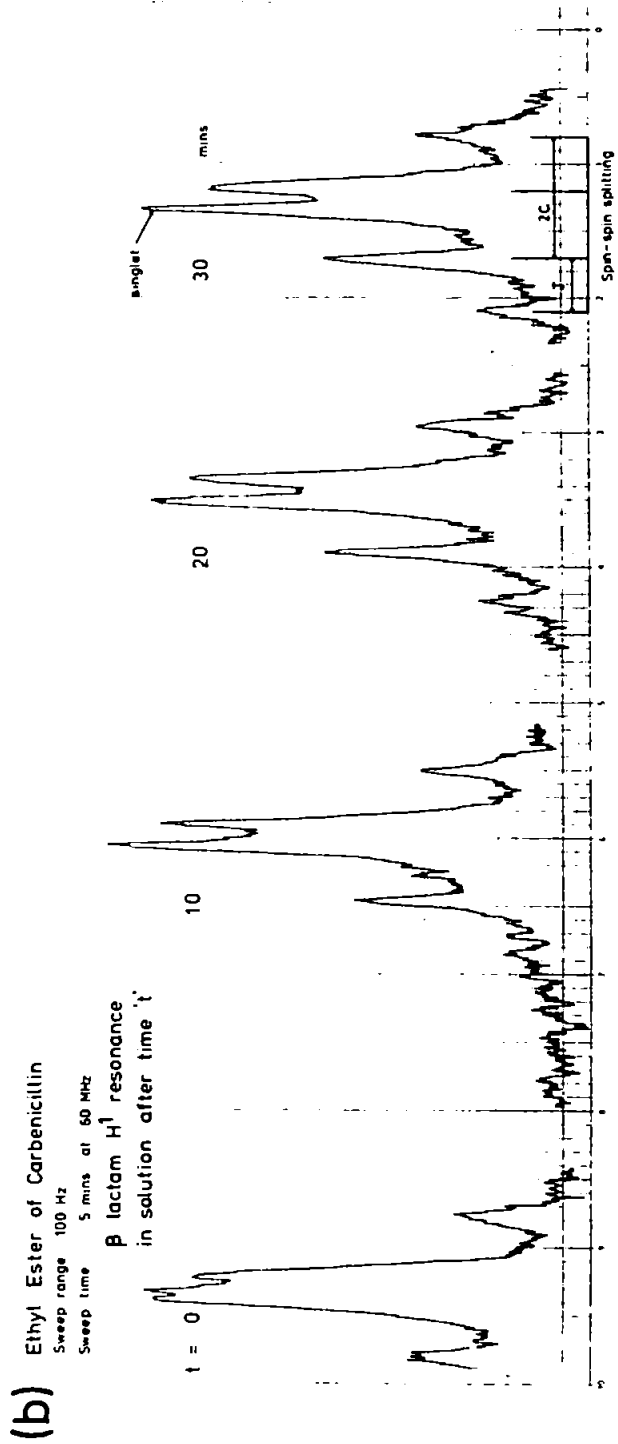
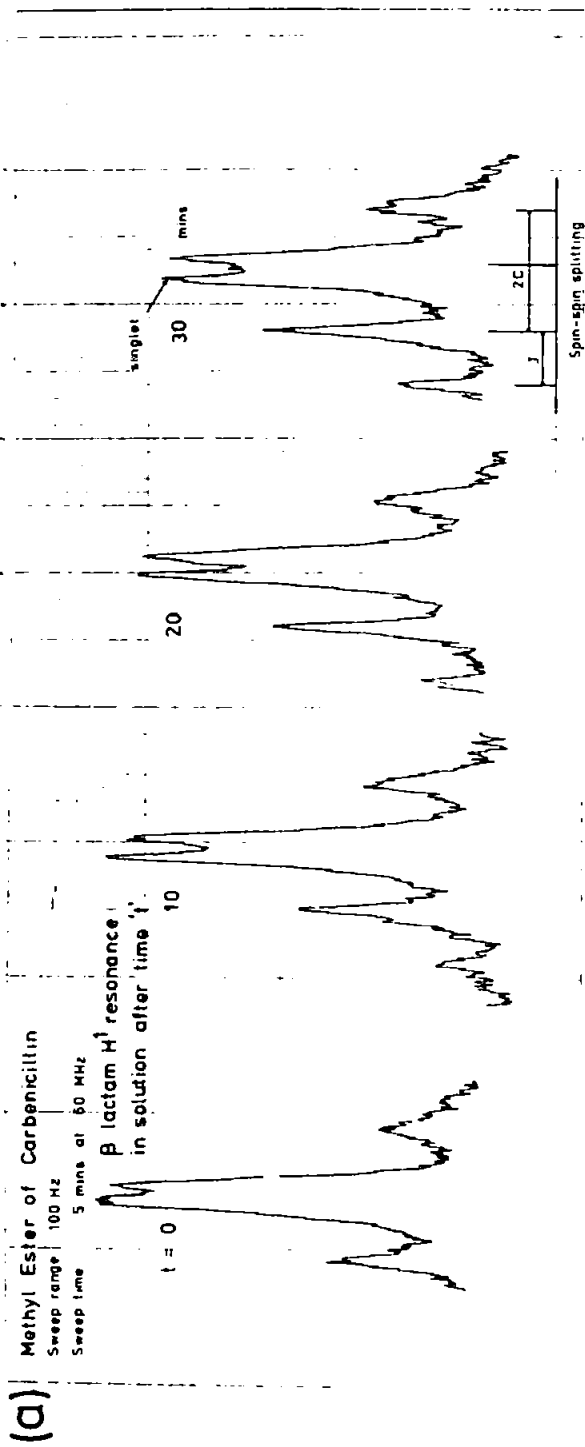
(a) Methyl Ester of Carbenicillin
Sweep range 10 ppm
Sweep time 5 mins at 60 MHz



(b) Methyl Ester of Carbenicillin
Sweep range 10 ppm
Sweep time 5 mins at 60 MHz

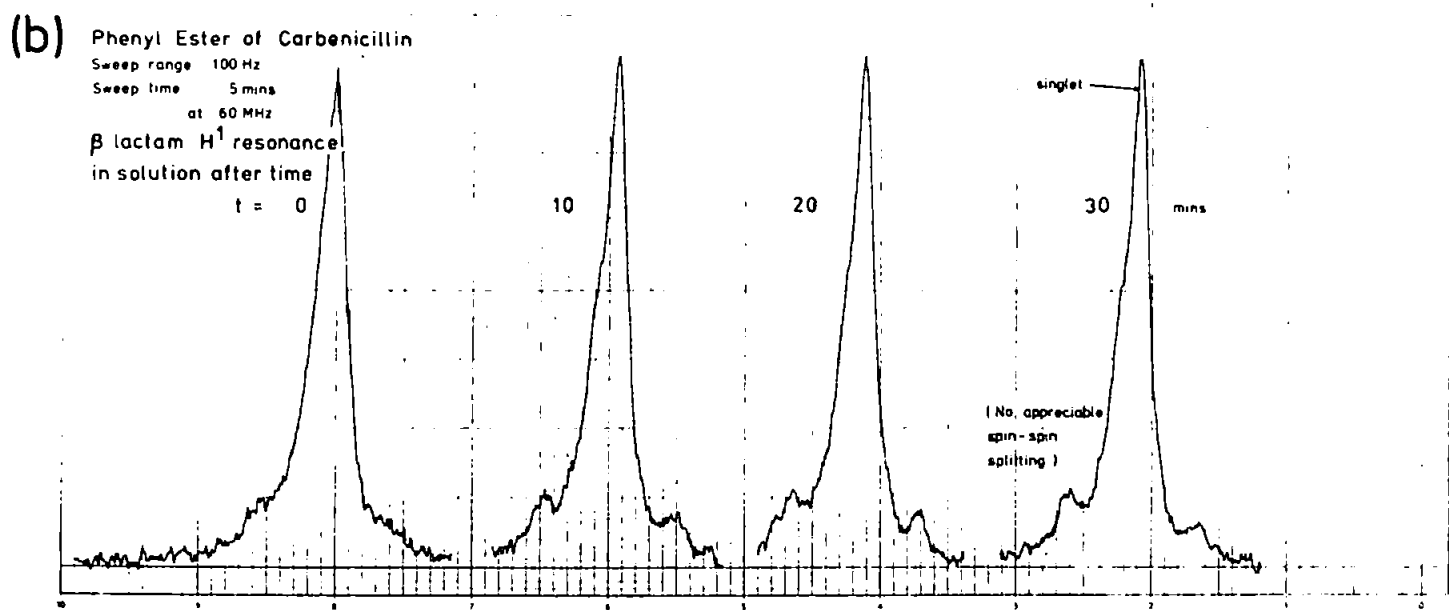
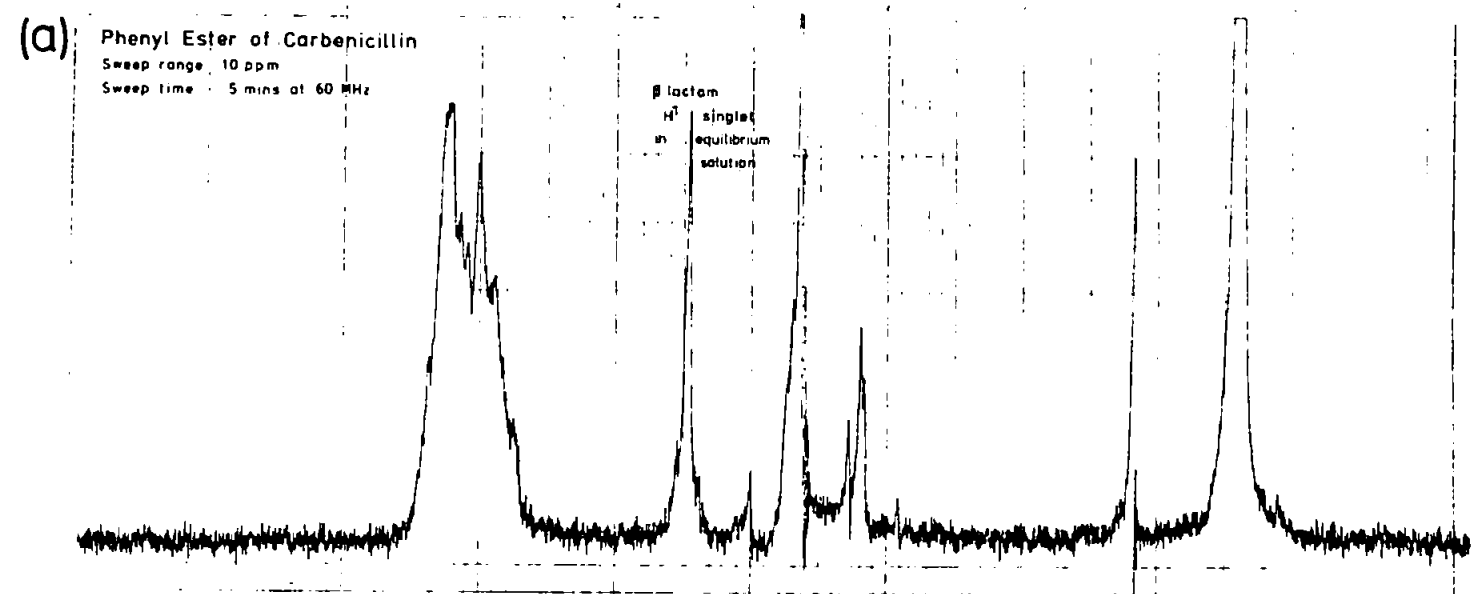


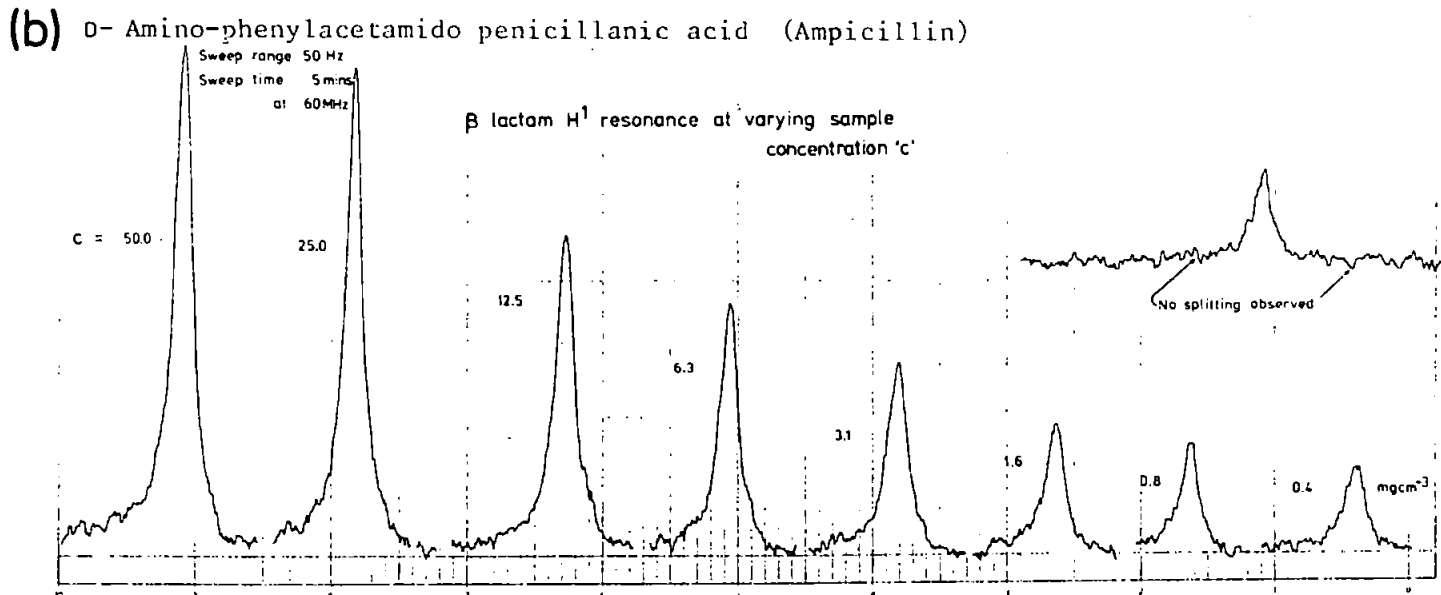
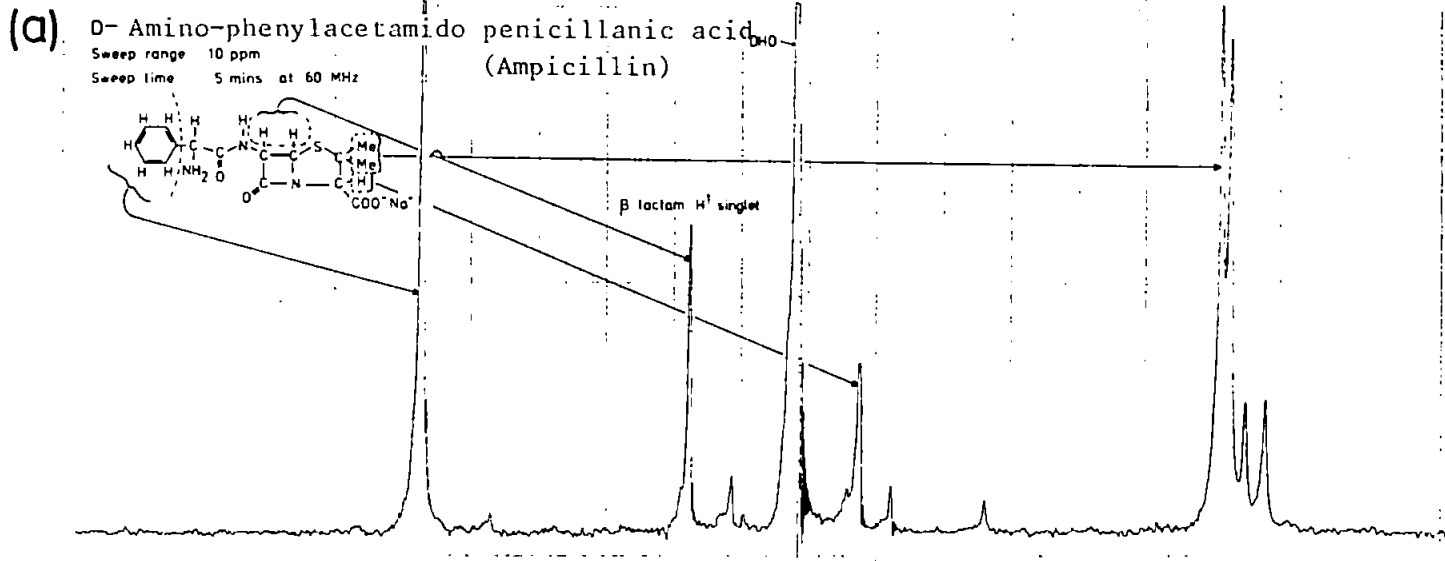




Trace 3

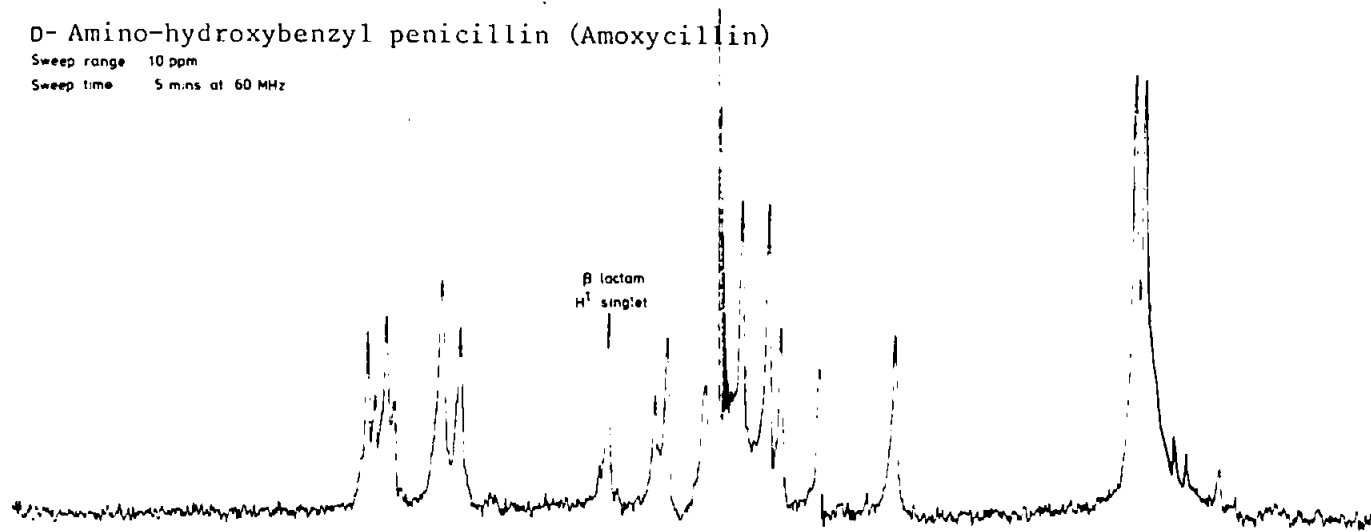
Trace 4





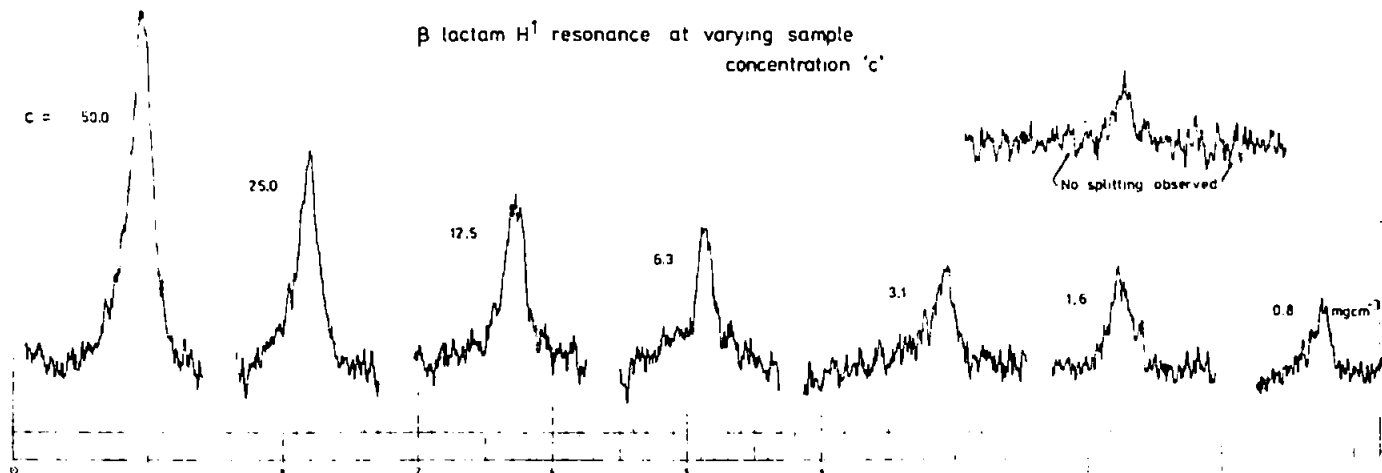
(a) D- Amino-hydroxybenzyl penicillin (Amoxycillin)

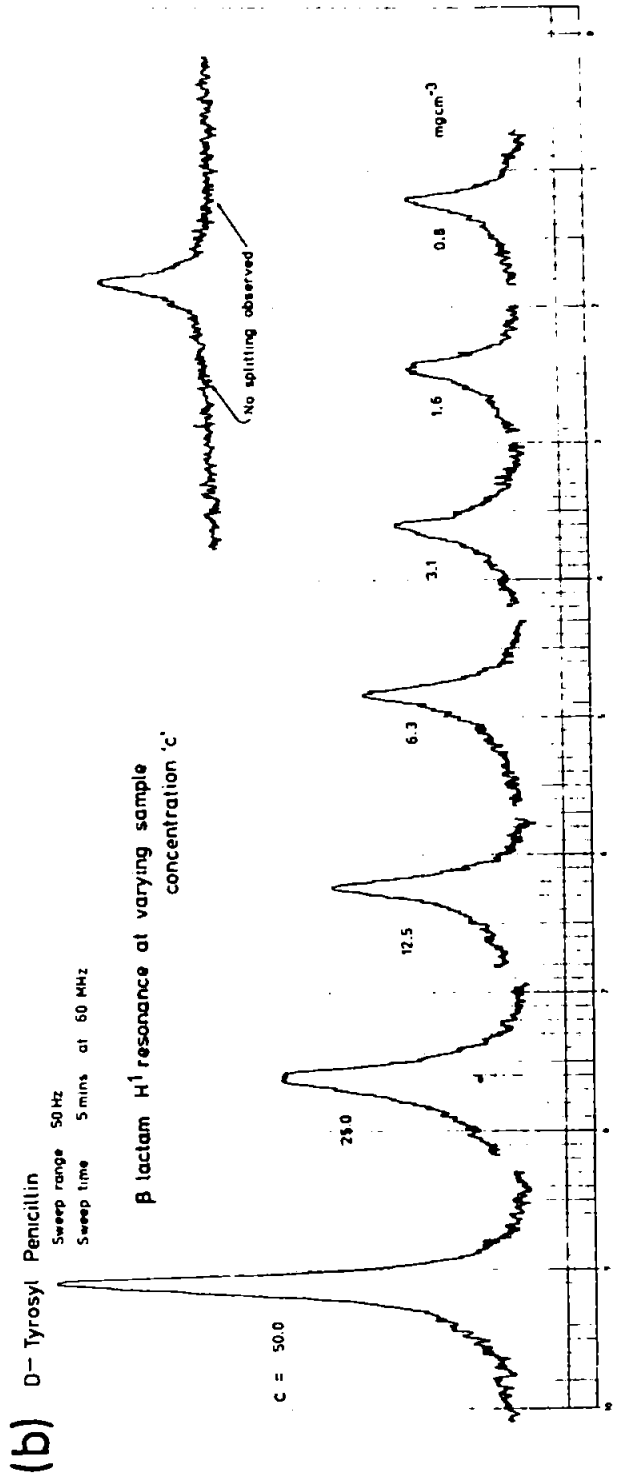
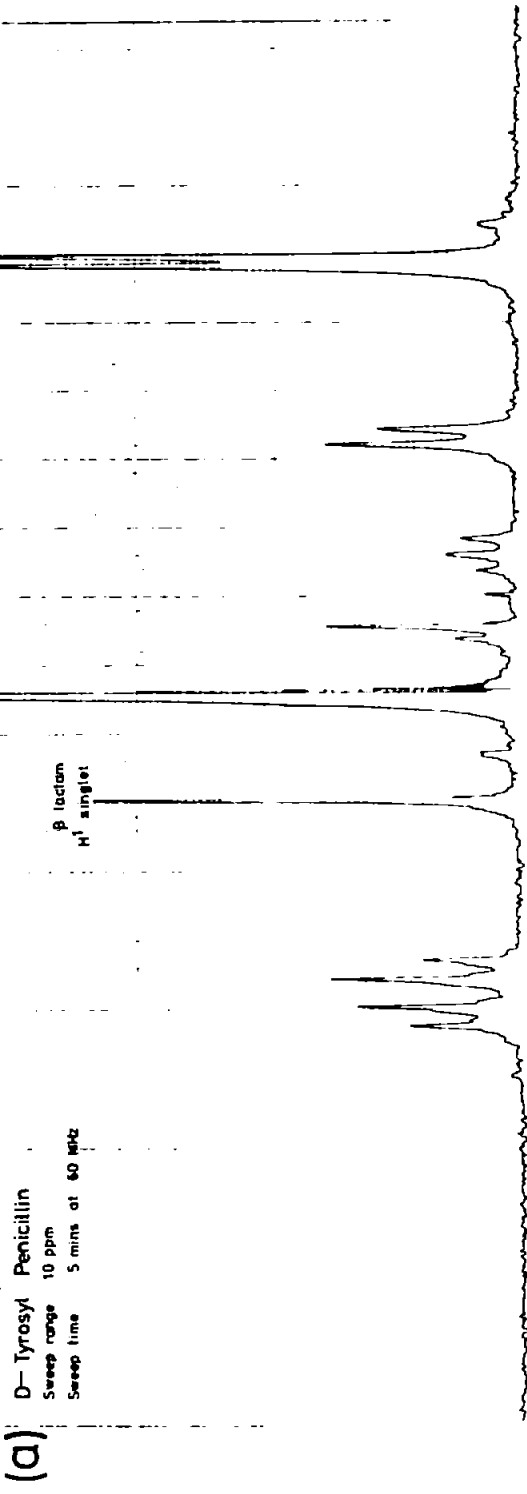
Sweep range 10 ppm
Sweep time 5 mins at 60 MHz



(b) D- Amino-hydroxybenzyl penicillin (Amoxycillin)

Sweep range 50 Hz
Sweep time 5 mins at 60 MHz



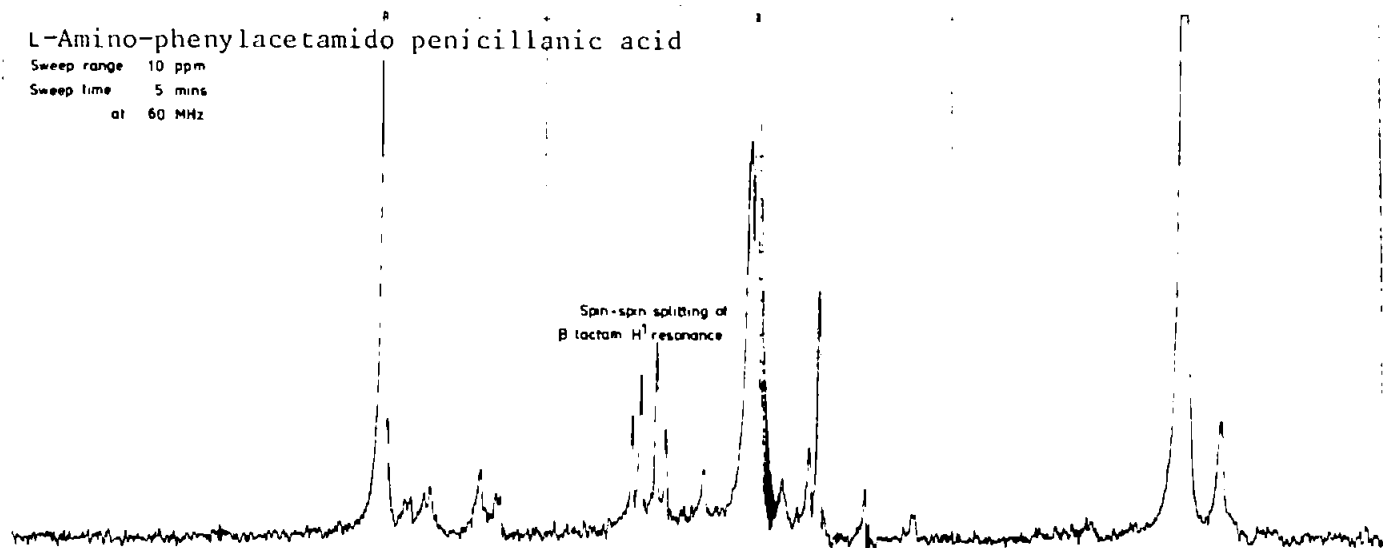


(a) L-Amino-phenylacetamido penicillanic acid

Sweep range 10 ppm

Sweep time 5 mins

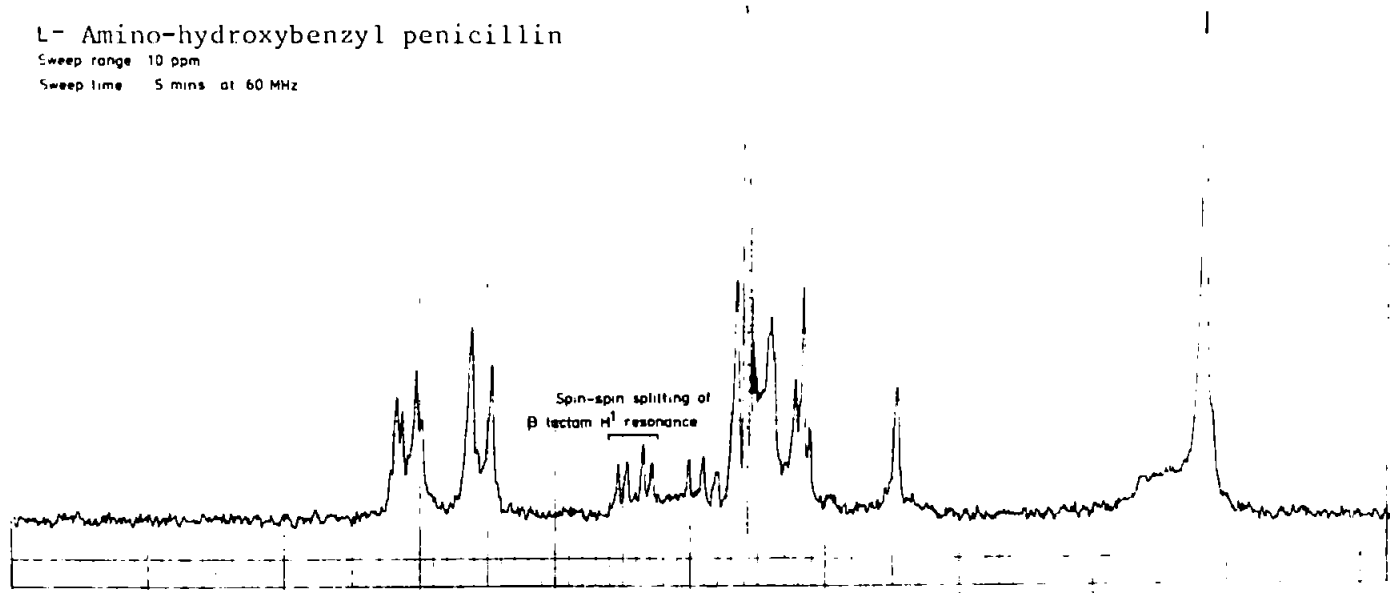
at 60 MHz



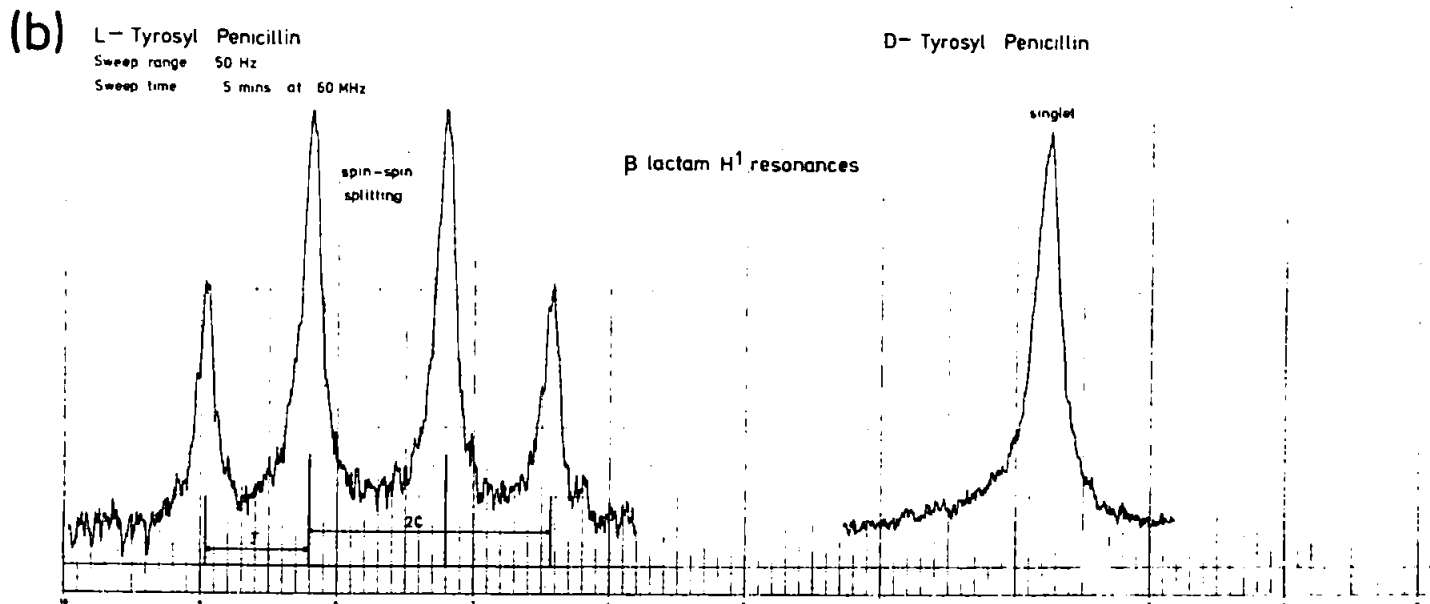
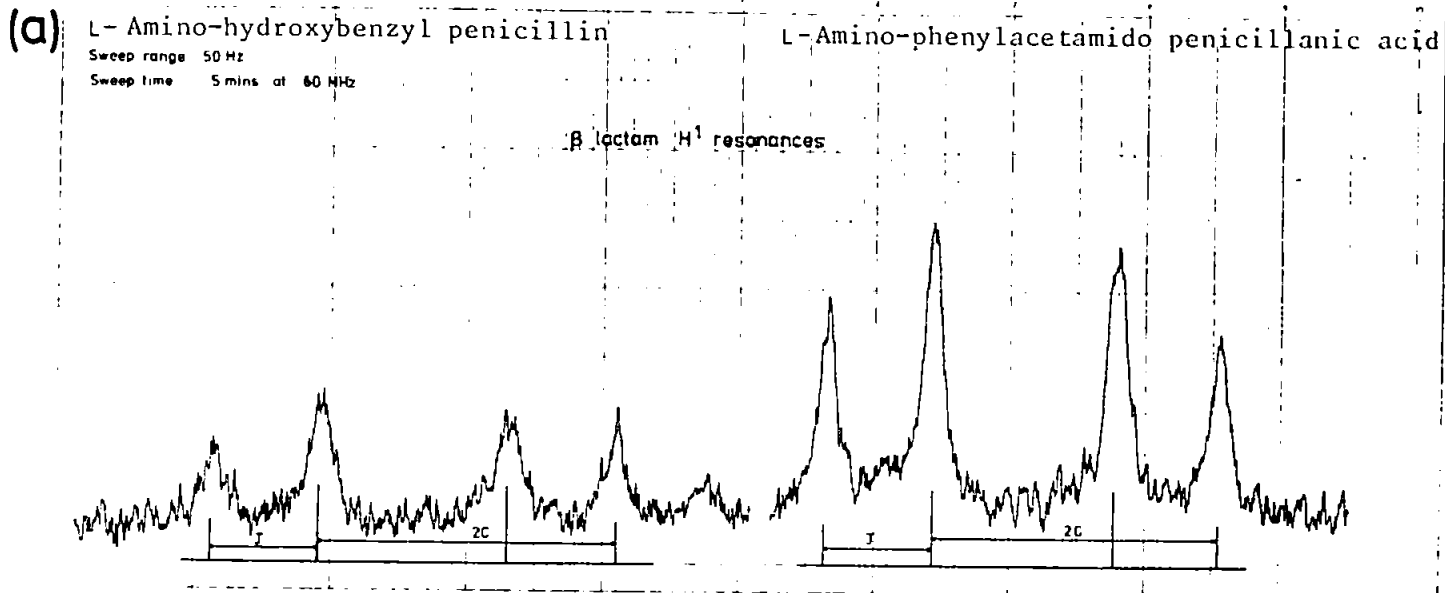
(b) L- Amino-hydroxybenzyl penicillin

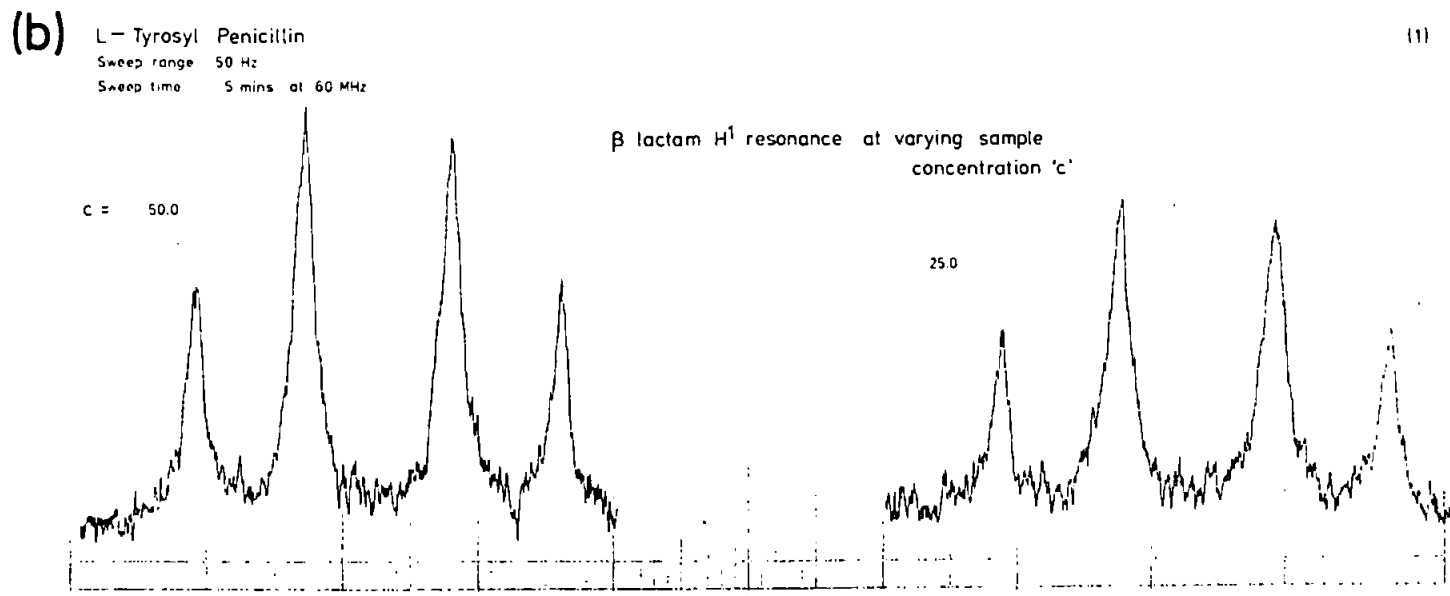
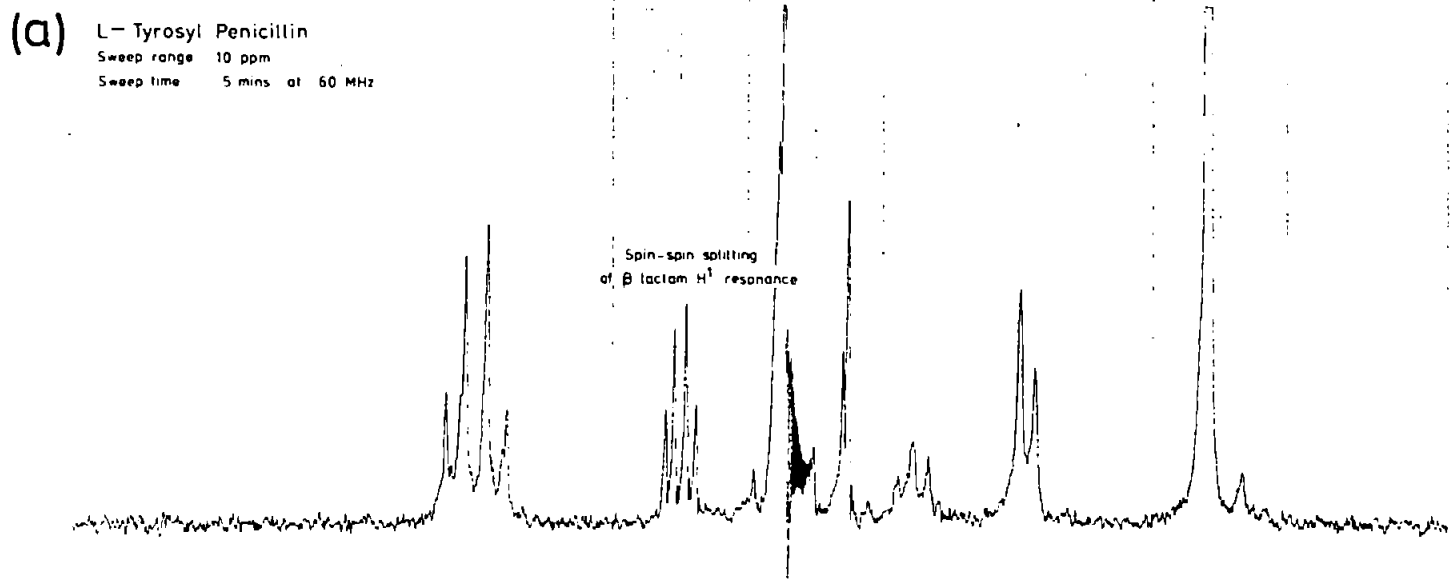
Sweep range 10 ppm

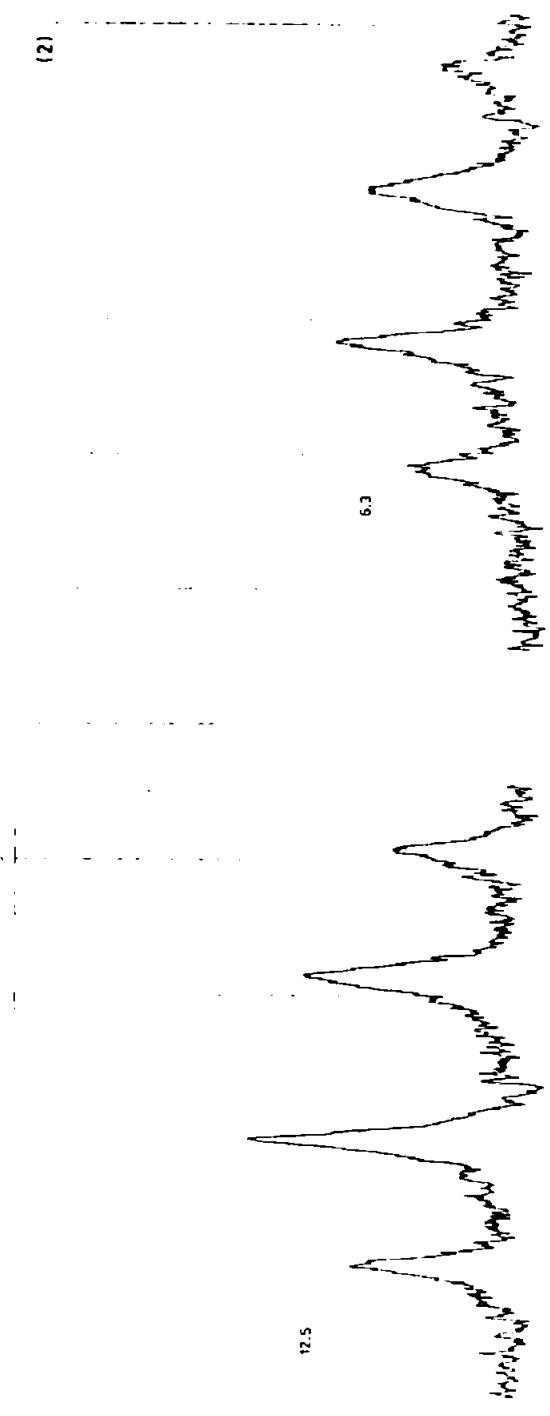
Sweep time 5 mins at 60 MHz



Trace 8

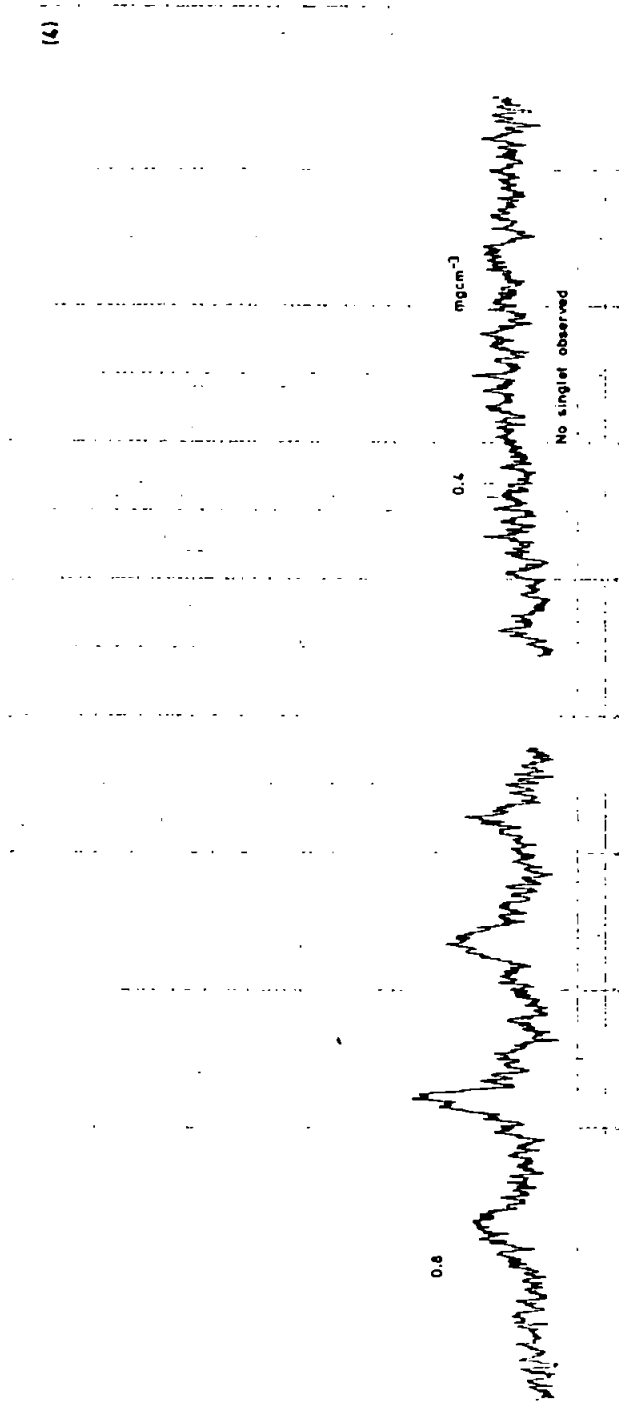






Trace 10 (b) contd.

(4)



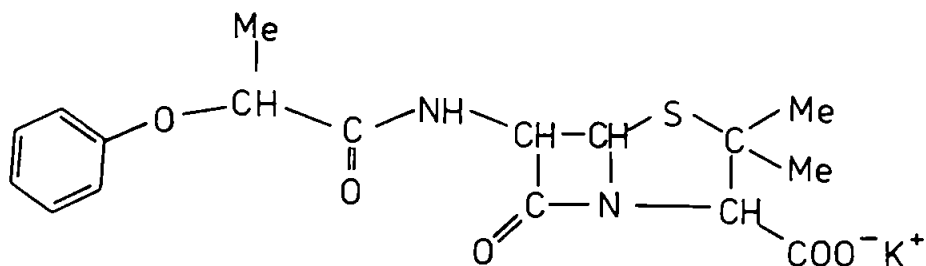
Trace 10 (b) contd.

Table 5.1 β lactam proton magnetic resonance spin-spin splitting coupling constants, J, and chemical shifts, δ , in solution at 35°C.

	J(Hz)	δ (p.p.m.)	Solvent
L-Tyrosyl penicillin,	3.80	0.13	D ₂ O/NaOD
L-Amino-phenylacetamido penicillanic acid,	3.90	0.16	"
L-Amino-hydroxybenzyl penicillin,	3.95	0.17	"
Methyl ester of carbenicillin,	4.00	0.13	D ₂ O
Ethyl ester of carbenicillin.	4.00	0.13	" } after equilibration

5.4 Side Chain Configuration and Associated Circular Dichroism

Stenlake, et al, (1972)⁵⁶, used the chiroptical technique of circular dichroism, (CD), as a method of assay to determine the proportions of D and L diastereoisomers in samples of phenethicillin potassium.



The spectrum obtained for the D and L epimers alone is shown in CD(1) where $\Delta\epsilon$ is the difference ($\epsilon_L - \epsilon_R$) between left and right circularly polarised light. The reversal in Cotton Effect, (CE), between the (+)ve $\Delta\epsilon$ value for the D and the (-)ve value for the L compounds both at 269nm and 276nm was shown to follow a linear relationship.

Boyd, et al, (1975)⁵⁷, computed a theoretical CD spectrum for penicillin nuclei using a molecular orbital model based on 6-aminopenicillanic acid, (6-APA). The predicted CD spectrum based on Extended Huckel Molecular Orbital theory is shown in CD(2), in which the exponential half-

width parameter for the transitions has a value chosen to most closely agree with experimental spectra of 6-APA. Two main features are evident: (i) the (+)ve CE at about 236nm is predicted to involve molecular orbitals designated S-N $\pi \rightarrow$ amide π^* with some mixing from S $n \rightarrow$ amide π^* ie. the sulphide chromophoric behaviour shows a dependence upon the relative vicinity of the β lactam amide chromophore; (ii) the shorter wavelength (-)ve CE at about 199nm is assigned to the β lactam $n \rightarrow \pi^*$ transition, however, a reversal to a (+)ve CE has been noted experimentally under conditions of varying pH. The (-)ve CE seems consistent with experimentally low pH values (~ 3.0), and the reversal of CE for higher pH values could be explained by a small mixing of the amino group orbitals into the amide orbitals.

An empirical discussion of the contribution made by the side chain chromophores to the CD spectra of penicillin derivatives is facilitated by the observance of features modifying the spectrum of the penicillin nucleus discussed above.

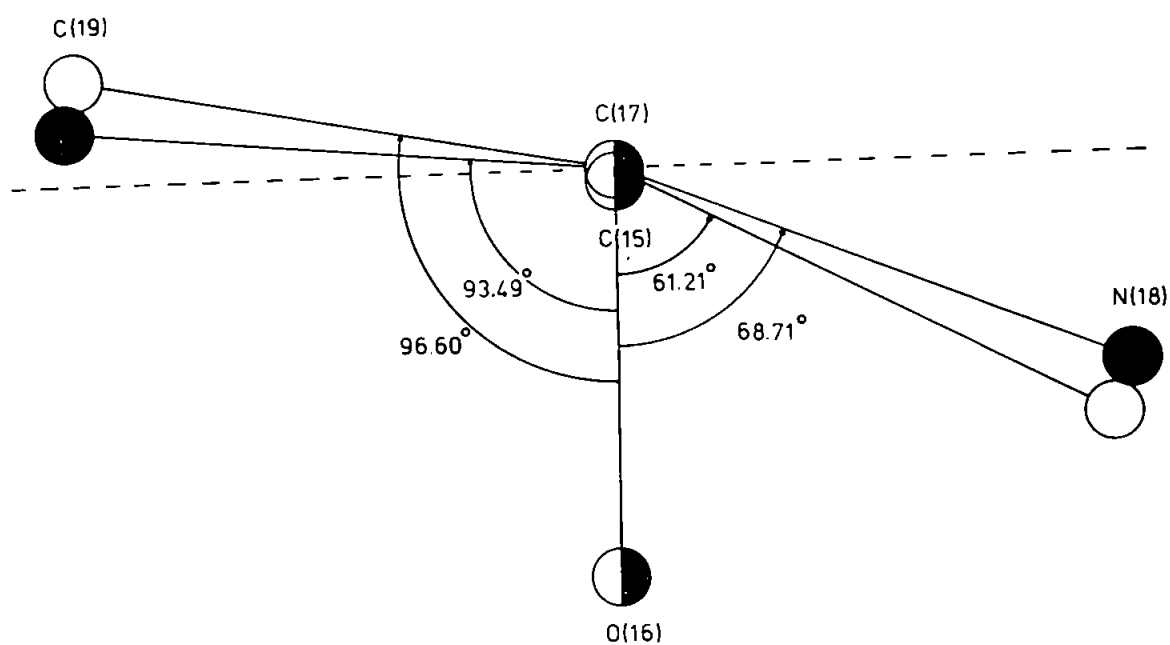
The CD spectrum of amino-phenylacetamido penicillanic acid is shown in CD(3). The spectrum for the D epimer resembles closely that of the penicillin nucleus alone CD(2), however, the short wavelength (-)ve CE occurs at 206nm compared with the unperturbed β lactam amide transition at 199nm. As in the case of phenethicillin potassium CD(1), a (+)ve CE is noted in the long wavelength region at 259nm and 267nm. The spectrum of the L epimer, however, differs by a reversal of sign of $\Delta\epsilon$ at 206nm and at the long wavelength CE at 261 nm and 266 nm. The reversal in CE at the short wavelength must be associated with the difference in side chain configuration since no pH change occurred to effect any change in the amide $n \rightarrow \pi^*$ transition. Similarly, the longer wavelength CE reversal must also be associated with the side chain configurational change since little or no contribution to the spectrum by the penicillin nucleus is apparent at such wavelengths. The side chain chromophores sensitive to configurational change about

C(17) are those that are either substituents of C(17) or suffer no insulation from chromophores in such a site. Thus, the study of the CD spectra of selected penicillin derivatives enables an assignment to be made of which chromophore(s) contributes the variation in spectra both between each derivative and their respective D and L diastereoisomers.

In the case of amino-phenylacetamido penicillanic acid, the differing spectral features, ie, reversal of CE's between the D and L forms already described, could be assigned to the possible chromophoric transitions in either the benzene, amine or carbonyl C(17) substituents.

Amino-hydroxybenzyl penicillin differs from amino-phenylacetamido penicillanic acid in respect to the para-substituted hydroxyl of the C(17) benzene substituent only. The absorption wavelength for a disubstituted benzene is not greatly affected by para-substitution of an electron donating group and as shown in CD(4), the spectrum of amino-hydroxybenzyl penicillin shows CE's associated with the diastereoisomeric configuration, at only slightly longer wavelengths than those of amino-phenylacetamido penicillanic acid. However, change of sign of the CE at 270-278 nm between the D and L forms of amino-hydroxybenzyl penicillin is opposite to that of amino-phenylacetamido penicillanic acid suggesting that this band is due either to a weak benzene $\pi \rightarrow \pi^*$ transition or pH sensitive amine transitions. Fig. 5.6 illustrates the C(17) substituent orientations relative to the C(17) carbonyl substituent C(15) = O(16) in amoxycillin and ampicillin (the D epimers of amino-hydroxybenzyl penicillin and phenylacetamido penicillanic acid respectively), (James, Hall and Hodgkin, (1968)⁴¹ Boles and Girven, (1976a)³⁴ and Boles, Girven and Gane, (1978)⁴⁰, in which it can be seen that any CE due to the carbonyl chromophore should exhibit very little difference between like isomeric configurations of the two compounds, thus, again confining the 270-278 nm absorption band as representative of weak benzene or amine transitions as described above.

- Atomic sites for
the D-epimers :
-  Amoxicillin,
 -  Ampicillin,
 -  Amoxicillin/ampicillin
joint occupation.



Conformation of the C(15)=O(16) chromophore with respect
to C(17) substituents in amoxicillin and ampicillin.

Fig.5.6

* CD is sensitive to relative configuration of those chromophores in the immediate vicinity of C(17). Since two of the chromophores are carbonyl groups and, therefore, identical, C(17) can be regarded as not constituting an asymmetric centre for the purpose of CD measurements.

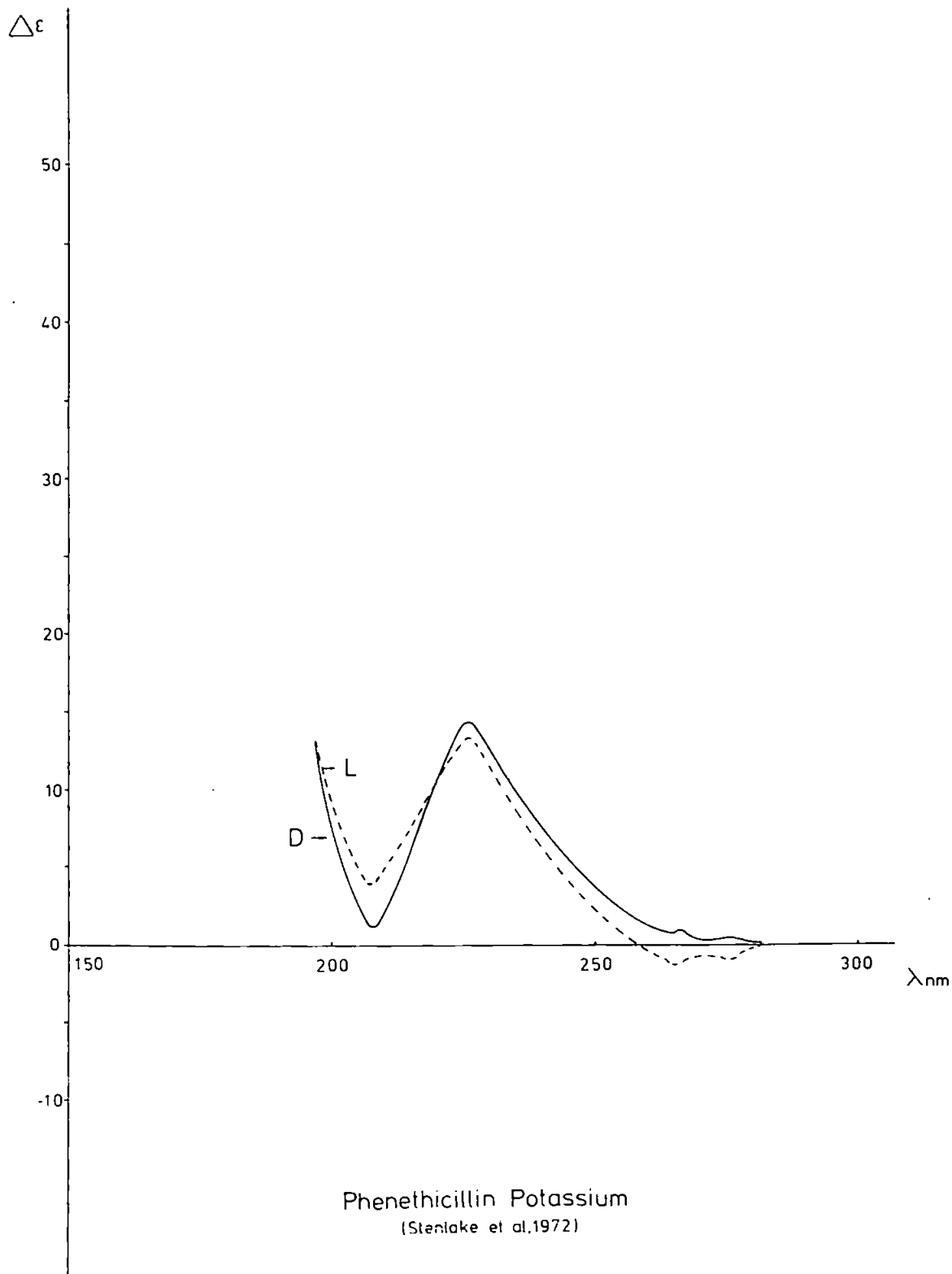
The tyrosyl penicillin provides the opportunity to study the CD spectrum of a derivative very similar to amino-hydroxybenzyl penicillin and amino-phenylacetamido penicillanic acid but with chromophoric insulation of the benzene ring by the intervening C(17) substituent methylene group. The spectrum shown in CD(5) exhibits no reversal of CE between the D and L forms ie. the insulation of the benzene has removed any CE sensitivity to side chain configuration within the recorded wavelength range, and thus, it can be concluded that both the long and short wavelength absorption bands are associated with π electron transitions of the benzene chromophore. Some reduction in the (+)ve $\Delta\epsilon$ at 190-195 nm for the L form could be attributed to the carbonyl or amine chromophores.

The absence of CE reversal between the spectra for D and L phenethicillin potassium in the short wavelength band would indicate that either some mixing of the absorption by the amine substituent, present in the above compounds, but replaced by a methyl group in phenethicillin, or the remoteness of the benzene due to the intervening oxygen, have a marked effect on the benzene absorption at this wavelength.

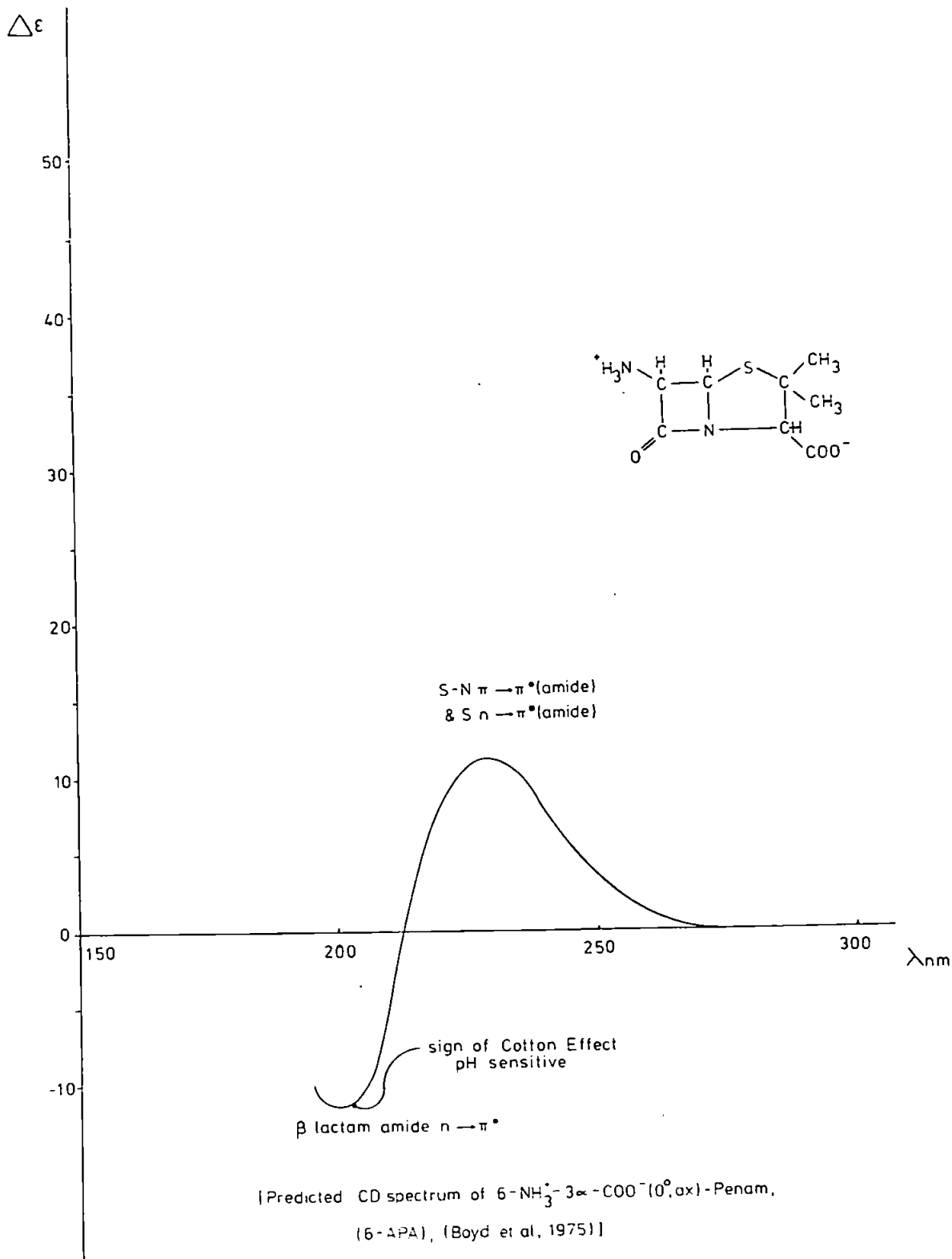
The methyl, ethyl and phenyl esters of carbenicillin show distinctive (-)ve CE's at 206-208 nm, in fresh solution, similar to the D forms, amoxicillin and ampicillin. Although C(17) does not constitute an asymmetric centre in the case of carbenicillin,* the short wavelength CE is sensitive to mutarotation. CD(6), CD(7) and CD(8) show the CD spectra of the methyl, ethyl and phenyl esters respectively, in fresh solution and subsequently at 10, 20 and 30 minutes and after 24 hours. All three esters exhibit mutarotation and the (-)ve CE at 206-208 nm in fresh solution virtually disappears when equilibrium is reached between the two side chain substituent configurations in good agreement with the H^1 n.m.r. spectra previously discussed. The phenyl ester reaches equilibrium more rapidly than either the methyl or ethyl esters

suggesting that the mechanism is susceptible to the molecular environment. The CD spectra, recorded at 27°C show slower rates of equilibration than those recorded at 35°C for the methyl and ethyl esters during H¹ n.m.r. studies. Hence, the mechanism would appear to involve the temporary separation of the mildly acidic hydrogen H(C(17)), as suggested in the model previously used to describe the anomalous behaviour of the H¹ n.m.r. spectrum of the phenyl ester after equilibration, (§. 5.3).

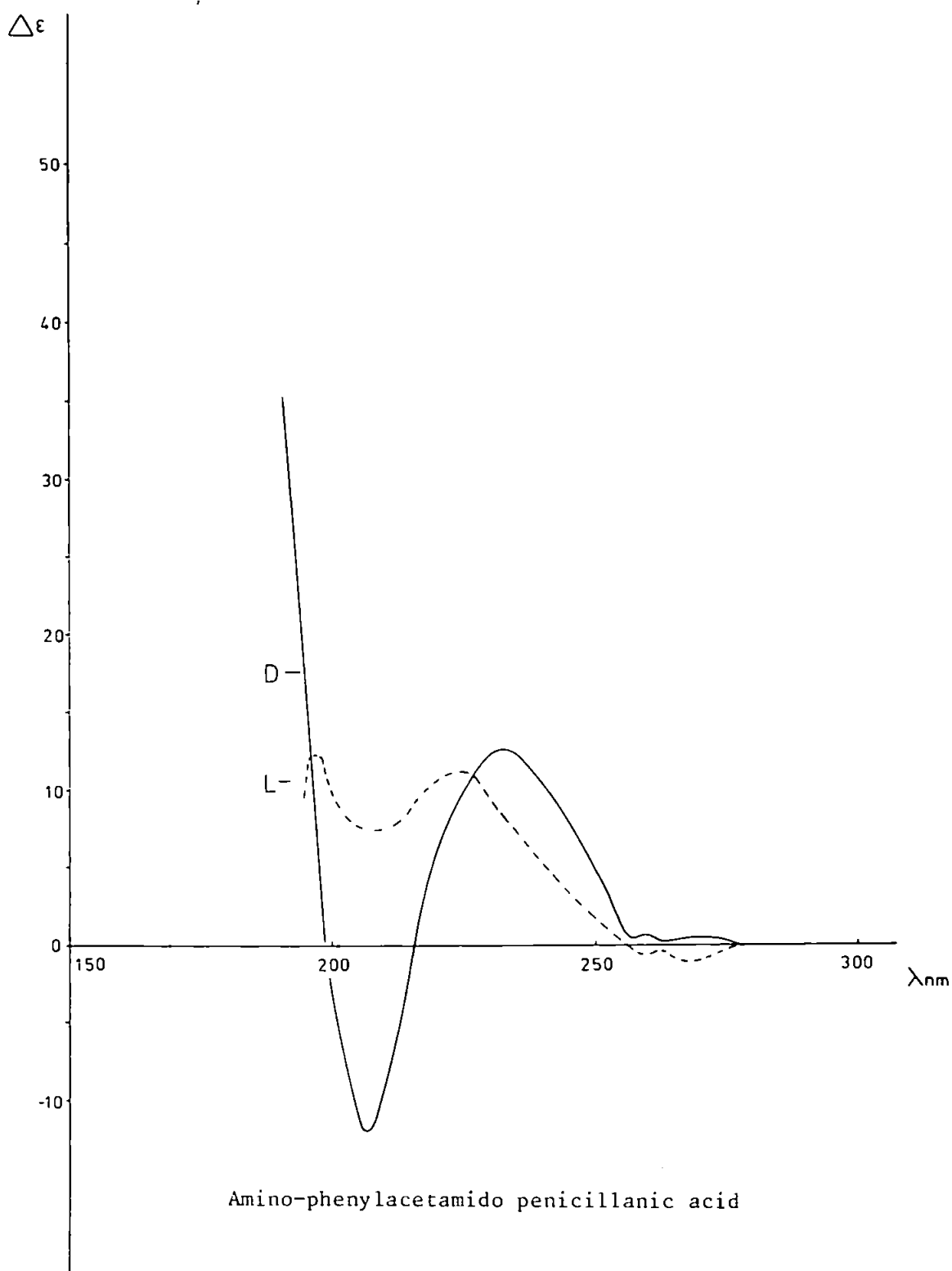
The $\Delta\epsilon$ values for the salient CE's for the D and L epimers of amino-phenylacetamido penicillanic acid, amino-hydroxybenzyl penicillin, the tyrosyl penicillin and the methyl, ethyl and phenyl esters of carbenicillin are given in Table 5.2; the spectra being recorded in aqueous solution at 27°C.



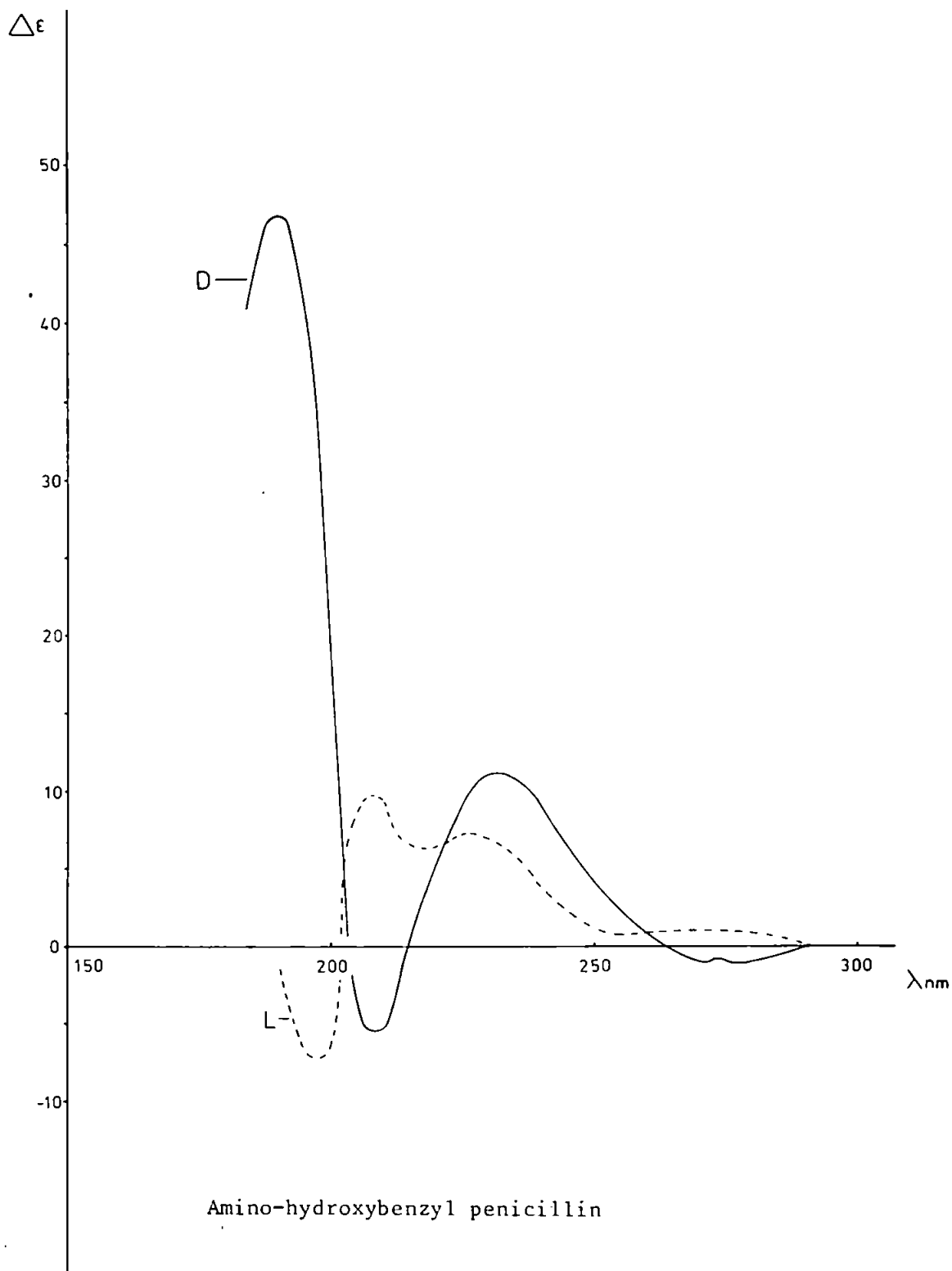
CD(1)



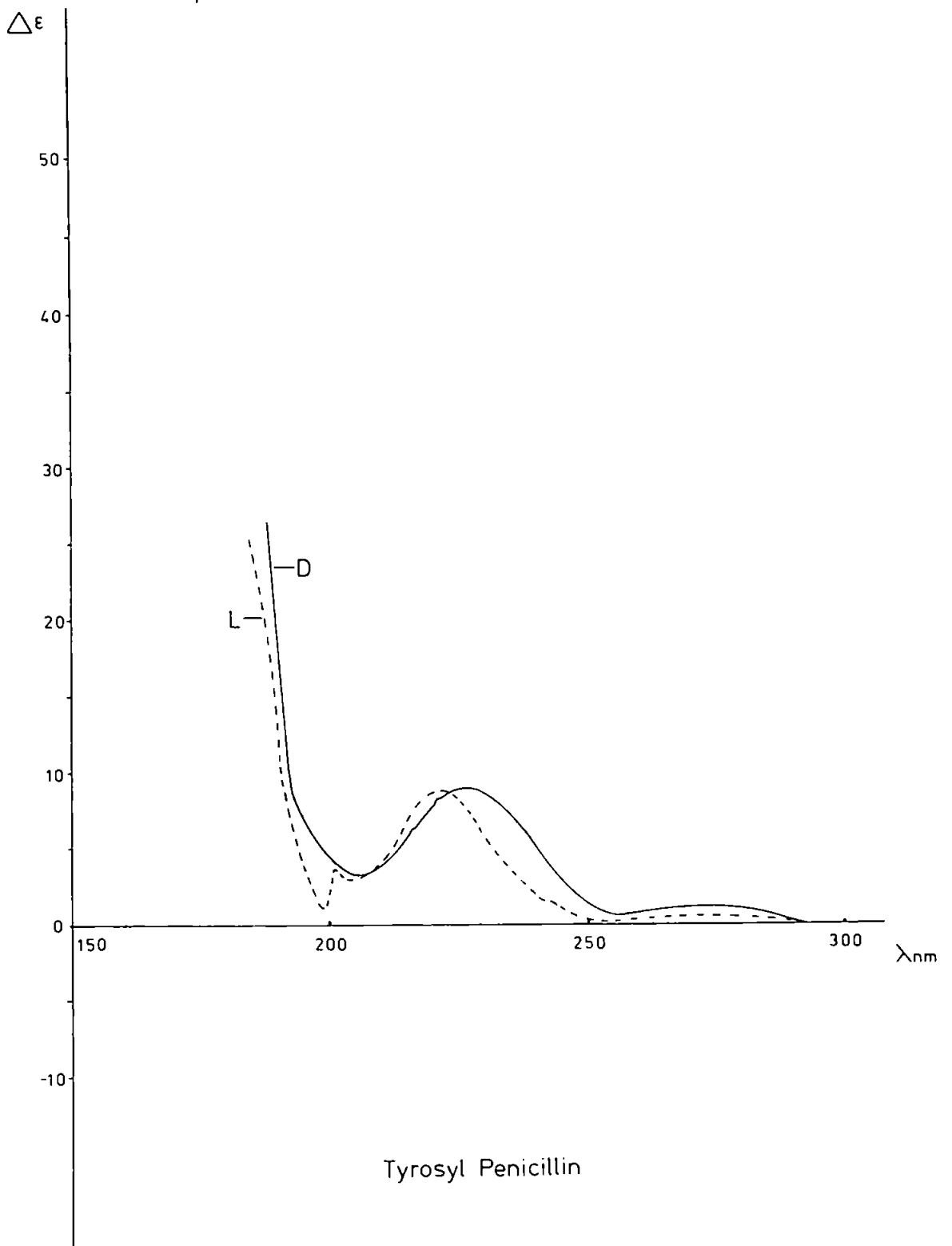
CD (2)



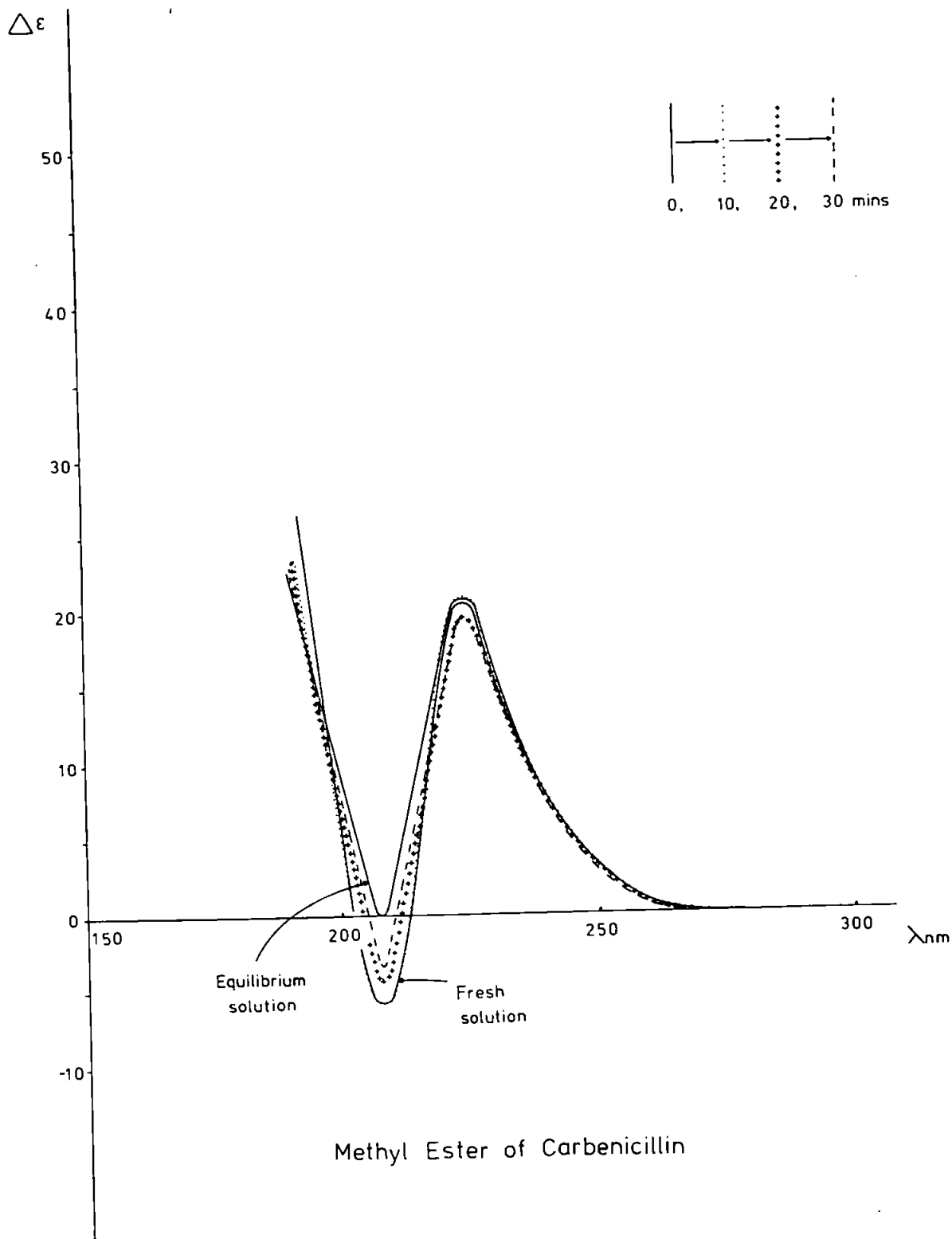
CD(3)



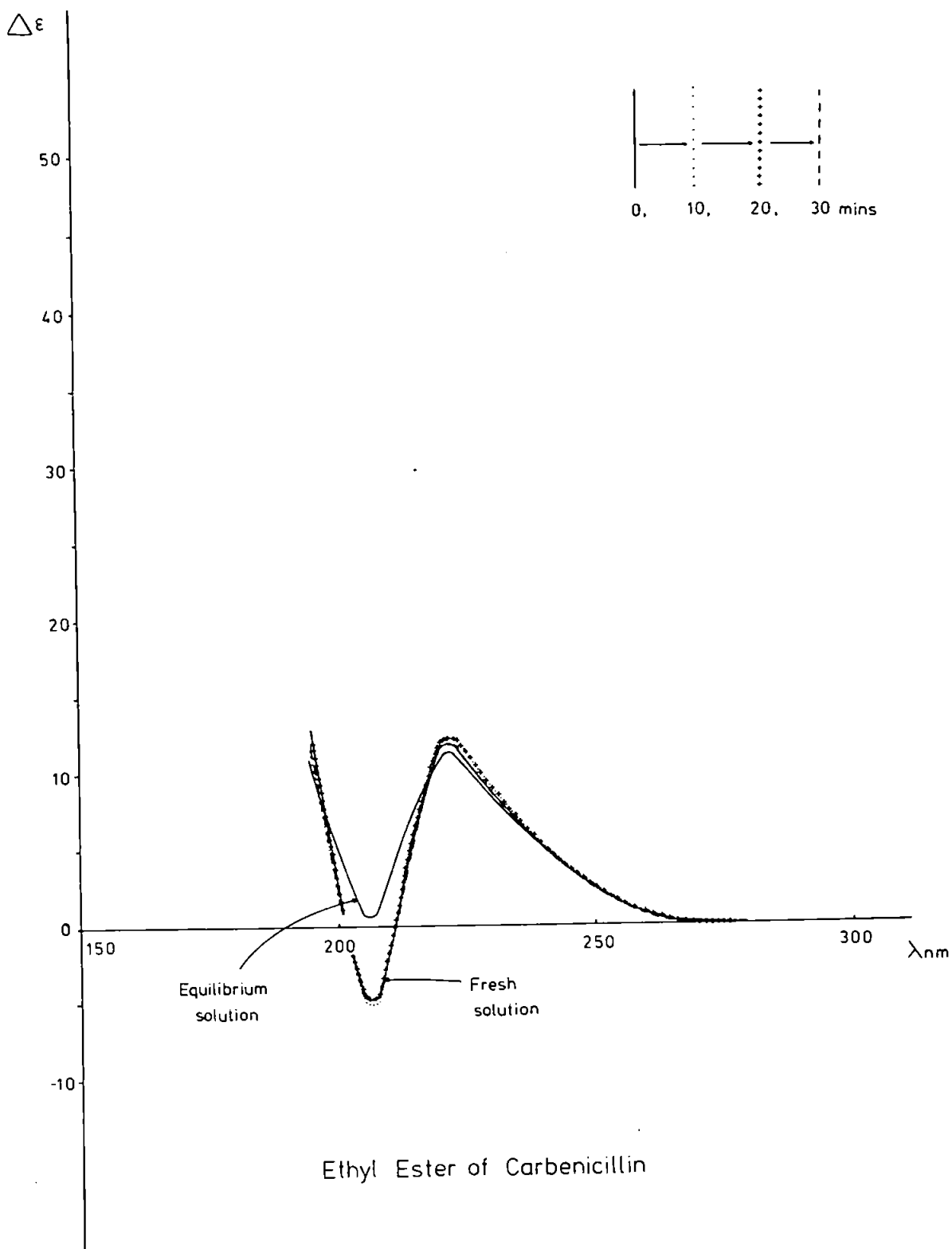
CD(4)



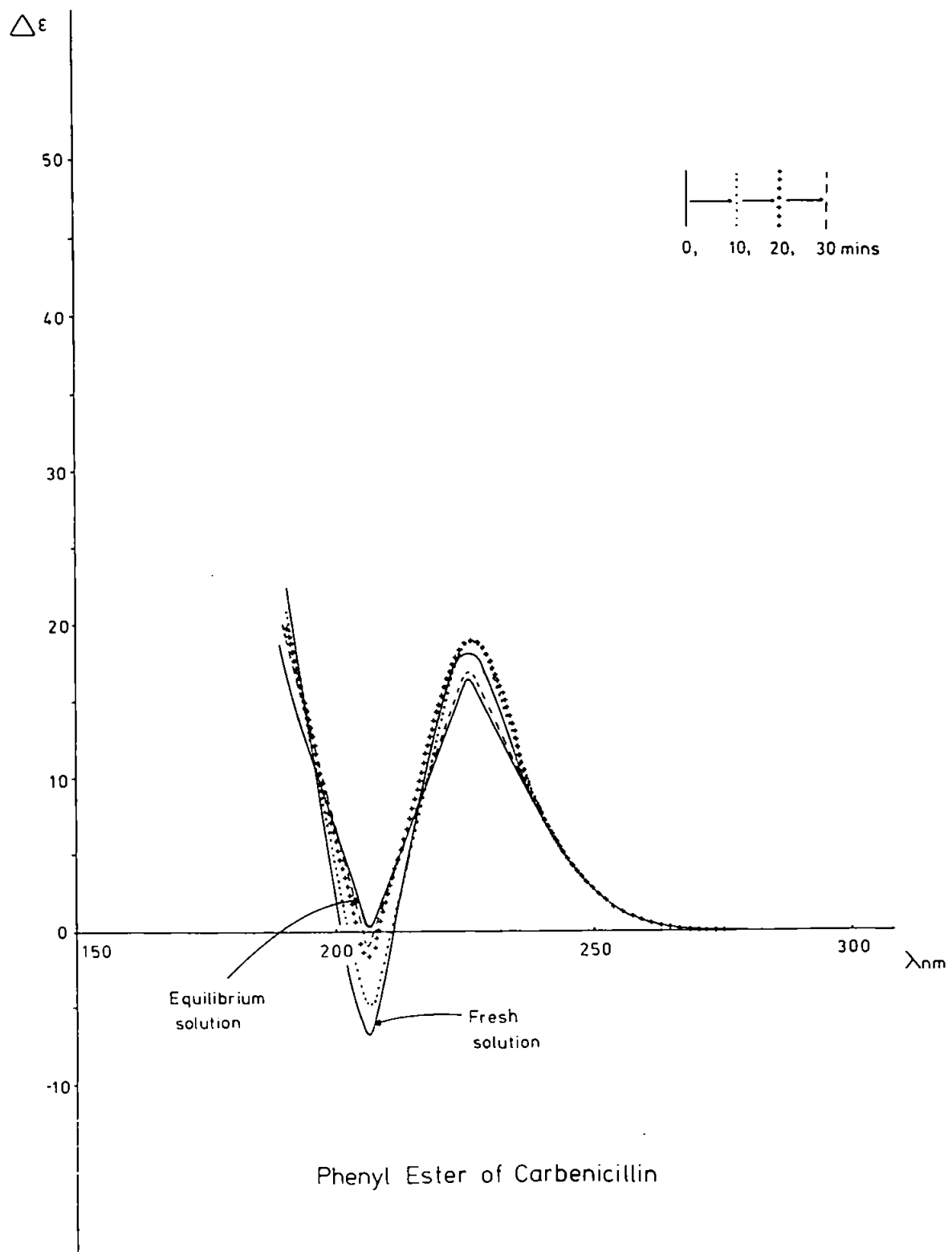
CD (5)



CD(6)



CD (7)



CD(8)

Table 5.2. Circular dichroism data for the principal Cotton Effects of the following penicillin derivatives in aqueous solution at 27°C. The units of the molar extinction coefficient, ϵ , are given in $\text{dm}^3 \text{mol}^{-1} \text{cm}^{-1}$, where $\Delta\epsilon [=(\epsilon_L - \epsilon_R)]$ expresses the difference in absorption between left and right circularly polarised light.

	$\Delta\epsilon$	$\lambda(\text{nm})$
D-Tyrosyl penicillin monohydrate	+ 0.29	275
	+ 8.75	235
	+ 7.10	221
	+ 5.74	217
	+ 7.38	195*
L-Tyrosyl penicillin trihydrate	+ 0.15	275
	+ 7.46	228
	+ 3.37	202
	+10.10	190*
D-Amino-phenylacetamido penicillanic acid anhydrate (Ampicillin anhydrate)	+ 0.64	268
	+ 0.96	260
	+12.48	232
	-10.24	206
	+ 4.16	195*
D-Amino-phenylacetamido penicillanic acid trihydrate (Ampicillin trihydrate)	+ 0.34	267
	+ 0.67	259
	+12.73	232
	-11.39	206
	+29.82	192*
L-Amino-phenylacetamido penicillanic acid trihydrate	- 0.31	266
	- 0.13	261
	+10.59	224
	+11.65	198*
D-Amino-hydroxybenzyl penicillin trihydrate (Amoxycillin trihydrate)	- 0.49	278
	- 0.74	270
	+10.83	234
	- 6.40	207
	+46.25	190*
L-Amino-hydroxybenzyl penicillin trihydrate	+ 0.96	275
	+ 2.89	243
	+ 7.45	226
	+ 9.62	208
	- 7.45	198*

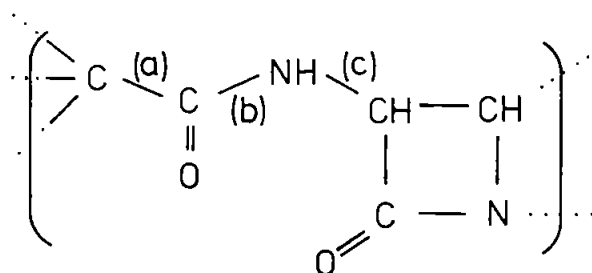
* denotes the shortest recorded wavelength

5.5 Further possibilities for conformational change outside the penicillin nucleus

The discussion related to the spectroscopic evidence above has been confined to a description of the relative orientation of side-chain substituents of C(17) only. It has been suggested, (§. 5.3), that this description is satisfactory in explaining the characteristic behaviour of the β lactam proton resonance and precludes the possibility of changes in conformation elsewhere within the molecule.

It is of interest to speculate what other possible conformational changes might take place in solution and how, if at all, such changes would be reflected in the relevant proton resonance and circular dichroism spectra.

The penicillin derivatives used in the previous discussion, (§. 5.2, 5.3, and 5.4), all have the common side-chain and β lactam constituents, with bonds labelled (a), (b) and (c) for convenience.



The constraining nature of the interstitial carbonyl group in the side-chain provides conformational stability of the bonds (a) and (b), where (b) takes on the nature of an amide-carbonyl bond common to rigid chain protein structures. Thus, possible conformational change of the side-

chain is limited to bond (c) where linkage is made with the β lactam of the penicillin nucleus. Rotation about (c) is, however, a remote possibility due to the constraints applied by possible repelling effects of the carbonyl groups in the side-chain and β lactam respectively.

Any progressive change of conformation of the side-chain in solution would be evidenced in both the proton resonance and circular dichroism spectra by either a superposition of shielding and unshielding effects or a progressive change in Cotton Effect for all the penicillin derivatives.

Free rotation of the side-chain in solution would result in the characteristic β lactam proton resonance being time averaged between the shielded and unshielded extrema.

It may therefore be concluded that the discrete nature of the differences in the respective H^1 n.m.r. and CD spectra of the D and L side-chain C(17) epimers precludes interpretation which does not include the constraints of rigidity within the side-chain substituents of the stable diastereoisomeric configurations.

APPENDIX A

COMPUTER PROGRAMS FOR THE CALCULATION OF
ORTHORHOMBIC PATTERSON FUNCTION, (1), AND ELECTRON DENSITY
FOURIER SYNTHESIS, (2), IN SPACE GROUP P2₁2₁2.

FORTRAN COMPILATION BY #XFAT MK 5A DATE

```
0001            LIST  
0002            WORK(ED,ICLF-DEFAULT)  
0003            PROGRAM(GANE)  
0004            INPUT 1,2=CRO  
0005            OUTPUT 1=LP1  
0006            OUTPUT 2=TP6  
0007            COMPILER INTEGER AND LOGICAL  
0008            TRACE 2  
0009            END
```

Program (1)

```

0010      MASTER PATT
0011      C
0012      C      PATTERN FUNCTION FOR ORTHORHOMBIC SYSTEM
0013      C
0014      DIMENSION NA(2000),NK(2000),NL(2000),FOPSS(2000)
0015      DIMENSION COSRU(11,11),COSRV(31,31),COSRW(31,31)
0016      DIMENSION NPATT(31),FPATT(31,31,10)
0017      DIMENSION FSCAT(10),F(5),NPATT(31)
0018      DIMENSION LINE(31)
0019      DIMENSION FIMH(2000)
0020      READ (2,303) MAST,IBLK
0021      303  FORMAT(2A3)
0022      C      READ IN ATOM TYPE AND TEMPERATURE FACTOR
0023      READ(2,5) NTYPE,BETA
0024      5    FORMAT(15,F10,5)
0025      WRITE(3,600) NTYPE,BETA
0026      600  FORMAT(24H SHARPENDING ATOM TYPE = ,15,4X,5H B = ,F10,5)
0027      C      READ IN UNIT CELL DIMENSIONS
0028      READ(2,10) A,B,C
0029      10   FORMAT(3F10,3)
0030      ASQ = A**2
0031      BSQ = B**2
0032      CSQ = C**2
0033      C      READ IN SCATTERING FACTORS
0034      DO 100 J = 1,5
0035      READ(2,10) F
0036      10   FORMAT(13)
0037      FJ = 14-N*14
0038      LUT = IFIX((FJ+1.5))
0039      DO 200 I = 1,14
0040      FI = LUT + I
0041      READ(2,3) FSCAT(FI)
0042      3    FORMAT(F10,3)
0043      200  CONTINUE
0044      100  CONTINUE
0045      FURIS = 0
0046      FURK = 0
0047      NA = 1
0048      NPATT(1) = 0
0049      C      READ IN H,K,L AND OBSERVED F(HKL)
0050      11   READ(2,70) J,K,L,F100
0051      70   FORMAT (3I5,F9,5)
0052      IF(J=000) GOTO 300
0053      3    SCALE = F100
0054      DO 10 11
0055      10   IF(J=000) GOTO 200
0056      C      CALCULATE S11(THETA)/LAMBDA FOR HKL REFLECTION
0057      9    DJKL = SQRT((J**2/ASQ) + (K**2/BSQ) + (L**2/CSQ))
0058      IF(J=000) GOTO 300
0059      IF(J=001) GOTO 300
0060      DO 10 101
0061      100  NA = NA + 1
0062      NPATT(NA) = DJKL
0063      301  SINLAM = 0.5 * DJKL
0064      NDIR = NDIR + 1
0065      NH(DIR) = J
0066      NK(DIR) = K
0067      NL(DIR) = L
0068      C      INTERPOLATE SCATTERING FACTOR FOR INCREASING THETA
0069      RANGE = 0.05
0070      N = 1
0071      17   IF(SINLAM-RANGE) 14,14,16
0072      16   RANGE = RANGE + 0.05

```

```

0073          N = N + 1
0074          GO TO 17
0075          DO 14 H = 1, 5
0076          FU = 14 * MN - 14
0077          HWT = FIX(FU * 0.5)
0078          NU = HWT + 1
0079          F(HH) = 20 + (FSCAT(HH) - FSCAT(HH + 1)) * (RANGE - SINLAM) + FSCAT(HH + 1)
0080          15 CONTINUE
0081          C SHARPE THE OBSERVED F(HKL)
0082          FUS = FORS / SCALE
0083          FUBS = FOBS / F(CTYPE) * EXP(BEYTA * SINLAM * SINLAM)
0084          FUIS = FOBS * FUS
0085          C REDUCE THE SYMMETRY FACTOR FOR H, K OR L = 0
0086          IF(J) 52, 53, 52
0087          53 FUBS2 = 0.5 * FUBS2
0088          52 IF(K) 54, 55, 54
0089          55 FUBS2 = 0.5 * FUBS2
0090          54 IF(L) 56, 57, 56
0091          57 FUBS2 = 0.5 * FUBS2
0092          56 FUIS2 = FUBS2 * FUIS
0093          FUBSS(NH) = FUBS2
0094          GO TO 11
0095          C SET UP TRIGONOMETRIC ARRAYS
0096          16 NA = N + 1
0097          WRITE (5, 400) NA
0098          400 FORMAT (10H NA = 14X N + 2 = , I5)
0099          NULH(1) = NU * 4
0100          DO 61 I = 1, 51
0101          DO 61 IJ = 1, 51
0102          FI = I - 1
0103          FJ = IJ - 1
0104          COSA(I, IJ) = COS(0.104719 * FI * FJ)
0105          COSA2(I, IJ) = COS(0.209439 * FI * FJ)
0106          61 CONTINUE
0107          60 CONTINUE
0108          DO 211 I = 1, 11
0109          DO 211 IJ = 1, 11
0110          FI = I - 1
0111          FJ = IJ - 1
0112          COSA(K, IJ) = COS(0.314159 * FI * FJ)
0113          201 CONTINUE
0114          202 CONTINUE
0115          C CALCULATE PATTERSON FUNCTION IN VV PLANE FOR BLOCKS OF H
0116          NJI = IN(NH) + 1
0117          WRITE (5, 410) NJI
0118          410 FORMAT (10H NJI = 14X I + 1 = , I5)
0119          DO 972 JI = 1, 51
0120          DO 971 JI = 1, 51
0121          DO 973 NI = 1, NJI
0122          NI = NI + 1
0123          NU = INH(NI) + 1
0124          NU = INH(43 + 1)
0125          IF (10 * ST .AND. 3) TO 101)
0126          DO 974 I = NI, NU
0127          NI = IN(I) + 1
0128          NLI = NL(I) + 1
0129          FPATT(NV, NI, NU) = FPATT(NV, NI, NI) + FOBS(I) * COSRV(NKI, NU)
0130          C *COSRV(NLI, NU)
0131          904 CONTINUE
0132          903 CONTINUE
0133          901 CONTINUE
0134          902 CONTINUE
0135          DO 300 JU = 1, 11
0136          WRITE (3, 307)
0137          307 FORMAT ('1', /)
0138          NTH = NU + 1
          WRITE (3, 306) NTH

```

```

0139      306      FORMAT(1X,134 SECTION J = ,13)
0140      DO 302 NW = 1,31
0141      DO 301 I = 1,31
0142      WPATT(I) = 0
0143      700      CONTINUE
0144      DO 302 NW = 1,31
0145      DO 302 IB = 1,31
0146      C      CALCULATE THE PATTERSON FUNCTION
0147      WPATT(NV) = WPATT(NV) + COSRU(MH,NU)*FPATT(NV,NW,MB)
0148      402      CONTINUE
0149      C      PRINT OUT A GRID REPRESENTING THE AMPLITUDE (● REFERS TO >99)
0150      WPATT(NV) = IFIX((WPATT(NV)*99./FORIG*10.) + 0.5)
0151      LINE(NV) = 13LK
0152      IF (WPATT(NV).GT.99) GO TO 500
0153      IF (WPATT(NV).LT.-99) GO TO 501
0154      GO TO 301
0155      500      WPATT(NV) = 99
0156      LINE(NV) = NAST
0157      GO TO 301
0158      501      WPATT(NV) = -99
0159      LINE(NV) = NAST
0160      301      CONTINUE
0161      WRITE(3,309) (WPATT(I),I = 1,31)
0162      309      FORMAT('D',3115)
0163      WRITE(3,702) (LINE(I),I = 1,31)
0164      702      FORMAT(' ',31A3)
0165      302      CONTINUE
0166      300      CONTINUE
0167      1000     STOP
0168      END

```

END OF SEGMENT, LENGTH 992, NAME PATT

Program (1) performs the computation of the function

$$P(u,v,w) = \frac{8}{V} \sum_{(hkl)} |F(hkl)|^2 \cos 2\pi hu \cos 2\pi kv \cos 2\pi lw$$

... Eqn A.1

for all observed reflexions (hkl) at discrete chosen values of (u,v,w). The output format is that of a discrete plot of P(u,v,w) over a 31 x 31 array of points (v,w) for 11 fixed values of u, ranging one quarter of the unit cell.

<u>FORTTRAN ARRAY VARIABLE</u>	<u>DEFINITION</u>
NH(I)	Reflexion indices h
NK(I)	k
NL(I)	l
COSRU(I,J)	Discrete values of the cosine components in Eqn A.1.
COSRV(I,J)	
COSRW(I,J)	
UPATT(I)	Values of the Patterson function during synthesis.
FPATT(I,J,K)	
FSCAT(I)	Scattering factors used in the Sharpening function.
F(I)	Value of scattering factor for given Bragg angle.
NPATT(I)	Integer value of scaled Patterson function.
LINE(I)	Overprint variable of NPATT(I).
NUMH(I)	Number of reflexions of given h index.
<u>LINES</u>	
14	Set array variable dimensions.
:	
19	
20	Input NAST as ** and IBLK as 'blank'.
21	
22	Input the element (NTYPE), used as the average scattering atom, whose scattering factors are used in the sharpening process, and an average isotropic temperature factor (BETA).
:	
:	
26	
27	Input unit cell dimepsions. (D = a, E = b, C = cA)
:	
32	

33 Input scattering factors (Int. Tables for
: X-ray Crystallography Vol. 3.) in order of
44 atom type 1...5.

45 Set variables FORIG (value of Patterson
: function at the origin) and counters NUMR
48 (number of input reflexions), MA and NUMH(I).

49 (hkl) and observed $|F_0(hkl)|$ read in as variables
: J,K,L, and FOBS.
51

52 If J is given the value of 100, FOBS is the
53 layer scale factor for given data.
54

55 Test for J = 999 as end of reflexion data flag.

56 Calculates d_{hkl} as DJKL and places hkl data
: in layers of given h provided input is also
67 in layers of given ascending h.

68 Interpolates the scattering factor data for
: that value of $(\sin\theta)/\lambda$, for reflexion hkl,
80 using a difference formula.

81 Applies the Sharpening factor (if required)
: as expressed in Eqn. 1.64.
84

85 Applies symmetry reduction factor to $|F_0(hkl)|^2$
: for h, k or l = 0.
91

92 Sums contribution by $|F_0(hkl)|^2$ at the origin.

93 Places Patterson coefficients in array for
94 each reflexion.

95 Calculates discrete values of $\cos 2\pi kv$ and
: $\cos 2\pi \ell w$ for arrays of $\left. \begin{matrix} k \\ \ell \end{matrix} \right\} 0 \dots 30$
: and $\left. \begin{matrix} v \\ w \end{matrix} \right\} 0 \dots 30$
114

115 Calculates the Patterson function at discrete
: values of (v,w) for blocks of fixed h index,
133 excluding u variation.

134 Print section U = section number heading.
:
139

140 Sets up nested DO LOOPS for output map.
:
145

146
:
:
148

149
:
:
:
:
:
:
168

Calculates the Patterson function for varying discrete u levels.

The value of the Patterson function is scaled such that $P'(u,v,w) = \frac{P(u,v,w) \times 99}{P(0,0,0) \times 10}$ and then output as an integer. If $|P'(u,v,w)| > 99$, then $P'(u,v,w)$ is set to 99 and overprinted by **. This scaling was found the most convenient for the problem in hand.

Program-(2)

```

0010      MASTER SFED
0011      C
0012      C      P4(1)2(1)2
0013      C
0014      DIMENSION X(100),Y(100),Z(100),FSCAT(100)
0015      DIMENSION AFUD(31,11),BFUD(31,11),APUD(31,11),BPUU(31,11)
0016      DIMENSION A(2000),B(2000)
0017      DIMENSION AZ(2000),BZ(2000),WK(2000)
0018      DIMENSION NL(2000),NPAR(2000),NH(12),NUMH(12)
0019      DIMENSION HTYPE(100),F(5),COSRA(31,61),COSRX(11,21),SINRX(11,21)
0020      DIMENSION SINRA(31,61),NGRID(10600),GRID(11,31)
0021      NUT = 1
0022      DO 110 I = 1,31
0023      DO 115 J = 1,11
0024      AFUD(I,J) = 0
0025      BFUD(I,J) = 0
0026      APUD(I,J) = 0
0027      BPUU(I,J) = 0
0028      115 CONTINUE
0029      110 CONTINUE
0030      SCALE = 1.0
0031      DO 111 I=1,2000
0032      AZ(I)=1
0033      BZ(I)=1
0034      WK(I)=0
0035      NL(I)=0
0036      NPAR(I)=0
0037      A(I)=0
0038      B(I)=0
0039      111 CONTINUE
0040      DO 230 I=1,11
0041      DO 231 J=1,31
0042      NGRID(I,J)=0
0043      231 CONTINUE
0044      230 CONTINUE
0045      DO 112 I=1,12
0046      NH(I)=1
0047      NUMH(I)=0
0048      112 CONTINUE
0049      NY=1
0050      J=1
0051      IJ=1
0052      NINI=200
0053      TUNE=0
0054      TIME=0
0055      N=1
0056      5 READ(2,101) X(N),Y(N),Z(N),HTYPE(N)
0057      WRITE(3,101) X(N),Y(N),Z(N),HTYPE(N)
0058      101 FORMAT(3F7.4,15)
0059      L=N
0060      N=N+1
0061      IF(X(L)-2)5,2,2
0062      2 NA=N-2
0063      READ(2,102) D,E,C
0064      102 FORMAT(3F10.5)
0065      ASQ=D*D
0066      BSQ=E*E
0067      CSQ=C*C
0068      DU=3 NH=1,5
0069      READ(2,104)N
0070      104 FORMAT(I3)
0071      FUM=14*N-14
0072      NUT= IFIX(FUM*.5)

```

```

0073      DO 6 I=1,14
0074      N1 = IJT+1
0075      READ(2,103) FSCAT(IH)
0076      6 CONTINUE
0077      3 CONTINUE
0078      103 FJRIAT(F10,3)
0079      11 READ(2,105) J,K,L,FOBS
0080      105 FJRIAT(313,14,2)
0081      IF(J-1)GOTO 7,4,7
0082      4 SCALE=FJRS
0083      GO TO 11
0084      7 IF(J-909) GOTO 9,10,9
0085      9 DJKL=SQRT(J+J/350+K+K/350+L+L/350)
0086      STILLA=(J+K+L)/4.0
0087      RANGE = 0.35
0088      V=1
0089      17 IF(STILLA-RANGE) 14,14,16
0090      16 RANGE=RANGE+.35
0091      V=V+1
0092      GO TO 17
0093      14 GO 15 I=1,5
0094      FJ=14+I-14
0095      QUT=IFIX(FJ+.5)
0096      V=IJT+V
0097      F(IH)=20*(FSCAT(QU)-FSCAT(IQ+1))*(RANGE-STILLA)+FSCAT(IQ+1)
0098      15 CONTINUE
0099      SUMFA=0
0100      SUMFB=0
0101      DO 13 I=1,14
0102      FJNL=(J+K+L)/4.0
0103      C1I=(K+L)/4.0
0104      C1KFE=L+20.0
0105      G=4*C1I*(6.283185+C1NF)*COS(6.283185*C1KFE)+C1I*(6.283185+C1KFE)
0106      H=4*C1I*(6.283185+C1NE)*SIN(6.283185+C1I)+C1I*(6.283185+C1KFE)
0107      QH=HTYPE(I)
0108      SUMFA=SUMFA+F(IH)*G)
0109      SUMFB=SUMFB+F(IH)*H)
0110      13 CONTINUE
0111      FINT=SQRT((SUMFA+SUMFB)*(SUMFB+SUMFB))
0112      FINT = FINT/EXP(5.0*SINLAM*SINLAM)
0113      FPAR=0.3 + FINT
0114      IF(FINT-FPAR)11,11,21
0115      ACCEPT FOBS IF FINT.GT.0.3*FOBS
0116
0117      21 SUMFA = FOBS*SUMFA/FINT
0118      SUMFB=FOBS*SUMFB/FINT
0119      NK(IJ)=K
0120      NL(IJ)=L
0121      JKSUM=J+K
0122      IF(K=NYIX) GOTO 197,197
0123      197 NYIX = K + 1
0124      23 IF(JKSUM)24,25,26
0125      25 NPAR(IJ)=1
0126      GO TO 27
0127      24 NPAR(IJ)=2
0128      GO TO 27
0129      26 JKSUM=JKSUM-2
0130      GO TO 23
0131      27 NK(IJ)=NK(IJ)+1
0132      NL(IJ)=NL(IJ)+1
0133      IF(J=NINI)31,32,31
0134      31 NH(I) = J + 1
0135      IF(IJ-1)41,42,41
0136      41 NUMH(I-1)=NH(I)
0137      42 NH(I)=J
0138      NUM=1

```

```

0134          I=I+1
0140          GO TO 43
0141          32 NUH=NUMI+1
0142          43 IF(J) 52,53,54
0143          53 SU1FA=0.5 * SUMFA
0144          SU1FB=0.5 * SUMFB
0145          52 IF(NK(IJ)-1) 54,55,54
0146          55 SU1FA=0.5 * SUMFA
0147          SU1FB=0.5 * SUMFB
0148          54 IF(L)191,192,191
0149          192 SU1FA=0.5*SUMFA
0150          SU1FB=0.5*SUMFB
0151          191 A(IJ)=SUMFA
0152          R(IJ)=SUMFB
0153          IJ=IJ+1
0154          GO TO 11
0155          10 NUH(I-1) = NUH
0156          IJ = IJ - 1
0157          WRITE (7,301) IJ
0158          301 FORMAT(10)
0159          NU1=I-1
0160          DO 60 I=1,NU1
0161          DO 61 J=1,NU1
0162          FI=I-1
0163          FJ=J-1
0164          COSRA(I,J)=COS(0.10472 * FI * FJ)
0165          SINRA(I,J) = SIN(0.10472 * FI * FJ)
0166          61 CONTINUE
0167          60 CONTINUE
0168          DO 200 I=1,11
0169          DO 201 J=1,21
0170          FI=I-1
0171          FJ=J-1
0172          COSRX(I,J)=COS(.314159 * FI * FJ)
0173          SINRX(I,J) = SIN(.314159 * FI * FJ)
0174          201 CONTINUE
0175          200 CONTINUE
0176          DO 70 IZ=1,31
0177          NZTLF=2*-IZ-1
0178          NZZ=IZ-1
0179          WRITE(7,199) NZZ
0180          199 FORMAT(I)
0181          DO 70 I=1,IJ
0182          JL = JL(I)
0183          AZ(I)=A(I)*COSRA(NC,NZTLF)
0184          BZ(I)=B(I)*SINRA(NC,NZTLF)
0185          70 CONTINUE
0186          I = 1
0187          DO 31 JK = 1,NUMI
0188          JK = I(JK)
0189          IS = NUMB(JK)
0190          DO 83 KL = 1,IS
0191          KT = NK(I)
0192          IF(NPAR(I) - 1) 92,92,91
0193          APJD(KT,JK) = APUD(KT,JK) + AZ(I)
0194          BPJD(KT,JK) = BPUD(KT,JK) + BZ(I)
0195          GO TO 95
0196          91 APJD(KT,JK) = APUD(KT,JK) + AZ(I)
0197          BPJD(KT,JK) = BPUD(KT,JK) + BZ(I)
0198          93 I = I + 1
0199          83 CONTINUE
0200          81 CONTINUE
0201          DO 80 IY = 1,31
0202          IYY = IY - 1
0203          DO 300 JK = 1,NUMI
0204          DO 164 I00 = 1,NYMX

```

```

0205      JN = 01(JY)
0206      TUNE=TONE*APUD(I0U,JN)*COSRA(I0J,NY)
0207      C =BFUD(I0U,JN)*COSRA(I0U,NY)
0208      T10U=TT0U*BPUD(I0U,JN)*SINRA(I0J,NY)
0209      C =AFUD(I0U,JN)*SINRA(I0U,NY)
0210      164  CUITI4JE
0211          DU 203 IXX = 1,11
0212          GRID(IXX,XY) = GRID(NXX,NY) + (COSRX(JN,NXX)*TUNU)
0213          C * (SINRX(JN,NXX)*TTUO)
0214      203  CUITI4JE
0215          TUNE = 0
0216          T10U = 0
0217      300  CUITI4JE
0218      80  CUITI4JE
0219          DU 500 I0U = 1,NYMX
0220          DU 501 JK = 1,0U:1
0221          JN = 41(JY)
0222          APUD(I0U,JN) = 0
0223          BPUD(I0U,JN) = 0
0224          AFUD(I0U,JN) = 0
0225          SFUD(I0U,JN) = 0
0226      301  CUITI4JE
0227      300  CUITI4JE
0228          DU 23 I=1,11
0229          DU 24 IP=1,31
0230          LPI=(31+.22)*9.51*(I-1)+10
0231          HURID(I,PA)=FIX(GRID(I,IP)+U,5)
0232      84  CUITI4JE
0233      83  CUITI4JE
0234          DU 450 I=1,11
0235          DU 451 J=1,31
0236          GRID(I,J) = 0
0237      431  CUITI4JE
0238      430  CUITI4JE
0239      70  CUITI4JE
0240          PA=0
0241          DU 151 I=1,100/1
0242          IF(NGRID(I)-PA)152,152,153
0243      153  PX=NGRID(I)
0244      152  CUITI4JE
0245      151  CUITI4JE
0246          T = 95/PA
0247          DU 154 I=1,100/1
0248          HGRID(I)=FIX((GPID(I)+T)
0249      154  CUITI4JE
0250          DU 211 I1=1,11
0251          Y14=4I-1
0252          WRITE(5,53)
0253      58  FUR:IAT('1',7)
0254          WRITE(7,114) 4TH
0255      114  FUR:IAT(1X,13H SECTION X = ,13)
0256          I=961+(I1-1)*1
0257      211  WRITE(7,600) (HGRID(J),J=I,961+1)
0258      400  FUR:IAT('0',5113)
0259          STOP
0260          END

```

LN11300

END OF SEGMENT, LENGTH 1865, NAME SFED

Program (2) performs the computation of the function

$$\rho(X,Y,Z) = \frac{8}{V} \left\{ \begin{aligned} &\sum_{\substack{(hkl) \\ h+k=2n}} |F(hkl)| [\cos 2\pi hX \cos 2\pi kY \cos 2\pi lZ \cos \alpha(hkl) \\ &- \sin 2\pi hX \sin 2\pi kY \sin 2\pi lZ \sin \alpha(hkl)] \\ &- \sum_{\substack{(hkl) \\ h+k=2n+1}} |F(hkl)| [\sin 2\pi hX \sin 2\pi kY \cos 2\pi lZ \cos \alpha(hkl) \\ &- \cos 2\pi hX \cos 2\pi kY \sin 2\pi lZ \sin \alpha(hkl)] \end{aligned} \right\} \dots \text{Eqn. A.2}$$

$$\text{where } \alpha(hkl) = \tan^{-1} \left(\frac{B}{A} \right) \dots \text{Eqn. A.3}$$

where A, B depend upon atom co-ordinates (x,y,z) such that

$$\left. \begin{aligned} A &= 4 \cos 2\pi \left(hx + \frac{h+k}{4} \right) \cos 2\pi \left(ky - \frac{h+k}{4} \right) \cos 2\pi lz \\ B &= -4 \sin 2\pi \left(hx + \frac{h+k}{4} \right) \sin 2\pi \left(ky - \frac{h+k}{4} \right) \sin 2\pi lz \end{aligned} \right\} \dots \text{Eqns. A.4}$$

Intensity symmetry in space group $P2_12_12$ results in

$$|F(hkl)| = |F(\bar{h}\bar{k}\bar{l})| = |F(\bar{h}k\bar{l})| = |F(h\bar{k}\bar{l})| = |F(hk\bar{l})|$$

and

$$\alpha(hkl) = -\alpha(\bar{h}\bar{k}\bar{l}) = -\alpha(\bar{h}k\bar{l}) = -\alpha(h\bar{k}\bar{l}) = -\alpha(hk\bar{l})$$

$$\forall h + k = 2n$$

and

$$\alpha(hkl) = -\alpha(\bar{h}\bar{k}\bar{l}) = \pi - \alpha(\bar{h}k\bar{l}) = \pi - \alpha(h\bar{k}\bar{l}) = -\alpha(hk\bar{l})$$

$$\forall h + k = 2n + 1$$

where n is integer.

The output format is that of a discrete plot of $\rho(X,Y,Z)$ over an array of points (Y,Z) for 11 fixed values of X, ranging one quarter of the unit cell.

FORTRAN ARRAY VARIABLE

DEFINITION

X(I)

Input atomic co-ordinates x

Y(I)

y

Z(I)

z

AFUD(I,J)

$$= \sum_{hkl} |F(hkl)| \cos \alpha(hkl) \cos 2\pi lZ \left. \vphantom{\sum_{hkl}} \right\} h + k = 2n$$

BFUD(I,J)

$$= \sum_{hkl} |F(hkl)| \sin \alpha(hkl) \sin 2\pi lZ$$

APUD(I,J)	$= \left. \begin{array}{l} \sum_{hkl} F(hkl) \cos\alpha(hkl) \cos 2\pi\ell Z \\ \sum_{hkl} F(hkl) \sin\alpha(hkl) \sin 2\pi\ell Z \end{array} \right\} h + k = 2n + 1$	
BPUD(I,J)		
A(I)	Calculated A for each reflexion.	
B(I)		B
AZ(I)	A(I) $\cos 2\pi\ell Z$	
BZ(I)		B(I) $\sin 2\pi\ell Z$
NH(I)	Reflexion indices h	
NK(I)		k
NL(I)		ℓ
NPAR(I)	Parity store distinguishing $h + k = 2n$ and $h + k = 2n + 1$.	
NUMH(I)	Number of reflexions of given h.	
NTYPE(I)	Atom type number to distinguish scattering factors.	
F(I)	Scattering factor store.	
COSRX(I,J)	Arrays of discrete values for $\cos 2\pi hX$.	
SINRX(I,J)		$\sin 2\pi hX$
COSRA(I,J)	Arrays of discrete values for $\cos 2\pi kY$, $\cos 2\pi\ell Z$	
SINRA(I,J)		$\sin 2\pi kY$, $\sin 2\pi\ell Z$
GRID(I,J)	Calculated value of $\rho(X,Y,Z)$ for fixed X	
NGRID(I)	Calculated integer value of $\rho(X,Y,Z)$ for complete map.	
<u>LINES</u>		
14	Set array variable dimensions.	
:		
20		
21	Set arrays to zero (only needed for previously occupied array storage).	
:		
48		
49	Set values for counters and end of data flag NINI = 999.	
:		
55		
56	Input atom co-ordinates x,y,z and atom type for selection of scattering factors.	
:		
62		
63	Input unit cell dimensions D = a E = b ₀ C = cÅ	
:		
67		

69
 :
 78 Input scattering factors in order of atom
 type N.

79
 :
 :
 :
 :
 :
 :
 98 Input reflexion data in terms of indices (hkl)
 and observed $|F_0(hkl)|$. Layer scale factors
 are input as F_0 data when h = 100 preceding
 each layer data batch. Scattering factors
 are difference interpolated for the calculated
 $(\sin\theta)/\lambda$ of each reflexion.

99
 :
 :
 110 Calculation of $\sum_{hkl} |F_c(hkl)|A$
 and $\sum_{hkl} |F_c(hkl)|B$

111
 :
 116 Calculated $|F_c(hkl)|$ produced and tested for
 significant contribution to observed $|F_0(hkl)|$
 using inequality Eqn. 2.8.

117
 118 If $|F_0(hkl)|$ accepted as Fourier coefficient,
 it becomes phased on the input atoms.

119
 :
 141 Parity and counters set for each reflexion.

142
 :
 :
 150 Symmetry factor reduction of A and B in the
 case of h, k or l = 0.

151
 :
 159 A and B stored in arrays A(I), B(I) and the
 number of accepted reflexions counted and output.

160
 :
 175 Discrete arrays for spatial cosine and sine
 variations calculated.

176
 :
 185 A and B are computed in conjunction with (l,Z)
 variation within the synthesis i.e.
 $\cos 2\pi lZ \cos \alpha(hkl)$ and $\sin 2\pi lZ \sin \alpha(hkl)$.

186
 :
 200 Calculation of APUD(I,J), BPUD(I,J);
 AFUD(I,J), BFUD(I,J);
 as defined in array variable, for given Z.

201
 :
 210 Calculation of terms including all Y variation
 in batches of given Z.

211
 :
 214 GRID(I,J) contains values of the synthesis
 for X and Y variation for fixed Z.

215 : 227	Disused arrays reset to zero for recycling.
228 : : : 233	Values for the completed synthesis are placed in NGRID(I) for Y = 0.....30 for each X = 0.....10 in turn for each Z = 0.....30
234 : 249	Scales the maximum value of $ \rho(X,Y,Z) $ to 99.
250 : 260	Outputs discrete values of integer $\rho(X,Y,Z)$ on 11 levels of X for a 31 x 31 array of (Y,Z) points.

APPENDIX B

LIST OF STRUCTURE FACTORS FOR

(i) SH62 P2(1)2(1)2: 7-chloro-2-methyl-5-phenyl-3-propyl[2,3-b]-imidazolyl quinoline.

(ii) SNP P2(1)/C: Methyl ester of 5,5-dimethyl-2-(2-phenoxyethyl-5-oxo-1,3-oxazolin-4-ylidene)-1,3-thiazolidine-4-carboxylic acid.

(iii) CARF P2(1): Phenyl ester of carbenicillin.

(i)

OBSERVED AND CALCULATED STRUCTURE FACTORS FOR SH6Z P2(1)2(1)2

PAGE 1

H	K	L	TOFD	TOFC	H	K	L	TOFD	TOFC	H	K	L	TOFD	TOFC	H	K	L	TOFD	TOFC	H	K	L	TOFD	TOFC
1	3	0	126	120	0	10	0	315	253	6	17	0	107	81	0	2	1	96	49	-6	6	1	120	114
2	3	0	84	77	2	10	0	453	427	0	18	0	64	56	1	2	1	485	520	-5	6	1	81	93
3	3	0	371	356	4	10	0	75	76	1	18	0	475	474	3	2	1	133	118	-4	6	1	266	250
5	3	0	229	217	6	10	0	169	148	2	18	0	255	281	5	2	1	186	168	-3	6	1	186	170
6	3	0	709	783	4	11	0	257	201	3	18	0	118	104	6	2	1	221	222	-2	6	1	198	226
8	4	0	173	66	3	11	0	236	230	6	18	0	93	85	-6	3	1	491	489	-1	6	1	308	320
1	4	0	563	651	6	11	0	194	204	1	19	0	136	135	-4	3	1	479	483	0	6	1	453	414
2	4	0	59	79	0	12	0	324	312	4	19	0	218	251	-3	3	1	324	336	1	6	1	322	304
3	4	0	437	440	1	12	0	235	252	5	19	0	61	57	-2	3	1	359	318	2	6	1	242	197
4	4	0	121	114	3	12	0	380	371	6	19	0	69	60	-1	3	1	487	492	3	6	1	203	162
6	4	0	490	494	5	12	0	136	127	0	20	0	76	75	0	3	1	58	40	4	6	1	258	246
2	5	0	121	97	6	12	0	99	102	1	20	0	317	323	1	3	1	479	493	5	6	1	97	84
3	5	0	102	80	1	13	0	389	393	2	20	0	109	92	2	3	1	361	335	6	6	1	118	116
4	5	0	177	186	2	13	0	86	81	3	20	0	124	109	3	3	1	380	326	-6	7	1	91	92
5	5	0	44	57	4	13	0	87	101	1	21	0	174	177	4	3	1	548	491	-5	7	1	307	303
6	5	0	459	479	5	13	0	97	96	3	21	0	156	157	6	3	1	442	488	-4	7	1	94	108
0	6	0	831	985	6	13	0	230	228	4	21	0	57	54	-6	4	1	384	344	-3	7	1	294	287
2	6	0	113	56	0	14	0	389	273	3	21	0	111	108	-5	4	1	178	171	-2	7	1	165	138
3	6	0	83	53	1	14	0	220	206	0	22	0	160	132	-4	4	1	182	149	-1	7	1	120	119
4	6	0	163	147	2	14	0	112	89	2	22	0	57	45	-3	4	1	197	192	0	7	1	695	683
5	6	0	175	165	3	14	0	145	155	3	22	0	168	192	-2	4	1	285	246	1	7	1	99	131
6	6	0	181	166	4	14	0	164	158	3	22	0	44	37	0	4	1	130	111	2	7	1	169	145
1	7	0	65	70	5	14	0	265	254	1	23	0	141	155	2	4	1	273	255	3	7	1	308	291
2	7	0	247	233	1	15	0	278	268	2	23	0	58	51	3	4	1	215	195	4	7	1	86	108
3	7	0	166	173	2	15	0	121	105	3	23	0	126	50	4	4	1	165	171	5	7	1	309	305
4	7	0	90	94	3	15	0	74	74	0	24	0	63	59	5	4	1	180	166	-6	8	1	132	131
5	7	0	145	143	4	15	0	78	84	2	24	0	58	64	6	4	1	357	345	-5	8	1	305	286
1	8	0	326	308	5	15	0	291	301	3	24	0	97	114	-6	3	1	86	76	-4	8	1	162	179
2	8	0	357	290	0	16	0	534	507	4	24	0	66	61	-4	3	1	164	171	-3	3	1	80	65
4	8	0	35	43	2	16	0	211	205	2	25	0	76	94	-2	3	1	275	274	-2	8	1	269	231
5	8	0	121	101	3	16	0	325	338	6	0	1	71	72	-1	3	1	522	498	-1	8	1	334	328
1	9	0	380	289	4	16	0	95	82	-6	1	1	55	42	0	3	1	166	125	0	8	1	538	491
2	9	0	359	316	5	16	0	253	241	-6	2	1	243	224	1	3	1	505	499	1	8	1	346	313
3	9	0	339	343	1	17	0	129	122	-5	2	1	147	178	2	3	1	298	261	2	8	1	231	237
4	9	0	131	136	2	17	0	198	201	-3	2	1	107	122	4	3	1	175	157	3	8	1	91	59
6	9	0	157	124	3	17	0	220	231	-1	2	1	441	500	6	3	1	60	54	4	8	1	168	168

OBSERVED AND CALCULATED STRUCTURE FACTORS FOR SH2 P2(1)2(1)2

PAGE 2

H	K	L	10FO	10FC	H	K	L	10FO	10FC	H	K	L	10FO	10FC	H	K	L	10FO	10FC	H	K	L	10FO	10FC
5	8	1	301	294	-4	12	1	89	87	-4	15	1	243	250	-1	18	1	61	28	1	22	1	57	45
6	8	1	141	131	-3	12	1	91	81	-3	15	1	155	158	0	18	1	216	222	2	22	1	94	90
-5	9	1	91	112	-2	12	1	330	316	-2	15	1	138	135	2	18	1	193	180	5	22	1	118	143
-4	9	1	107	80	-1	12	1	479	472	0	15	1	429	385	3	18	1	81	88	-4	23	1	79	88
-3	9	1	361	357	0	12	1	253	227	2	15	1	144	137	5	18	1	135	133	-2	23	1	48	48
-2	9	1	181	174	1	12	1	491	462	3	15	1	168	153	-5	19	1	88	89	-1	23	1	70	75
-1	9	1	125	116	2	12	1	334	322	4	15	1	244	250	-4	19	1	94	109	0	23	1	155	152
1	9	1	120	116	3	12	1	101	75	5	15	1	202	198	-3	19	1	227	221	1	23	1	62	79
2	9	1	188	169	4	12	1	74	96	6	15	1	128	125	-2	19	1	131	138	4	23	1	76	88
3	9	1	373	359	5	12	1	101	102	-6	16	1	89	77	-1	19	1	184	185	-3	24	1	70	83
4	9	1	101	85	-6	13	1	186	191	-5	16	1	107	111	0	19	1	107	9	-2	24	1	105	124
5	9	1	101	104	-5	13	1	168	157	-4	16	1	165	192	1	19	1	190	178	-1	24	1	97	115
6	9	1	86	69	-4	13	1	154	148	-3	16	1	163	158	2	19	1	136	138	0	24	1	134	17
-5	10	1	101	96	-3	13	1	227	215	-2	16	1	329	336	3	19	1	225	224	1	24	1	101	111
-4	10	1	116	114	-2	13	1	182	212	-1	16	1	224	236	4	19	1	97	105	2	24	1	110	117
-3	10	1	195	171	-1	13	1	181	160	0	16	1	177	168	5	19	1	89	84	3	24	1	67	84
-2	10	1	87	89	0	13	1	234	206	1	16	1	244	222	-5	20	1	109	114	4	24	1	59	77
-1	10	1	563	524	1	13	1	161	169	2	16	1	337	335	-4	20	1	71	78	-3	25	1	39	77
0	10	1	154	126	2	13	1	199	199	3	16	1	168	163	-3	20	1	127	121	-2	25	1	50	56
1	10	1	532	540	3	13	1	227	217	4	16	1	176	179	-2	20	1	63	60	-1	25	1	72	79
2	10	1	92	91	4	13	1	149	145	5	16	1	108	102	-1	20	1	58	48	0	25	1	100	112
3	10	1	201	169	5	13	1	164	160	6	16	1	94	75	1	20	1	67	52	1	25	1	69	85
4	10	1	110	100	6	13	1	189	187	-5	17	1	148	145	2	20	1	65	58	2	25	1	49	60
5	10	1	100	66	-6	14	1	172	176	-4	17	1	79	84	3	20	1	127	124	3	25	1	40	76
-6	11	1	115	107	-5	14	1	93	89	-3	17	1	107	125	4	20	1	65	83	-2	26	1	70	82
-4	11	1	84	74	-4	14	1	217	239	-2	17	1	139	150	5	20	1	113	106	1	0	2	247	264
-3	11	1	206	196	-2	14	1	207	211	-1	17	1	256	236	-5	21	1	150	153	2	0	2	166	148
-2	11	1	140	142	-1	14	1	88	75	0	17	1	390	365	-3	21	1	69	58	3	0	2	118	103
-1	11	1	622	624	0	14	1	117	102	1	17	1	248	248	-1	21	1	104	99	4	0	2	243	255
0	11	1	376	354	1	14	1	87	75	2	17	1	148	142	0	21	1	74	59	5	0	2	45	41
1	11	1	592	615	2	14	1	213	209	3	17	1	124	104	1	21	1	104	98	6	0	2	99	118
2	11	1	138	145	4	14	1	219	235	4	17	1	86	80	5	21	1	142	137	-6	1	2	151	144
3	11	1	208	192	5	14	1	88	88	5	17	1	147	143	-5	22	1	114	139	-5	1	2	97	129
4	11	1	73	82	6	14	1	171	179	-5	18	1	145	130	-2	22	1	93	86	-4	1	2	79	67
6	11	1	128	114	-6	15	1	147	140	-3	18	1	84	89	-1	22	1	59	48	-3	1	2	103	114
-5	12	1	98	108	-5	15	1	201	195	-2	18	1	194	181	0	22	1	58	62	-1	1	2	336	387

OBSERVED AND CALCULATED STRUCTURE FACTORS FOR SH6Z P2(1)2(1)2

PAGE 3

H	K	L	10FO	10FC	H	K	L	10FO	10FC	H	K	L	10FO	10FC	H	K	L	10FO	10FC	H	K	L	10FO	10FC
1	1	2	353	370	-1	4	2	299	262	-1	7	2	248	262	-2	10	2	313	297	-1	13	2	155	149
2	1	2	639	757	0	4	2	310	283	0	7	2	312	294	-1	10	2	324	298	0	13	2	104	87
3	1	2	117	110	1	4	2	298	274	1	7	2	271	248	0	10	2	390	361	1	13	2	136	162
4	1	2	81	83	2	4	2	248	229	2	7	2	336	287	1	10	2	309	310	2	13	2	67	49
5	1	2	104	121	3	4	2	343	295	3	7	2	264	272	2	10	2	315	311	4	13	2	57	72
6	1	2	126	141	4	4	2	81	112	4	7	2	200	218	3	10	2	73	66	5	13	2	208	204
-6	2	2	95	82	5	4	2	97	87	5	7	2	61	58	4	10	2	214	221	-5	14	2	152	146
-5	2	2	37	33	6	4	2	220	214	-6	8	2	104	99	5	10	2	164	160	-4	14	2	92	74
-4	2	2	324	332	-6	5	2	249	236	-5	8	2	191	165	6	10	2	132	145	-3	14	2	224	201
-3	2	2	338	379	-5	5	2	195	223	-4	8	2	191	171	-6	11	2	158	142	-1	14	2	175	177
-2	2	2	384	361	-4	5	2	58	46	-3	8	2	335	321	-5	11	2	94	80	0	14	2	140	130
-1	2	2	349	373	-3	5	2	242	266	-2	8	2	313	297	-4	11	2	208	185	-1	14	2	180	169
0	2	2	516	723	-2	5	2	65	39	-1	8	2	309	303	-3	11	2	279	265	2	14	2	124	36
1	2	2	352	391	-1	5	2	437	489	0	8	2	123	87	-2	11	2	197	178	3	14	2	204	225
2	2	2	383	365	0	5	2	85	55	1	8	2	313	316	-1	11	2	213	205	4	14	2	83	79
3	2	2	375	361	1	5	2	479	465	2	8	2	315	302	0	11	2	131	127	5	14	2	141	143
4	2	2	326	326	2	5	2	65	46	3	8	2	335	306	1	11	2	222	195	-5	15	2	173	151
5	2	2	37	23	3	5	2	299	268	4	8	2	177	169	2	11	2	189	191	-4	15	2	80	79
6	2	2	95	98	4	5	2	53	53	5	8	2	179	175	3	11	2	300	262	-3	15	2	64	65
-6	3	2	71	48	5	5	2	205	217	-6	8	2	109	105	4	11	2	187	204	-2	15	2	134	131
-5	3	2	173	192	6	5	2	221	233	-6	9	2	97	93	5	11	2	83	84	-1	15	2	167	151
-4	3	2	321	299	-6	6	2	74	62	-5	9	2	135	139	6	11	2	157	147	0	15	2	132	112
-3	3	2	129	133	-5	6	2	146	153	-4	9	2	142	136	-6	12	2	100	101	1	15	2	151	163
-2	3	2	254	230	-4	6	2	229	244	-3	9	2	173	144	-5	12	2	128	123	2	15	2	158	153
-1	3	2	417	445	-3	6	2	255	244	-2	9	2	233	193	-3	12	2	252	246	4	15	2	77	76
0	3	2	28	29	-2	6	2	91	65	-1	9	2	225	234	-2	12	2	142	127	5	15	2	150	164
1	3	2	418	443	-1	6	2	440	432	0	9	2	308	250	-1	12	2	166	182	-4	16	2	131	115
2	3	2	220	239	0	6	2	464	444	1	9	2	236	226	0	12	2	143	130	-3	16	2	211	233
3	3	2	136	143	1	6	2	441	445	2	9	2	227	209	1	12	2	189	165	-2	16	2	86	92
4	3	2	294	301	2	6	2	101	94	3	9	2	164	158	2	12	2	141	137	-1	16	2	102	82
5	3	2	182	139	3	6	2	251	257	4	9	2	130	145	3	12	2	267	235	0	16	2	171	156
-6	4	2	255	212	4	6	2	243	234	5	9	2	133	138	4	12	2	121	126	1	16	2	95	92
-5	4	2	93	94	5	6	2	158	147	6	9	2	105	94	5	12	2	111	112	2	16	2	93	89
-4	4	2	97	101	-4	7	2	228	212	-6	10	2	129	135	-5	13	2	204	210	3	16	2	219	232
-3	4	2	292	310	-3	7	2	261	263	-5	10	2	167	159	-4	13	2	56	62	4	16	2	131	112
-2	4	2	234	227	-2	7	2	319	304	-4	10	2	234	206	-2	13	2	53	58	-3	17	2	100	109

OBSERVED AND CALCULATED STRUCTURE FACTORS FOR SH62 P2(1)2(1)2

PAGE 4

H	K	L	10FO	10FC	H	K	L	10FO	10FC	H	K	L	10FO	10FC	H	K	L	10FO	10FC	H	K	L	10FO	10FC
-2	17	2	209	210	-2	21	2	55	63	-5	1	3	97	83	-6	4	3	168	57	6	6	3	97	97
-1	17	2	192	186	-1	21	2	78	77	-4	1	3	61	78	-5	4	3	51	50	-5	7	3	133	134
0	17	2	61	52	1	21	2	80	73	-3	1	3	313	329	-4	4	3	344	330	-4	7	3	188	184
1	17	2	189	188	2	21	2	61	59	-2	1	3	444	426	-3	4	3	181	165	-3	7	3	109	115
2	17	2	219	206	3	21	2	97	107	-1	1	3	86	58	-2	4	3	68	84	-2	7	3	454	450
3	17	2	110	102	4	21	2	186	119	0	1	3	72	90	-1	4	3	103	93	-1	7	3	277	268
4	17	2	111	46	-4	22	2	89	12	1	1	3	84	69	0	4	3	194	166	0	7	3	345	376
5	17	2	73	62	-3	22	2	96	102	2	1	3	451	433	1	4	3	105	92	1	7	3	269	265
-4	18	2	133	134	-2	22	2	73	68	3	1	3	328	339	2	4	3	70	85	3	7	3	115	116
-3	18	2	113	121	-1	22	2	72	73	4	1	3	67	69	3	4	3	188	153	4	7	3	190	171
-2	18	2	100	83	1	22	2	73	71	5	1	3	101	85	4	4	3	314	329	4	7	3	135	137
-1	18	2	186	177	2	22	2	69	72	6	1	3	129	124	5	4	3	56	55	-5	8	3	239	242
0	18	2	269	230	3	22	2	85	106	-5	2	3	100	83	-6	5	3	169	155	-4	8	3	64	72
1	18	2	191	168	-4	23	2	61	77	-4	2	3	231	221	-5	5	3	85	108	-3	8	3	293	318
2	18	2	91	94	-1	23	2	84	67	-3	2	3	254	275	-4	5	3	165	159	-2	8	3	328	327
3	18	2	127	113	0	23	2	70	62	-2	2	3	262	267	-3	5	3	134	119	-1	8	3	173	170
4	18	2	118	140	1	23	2	71	72	-1	2	3	290	266	-2	5	3	209	203	0	8	3	652	717
-5	19	2	34	71	4	23	2	68	74	0	2	3	278	290	-1	5	3	335	364	1	8	3	181	181
-4	19	2	74	71	-3	24	2	66	81	1	2	3	268	281	0	5	3	389	386	2	8	3	360	312
-3	19	2	87	91	-2	24	2	62	71	2	2	3	264	257	1	5	3	318	359	3	8	3	324	301
-2	19	2	147	131	-1	24	2	75	74	3	2	3	275	267	2	5	3	225	208	4	8	3	81	61
-1	19	2	171	167	1	24	2	65	80	4	2	3	215	212	3	5	3	133	124	5	8	3	267	231
0	19	2	168	168	2	24	2	65	67	5	2	3	82	98	4	5	3	141	160	-4	9	3	131	125
1	19	2	142	142	3	24	2	64	77	-6	3	3	171	151	5	5	3	98	103	-4	9	3	126	126
2	19	2	87	63	-2	25	2	56	66	-5	3	3	137	148	6	5	3	141	142	-3	9	3	382	363
3	19	2	78	78	-1	25	2	91	107	-6	3	3	96	102	-6	6	3	120	101	-2	9	3	292	271
4	19	2	64	73	0	25	2	57	64	-3	3	3	142	101	-4	6	3	236	251	-1	9	3	163	164
-5	20	2	91	102	1	25	2	94	104	-2	3	3	238	238	-3	6	3	319	306	0	9	3	56	70
-2	20	2	105	111	2	25	2	62	67	-1	3	3	409	453	-2	6	3	395	385	1	9	3	187	147
-1	20	2	114	116	1	0	3	111	128	0	3	3	217	229	-1	6	3	288	278	2	9	3	307	276
0	20	2	124	122	2	0	3	129	30	1	3	3	412	437	0	6	3	61	35	3	9	3	398	376
1	20	2	111	114	3	0	3	391	408	2	3	3	248	262	1	6	3	296	275	4	9	3	148	114
2	20	2	108	111	4	0	3	141	141	3	3	3	144	110	2	6	3	416	389	6	9	3	120	122
3	20	2	99	97	5	0	3	248	290	4	3	3	183	92	3	6	3	343	319	-5	10	3	85	88
-4	21	2	109	116	6	0	3	103	93	5	3	3	142	148	4	6	3	243	233	-4	10	3	236	217
-3	21	2	100	107	-6	1	3	136	122	6	3	3	132	132	5	6	3	69	54	-3	10	3	166	161

OBSERVED AND CALCULATED STRUCTURE FACTORS FOR SH62 P2(1)2(1)2

PAGE 5

H	K	L	TOFO	TOFC	H	K	L	TOFO	TOFC	H	K	L	TOFO	TOFC	H	K	L	TOFO	TOFC					
-2	10	3	254	242	3	13	3	180	179	-4	17	3	110	123	-3	22	3	77	87	-5	2	4	86	86
-1	10	3	396	355	5	13	3	87	78	-3	17	3	152	159	-2	22	3	84	86	-4	2	4	138	137
0	10	3	64	50	5	13	3	154	154	-2	17	3	130	130	-1	22	3	48	42	-3	2	4	101	111
1	10	3	379	376	-5	14	3	82	75	0	17	3	71	58	1	22	3	53	33	-2	2	4	126	125
2	10	3	260	240	-4	14	3	139	100	2	17	3	132	131	2	22	3	87	83	-1	2	4	203	207
3	10	3	174	160	-3	14	3	202	187	3	17	3	160	152	3	22	3	67	95	0	2	4	87	95
4	10	3	206	221	-2	14	3	210	210	4	17	3	110	121	-1	23	3	76	67	1	2	4	223	187
5	10	3	87	93	-1	14	3	103	104	-3	18	3	83	91	0	23	3	108	99	2	2	4	118	130
-5	11	3	77	69	0	14	3	225	218	-4	18	3	100	110	1	23	3	67	75	3	2	4	102	115
-4	11	3	195	182	1	14	3	113	97	-2	18	3	112	109	2	23	3	99	63	4	2	4	136	137
-3	11	3	71	70	2	14	3	229	218	-1	18	3	148	137	4	23	3	41	35	5	2	4	89	80
-2	11	3	60	82	3	14	3	194	202	0	18	3	52	52	-3	24	3	58	75	-6	3	4	183	178
-1	11	3	332	329	4	14	3	175	147	1	18	3	146	134	-2	24	3	72	78	-5	3	4	60	64
0	11	3	33	20	-6	15	3	91	79	2	18	3	103	112	2	24	3	73	76	-4	3	4	226	181
1	11	3	347	319	-5	15	3	131	114	4	18	3	113	109	3	24	3	58	72	-3	3	4	76	95
2	11	3	84	68	-4	15	3	86	95	3	18	3	85	85	-2	25	3	40	40	-2	3	4	104	106
4	11	3	188	182	-2	15	3	214	250	-5	10	3	60	70	-1	25	3	55	74	-1	3	4	142	147
5	11	3	75	67	-1	15	3	160	119	-4	19	3	96	102	1	25	3	61	66	0	3	4	260	288
-6	12	3	119	103	1	15	3	197	182	-3	19	3	70	83	0	0	4	527	606	1	3	4	163	125
-4	12	3	189	205	1	15	3	126	131	-1	19	3	106	107	1	0	4	288	287	2	3	4	120	96
-3	12	3	158	167	2	15	3	240	241	0	10	3	86	70	2	0	4	76	73	3	3	4	86	89
-2	12	3	61	64	4	15	3	100	86	1	19	3	105	111	3	0	4	186	216	4	3	4	202	196
-1	12	3	255	253	5	15	3	116	123	3	10	3	78	81	4	0	4	160	151	5	3	4	71	63
1	12	3	261	247	6	15	3	89	89	4	19	3	99	101	-6	1	4	78	73	6	3	4	187	174
2	12	3	53	75	-5	16	3	99	114	5	19	3	75	68	-5	1	4	78	93	-4	4	4	192	164
3	12	3	180	153	-4	16	3	108	117	-2	20	3	60	59	-4	1	4	140	154	-5	4	4	126	134
4	12	3	203	192	-3	16	3	68	62	-1	20	3	91	101	-3	1	4	131	159	-4	4	4	114	96
6	12	3	113	100	-2	16	3	117	121	0	20	3	82	80	-2	1	4	400	400	-3	4	4	204	217
-6	13	3	176	164	-1	16	3	83	97	1	20	3	96	98	-1	1	4	317	309	-2	4	4	116	105
-5	13	3	91	80	0	16	3	262	239	2	20	3	68	51	0	1	4	63	28	-1	4	4	180	154
-3	13	3	174	184	1	16	3	97	83	4	20	3	64	48	1	1	4	304	317	0	4	4	54	24
-2	13	3	134	136	2	16	3	131	112	-2	21	3	56	55	2	1	4	385	410	1	4	4	172	167
-1	13	3	139	134	3	16	3	74	61	-1	21	3	62	61	3	1	4	152	145	2	4	4	98	125
0	13	3	236	240	4	16	3	130	115	1	21	3	56	63	4	1	4	138	139	3	4	4	231	206
1	13	3	130	143	5	16	3	97	110	2	21	3	60	55	5	1	4	74	99	4	4	4	107	103
2	13	3	151	125	-6	17	3	73	100	4	21	3	68	56	6	1	4	80	71	5	4	4	131	131

OBSERVED AND CALCULATED STRUCTURE FACTORS FOR SH62 P2(1)2(1)2

PAGE 6

H	K	L	10FO	10FC	H	K	L	10FO	10FC	H	K	L	10FO	10FC	H	K	L	10FO	10FC	H	K	L	10FO	10FC
6	4	4	177	173	-6	8	4	102	105	-4	11	4	244	242	-4	14	4	191	193	1	17	4	157	163
-6	5	4	170	176	-5	8	4	88	76	-3	11	4	221	234	-3	14	4	164	161	2	17	4	139	144
-5	5	4	107	118	-4	8	4	139	115	-2	11	4	124	140	-2	14	4	81	102	3	17	4	81	69
-3	5	4	62	75	-3	8	4	88	104	0	11	4	223	213	-1	14	4	78	98	4	17	4	70	71
-2	5	4	227	223	-2	8	4	198	196	1	11	4	47	49	0	14	4	140	146	5	17	4	78	88
-1	5	4	264	277	-1	8	4	292	305	2	11	4	143	123	1	14	4	84	87	-2	18	4	63	48
0	5	4	237	204	0	8	4	364	346	3	11	4	217	233	2	14	4	97	85	-1	18	4	121	124
1	5	4	264	260	1	8	4	310	298	4	11	4	235	256	3	14	4	153	173	0	18	4	125	99
2	5	4	236	222	2	8	4	202	205	6	11	4	162	159	4	14	4	191	195	1	18	4	131	113
3	5	4	69	77	3	8	4	98	97	-6	12	4	98	98	5	14	4	108	98	2	18	4	59	52
5	5	4	121	109	4	8	4	128	127	-5	12	4	210	200	6	14	4	138	143	-5	19	4	61	53
6	5	4	160	132	5	8	4	86	74	-4	12	4	134	134	-5	15	4	120	113	-4	19	4	121	116
-6	6	4	138	127	6	8	4	91	95	-3	12	4	92	113	-4	15	4	96	97	-3	19	4	129	155
-5	6	4	178	172	-5	9	4	101	97	-2	12	4	128	111	-3	15	4	78	63	-2	19	4	107	116
-4	6	4	290	282	-4	9	4	63	60	-1	12	4	165	152	-1	15	4	162	151	0	19	4	129	124
-3	6	4	176	204	-3	9	4	111	128	1	12	4	165	153	0	15	4	287	272	2	19	4	122	103
-2	6	4	102	133	-2	9	4	264	263	2	12	4	113	130	1	15	4	144	166	3	19	4	127	151
-1	6	4	221	198	-1	9	4	317	313	3	12	4	104	102	3	15	4	76	67	4	19	4	108	123
0	6	4	116	99	0	9	4	305	276	4	12	4	130	137	4	15	4	98	95	-5	20	4	64	74
1	6	4	202	212	1	9	4	329	317	5	12	4	205	201	5	15	4	111	111	-2	20	4	92	88
2	6	4	131	112	2	9	4	267	280	6	12	4	106	106	-4	16	4	143	146	-1	20	4	76	76
3	6	4	198	203	3	9	4	125	112	-6	13	4	116	119	-3	16	4	83	82	1	20	4	67	81
4	6	4	272	233	4	9	4	57	55	-5	13	4	78	59	-2	16	4	254	284	2	20	4	91	91
5	6	4	198	188	5	9	4	102	100	-4	13	4	100	95	-1	16	4	105	101	3	20	4	63	73
6	6	4	133	131	-5	10	4	143	135	-3	13	4	84	82	0	16	4	139	137	-4	21	4	105	125
-5	7	4	120	127	-5	10	4	96	106	-2	13	4	249	254	1	16	4	112	94	-2	21	4	97	101
-4	7	4	89	84	-3	10	4	62	34	-1	13	4	141	138	2	16	4	255	288	-1	21	4	102	107
-3	7	4	264	251	-2	10	4	109	93	0	13	4	201	192	3	16	4	72	82	1	21	4	98	110
-2	7	4	158	137	-1	10	4	192	196	1	13	4	147	140	4	16	4	138	152	2	21	4	91	109
-1	7	4	155	160	0	10	4	105	114	2	13	4	257	259	6	16	4	50	72	4	21	4	112	121
0	7	4	162	170	1	10	4	208	185	3	13	4	77	80	-5	17	4	92	83	-4	22	4	52	61
1	7	4	155	166	2	10	4	102	103	4	13	4	94	92	-4	17	4	69	64	-3	22	4	63	75
2	7	4	174	184	3	10	4	58	39	5	13	4	66	62	-3	17	4	69	81	-2	22	4	84	93
3	7	4	270	253	5	10	4	99	103	6	13	4	116	123	-2	17	4	154	131	-1	22	4	57	49
4	7	4	77	89	6	10	4	154	145	-6	14	4	146	144	-1	17	4	165	165	0	22	4	89	98
5	7	4	151	149	-6	11	4	163	161	-5	14	4	105	101	0	17	4	279	272	1	22	4	45	50

OBSERVED AND CALCULATED STRUCTURE FACTORS FOR SH62 P2(1)2(1)2

PAGE 7

H	K	L	TOFO	TOFC	H	K	L	TOFO	TOFC	H	K	L	TOFO	TOFC	H	K	L	TOFO	TOFC					
2	22	4	89	87	2	2	5	319	363	0	5	5	158	161	5	8	5	60	58	0	12	5	170	156
3	22	4	55	78	3	2	5	132	129	1	5	5	335	324	-6	9	5	107	106	1	12	5	130	134
4	22	4	53	62	4	2	5	327	331	2	5	5	142	144	-5	9	5	77	69	2	12	5	146	147
-4	23	4	52	66	5	2	5	188	206	3	5	5	181	165	-4	9	5	129	137	3	12	5	133	130
-2	23	4	60	62	-6	3	5	226	230	4	5	5	127	135	-3	9	5	82	90	4	12	5	55	43
-1	23	4	68	73	-5	3	5	171	169	5	5	5	86	88	-2	9	5	208	211	5	12	5	82	71
0	23	4	145	175	-4	3	5	133	142	6	5	5	175	176	-1	9	5	129	113	-6	13	5	131	127
1	23	4	76	69	-3	3	5	260	256	-6	6	5	104	101	1	9	5	135	116	-5	13	5	118	102
2	23	4	57	57	-2	3	5	117	91	-5	6	5	89	103	2	9	5	219	208	-4	13	5	66	57
-2	24	4	116	142	-1	3	5	126	170	-6	6	5	69	74	3	9	5	88	78	-3	13	5	129	146
-1	24	4	76	68	0	3	5	187	217	-2	6	5	81	97	4	9	5	131	142	-2	13	5	86	90
1	24	4	66	70	1	3	5	157	191	-1	6	5	254	232	5	9	5	72	72	-1	13	5	208	208
2	24	4	127	142	2	3	5	118	99	0	6	5	122	94	6	9	5	101	106	0	13	5	85	65
3	24	4	42	64	3	3	5	254	263	1	6	5	244	238	-4	10	5	173	171	1	13	5	210	208
1	0	5	463	463	4	3	5	147	132	2	6	5	88	93	-3	10	5	79	87	2	13	5	94	83
2	0	5	222	240	5	3	5	180	165	4	6	5	67	78	-2	10	5	181	184	3	13	5	132	134
3	0	5	299	271	6	3	5	229	234	5	6	5	86	104	-1	10	5	185	172	4	13	5	65	62
6	0	5	135	143	-6	4	5	104	99	6	6	5	103	101	0	10	5	86	81	5	13	5	106	107
-5	1	5	142	143	-5	4	5	110	106	-5	7	5	143	146	1	10	5	171	186	6	13	5	139	121
-4	1	5	110	98	-4	4	5	74	80	-6	7	5	69	70	2	10	5	189	186	-5	14	5	136	149
-3	1	5	171	169	-3	4	5	203	219	-2	7	5	183	198	3	10	5	76	91	-4	14	5	98	105
-2	1	5	308	330	-2	4	5	193	178	-1	7	5	164	129	4	10	5	168	173	-2	14	5	110	104
-1	1	5	438	452	-1	4	5	258	244	1	7	5	126	137	-5	11	5	173	173	-1	14	5	203	196
0	1	5	202	167	0	4	5	306	291	2	7	5	191	192	-3	11	5	129	127	0	14	5	119	127
1	1	5	447	442	1	4	5	268	238	4	7	5	81	60	-2	11	5	170	166	1	14	5	205	195
2	1	5	307	323	2	4	5	190	192	5	7	5	149	147	-1	11	5	95	91	2	14	5	119	96
3	1	5	156	176	3	4	5	228	223	-5	8	5	54	53	0	11	5	135	124	4	14	5	99	100
4	1	5	114	136	4	4	5	77	70	-6	8	5	129	122	1	11	5	90	102	5	14	5	133	131
5	1	5	150	137	5	4	5	113	103	-3	8	5	189	193	2	11	5	178	175	-5	15	5	136	155
-5	2	5	188	204	6	4	5	102	97	-2	8	5	54	54	-3	11	5	131	136	-4	15	5	134	158
-4	2	5	341	331	-6	5	5	187	184	-1	8	5	221	215	5	11	5	169	170	-2	15	5	182	201
-3	2	5	121	137	-5	5	5	98	73	0	8	5	492	465	-5	12	5	85	77	-1	15	5	69	61
-2	2	5	334	372	-4	5	5	136	129	1	8	5	228	202	-4	12	5	52	51	0	15	5	102	87
-1	2	5	313	264	-3	5	5	172	165	2	8	5	70	63	-3	12	5	133	128	1	15	5	65	72
0	2	5	252	213	-2	5	5	141	136	3	8	5	190	194	-2	12	5	148	136	2	15	5	189	196
1	2	5	297	280	-1	5	5	336	330	4	8	5	127	118	-1	12	5	113	144	3	15	5	68	70

OBSERVED AND CALCULATED STRUCTURE FACTORS FOR SH62 P2(1)2(1)2

PAGE 8

H	K	L	10FO	10FC	H	K	L	10FO	10FC	H	K	L	10FO	10FC	H	K	L	10FO	10FC	H	K	L	10FO	10FC
4	15	5	158	152	2	10	5	62	72	-1	1	6	58	40	-2	4	6	227	255	-1	7	6	84	84
5	15	5	142	159	3	19	5	100	123	0	1	6	104	72	-1	4	6	221	196	0	7	6	174	174
-5	16	5	72	76	4	19	5	103	98	2	1	6	218	208	0	4	6	233	194	1	7	6	76	95
-4	16	5	108	111	5	19	5	103	101	3	1	6	262	242	1	4	6	220	193	2	7	6	47	63
-3	16	5	206	209	-5	20	5	56	63	4	1	6	201	200	2	4	6	241	251	3	7	6	211	221
-2	16	5	121	125	-3	20	5	66	63	6	1	6	101	87	3	4	6	137	114	4	7	6	108	111
-1	16	5	206	219	-1	20	5	101	125	-6	2	6	105	98	4	4	6	82	95	5	7	6	90	93
0	16	5	288	280	0	20	5	71	63	-5	2	6	124	135	3	4	6	92	89	6	7	6	132	119
1	16	5	218	212	1	20	5	109	117	-4	2	6	153	151	6	4	6	127	110	-6	8	6	121	129
2	16	5	127	118	3	20	5	61	69	-3	2	6	65	61	-6	5	6	119	113	-5	8	6	182	164
3	16	5	194	214	5	20	5	54	66	-2	2	6	226	198	-4	5	6	142	152	-2	8	6	145	164
4	16	5	114	104	-3	21	5	56	69	-1	2	6	106	108	-3	5	6	120	126	-1	8	6	151	145
5	16	5	75	78	-1	21	5	93	97	0	2	6	85	46	-2	5	6	185	187	0	8	6	312	283
-4	17	5	101	107	0	21	5	59	57	1	2	6	120	94	-1	5	6	275	277	1	8	6	150	150
-2	17	5	116	126	1	21	5	93	97	2	2	6	225	209	0	5	6	130	124	2	8	6	147	158
-1	17	5	99	94	3	21	5	66	62	3	2	6	77	60	1	5	6	285	268	5	8	6	179	170
0	17	5	97	99	-3	22	5	50	68	4	2	6	150	146	2	5	6	202	181	6	8	6	121	127
1	17	5	88	103	-2	22	5	64	63	5	2	6	130	124	3	5	6	129	124	-6	9	6	109	104
2	17	5	126	119	-1	22	5	48	45	6	2	6	74	94	4	5	6	143	146	-5	9	6	91	95
4	17	5	98	108	1	22	5	53	43	-6	3	6	153	143	5	5	6	58	39	-4	9	6	71	75
-5	18	5	75	34	2	22	5	58	62	-5	3	6	103	110	6	5	6	106	103	-3	9	6	152	154
-4	18	5	79	73	3	22	5	48	66	-6	3	6	155	128	-6	6	6	111	115	-1	9	6	87	99
-3	18	5	115	129	-1	23	5	57	53	-3	3	6	110	125	-5	6	6	125	137	1	9	6	96	91
-2	18	5	148	150	3	23	5	63	63	-2	3	6	118	108	-4	6	6	228	231	2	9	6	44	23
-1	18	5	196	195	1	23	5	59	55	-1	3	6	131	114	-2	6	6	70	82	3	9	6	152	162
1	18	5	181	203	-2	24	5	34	37	0	3	6	370	383	-1	6	6	220	225	4	9	6	72	76
2	18	5	148	152	2	24	5	40	33	1	3	6	126	124	0	6	6	209	160	5	9	6	92	92
3	18	5	113	129	1	0	6	130	132	2	3	6	123	107	1	6	6	224	220	6	9	6	116	106
4	18	5	74	69	2	0	6	199	104	3	3	6	126	114	2	6	6	84	80	-4	10	6	67	77
5	18	5	78	79	3	0	6	50	45	4	3	6	142	140	4	6	6	232	222	-3	10	6	83	87
-5	19	5	99	103	4	0	6	60	67	5	3	6	106	108	5	6	6	142	132	-1	10	6	256	246
-4	19	5	99	98	5	0	6	130	123	6	3	6	153	148	6	6	6	111	113	0	10	6	166	167
-3	19	5	111	118	-5	1	6	98	89	-6	4	6	119	105	-6	7	6	129	122	1	10	6	247	260
-2	19	5	74	63	-4	1	6	193	207	-5	4	6	87	89	-5	7	6	92	92	2	10	6	51	38
-1	19	5	109	105	-3	1	6	243	261	-4	4	6	94	81	-4	7	6	104	118	3	10	6	93	86
1	19	5	113	105	-2	1	6	213	203	-3	4	6	120	121	-3	7	6	212	215	4	10	6	72	75

OBSERVED AND CALCULATED STRUCTURE FACTORS FOR SH62 P2(1)2(1)2

PAGE 9

H	K	L	10FO	10FC	H	K	L	10FO	10FC	H	K	L	10FO	10FC	H	K	L	10FO	10FC	H	K	L	10FO	10FC
6	10	6	82	74	1	14	6	126	116	1	18	6	149	136	1	1	7	115	84	3	4	7	66	88
-6	11	6	123	111	6	14	6	151	161	2	18	6	67	66	2	1	7	80	68	4	4	7	182	178
-5	11	6	75	79	5	14	6	83	83	3	18	6	71	69	3	1	7	220	242	5	4	7	110	113
-3	11	6	80	62	6	14	6	96	89	4	18	6	45	53	4	1	7	68	77	6	4	7	110	105
-2	11	6	132	150	-6	15	6	93	105	-5	19	6	58	71	5	1	7	75	72	-4	5	7	168	169
-1	11	6	234	234	-5	15	6	76	76	-4	19	6	52	49	-5	2	7	79	82	-5	5	7	183	189
1	11	6	244	230	-4	15	6	95	88	-3	19	6	134	160	-4	2	7	145	137	-4	5	7	183	187
2	11	6	132	146	-3	15	6	158	166	-2	19	6	59	59	-3	2	7	236	236	-3	5	7	194	194
5	11	6	75	78	-2	15	6	79	80	2	19	6	62	58	-2	2	7	179	192	-2	5	7	130	129
6	11	6	133	118	-1	15	6	139	131	3	19	6	138	154	-1	2	7	125	92	-1	5	7	158	148
-5	12	6	152	154	0	15	6	106	94	4	19	6	47	52	0	2	7	141	127	0	5	7	87	94
-4	12	6	67	63	1	15	6	128	138	5	19	6	61	70	1	2	7	114	100	1	5	7	131	134
-3	12	6	113	116	2	15	6	76	84	-2	20	6	56	55	2	2	7	179	197	2	5	7	128	131
-1	12	6	127	131	3	15	6	154	167	-1	20	6	69	77	3	2	7	250	227	3	5	7	215	194
0	12	6	320	309	4	15	6	84	95	0	20	6	63	53	4	2	7	133	146	4	5	7	182	186
1	12	6	142	120	5	15	6	65	72	1	20	6	78	77	5	2	7	98	84	5	5	7	104	111
3	12	6	106	113	-5	16	6	66	68	2	20	6	57	54	-6	3	7	139	136	6	5	7	177	169
4	12	6	72	61	-3	16	6	137	145	3	20	6	51	57	-5	3	7	110	107	-6	6	7	91	82
5	12	6	154	156	-2	16	6	126	123	-3	21	6	42	52	-4	3	7	91	81	-5	6	7	138	124
6	12	6	88	81	-1	16	6	64	72	-2	21	6	69	68	-3	3	7	71	74	-4	6	7	152	166
-6	13	6	114	130	1	16	6	65	73	0	21	6	56	50	-2	3	7	79	65	-3	6	7	212	219
-5	13	6	189	95	2	16	6	123	123	-1	22	6	38	46	-1	3	7	129	113	-2	6	7	176	181
-3	13	6	154	154	3	16	6	134	146	2	22	6	40	53	0	3	7	207	191	-1	6	7	108	89
-2	13	6	172	181	4	16	6	80	60	2	22	6	45	56	1	3	7	133	189	0	6	7	348	329
-1	13	6	124	128	5	16	6	73	61	0	0	7	90	27	2	3	7	67	73	1	6	7	98	92
1	13	6	129	122	-2	17	6	46	47	1	0	7	85	74	3	3	7	79	72	2	6	7	183	188
2	13	6	175	177	-1	17	6	215	210	2	0	7	64	46	4	3	7	91	82	3	6	7	206	230
3	13	6	157	156	0	17	6	141	133	3	0	7	83	92	5	3	7	111	114	4	6	7	168	168
5	13	6	98	98	1	17	6	206	212	5	0	7	97	89	6	3	7	142	134	5	6	7	146	120
6	13	6	117	127	2	17	6	52	47	6	0	7	165	172	-6	4	7	104	102	6	6	7	97	86
-6	14	6	79	86	3	17	6	62	50	-5	1	7	73	77	-5	4	7	99	115	-4	7	7	92	101
-5	14	6	85	86	-4	18	6	53	49	-4	1	7	82	69	-4	4	7	189	181	-5	7	7	188	126
-4	14	6	155	164	-3	18	6	73	72	-3	1	7	233	239	-3	4	7	71	69	-4	7	7	183	173
-2	14	6	52	38	-2	18	6	75	83	-2	1	7	72	67	-1	4	7	100	103	-3	7	7	87	108
-1	14	6	123	117	-1	18	6	144	144	-1	1	7	112	89	0	4	7	131	125	-2	7	7	274	298
0	14	6	101	96	0	18	6	75	80	0	1	7	137	119	1	4	7	103	97	-1	7	7	192	203

OBSERVED AND CALCULATED STRUCTURE FACTORS FOR S462 P2(1)2(1)2

PAGE 10

H	K	L	10FO	10FC	H	K	L	10FO	10FC	H	K	L	10FO	10FC	H	K	L	10FO	10FC	H	K	L	10FO	10FC
0	7	7	125	107	2	10	7	227	246	6	13	7	100	110	-3	18	7	52	53	-2	2	8	222	232
1	7	7	205	196	3	10	7	186	196	-5	14	7	96	96	-1	18	7	73	83	-1	2	8	141	148
2	7	7	287	288	4	10	7	284	292	-4	14	7	74	70	0	18	7	108	90	0	2	8	48	43
3	7	7	93	99	5	10	7	175	181	-3	14	7	151	138	1	18	7	76	83	1	2	8	154	138
4	7	7	166	181	6	10	7	82	80	-2	14	7	57	43	4	18	7	117	121	2	2	8	225	220
5	7	7	121	114	-6	11	7	93	119	-1	14	7	139	140	3	18	7	67	55	3	2	8	133	129
6	7	7	104	103	-5	11	7	85	74	0	14	7	107	97	-4	19	7	67	56	4	2	8	180	185
-5	8	7	202	199	-4	11	7	169	155	1	14	7	144	134	-2	19	7	66	57	5	2	8	72	70
-4	8	7	151	161	-3	11	7	228	244	3	14	7	135	153	2	19	7	55	65	-6	3	8	136	123
-3	8	7	346	398	-1	11	7	243	244	4	14	7	79	69	4	19	7	52	58	-4	3	8	187	183
-2	8	7	94	108	1	11	7	247	236	5	14	7	94	93	-2	20	7	71	81	-3	3	8	80	83
-1	8	7	182	181	3	11	7	232	244	-9	15	7	136	125	0	20	7	88	88	-2	3	8	44	41
0	8	7	64	77	4	11	7	161	163	-3	15	7	79	100	2	20	7	74	80	-1	3	8	89	82
1	8	7	179	186	5	11	7	85	80	-2	15	7	116	110	-2	21	7	74	78	0	3	8	154	132
2	8	7	100	116	6	11	7	131	121	2	15	7	115	108	-1	21	7	50	50	1	3	8	87	85
3	8	7	387	383	-6	12	7	114	116	3	15	7	84	99	1	21	7	51	68	2	3	8	50	38
4	8	7	159	161	-5	12	7	85	72	5	15	7	128	134	2	21	7	71	77	3	3	8	87	75
5	8	7	198	201	-4	12	7	182	178	-5	16	7	78	86	0	0	8	212	197	4	3	8	143	136
-6	9	7	118	136	-3	12	7	102	120	-4	16	7	92	90	1	0	8	133	138	6	3	8	139	129
-3	9	7	202	223	-2	12	7	156	166	-3	16	7	136	149	2	0	8	190	176	-6	4	8	106	106
-2	9	7	279	278	0	12	7	67	76	-1	16	7	81	74	3	0	8	129	121	-5	4	8	78	82
-1	9	7	229	246	2	12	7	160	163	0	16	7	134	122	4	0	8	89	104	-4	4	8	304	305
0	9	7	325	308	3	12	7	115	108	1	16	7	77	77	-5	1	8	107	107	-3	4	8	131	30
1	9	7	233	243	4	12	7	185	177	2	16	7	58	61	-4	1	8	86	71	-2	4	8	118	138
2	9	7	282	292	5	12	7	85	74	3	16	7	136	144	-3	1	8	106	121	-1	4	8	70	66
3	9	7	214	223	6	12	7	136	122	4	16	7	108	84	-2	1	8	202	204	1	4	8	62	67
4	9	7	39	31	-6	13	7	98	110	5	16	7	77	89	-1	1	8	146	143	2	4	8	136	126
5	9	7	131	136	-5	13	7	144	155	-2	17	7	132	136	0	1	8	76	66	4	4	8	275	308
-6	10	7	87	86	-3	13	7	190	194	-1	17	7	79	74	1	1	8	144	148	5	4	8	88	79
-5	10	7	178	180	-2	13	7	186	112	0	17	7	57	43	2	1	8	193	207	6	4	8	116	189
-4	10	7	283	283	-1	13	7	136	120	1	17	7	74	77	3	1	8	112	117	-6	5	8	167	174
-3	10	7	183	180	0	13	7	30	49	2	17	7	136	131	4	1	8	74	74	-5	5	8	108	86
-2	10	7	232	238	1	13	7	120	134	4	17	7	63	43	5	1	8	109	111	-4	5	8	151	155
-1	10	7	116	118	2	13	7	111	108	5	17	7	55	51	-6	2	8	166	62	-3	5	8	67	77
0	10	7	201	182	3	13	7	186	194	-5	18	7	67	56	-4	2	8	185	181	-2	5	8	245	260
1	10	7	114	122	5	13	7	130	143	-4	18	7	118	120	-3	2	8	131	130	-1	5	8	72	83

OBSERVED AND CALCULATED STRUCTURE FACTORS FOR SH62 P2(1)2(1)2

PAGE 11

H	K	L	TOFO	TOFC	H	K	L	TOFO	TOFC	H	K	L	TOFO	TOFC	H	K	L	TOFO	TOFC	H	K	L	TOFO	TOFC
0	5	8	52	51	0	8	8	368	358	4	11	8	174	185	0	16	8	45	37	3	2	9	179	198
1	5	8	75	84	1	8	8	200	193	5	11	8	78	91	2	16	8	58	49	5	2	9	62	68
2	5	8	247	263	2	8	8	355	378	-5	12	8	106	95	4	16	8	60	58	6	2	9	109	104
3	5	8	194	74	3	8	8	82	83	-4	12	8	177	173	5	16	8	72	78	-6	3	9	40	58
4	5	8	137	162	4	8	8	155	147	-3	12	8	112	111	-4	17	8	52	52	-4	3	9	55	26
5	5	8	100	87	-6	9	8	77	79	-2	12	8	110	119	-3	17	8	82	86	-3	3	9	212	193
6	5	8	169	168	-4	9	8	187	189	-1	12	8	138	143	3	17	8	78	87	-1	3	9	226	228
-4	6	8	132	151	-3	9	8	168	163	1	12	8	133	133	4	17	8	46	50	1	3	9	218	237
-5	6	8	138	154	-2	9	8	86	76	2	12	8	111	117	-2	18	8	87	86	3	3	9	211	194
-6	6	8	189	183	-1	9	8	119	118	3	12	8	118	110	-1	18	8	113	120	6	3	9	30	38
-3	6	8	259	284	0	9	8	190	174	4	12	8	171	170	1	18	8	119	121	-6	4	9	181	212
-2	6	8	305	298	1	9	8	130	113	5	12	8	186	188	2	18	8	84	85	-5	4	9	75	86
-1	6	8	134	129	2	9	8	88	75	-4	13	8	70	54	-3	19	8	49	67	-3	4	9	152	136
0	6	8	156	134	3	9	8	173	171	-3	13	8	97	102	-2	19	8	72	70	-1	4	9	51	48
1	6	8	131	125	4	9	8	180	189	-2	13	8	117	122	-1	19	8	59	55	3	4	9	148	145
2	6	8	286	309	5	9	8	68	58	0	13	8	59	36	0	19	8	60	48	5	4	9	88	88
3	6	8	273	235	-5	10	8	88	86	2	13	8	114	124	1	19	8	60	57	6	4	9	203	213
4	6	8	185	174	-4	10	8	189	163	3	13	8	101	98	2	19	8	68	71	-5	5	9	164	186
5	6	8	144	149	-3	10	8	164	164	4	13	8	48	61	-1	20	8	48	49	-4	5	9	134	149
6	6	8	162	149	-2	10	8	139	176	-5	14	8	182	97	1	20	8	43	49	-3	5	9	209	225
-5	7	8	158	137	-1	10	8	231	212	-3	14	8	130	137	1	0	9	52	28	-1	5	9	91	106
-4	7	8	116	135	0	10	8	237	235	-2	14	8	128	124	2	0	9	87	98	0	5	9	146	143
-3	7	8	167	198	1	10	8	227	223	-1	14	8	62	60	3	0	9	326	337	1	5	9	100	96
-2	7	8	173	187	2	10	8	161	173	1	14	8	64	68	5	0	9	177	198	3	5	9	226	226
-1	7	8	248	259	3	10	8	162	166	2	14	8	119	132	-4	1	9	65	70	4	5	9	149	147
0	7	8	147	149	4	10	8	171	167	3	14	8	126	138	-3	1	9	117	127	5	5	9	195	193
1	7	8	255	259	5	10	8	89	84	5	14	8	103	97	-1	1	9	94	91	6	5	9	77	82
2	7	8	175	182	-5	11	8	83	91	-5	15	8	57	62	0	1	9	193	188	-6	6	9	84	99
3	7	8	192	188	-4	11	8	190	189	-4	15	8	71	66	1	1	9	103	87	-4	6	9	115	111
4	7	8	123	129	-3	11	8	87	77	0	15	8	67	63	3	1	9	123	127	-3	6	9	128	141
5	7	8	154	138	-2	11	8	144	170	1	15	8	54	55	4	1	9	71	72	0	6	9	102	77
6	7	8	83	83	-1	11	8	92	98	4	15	8	63	72	6	1	9	82	79	3	6	9	145	132
-4	8	8	155	144	0	11	8	43	59	5	15	8	60	63	-3	2	9	184	191	4	6	9	118	110
-3	8	8	86	85	1	11	8	88	94	-3	16	8	72	81	-1	2	9	91	108	5	6	9	61	58
-2	8	8	369	384	2	11	8	153	168	-4	16	8	73	56	0	2	9	59	62	6	6	9	93	102
-1	8	8	188	200	3	11	8	76	88	-2	16	8	58	51	1	2	9	98	99	-5	7	9	146	143

OBSERVED AND CALCULATED STRUCTURE FACTORS FOR SH62 P2(1)2(1)2

PAGE 12

H	K	L	10FO	10FC	H	K	L	10FO	10FC	H	K	L	10FO	10FC	H	K	L	10FO	10FC					
-4	7	9	114	100	1	10	9	157	147	-2	10	9	58	81	1	6	10	140	135	0	12	10	55	52
-3	7	9	105	112	2	10	9	78	76	2	19	9	50	76	3	6	10	97	109	1	12	10	79	78
-2	7	9	170	176	3	10	9	108	117	3	0	10	63	49	4	6	10	74	84	2	12	10	59	64
-1	7	9	104	93	4	10	9	85	83	-5	1	10	118	118	5	6	10	104	99	4	12	10	60	59
0	7	9	319	316	5	10	9	80	70	-3	1	10	99	101	-5	7	10	74	73	-4	13	10	40	43
1	7	9	91	101	-5	11	9	62	47	-2	1	10	110	114	-4	7	10	100	42	4	13	10	44	42
2	7	9	180	172	-4	11	9	101	88	-1	1	10	57	76	-3	7	10	82	74	-2	14	10	63	58
3	7	9	103	113	-2	11	9	120	144	0	1	10	167	174	-2	7	10	82	92	-1	14	10	63	62
4	7	9	96	105	0	11	9	102	110	1	1	10	74	80	0	7	10	74	87	0	14	10	101	76
5	7	9	144	139	2	11	9	122	135	2	1	10	108	115	2	7	10	78	94	1	14	10	58	60
-5	8	9	65	71	4	11	9	108	90	3	1	10	104	97	3	7	10	87	71	2	14	10	66	52
-4	8	9	86	76	5	11	9	48	51	5	1	10	104	119	5	7	10	75	72	0	15	10	66	62
-3	8	9	123	123	-5	12	9	72	87	-5	2	10	63	52	-5	8	10	99	85	-2	16	10	67	64
-2	8	9	52	31	-3	12	9	64	63	-4	2	10	75	69	-3	8	10	64	66	2	16	10	65	69
-1	8	9	68	70	0	12	9	48	38	-3	2	10	65	65	-1	8	10	110	108	5	0	11	98	108
0	8	9	226	197	3	12	9	61	79	-2	2	10	97	96	0	8	10	132	40	-3	1	11	55	71
1	8	9	70	68	5	12	9	89	87	0	2	10	105	103	1	8	10	116	102	-2	1	11	62	61
2	8	9	56	28	-4	13	9	57	71	1	2	10	172	156	5	8	10	99	85	0	1	11	46	21
3	8	9	121	125	-2	13	9	100	102	2	2	10	96	97	-5	9	10	66	59	2	1	11	58	66
4	8	9	70	81	-1	13	9	58	54	3	2	10	75	63	-1	9	10	55	36	3	1	11	66	73
5	8	9	64	68	0	13	9	79	81	5	2	10	50	52	1	9	10	54	39	-4	2	11	70	74
-4	9	9	83	94	1	13	9	59	56	-4	3	10	84	88	4	9	10	56	64	-3	2	11	60	69
-3	9	9	131	130	2	13	9	96	105	-1	3	10	177	204	5	9	10	66	61	-2	2	11	43	46
-2	9	9	184	191	-3	14	9	78	100	0	3	10	96	79	-4	10	10	52	63	-1	2	11	66	84
-1	9	9	150	150	-2	14	9	86	85	1	3	10	196	200	-1	10	10	56	33	3	2	11	57	72
0	9	9	179	188	2	14	9	85	86	4	3	10	75	85	0	10	10	145	37	4	2	11	64	77
1	9	9	149	151	3	14	9	85	92	-3	4	10	105	113	1	10	10	56	31	-3	3	11	195	21
2	9	9	176	199	-1	16	9	45	54	-2	4	10	76	78	4	10	10	59	63	-1	3	11	102	100
3	9	9	135	127	1	16	9	52	50	2	4	10	82	74	-1	11	10	75	73	-3	4	11	79	83
4	9	9	92	88	-2	17	9	49	49	3	4	10	106	112	0	11	10	86	98	3	4	11	71	84
-5	10	9	83	72	2	17	9	50	50	5	4	10	53	37	1	11	10	79	71	5	4	11	51	62
-4	10	9	90	82	-2	18	9	46	51	1	5	10	102	93	3	11	10	55	67	-1	5	11	94	85
-3	10	9	112	115	-1	18	9	64	56	-5	6	10	105	101	-4	12	10	52	62	1	5	11	83	81
-2	10	9	81	75	0	18	9	87	81	-4	6	10	72	87	-3	12	10	50	57	-1	6	11	81	66
-1	10	9	152	150	1	18	9	53	59	-3	6	10	109	109	-2	12	10	61	62	1	6	11	70	68
0	10	9	53	50	2	18	9	48	48	-1	6	10	143	134	-1	12	10	81	74	5	6	11	58	54

OBSERVED AND CALCULATED STRUCTURE FACTORS FOR SH62 P2(1)2(1)2

PAGE 13

H	K	L	TOFO	TOFC	H	K	L	TOFO	TOFC	H	K	L	TOFO	TOFC	H	K	L	TOFO	TOFC					
-4	7	11	42	55	-2	11	11	48	40	0	2	12	37	29	-3	6	12	51	51	0	8	12	166	152
4	7	11	47	56	-1	13	11	60	64	2	2	12	74	58	-2	6	12	103	92	2	8	12	90	92
-4	8	11	41	30	1	13	11	68	61	4	2	12	37	43	-1	6	12	63	48	-2	9	12	82	81
-2	8	11	71	60	-2	14	11	64	41	-2	3	12	55	48	1	6	12	62	47	-1	9	12	49	46
-1	8	11	62	57	0	14	11	100	42	-1	3	12	53	62	2	6	12	95	93	1	9	12	54	45
1	8	11	67	60	2	14	11	41	41	1	3	12	57	59	3	6	12	40	54	2	9	12	76	83
2	8	11	70	61	0	0	12	180	170	2	3	12	51	46	-2	7	12	91	81	2	1	13	36	40
-2	9	11	53	56	-3	1	12	63	50	-2	5	12	50	39	0	7	12	117	78	-2	2	13	35	47
0	9	11	59	59	2	1	12	83	76	-1	5	12	56	41	2	7	12	86	79	2	2	13	41	46
2	9	11	49	60	4	1	12	46	43	1	5	12	57	44	-2	8	12	92	94	-1	4	13	104	25
0	10	11	55	31	-2	2	12	78	60	2	5	12	51	40										

(ii)

OBSERVED AND CALCULATED STRUCTURE FACTORS FOR SNP D2(1)/C

PAGE 1

H	K	L	10FO	10FC	H	K	L	10FO	10FC	H	K	L	10FO	10FC	H	K	L	10FO	10FC	H	K	L	10FO	10FC
2	0	0	238	-256	7	4	0	111	-95	6	4	0	100	94	0	18	0	70	-82	-7	3	1	61	-71
3	0	0	361	401	9	4	0	102	-81	7	4	0	172	171	1	18	0	70	-69	-5	3	1	182	162
4	0	0	151	113	10	4	0	144	-128	9	4	0	70	56	3	18	0	69	-112	-4	3	1	475	-455
6	0	0	391	304	1	5	0	768	-786	10	4	0	119	106	-11	1	1	39	-50	-3	3	1	409	-415
7	0	0	66	70	2	5	0	249	-231	0	10	0	353	376	-9	1	1	156	126	-2	3	1	302	307
9	0	0	114	97	6	5	0	115	112	1	10	0	87	82	-7	1	1	156	-110	-1	3	1	1043	1018
1	1	0	183	-216	7	5	0	178	-157	2	10	0	69	-45	-6	1	1	250	-217	0	3	1	98	-54
2	1	0	135	107	3	5	0	85	61	3	10	0	133	115	-5	1	1	190	-174	1	3	1	112	110
3	1	0	257	271	9	5	0	95	-84	4	10	0	95	69	-4	1	1	456	-521	2	3	1	516	-508
4	1	0	94	103	0	6	0	392	-462	6	10	0	279	275	-3	1	1	648	-732	4	3	1	111	79
5	1	0	304	324	1	6	0	453	-466	9	10	0	49	80	-2	1	1	117	-110	5	3	1	227	207
6	1	0	261	-245	2	6	0	76	-46	2	11	0	85	-74	3	1	1	148	-145	7	3	1	55	62
8	1	0	91	-77	3	6	0	316	-348	3	11	0	262	258	4	1	1	287	-299	8	3	1	188	-208
2	2	0	101	68	4	6	0	156	-137	4	11	0	183	196	3	1	1	541	-562	-10	4	1	78	80
3	2	0	454	516	6	6	0	350	-358	6	11	0	108	96	3	1	1	276	254	-2	4	1	67	63
4	2	0	125	-100	7	6	0	94	-90	7	11	0	84	61	7	1	1	115	-95	-8	4	1	274	-235
5	2	0	139	115	9	6	0	134	-116	0	12	0	105	84	6	1	1	126	-102	-6	4	1	52	62
6	2	0	336	331	10	6	0	151	-133	3	12	0	211	230	4	1	1	134	-149	-4	4	1	46	55
7	2	0	71	73	2	7	0	82	-83	5	12	0	142	128	-10	2	1	36	50	-3	4	1	247	234
8	2	0	103	83	3	7	0	101	-48	6	12	0	222	223	-9	2	1	90	79	-2	4	1	485	460
11	2	0	63	43	4	7	0	209	-175	8	12	0	112	98	-3	2	1	74	-92	-1	4	1	1434	1492
1	3	0	2068	-2035	5	7	0	131	-117	9	12	0	74	-97	-7	2	1	113	116	0	4	1	500	471
2	3	0	294	-279	6	7	0	87	64	1	13	0	87	-49	-6	2	1	65	-44	2	4	1	442	403
3	3	0	167	-145	7	7	0	271	255	4	13	0	127	-103	-4	2	1	333	332	3	4	1	339	335
4	3	0	474	-512	8	7	0	81	-72	5	13	0	110	114	-3	2	1	415	415	4	4	1	284	298
5	3	0	265	257	10	7	0	90	62	2	14	0	89	106	-2	2	1	406	573	5	4	1	224	197
7	3	0	230	-212	9	8	0	361	-335	3	14	0	180	191	1	2	1	333	302	6	4	1	290	284
9	3	0	101	79	1	8	0	372	-392	4	14	0	191	-221	2	2	1	266	286	7	4	1	92	87
11	3	0	46	-9	2	3	0	170	169	6	14	0	69	32	3	2	1	41	56	8	4	1	105	118
0	4	0	164	-132	3	8	0	74	-71	1	15	0	101	-87	4	2	1	219	-201	9	4	1	70	75
1	4	0	712	713	4	8	0	138	-138	2	15	0	85	94	5	2	1	835	835	-10	5	1	99	95
2	4	0	453	-469	6	8	0	69	-67	0	16	0	122	-91	7	2	1	115	105	-9	5	1	55	16
3	4	0	334	324	9	8	0	101	-87	1	16	0	127	-133	10	2	1	132	142	-8	5	1	177	183
4	4	0	217	-230	2	9	0	114	-75	3	16	0	110	-103	11	2	1	56	79	-7	5	1	186	176
5	4	0	337	-319	3	9	0	83	-76	6	16	0	63	-8	-9	3	1	59	-58	-5	5	1	294	300
6	4	0	256	-239	4	9	0	132	109	4	17	0	74	-57	-8	3	1	250	217	-4	5	1	93	97

OBSERVED AND CALCULATED STRUCTURE FACTORS FOR SNP P2(1)/C

PAGE 2

H	K	L	10FO	10FC	H	K	L	10FO	10FC	H	K	L	10FO	10FC	H	K	L	10FO	10FC	H	K	L	10FO	10FC
-3	5	1	252	-276	-3	7	1	37	48	3	0	1	127	115	2	12	1	25	50	3	17	1	75	-92
-2	5	1	552	563	-2	7	1	512	517	4	0	1	110	-88	4	12	1	95	-88	4	17	1	76	90
-1	5	1	319	235	-1	7	1	163	115	5	0	1	294	-391	5	12	1	112	108	3	18	1	45	68
0	5	1	126	-102	1	7	1	233	220	6	0	1	85	97	0	12	1	34	78	4	18	1	44	74
1	5	1	429	423	2	7	1	215	-194	-9	10	1	70	62	1	12	1	91	-83	-10	0	2	90	88
3	5	1	311	300	3	7	1	278	265	-6	10	1	73	-61	-7	13	1	56	-60	-9	0	2	160	132
4	5	1	449	427	4	7	1	347	313	-5	10	1	267	278	-5	13	1	57	-62	-7	0	2	158	179
5	5	1	220	197	6	7	1	115	118	-4	10	1	110	-96	-4	13	1	215	-246	-6	0	2	76	78
6	5	1	56	54	7	7	1	89	-107	-3	10	1	168	-166	-3	13	1	35	-115	-5	0	2	408	-418
8	5	1	149	-155	8	7	1	72	-54	-2	10	1	82	54	-2	13	1	32	63	-4	0	2	162	187
9	5	1	122	131	11	7	1	44	-52	-1	10	1	124	-106	-1	13	1	30	-71	-3	0	2	203	-203
-8	6	1	93	72	-9	3	1	60	-52	2	10	1	166	139	1	13	1	119	105	-2	0	2	328	-355
-7	6	1	179	-160	-7	3	1	186	-160	4	10	1	162	-149	2	13	1	272	-322	4	0	2	87	117
-6	6	1	75	77	-6	3	1	67	-51	5	10	1	194	-195	3	13	1	117	-129	5	0	2	143	-119
-5	6	1	265	-264	-5	3	1	144	-135	6	10	1	31	-81	4	13	1	90	-76	6	0	2	208	-190
-4	6	1	196	-131	-4	3	1	342	-330	7	10	1	196	-202	-5	14	1	71	57	7	0	2	155	-152
-3	6	1	462	445	-3	3	1	87	63	8	10	1	115	-115	-4	14	1	120	145	8	0	2	193	-223
-2	6	1	607	533	-2	3	1	590	553	9	10	1	75	-75	-1	14	1	171	192	9	0	2	91	141
-1	6	1	115	120	-1	3	1	276	-258	-7	11	1	123	-116	0	14	1	112	109	-8	1	2	55	-74
0	6	1	445	-417	1	3	1	156	-123	-5	11	1	132	-151	2	14	1	148	212	-7	1	2	39	54
1	6	1	246	242	2	3	1	42	-11	-4	11	1	78	56	3	14	1	136	157	-6	1	2	195	-200
2	6	1	54	-58	3	3	1	177	133	-3	11	1	135	145	5	14	1	106	110	-5	1	2	339	-336
3	6	1	116	94	4	3	1	99	-91	-2	11	1	133	-141	0	14	1	58	70	-4	1	2	223	-221
4	6	1	352	313	5	3	1	175	-172	-1	11	1	388	-410	-4	15	1	134	-115	-3	1	2	176	-171
5	6	1	65	-43	6	3	1	249	-246	0	11	1	58	47	1	15	1	52	74	0	1	2	605	-555
6	6	1	88	-79	7	3	1	153	-133	1	11	1	152	-166	2	15	1	97	-130	3	1	2	363	351
7	6	1	83	-76	9	3	1	68	-62	2	11	1	128	-137	5	15	1	59	61	4	1	2	263	-291
8	6	1	106	-111	-3	9	1	43	43	-4	11	1	91	-81	-4	16	1	55	60	5	1	2	253	-243
9	6	1	79	77	-6	9	1	62	-62	-3	10	1	36	-83	-3	10	1	110	143	6	1	2	184	-195
-10	6	1	65	99	-5	9	1	106	-100	-2	10	1	192	-197	-2	10	1	94	102	8	1	2	85	-91
-10	7	1	37	46	-3	9	1	318	321	0	10	1	103	-106	0	10	1	51	74	9	1	2	126	-190
-8	7	1	75	61	-2	9	1	117	117	-5	12	1	83	72	1	10	1	94	-109	-10	2	2	81	69
-7	7	1	271	273	-1	9	1	294	-286	-4	12	1	176	206	3	10	1	54	71	-7	2	2	200	212
-6	7	1	149	-151	0	9	1	180	-153	-3	12	1	173	179	-2	17	1	65	73	-6	2	2	135	120
-5	7	1	352	368	1	9	1	65	61	-1	12	1	118	104	0	17	1	66	86	-5	2	2	74	-59
-4	7	1	419	414	2	9	1	97	83	1	12	1	256	260	1	17	1	61	86	-4	2	2	261	-227

OBSERVED AND CALCULATED STRUCTURE FACTORS FOR SNP P2(1)/C

PAGE 3

H	K	L	10FO	10FC	H	K	L	10FO	10FC	H	K	L	10FO	10FC	H	K	L	10FO	10FC	H	K	L	10FO	10FC
-3	2	2	324	-365	-10	5	2	65	68	0	7	2	394	589	-6	10	2	87	-89	1	14	2	205	247
-2	2	2	75	-96	-6	5	2	116	-111	1	7	2	403	591	-5	10	2	118	-130	2	14	2	77	83
-1	2	2	236	-256	-5	5	2	196	-210	2	7	2	134	159	-4	10	2	105	121	3	14	2	163	-195
0	2	2	1194	-1123	-4	5	2	221	-227	3	7	2	56	70	-3	10	2	87	104	4	14	2	86	-73
2	2	2	190	133	-3	5	2	43	6	4	7	2	157	160	-2	10	2	91	97	5	14	2	103	-114
3	2	2	215	-220	-2	5	2	92	-98	5	7	2	181	179	0	10	2	115	119	-3	15	2	104	-139
5	2	2	217	194	-1	5	2	100	-95	6	7	2	103	116	1	10	2	227	-224	-1	15	2	121	-144
7	2	2	78	37	0	5	2	133	-109	8	7	2	93	-131	2	10	2	89	-95	0	15	2	92	-85
9	2	2	105	-160	1	5	2	484	-458	-9	8	2	67	-55	3	10	2	94	79	5	15	2	128	-151
-8	3	2	114	-67	2	5	2	233	221	-6	8	2	127	-131	4	10	2	86	100	6	15	2	79	-95
-6	3	2	428	-447	3	5	2	214	-226	-4	8	2	77	-77	6	10	2	119	-122	-1	15	2	79	113
-5	3	2	212	-234	4	5	2	293	306	0	8	2	630	-669	7	10	2	86	-95	0	16	2	92	97
-3	3	2	141	-173	5	5	2	131	-128	1	8	2	114	122	-5	11	2	96	102	1	16	2	100	113
0	3	2	1822	-1731	6	5	2	321	-338	2	8	2	115	110	-3	11	2	124	140	3	16	2	82	-94
1	3	2	553	-515	7	5	2	95	-85	3	8	2	150	143	0	11	2	37	67	5	16	2	94	88
2	3	2	386	-362	8	5	2	159	-209	4	8	2	140	160	1	11	2	212	206	2	17	2	87	-141
3	3	2	568	-564	-7	6	2	102	-115	5	8	2	100	-105	2	11	2	306	332	3	17	2	82	-105
4	3	2	611	-604	-6	6	2	143	-144	7	8	2	70	92	3	11	2	251	270	0	18	2	81	103
5	3	2	115	-122	-4	6	2	193	207	11	8	2	62	-78	4	11	2	39	-74	-8	1	3	127	-114
6	3	2	204	-203	-3	6	2	135	-141	-9	9	2	86	88	7	11	2	87	-60	-7	1	3	105	98
7	3	2	205	-234	-2	6	2	77	-94	-7	9	2	144	136	-4	12	2	140	169	-6	1	3	203	196
10	3	2	99	-137	-1	6	2	407	-371	-6	9	2	115	116	-1	12	2	78	55	-5	1	3	220	-189
-6	4	2	126	-126	0	6	2	611	-606	-5	9	2	144	147	1	12	2	100	77	-4	1	3	72	55
-5	4	2	75	34	1	6	2	187	188	-4	9	2	198	214	2	12	2	177	201	-3	1	3	271	291
-4	4	2	81	104	2	6	2	179	-164	-3	9	2	160	176	3	12	2	170	-162	-2	1	3	159	-113
-3	4	2	335	-339	3	6	2	270	-247	-2	9	2	105	109	6	12	2	129	-138	-1	1	3	400	440
-2	4	2	138	131	4	6	2	621	625	0	9	2	266	283	-4	13	2	34	109	1	1	3	259	-256
0	4	2	169	-159	5	6	2	168	140	1	9	2	352	378	-2	13	2	175	-203	3	1	3	152	-153
1	4	2	269	-266	6	6	2	67	56	2	9	2	240	228	-1	13	2	170	-194	4	1	3	263	-296
3	4	2	210	-202	7	6	2	150	173	3	9	2	459	490	0	13	2	138	-142	5	1	3	185	164
4	4	2	75	-53	8	6	2	82	-153	4	9	2	210	203	3	13	2	94	-110	7	1	3	191	171
5	4	2	54	-42	-3	7	2	97	73	5	9	2	78	99	4	13	2	212	-223	8	1	3	173	161
6	4	2	80	53	-6	7	2	228	249	6	9	2	167	177	6	13	2	103	-121	9	1	3	314	387
7	4	2	99	119	-3	7	2	72	75	7	9	2	180	-229	8	13	2	68	-70	10	1	3	147	210
8	4	2	76	-104	-2	7	2	400	382	8	9	2	104	126	-4	14	2	86	105	-10	2	3	71	65
9	4	2	82	-36	-1	7	2	52	-19	9	9	2	79	101	-1	14	2	260	295	-8	2	3	167	157

OBSERVED AND CALCULATED STRUCTURE FACTORS FOR SNP P2(1)/C

PAGE 4

H	K	L	10FO	10FC	H	K	L	10FO	10FC	H	K	L	10FO	10FC	H	K	L	10FO	10FC					
-7	2	3	162	148	-2	5	3	84	-59	8	7	3	127	-140	-7	11	3	90	82	-3	0	4	78	46
-4	2	3	320	303	-1	5	3	590	-662	9	7	3	117	-143	-4	11	3	275	265	-2	0	4	288	-265
-3	2	3	180	150	0	5	3	381	-355	10	7	3	89	-84	-2	11	3	140	-149	-1	0	4	421	-417
-2	2	3	104	97	1	5	3	71	35	-9	8	3	62	-59	-1	11	3	261	219	5	0	4	575	-625
-1	2	3	401	411	2	5	3	155	103	-8	8	3	91	-70	0	11	3	272	249	6	0	4	394	-420
2	2	3	169	-145	3	5	3	376	-363	-7	8	3	101	-94	2	11	3	140	135	7	0	4	247	-278
3	2	3	212	236	4	5	3	110	-92	-6	8	3	112	85	3	11	3	234	241	9	0	4	176	250
4	2	3	163	153	5	5	3	118	-120	-5	8	3	290	-272	5	11	3	137	-123	-8	1	4	75	51
5	2	3	493	545	6	5	3	181	-168	-4	8	3	114	-114	6	11	3	195	162	-6	1	4	81	-69
6	2	3	167	-115	7	5	3	193	-169	-2	8	3	568	-362	-2	12	3	230	-232	-5	1	4	158	-133
7	2	3	174	144	9	5	3	101	-100	-1	8	3	425	-434	-1	12	3	226	-213	-3	1	4	92	61
8	2	3	98	64	-8	6	3	85	65	0	8	3	131	-126	4	12	3	143	-167	-2	1	4	194	182
9	2	3	144	163	-7	6	3	71	74	2	8	3	259	-252	5	12	3	94	89	-1	1	4	98	118
-8	3	3	121	-104	-5	6	3	47	-47	3	8	3	266	-231	-5	13	3	113	-123	0	1	4	97	-77
-6	3	3	74	34	-4	6	3	96	-79	4	8	3	91	-74	-1	13	3	262	253	1	1	4	398	-398
-2	3	3	115	74	-2	6	3	156	-138	5	8	3	297	-278	0	13	3	185	173	2	1	4	211	198
1	3	3	273	-299	1	6	3	264	240	6	8	3	136	-103	1	13	3	134	-107	3	1	4	434	440
4	3	3	151	35	2	6	3	107	-100	7	8	3	85	86	2	13	3	203	195	4	1	4	328	-350
5	3	3	104	105	3	6	3	251	-212	9	8	3	89	-84	3	13	3	93	95	5	1	4	154	138
7	3	3	224	-213	4	6	3	364	334	10	8	3	86	-69	4	13	3	115	111	6	1	4	90	-83
8	3	3	366	374	5	6	3	96	-53	-3	9	3	253	248	6	13	3	100	-101	7	1	4	232	221
-6	4	3	175	-136	6	6	3	117	-80	-2	9	3	131	-143	8	13	3	135	116	8	1	4	155	-172
-5	4	3	123	103	7	6	3	83	59	0	9	3	130	121	-5	14	3	126	74	-9	2	4	106	-93
-4	4	3	194	159	8	6	3	94	103	1	9	3	102	63	-1	14	3	74	86	-8	2	4	97	-68
-3	4	3	77	68	9	6	3	92	-87	2	9	3	103	85	2	14	3	174	185	-5	2	4	128	-125
-2	4	3	485	516	-7	7	3	185	-171	3	9	3	305	290	-5	15	3	85	-90	-4	2	4	186	-162
-1	4	3	606	643	-5	7	3	239	214	-7	10	3	92	-74	-2	15	3	89	-91	-3	2	4	249	216
1	4	3	324	-304	-4	7	3	72	66	-6	10	3	89	79	2	15	3	100	114	-2	2	4	198	-178
4	4	3	410	393	-3	7	3	138	125	-4	10	3	296	-286	-4	16	3	94	120	-1	2	4	137	-104
5	4	3	239	263	-2	7	3	104	-104	-3	10	3	306	-310	3	16	3	74	-61	0	2	4	625	609
8	4	3	273	287	-1	7	3	432	-439	-2	10	3	484	-490	5	16	3	43	-86	1	2	4	321	328
10	4	3	114	-132	0	7	3	398	-403	-1	10	3	339	-323	-3	17	3	78	-87	2	2	4	473	-516
-7	5	3	235	-189	1	7	3	536	-568	1	10	3	89	-60	3	17	3	70	-94	4	2	4	121	-117
-5	5	3	164	-140	3	7	3	257	-242	2	10	3	240	-236	-6	0	4	133	-117	5	2	4	308	-328
-4	5	3	127	-89	5	7	3	92	54	5	10	3	97	-78	-5	0	4	174	-166	6	2	4	175	-165
-3	5	3	58	-40	6	7	3	372	-373	7	10	3	126	-96	-4	0	4	89	-69	7	2	4	76	-66

OBSERVED AND CALCULATED STRUCTURE FACTORS FOR SNP D2(1)7C

PAGE 5

H	K	L	10FO	10FC	H	K	L	10FO	10FC	H	K	L	10FO	10FC	H	K	L	10FO	10FC					
-9	3	4	76	-76	-1	5	4	276	280	-4	8	4	85	-81	-5	11	4	107	88	-2	1	5	262	271
-6	3	4	230	-207	0	5	4	99	-99	-3	8	4	132	133	-1	11	4	92	78	-1	1	5	499	524
-5	3	4	104	-66	1	5	4	362	-321	-2	8	4	192	195	0	11	4	74	50	0	1	5	466	501
-4	3	4	152	126	2	5	4	304	-291	1	8	4	147	131	1	11	4	115	115	2	1	5	63	-51
-3	3	4	148	-127	3	5	4	159	143	2	8	4	346	357	-7	12	4	92	-116	3	1	5	148	162
-1	3	4	144	139	4	5	4	149	104	3	8	4	314	315	-5	12	4	111	-108	4	1	5	58	73
0	3	4	153	-174	5	5	4	293	-304	4	8	4	167	-169	-4	12	4	136	-144	5	1	5	339	-289
1	3	4	594	-578	6	5	4	344	361	5	8	4	219	186	-3	12	4	169	-167	7	1	5	87	90
2	3	4	162	-139	7	5	4	74	66	6	8	4	234	191	-2	12	4	135	-133	8	1	5	53	-48
3	3	4	110	-90	-3	6	4	100	96	8	8	4	145	132	-1	12	4	210	-222	9	1	5	86	120
4	3	4	157	-135	-5	6	4	276	280	9	8	4	96	-40	0	12	4	95	-101	-5	2	5	48	-22
5	3	4	441	410	-4	6	4	320	328	-8	9	4	69	80	1	12	4	98	-107	-4	2	5	112	-100
6	3	4	262	267	-3	6	4	263	256	-6	9	4	82	85	2	12	4	122	-118	-3	2	5	171	-168
7	3	4	242	244	-2	6	4	299	303	-5	9	4	125	111	3	12	4	147	-152	-2	2	5	228	191
8	3	4	217	251	-1	6	4	314	-294	-4	9	4	92	96	4	12	4	207	-175	-1	2	5	282	-258
9	3	4	131	217	0	6	4	542	576	-3	9	4	178	-182	5	12	4	88	-85	0	2	5	115	64
-8	4	4	92	91	1	6	4	275	262	-2	9	4	242	-219	7	12	4	64	-83	1	2	5	179	-128
-7	4	4	109	-104	2	6	4	415	423	-1	9	4	118	-100	6	12	4	138	-172	2	2	5	591	-596
-6	4	4	192	131	3	6	4	438	467	0	9	4	283	287	8	12	4	70	-63	3	2	5	185	-137
-5	4	4	152	150	4	6	4	348	347	1	9	4	159	-148	-2	13	4	99	-99	4	2	5	437	-445
-4	4	4	184	165	5	6	4	362	374	2	9	4	101	93	-1	13	4	151	151	5	2	5	140	-149
-3	4	4	313	325	6	6	4	180	184	3	9	4	124	-98	1	13	4	89	117	6	2	5	68	48
-2	4	4	209	209	7	6	4	65	63	7	9	4	210	179	5	13	4	154	140	7	2	5	163	-195
-1	4	4	252	249	-5	7	4	102	-93	8	9	4	87	50	6	13	4	102	94	9	2	5	174	-248
1	4	4	412	397	-4	7	4	93	-77	-7	10	4	102	-89	-4	14	4	140	-152	10	2	5	53	-120
2	4	4	251	222	-3	7	4	106	105	-2	10	4	327	-349	-3	14	4	113	-113	-8	3	5	70	71
3	4	4	190	197	-2	7	4	133	-71	-1	10	4	69	-55	-1	14	4	113	-109	-6	3	5	60	50
4	4	4	174	176	-1	7	4	90	-79	0	10	4	170	-155	1	14	4	171	-168	-5	3	5	182	169
5	4	4	76	-41	0	7	4	92	-75	1	10	4	213	-221	2	14	4	80	-92	-4	3	5	132	-114
6	4	4	98	94	1	7	4	226	-201	2	10	4	124	-124	5	14	4	112	-110	-3	3	5	177	-176
8	4	4	188	242	2	7	4	314	-322	3	10	4	168	155	0	15	4	139	124	-2	3	5	197	179
9	4	4	138	191	5	7	4	64	-85	4	10	4	215	-189	4	10	4	104	88	-1	3	5	71	37
-6	5	4	196	-133	6	7	4	78	75	5	10	4	155	-122	-1	17	4	64	-75	1	3	5	177	164
-4	5	4	69	50	7	7	4	245	256	8	10	4	128	-109	-8	1	5	93	35	2	3	5	125	69
-3	5	4	167	-127	3	7	4	70	86	10	10	4	75	-113	-7	1	5	128	137	3	3	5	58	-43
-2	5	4	280	-276	-5	8	4	203	192	-6	11	4	112	87	-6	1	5	54	-53	4	3	5	169	161

OBSERVED AND CALCULATED STRUCTURE FACTORS FOR SNP P2(1)/C

PAGE 6

H	K	L	10FO	10FC	H	K	L	10FO	10FC	H	K	L	10FO	10FC	H	K	L	10FO	10FC	H	K	L	10FO	10FC
5	3	5	393	-375	-3	6	5	300	310	4	8	5	134	-96	9	11	5	121	135	0	0	6	82	-64
6	3	5	398	-304	-2	6	5	111	69	5	8	5	119	108	-3	12	5	109	-105	1	0	6	296	-300
7	3	5	127	120	-1	6	5	157	146	6	8	5	215	195	-2	12	5	111	-105	4	0	6	371	-404
8	3	5	75	93	1	6	5	204	208	7	8	5	221	220	-1	12	5	208	227	7	0	6	341	410
9	3	5	89	-122	1	6	5	305	303	8	8	5	123	130	3	12	5	167	-181	-8	1	6	54	47
-7	4	5	89	-93	2	6	5	128	-116	10	8	5	112	165	4	12	5	72	-58	-5	1	6	56	55
-6	4	5	50	-85	3	6	5	107	85	11	8	5	51	89	6	12	5	85	57	-4	1	6	149	124
-5	4	5	71	70	4	6	5	74	74	-6	9	5	44	-51	8	12	5	39	-45	-3	1	6	169	130
-4	4	5	53	36	5	6	5	172	-130	-3	9	5	123	103	-5	13	5	55	67	-2	1	6	218	208
-3	4	5	140	116	6	6	5	85	79	-2	9	5	224	-203	-2	13	5	201	240	0	1	6	264	-284
-2	4	5	235	245	7	6	5	226	257	-1	9	5	49	-18	1	13	5	164	168	1	1	6	469	477
-1	4	5	191	197	8	6	5	96	-144	1	9	5	37	40	4	13	5	199	184	3	1	6	182	194
0	4	5	231	-246	-3	7	5	69	-60	2	9	5	107	-104	3	13	5	114	-143	4	1	6	256	-255
1	4	5	553	-542	-5	7	5	71	69	3	9	5	94	101	6	13	5	96	86	5	1	6	80	-55
2	4	5	331	-306	-4	7	5	54	-57	4	9	5	241	-247	8	13	5	54	70	5	1	6	267	313
3	4	5	414	-341	-3	7	5	226	-242	5	9	5	68	-63	9	13	5	37	61	7	1	6	52	61
4	4	5	321	-274	-2	7	5	229	-234	6	9	5	144	129	-3	14	5	70	-71	-7	2	6	80	71
5	4	5	492	-396	-1	7	5	303	-313	-3	10	5	131	-130	1	14	5	53	-57	-6	2	6	118	-115
7	4	5	83	-100	1	7	5	397	-372	-2	10	5	167	162	2	14	5	69	-56	-5	2	6	121	-119
8	4	5	39	-34	1	7	5	121	-103	-1	10	5	246	243	4	14	5	198	-113	-4	2	6	123	-122
10	4	5	95	-169	2	7	5	272	-251	0	10	5	210	221	8	14	5	62	-72	-3	2	6	260	-255
-6	5	5	56	-59	3	7	5	110	-97	2	10	5	209	214	-4	15	5	62	-65	-2	2	6	104	-100
-5	5	5	183	-170	4	7	5	73	-62	4	10	5	261	252	-2	15	5	126	155	-1	2	6	217	234
-3	5	5	151	-135	5	7	5	170	-144	5	10	5	163	147	0	15	5	105	-123	0	2	6	194	-165
-1	5	5	221	-198	6	7	5	99	71	6	10	5	60	69	4	15	5	129	140	1	2	6	294	-264
0	5	5	296	257	10	7	5	65	-86	8	10	5	145	144	-1	16	5	53	-56	2	2	6	74	-34
2	5	5	230	-207	-7	3	5	77	75	10	10	5	92	126	0	17	5	43	-58	3	2	6	180	140
3	5	5	285	-291	-5	3	5	55	53	-5	11	5	57	60	1	17	5	68	-72	5	2	6	197	-183
5	5	5	242	-250	-4	3	5	152	149	-4	11	5	109	122	2	17	5	54	-77	7	2	6	85	109
6	5	5	117	-111	-3	3	5	216	231	-2	11	5	84	68	-7	0	6	103	86	0	2	6	98	-118
7	5	5	165	-179	-2	3	5	378	397	-1	11	5	136	-129	-6	0	6	135	-114	-8	3	6	77	80
8	5	5	189	-207	-1	3	5	274	270	1	11	5	95	101	-5	0	6	302	-289	-7	3	6	55	-61
-8	6	5	63	31	0	3	5	178	175	5	11	5	158	139	-4	0	6	165	-124	-6	3	6	86	-81
-7	6	5	60	-47	1	3	5	69	46	6	11	5	174	169	-3	0	6	286	-286	-5	3	6	104	97
-6	6	5	80	75	2	3	5	160	175	7	11	5	152	144	-2	0	6	281	-266	-4	3	6	237	245
-4	6	5	111	-108	3	3	5	250	233	8	11	5	61	-89	-1	0	6	277	268	-3	3	6	212	207

OBSERVED AND CALCULATED STRUCTURE FACTORS FOR SNO D2(1)Z

PAGE 7

H	K	L	10FO	10FC	H	K	L	10FO	10FC	H	K	L	10FO	10FC	H	K	L	10FO	10FC	H	K	L	10FO	10FC
-2	3	6	385	465	4	6	6	150	157	2	9	6	245	-255	6	10	6	57	-71	5	3	7	75	67
-1	3	6	334	310	5	6	6	85	69	3	9	6	166	-164	2	17	6	68	-93	6	3	7	255	260
0	3	6	182	198	6	6	6	94	-61	4	9	6	154	-127	-5	1	7	116	-125	7	3	7	72	61
1	3	6	370	326	7	6	6	147	140	5	9	6	200	-202	-4	1	7	173	-182	8	3	7	230	208
2	3	6	472	460	-5	7	6	144	-133	6	9	6	151	-141	-3	1	7	86	-85	9	3	7	148	-137
3	3	6	112	110	-4	7	6	145	-170	7	9	6	580	-379	-1	1	7	57	-68	-6	4	7	112	-119
4	3	6	159	156	-3	7	6	85	111	8	9	6	264	-299	1	1	7	565	-613	-5	4	7	105	-113
5	3	6	340	331	-2	7	6	104	76	-4	10	6	84	96	2	1	7	106	-94	-3	4	7	132	-122
6	3	6	413	413	1	7	6	190	-194	-1	10	6	96	105	3	1	7	155	-137	-2	4	7	92	-33
7	3	6	140	125	1	7	6	116	-101	3	10	6	123	122	4	1	7	513	-685	-1	4	7	235	-268
-4	4	6	132	-124	2	7	6	220	-132	4	10	6	104	-103	5	1	7	190	176	0	4	7	343	-325
-3	4	6	276	-269	3	7	6	107	85	5	10	6	78	74	7	1	7	269	-281	1	4	7	331	-337
-2	4	6	100	-87	4	7	6	242	-239	6	10	6	72	59	8	1	7	144	-126	3	4	7	477	-466
1	4	6	60	59	5	7	6	234	-215	-1	11	6	67	-84	9	1	7	157	160	4	4	7	242	-206
2	4	6	238	-135	6	7	6	113	-127	3	11	6	120	-117	10	1	7	111	-89	5	4	7	131	33
3	4	6	345	-259	7	7	6	76	-70	5	11	6	118	-121	-6	2	7	65	-75	6	4	7	84	-74
5	4	6	142	-111	1	7	6	244	-340	7	11	6	160	-166	-5	2	7	216	-232	7	4	7	267	-259
6	4	6	65	49	-4	3	6	58	61	8	11	6	135	-145	-4	2	7	85	-86	8	4	7	236	223
-5	5	6	71	70	-3	3	6	160	164	9	11	6	18	-71	-1	2	7	63	-92	9	4	7	106	-96
-3	5	6	147	137	-2	3	6	83	86	-4	12	6	58	52	0	2	7	307	-309	10	4	7	226	-223
-2	5	6	296	323	-1	3	6	93	77	1	12	6	89	113	1	2	7	286	-320	-4	3	7	142	141
-1	5	6	206	178	0	3	6	135	-111	3	12	6	169	-186	2	2	7	36	18	-3	3	7	186	204
0	5	6	191	202	1	3	6	54	63	5	12	6	65	76	3	2	7	155	-147	-2	3	7	71	72
1	5	6	78	-61	2	3	6	139	115	9	12	6	68	101	4	2	7	97	-91	0	3	7	86	-76
2	5	6	464	433	3	3	6	135	-194	-4	13	6	53	52	3	2	7	86	50	1	3	7	217	193
4	5	6	79	-59	5	3	6	116	109	-2	13	6	109	140	6	2	7	330	-327	2	3	7	292	290
5	5	6	216	191	5	3	6	167	-144	2	13	6	134	142	7	2	7	101	-117	3	3	7	72	78
8	5	6	92	-72	3	3	6	91	-95	5	13	6	108	115	9	2	7	152	-117	4	3	7	172	155
-6	6	6	106	106	9	3	6	66	-94	-4	14	6	56	-63	10	2	7	152	-151	5	3	7	386	358
-5	6	6	82	77	-5	9	6	101	-97	0	14	6	67	-78	-6	3	7	58	76	6	3	7	154	135
-4	6	6	134	137	-4	9	6	118	-124	3	14	6	145	-151	-4	3	7	164	-170	7	3	7	197	200
-3	6	6	102	-108	-3	9	6	215	-216	8	14	6	69	74	-1	3	7	122	103	8	3	7	160	147
-2	6	6	222	-136	-2	9	6	81	-67	-2	15	6	74	94	0	3	7	330	-332	11	3	7	152	130
0	6	6	84	49	-1	9	6	132	123	-1	15	6	83	97	1	3	7	82	64	-5	3	7	88	-100
1	6	6	39	46	0	9	6	97	-95	4	15	6	119	140	3	3	7	53	42	-4	3	7	103	-112
3	6	6	383	-345	1	9	6	114	-115	5	15	6	51	78	4	3	7	138	137	-3	3	7	70	75

OBSERVED AND CALCULATED STRUCTURE FACTORS FOR SNP PZ(1)/C

PAGE 8

H	K	L	10FO	10FC	H	K	L	10FO	10FC	H	K	L	10FO	10FC	H	K	L	10FO	10FC	H	K	L	10FO	10FC
-2	6	7	160	-153	-2	11	7	97	111	1	16	7	96	-127	10	2	8	88	67	5	5	8	111	98
-1	6	7	179	-134	-1	10	7	93	-94	1	17	7	47	62	-4	3	8	165	165	6	5	3	139	135
1	6	7	184	174	0	10	7	109	96	2	17	7	61	98	-3	3	8	76	-69	8	5	3	130	114
2	6	7	197	-200	1	10	7	181	184	-4	0	8	154	135	-2	3	8	74	-60	9	5	3	88	45
4	6	7	33	30	2	10	7	110	122	-3	0	8	280	317	-1	3	8	119	113	10	5	3	172	-140
7	6	7	109	-104	3	10	7	171	157	-2	0	8	188	196	0	3	8	154	141	-3	5	3	137	-127
8	6	7	142	-117	4	10	7	319	318	1	0	8	190	-262	1	3	8	224	-261	-1	5	3	128	-115
9	6	7	132	-113	5	10	7	73	-72	2	0	8	177	226	3	3	8	186	-182	0	5	8	222	-265
-2	7	7	92	102	3	10	7	128	-118	4	0	8	136	-146	5	3	8	262	273	1	5	4	211	-227
-1	7	7	73	-64	3	10	7	84	-77	5	0	8	185	218	6	3	8	47	66	2	5	4	231	-260
1	7	7	72	-87	9	10	7	80	73	7	0	8	130	136	7	3	8	83	-53	3	5	3	107	-110
2	7	7	261	276	-5	11	7	72	-89	8	0	8	329	357	8	3	8	101	89	6	5	8	196	-198
4	7	7	337	253	-2	11	7	173	-211	9	0	8	304	205	9	3	8	228	-186	7	5	4	297	-286
5	7	7	496	470	1	11	7	89	-80	10	0	8	107	86	10	3	8	154	-100	8	5	3	284	-270
7	7	7	295	275	2	11	7	202	-206	11	0	8	179	138	12	3	8	110	-75	9	5	4	103	-94
8	7	7	100	99	4	11	7	150	-141	-1	1	8	114	-115	-3	4	8	44	-82	12	6	6	141	-89
9	7	7	154	-140	7	11	7	210	-225	0	1	8	113	64	-4	4	8	92	-96	-3	7	3	126	125
-3	8	7	112	131	3	11	7	123	-142	2	1	8	46	32	-3	4	8	112	107	-2	7	8	141	-135
-2	8	7	67	-65	10	11	7	73	-78	3	1	8	159	-169	0	4	8	147	-150	-1	7	3	109	-113
-1	8	7	133	-125	-2	12	7	113	153	4	1	8	178	-170	1	4	8	122	-136	0	7	3	86	-80
1	8	7	286	307	0	12	7	123	-137	5	1	8	199	210	2	4	8	210	-219	1	7	4	89	58
4	8	7	67	47	4	12	7	157	105	6	1	8	85	58	4	4	8	121	109	2	7	4	99	101
5	8	7	120	113	6	12	7	82	-76	9	1	8	178	-144	5	4	8	58	-53	3	7	4	275	309
7	8	7	153	158	7	12	7	181	-162	-5	2	8	73	81	6	4	8	246	-241	4	7	4	62	-70
8	8	7	149	-152	0	13	7	141	146	-4	2	8	92	74	7	4	8	51	-47	6	7	6	147	127
9	8	7	90	84	1	13	7	67	-54	-3	2	8	219	235	8	4	8	88	-69	7	7	8	312	340
-3	0	7	78	-35	4	13	7	154	-171	-2	2	8	134	145	9	4	8	138	93	8	7	8	118	88
-2	0	7	103	-114	3	13	7	176	-197	0	2	8	124	101	12	4	8	94	-65	-5	6	8	74	66
-1	0	7	156	133	6	13	7	74	-84	1	2	8	108	91	-4	5	8	102	97	-1	3	4	83	-90
0	0	7	111	124	9	13	7	63	-81	2	2	8	116	103	-3	5	8	92	55	0	3	4	89	-66
1	0	7	207	-225	0	14	7	134	-159	3	2	8	231	232	-2	5	8	170	-167	1	1	4	68	-56
2	0	7	163	-139	1	14	7	109	-123	4	2	8	63	63	-1	5	8	53	32	3	3	3	159	-132
3	0	7	71	-54	6	14	7	91	-111	5	2	8	54	39	1	5	8	49	53	5	3	4	39	-36
5	0	7	99	30	7	15	7	92	109	6	2	8	225	217	2	5	8	87	64	7	3	3	185	-173
7	0	7	153	-138	5	15	7	78	-98	8	2	8	201	207	3	5	8	67	-66	9	3	3	174	-159
11	0	7	72	69	6	15	7	73	-94	9	2	8	236	238	4	5	8	90	75	-3	9	4	88	-82

OBSERVED AND CALCULATED STRUCTURE FACTORS FOR SNP P2(1)/C

PAGE 9

H	K	L	10FO	10FC	H	K	L	10FO	10FC	H	K	L	10FO	10FC	H	K	L	10FO	10FC	H	K	L	10FO	10FC
-1	0	8	176	-176	0	1	0	160	-167	-5	4	0	57	61	-3	7	0	56	53	2	12	0	100	105
0	0	8	93	-15	2	1	0	44	49	-4	4	0	71	89	1	7	0	211	203	8	12	0	111	115
3	0	8	142	144	5	1	0	241	-247	-1	4	0	42	30	2	7	0	73	52	0	13	0	97	-109
4	0	8	193	168	4	1	0	274	-293	0	4	0	101	100	5	7	0	146	184	1	13	0	69	-75
8	0	8	182	158	5	1	0	317	-350	1	4	0	120	147	-4	7	0	362	366	2	13	0	71	-90
-1	10	8	111	103	5	1	0	333	-379	2	4	0	88	90	0	7	0	122	87	5	13	0	69	-75
0	10	8	128	112	7	1	0	184	-205	3	4	0	220	-214	7	7	0	96	97	4	13	0	59	-74
2	10	8	173	170	3	1	0	191	172	4	4	0	204	154	6	7	0	229	-202	5	13	0	57	-65
3	10	8	126	114	0	1	0	95	62	5	4	0	317	326	10	7	0	75	71	0	14	0	62	67
5	10	8	165	146	10	1	0	183	-180	6	4	0	266	275	-2	0	0	47	-66	1	14	0	70	74
6	10	8	214	206	11	1	0	117	-70	7	4	0	420	449	-1	0	0	62	-59	2	14	0	117	158
11	10	8	79	69	-5	2	0	60	64	8	4	0	250	245	1	6	0	99	-104	5	14	0	92	100
-4	11	8	79	-74	-4	2	0	110	107	11	4	0	154	129	2	0	0	261	-239	7	14	0	78	68
-3	11	8	143	-139	-3	2	0	86	74	-5	5	0	91	113	4	6	0	153	-128	-4	0	10	117	106
-2	11	8	92	-169	-2	2	0	35	80	-4	5	0	117	127	5	0	0	117	-105	-2	0	10	146	-141
-1	11	8	136	-158	1	2	0	230	253	-3	5	0	61	66	10	0	0	57	-64	-1	0	10	155	161
0	11	8	92	-14	2	2	0	86	77	0	5	0	163	126	13	6	0	52	-52	0	0	10	169	191
2	11	8	89	-10	3	2	0	106	93	1	5	0	273	305	-2	9	0	67	59	1	0	10	169	-186
3	11	8	96	-75	4	2	0	91	83	2	5	0	98	-69	-1	9	0	56	62	2	0	10	269	290
4	11	8	183	156	5	2	0	51	69	4	5	0	116	96	1	9	0	110	-131	3	0	10	30	-5
9	11	8	100	76	6	2	0	276	253	5	5	0	74	52	2	9	0	65	43	6	0	10	227	-205
0	12	8	161	124	7	2	0	351	348	6	5	0	60	41	3	9	0	137	123	8	0	10	76	-61
1	12	8	89	114	3	2	0	366	324	7	5	0	69	51	4	9	0	125	99	0	0	10	97	-86
3	12	8	179	168	9	2	0	174	-154	0	5	0	191	149	7	9	0	75	-53	10	0	10	57	-72
6	12	8	123	103	10	2	0	165	141	10	5	0	123	99	0	10	0	70	82	-4	1	10	52	-58
9	12	8	87	68	11	2	0	156	131	-2	6	0	73	-61	4	10	0	99	-108	0	1	10	163	-162
-2	13	8	57	-66	-5	3	0	47	42	0	6	0	90	121	5	10	0	122	-183	1	1	10	39	22
0	13	8	99	-116	-2	3	0	105	99	1	6	0	110	-132	7	10	0	119	-99	2	1	10	131	-130
6	13	8	79	-70	-1	3	0	63	-47	2	6	0	131	-119	-3	11	0	64	-70	3	1	10	122	-120
3	14	8	167	193	1	3	0	113	66	3	6	0	34	47	-1	11	0	102	-106	5	1	10	64	-61
5	14	8	100	-86	2	3	0	55	-49	5	6	0	172	-140	0	11	0	74	-52	6	1	10	139	-131
8	14	8	71	64	4	3	0	192	97	7	6	0	220	216	1	11	0	80	-91	8	1	10	138	-127
6	15	8	69	-38	5	3	0	178	-170	8	6	0	39	-66	4	11	0	42	-85	0	1	10	148	-147
5	16	8	69	-37	6	3	0	238	-238	-4	7	0	57	64	1	12	0	81	86	-3	2	10	74	-80
-5	1	9	53	-57	7	3	0	72	-62	-3	7	0	75	76	2	12	0	138	149	-2	2	10	121	-133
-1	1	9	86	-91	0	3	0	106	-98	-2	7	0	96	112	3	12	0	75	73	-1	2	10	58	64

OBSERVED AND CALCULATED STRUCTURE FACTORS FOR SNP P2(1)/C

PAGE 10

H	K	L	10FO	10FC	H	K	L	10FO	10FC	H	K	L	10FO	10FC	H	K	L	10FO	10FC	H	K	L	10FO	10FC
0	2	10	79	84	9	3	10	224	-215	0	6	10	84	-129	1	6	10	85	-87	5	10	10	120	-118
2	2	10	112	86	10	3	10	150	-126	1	6	10	74	80	2	6	10	131	-142	4	10	10	55	-48
3	2	10	23	-41	-2	6	10	69	-82	4	6	10	104	97	3	6	10	169	-167	5	10	10	85	81
4	2	10	76	-75	1	6	10	152	149	6	6	10	119	-103	4	6	10	129	137	7	10	10	193	-202
5	2	10	164	-160	3	4	10	159	151	7	6	10	184	147	6	6	10	85	-75	0	11	10	79	80
6	2	10	144	-141	5	4	10	277	-252	8	6	10	156	-132	8	6	10	42	-43	5	11	10	134	140
8	2	10	137	103	7	4	10	133	127	-3	7	10	52	45	10	6	10	96	87	9	11	10	94	71
9	2	10	144	-134	9	4	10	87	-69	-2	7	10	69	73	-3	9	10	78	78	-1	12	10	56	51
10	2	10	191	-104	-3	5	10	71	-77	-1	7	10	157	167	-2	9	10	56	61	0	12	10	46	-34
-3	3	10	127	-132	1	5	10	80	-62	0	7	10	145	166	-1	9	10	155	160	2	12	10	68	37
-1	3	10	89	102	3	5	10	326	-305	2	7	10	86	86	9	9	10	175	194	3	12	10	75	-85
0	3	10	275	-301	4	5	10	209	-208	4	7	10	193	-203	1	9	10	95	111	5	12	10	103	104
1	3	10	138	-152	5	5	10	90	-65	6	7	10	342	316	2	9	10	68	75	0	13	10	56	-65
2	3	10	138	-131	6	5	10	46	-55	7	7	10	63	59	3	9	10	180	177	1	13	10	63	-65
3	3	10	396	-394	7	5	10	67	-64	8	7	10	157	-136	6	7	10	142	124	4	13	10	51	-53
4	3	10	287	-288	8	5	10	121	-133	10	7	10	78	65	7	9	10	64	51	5	13	10	101	-101
5	3	10	136	-113	9	5	10	184	-173	-3	3	10	94	-105	9	9	10	167	152	6	13	10	91	-106
6	3	10	252	-262	-4	6	10	48	-53	-1	8	10	80	-79	0	10	10	93	-99	2	14	10	95	129
7	3	10	75	-73	-1	6	10	115	-138	0	8	10	42	-35	1	10	10	76	-46	5	14	10	62	74
8	3	10	145	-135																				

(iii)

OBSERVED AND CALCULATED STRUCTURE FACTORS FOR CARE P2(1)

PAGE 1

H	K	L	10FO	10FC	H	K	L	10FO	10FC	H	K	L	10FO	10FC	H	K	L	10FO	10FC	H	K	L	10FO	10FC
1	0	0	375	395	5	5	0	124	65	3	2	1	247	236	1	3	1	226	200	-7	2	2	128	161
2	0	0	202	134	-3	5	1	102	112	4	2	1	276	273	2	3	1	208	196	-5	2	2	122	170
4	0	0	363	509	-7	3	1	209	205	5	2	1	355	326	3	3	1	190	183	-3	2	2	446	516
5	0	0	503	529	-5	0	1	76	49	9	2	1	145	139	4	3	1	106	108	-2	2	2	156	192
6	0	0	137	115	-6	1	1	180	132	-6	3	1	120	122	-8	0	2	121	109	0	2	2	297	221
7	0	0	355	352	-2	0	1	152	147	-5	3	1	177	169	-7	0	2	105	99	1	2	2	381	383
8	0	0	135	117	-1	0	1	253	226	-4	3	1	150	139	-5	0	2	143	130	2	2	2	209	209
2	1	0	161	160	1	0	1	224	210	-3	1	1	134	134	-4	0	2	240	193	3	2	2	144	133
3	1	0	231	193	2	0	1	157	166	-2	3	1	317	291	-3	0	2	443	425	4	2	2	265	249
4	1	0	90	92	1	0	1	315	259	-1	3	1	164	151	-2	0	2	569	579	5	2	2	187	163
5	1	0	139	135	5	1	1	433	461	1	3	1	219	211	-1	0	2	308	305	6	2	2	147	136
6	1	0	137	139	6	1	1	193	192	2	3	1	325	317	0	1	2	159	136	7	2	2	119	127
7	1	0	160	141	5	0	1	121	109	3	3	1	402	323	1	0	2	366	383	-6	3	2	214	232
8	1	0	166	161	0	0	1	127	125	4	3	1	207	198	2	0	2	462	403	-5	3	2	69	85
9	1	0	150	144	-9	1	1	123	134	5	3	1	246	236	3	0	2	485	458	-4	3	2	134	147
1	2	0	129	119	-3	1	1	119	120	6	3	1	151	156	4	0	2	274	261	-5	3	2	135	129
2	2	0	111	113	-7	1	1	116	118	3	3	1	112	124	5	0	2	329	303	-2	3	2	319	292
3	2	0	253	244	-5	1	1	306	265	-8	4	1	91	101	6	0	2	368	346	-1	3	2	246	243
4	2	0	244	251	-4	1	1	370	347	-7	4	1	90	90	10	0	2	153	152	0	3	2	484	471
5	2	0	169	156	-3	1	1	345	319	-6	4	1	233	262	-8	1	2	240	251	1	3	2	88	70
6	2	0	155	124	-2	1	1	309	297	-4	4	1	114	102	-7	1	2	150	150	2	3	2	166	156
7	2	0	163	135	-1	1	1	452	519	-3	4	1	206	133	-6	1	2	246	233	3	3	2	295	257
8	2	0	171	164	1	1	1	157	163	-2	4	1	116	104	-5	1	2	154	143	4	3	2	316	306
1	3	0	556	519	2	1	1	336	311	-1	4	1	276	291	-4	1	2	262	265	5	3	2	123	101
2	3	0	167	172	1	1	1	124	93	1	4	1	33	16	-3	1	2	203	192	8	3	2	59	68
3	3	0	219	213	4	1	1	158	131	2	4	1	166	157	-2	1	2	415	402	9	3	2	149	163
4	3	0	114	95	5	1	1	105	99	3	4	1	268	246	-1	1	2	770	851	-7	4	2	182	167
5	3	0	96	97	6	1	1	234	252	4	4	1	210	192	1	1	2	394	384	-6	3	2	99	89
6	3	0	157	159	7	1	1	200	207	5	4	1	142	112	2	1	2	176	158	-5	4	2	124	149
1	4	0	262	239	1	1	1	149	156	6	4	1	97	107	3	1	2	244	203	-4	4	2	100	103
2	4	0	72	71	-5	2	1	129	116	-5	5	1	76	37	4	1	2	193	189	-3	4	2	143	133
3	4	0	223	219	-4	2	1	120	101	-4	5	1	71	131	5	1	2	236	225	-2	4	2	49	41
1	5	0	218	238	-3	2	1	425	461	-3	5	1	134	103	6	1	2	315	304	-1	4	2	242	283
2	5	0	144	130	-2	2	1	276	329	-2	5	1	160	95	7	1	2	107	97	0	4	2	235	223
3	5	0	196	198	-1	2	1	184	220	-1	5	1	164	171	-9	2	2	116	113	1	4	2	169	166
4	5	0	102	159	1	2	1	217	205	0	5	1	156	164	-8	4	2	143	146	2	4	2	104	129

OBSERVED AND CALCULATED STRUCTURE FACTORS FOR CARF P2(1)

PAGE 2

H	K	L	10FO	10FC	H	K	L	10FO	10FC	H	K	L	10FO	10FC	H	K	L	10FO	10FC					
3	4	2	170	153	2	1	3	434	440	-3	4	3	42	26	-7	1	4	164	164	2	3	4	210	193
4	4	2	277	258	3	1	3	328	301	-2	4	3	210	198	-6	1	4	109	95	3	3	4	151	120
8	4	2	88	99	5	1	3	105	98	-1	4	3	261	307	-5	1	4	98	95	4	3	4	245	237
-5	5	2	85	120	6	1	3	131	117	0	4	3	77	54	-4	1	4	182	178	6	3	4	243	233
-4	5	2	170	113	-4	2	3	111	111	1	4	3	274	262	-3	1	4	665	710	4	3	4	121	143
-2	5	2	176	165	-3	2	3	241	312	3	4	3	46	45	-2	1	4	347	323	-6	4	4	160	158
-1	5	2	126	133	-2	2	3	104	119	4	4	3	233	223	-1	1	4	219	203	-5	4	4	54	57
0	5	2	185	196	-1	2	3	106	184	5	4	3	124	135	0	1	4	241	206	-4	4	4	207	210
1	5	2	185	164	0	2	3	645	555	6	4	3	104	130	1	1	4	617	717	-2	4	4	64	66
2	5	2	354	330	2	2	3	482	452	7	4	3	62	72	2	1	4	512	495	-1	4	4	180	191
3	5	2	152	65	4	2	3	163	146	8	4	3	104	115	3	1	4	114	101	0	4	4	199	138
4	5	2	76	56	6	2	3	222	237	-5	5	3	112	115	4	1	4	251	232	1	4	4	106	116
5	5	2	72	124	3	2	3	145	141	-3	5	3	102	62	5	1	4	144	152	3	4	4	193	145
-8	0	3	166	172	-1	3	3	94	129	-2	5	3	174	157	6	1	4	206	192	4	4	4	100	111
-7	0	3	87	100	-2	3	3	140	203	-1	5	3	122	124	7	1	4	111	114	5	4	4	289	252
-6	0	3	224	132	-3	3	3	104	134	0	5	3	126	132	-5	2	4	146	151	4	4	4	215	223
-4	0	3	81	74	-5	3	3	145	146	1	5	3	192	190	-4	2	4	312	329	-3	3	4	150	72
-3	0	3	226	210	-4	3	3	125	122	2	5	3	244	208	-3	2	4	136	156	-1	3	4	129	142
-2	0	3	776	829	-3	3	3	266	251	3	5	3	105	132	-2	2	4	246	343	1	3	4	124	95
-1	0	3	312	315	-2	3	3	289	274	5	5	3	75	165	-1	2	4	174	236	1	3	4	187	183
1	0	3	451	1032	-1	3	3	510	500	-10	0	4	40	114	0	2	4	504	430	2	3	4	134	71
2	0	3	606	764	0	3	3	487	459	-9	0	4	192	202	1	2	4	304	265	3	3	4	132	193
3	0	3	355	353	1	3	3	216	204	-6	0	4	271	266	2	2	4	160	141	-10	3	5	94	97
4	0	3	235	237	2	3	3	92	64	-4	0	4	144	105	3	2	4	202	265	-7	3	5	188	167
5	0	3	346	337	3	3	3	220	167	-3	0	4	318	293	4	2	4	83	70	-6	3	5	343	324
6	0	3	281	268	4	3	3	117	99	-2	0	4	426	442	5	2	4	171	143	-5	3	5	127	122
7	0	3	131	110	5	3	3	222	216	-1	0	4	648	674	6	2	4	268	261	-4	3	5	349	307
-8	1	3	294	314	6	3	3	145	127	0	0	4	427	427	-8	3	4	121	116	-3	3	5	330	328
-7	1	3	234	231	7	3	3	134	121	2	0	4	208	160	-7	3	4	174	195	-1	3	5	57	56
-6	1	3	214	264	3	3	3	116	141	3	0	4	163	166	-5	3	4	188	197	0	3	5	498	585
-5	1	3	234	208	0	3	3	76	73	4	0	4	66	51	-4	3	4	87	73	1	3	5	691	756
-4	1	3	202	194	-3	4	3	86	105	5	0	4	367	362	-3	3	4	146	144	2	3	5	237	210
-3	1	3	563	563	-7	4	3	127	150	6	0	4	102	91	-2	3	4	340	344	3	3	5	353	332
-2	1	3	264	240	-6	4	3	177	232	7	0	4	128	134	-1	3	4	382	338	4	3	5	293	266
0	1	3	554	645	-5	4	3	206	196	8	0	4	84	83	0	3	4	366	351	5	3	5	307	288
1	1	3	185	132	-4	4	3	260	254	9	0	4	160	164	1	3	4	204	179	7	3	5	119	101

OBSERVED AND CALCULATED STRUCTURE FACTORS FOR CARF D2(1)

PAGE 5

H	K	L	10FO	10FC	H	K	L	10FO	10FC	H	K	L	10FO	10FC	H	K	L	10FO	10FC	H	K	L	10FO	10FC
8	0	5	290	386	5	3	5	102	170	3	0	6	120	109	-2	3	6	366	392	-4	1	7	247	223
9	0	5	160	128	6	3	5	245	243	6	0	6	104	82	-1	3	6	303	291	-5	1	7	162	133
-6	1	5	139	211	7	3	5	146	155	7	0	6	125	120	0	3	6	315	274	-3	1	7	394	382
-5	1	5	162	167	8	3	5	81	70	8	0	6	161	169	1	3	6	236	163	-2	1	7	581	584
-4	1	5	81	56	9	3	5	62	70	-10	1	6	97	108	2	3	6	55	60	-1	0	7	218	211
-3	1	5	256	261	-7	4	5	123	140	-8	1	6	73	95	3	3	6	200	189	0	0	7	303	264
-2	1	5	254	268	-5	4	5	190	203	-6	1	6	144	134	4	3	6	137	95	1	0	7	361	353
-1	1	5	283	173	-5	5	5	60	43	-5	1	6	161	169	5	3	6	136	155	3	0	7	502	493
0	1	5	430	411	-3	6	5	223	236	-4	1	6	290	258	6	3	6	90	75	4	0	7	96	107
1	1	5	453	433	-2	6	5	135	100	-3	1	6	423	431	8	3	6	86	97	5	1	7	127	118
2	1	5	319	264	-1	6	5	322	355	-2	1	6	374	375	9	3	6	111	125	-7	1	7	112	110
3	1	5	521	510	0	6	5	104	68	-1	1	6	147	142	-8	4	6	87	100	-6	1	7	139	114
4	1	5	247	240	1	4	5	202	170	0	1	6	506	497	-7	4	6	136	164	-5	1	7	243	228
6	1	5	127	103	2	4	5	221	193	1	1	6	114	112	-6	4	6	141	139	-4	1	7	276	277
-9	2	5	137	145	3	4	5	223	211	2	1	6	371	367	-5	4	6	64	60	-3	1	7	237	239
-8	2	5	146	114	5	4	5	202	176	3	1	6	551	554	-4	4	6	136	117	-2	1	7	192	161
-3	2	5	277	243	6	4	5	100	100	5	1	6	234	230	-3	4	6	232	227	-1	1	7	449	401
-2	2	5	270	368	7	4	5	69	74	6	1	6	159	158	-2	4	6	109	100	0	1	7	333	348
-1	2	5	156	146	-4	5	5	212	138	3	1	6	145	145	-1	4	6	239	266	1	1	7	163	135
0	2	5	130	118	-3	5	5	206	120	-6	2	6	233	202	0	4	6	94	100	2	1	7	611	613
1	2	5	276	274	-2	5	5	210	224	-5	2	6	131	145	1	4	6	97	116	3	1	7	525	522
2	2	5	150	126	-1	5	5	111	93	-4	2	6	193	202	2	4	6	346	303	5	1	7	173	168
3	2	5	134	122	0	5	5	122	141	-3	2	6	105	143	3	4	6	191	157	6	1	7	109	110
4	2	5	131	133	1	5	5	112	90	-2	2	6	66	46	4	4	6	104	89	7	1	7	155	154
6	2	5	149	131	2	5	5	111	135	-1	2	6	223	182	6	4	6	129	120	8	1	7	164	181
-8	3	5	133	157	4	5	5	139	135	0	2	6	264	259	7	4	6	93	110	-10	2	7	110	102
-7	3	5	146	175	-10	6	6	109	87	1	2	6	334	305	8	4	6	93	115	-6	2	7	201	245
-6	3	5	91	112	-7	6	6	283	285	2	2	6	187	145	-5	5	6	115	93	-4	2	7	96	107
-4	3	5	213	235	-6	6	6	104	73	4	2	6	255	231	-4	5	6	199	199	-3	2	7	147	207
-3	3	5	114	115	-5	6	6	303	302	6	2	6	252	276	-3	5	6	234	203	-2	2	7	270	351
-2	3	5	293	254	-4	6	6	417	395	-8	3	6	79	95	-1	5	6	160	98	-1	2	7	121	115
-1	3	5	292	279	-3	6	6	642	652	-7	3	6	83	89	0	5	6	93	89	0	2	7	221	204
1	3	5	246	213	-2	6	6	431	413	-6	3	6	161	177	1	5	6	114	125	1	2	7	83	73
2	3	5	234	245	-1	6	6	322	260	-5	3	6	152	139	2	5	6	107	116	2	2	7	162	118
3	3	5	148	160	0	6	6	501	576	-4	3	6	175	162	3	5	6	118	153	4	2	7	212	171
4	3	5	217	203	2	6	6	123	134	-3	3	6	184	173	-7	0	7	261	260	5	2	7	248	210

OBSERVED AND CALCULATED STRUCTURE FACTORS FOR CASE D2(1)

PAGE 4

H	K	L	10FO	10FC	H	K	L	10FO	10FC	H	K	L	10FO	10FC	H	K	L	10FO	10FC
6	2	7	162	166	-9	2	8	136	134	2	2	8	107	263	-4	0	8	188	162
6	2	7	95	113	-9	2	8	161	152	3	2	8	220	194	-3	0	8	228	236
-9	3	7	89	93	-3	2	8	195	193	5	2	8	191	156	-2	0	8	144	76
-7	3	7	165	153	-5	2	8	211	209	0	2	8	82	131	-1	0	8	117	66
-6	3	7	132	158	-4	2	8	141	121	-9	3	8	93	131	0	0	8	89	78
-5	3	7	95	114	-3	2	8	119	100	-8	3	8	95	126	1	5	8	134	40
-3	3	7	200	279	-1	2	8	564	574	-7	3	8	157	236	2	0	8	168	221
-2	3	7	129	121	-1	2	8	250	252	-6	3	8	125	156	-9	0	0	171	162
-1	3	7	427	425	0	2	8	220	190	-5	3	8	71	117	-7	0	0	102	84
0	3	7	414	514	1	2	8	280	262	-4	3	8	100	90	-6	0	0	124	130
1	3	7	149	112	2	2	8	226	206	-3	3	8	114	129	-5	0	0	366	342
2	3	7	286	279	4	2	8	333	322	-2	3	8	176	164	-4	0	0	190	169
3	3	7	307	276	0	2	8	136	176	-1	3	8	307	296	-3	0	0	345	346
4	3	7	159	169	2	2	8	117	135	0	3	8	204	211	-2	0	0	371	362
5	3	7	95	92	-7	1	8	233	225	1	3	8	194	144	-1	0	0	435	411
6	3	7	173	120	-5	1	8	154	135	2	3	8	222	219	0	0	0	440	324
7	3	7	146	142	-4	1	8	326	323	3	3	8	75	66	1	0	0	130	161
8	3	7	85	112	-1	1	8	133	120	4	3	8	133	120	2	0	0	263	212
-8	4	7	69	73	-2	1	8	270	242	5	3	8	193	136	3	0	0	220	234
-5	4	7	99	108	-1	1	8	132	76	6	3	8	180	175	4	0	0	268	236
-4	4	7	226	228	0	1	8	626	593	7	3	8	80	78	6	0	0	169	163
-3	4	7	222	231	2	1	8	254	220	1	3	8	147	156	8	0	0	121	124
-2	4	7	143	143	2	1	8	426	402	-7	4	8	85	111	-7	1	0	139	129
-1	4	7	214	169	3	1	8	286	265	-6	4	8	114	105	-6	1	0	135	116
0	4	7	156	144	4	1	8	139	139	-5	4	8	71	43	-4	1	0	190	160
1	4	7	213	217	5	1	8	127	132	-4	4	8	235	231	-3	1	0	425	387
2	4	7	256	227	7	1	8	160	174	-3	4	8	211	216	-2	1	0	126	120
4	4	7	221	119	-10	2	8	156	146	-2	4	8	222	214	-1	1	0	331	316
6	4	7	123	152	-8	2	8	169	167	-1	4	8	201	179	1	1	0	251	207
7	4	7	133	142	-6	2	8	196	219	0	4	8	147	131	2	1	0	159	127
-4	5	7	219	137	-5	2	8	231	241	1	4	8	313	325	3	1	0	118	120
-3	5	7	251	220	-4	2	8	203	224	3	4	8	264	170	4	1	0	240	247
-2	5	7	230	213	-3	2	8	120	137	4	4	8	162	116	-10	2	0	74	81
-1	5	7	96	137	-1	2	8	196	230	5	4	8	137	133	-5	2	0	353	390
1	5	7	89	90	0	2	8	210	180	6	4	8	81	90	-4	2	0	166	190
2	5	7	121	126	1	2	8	369	320	-7	5	8	142	110	-3	2	0	204	234

OBSERVED AND CALCULATED STRUCTURE FACTORS FOR CARE D2(1)

PAGE 5

H	K	L	10FO	10FC	H	K	L	10FO	10FC	H	K	L	10FO	10FC	H	K	L	10FO	10FC	H	K	L	10FO	10FC
0	5	9	85	78	-6	3	10	118	119	0	0	11	158	131	-1	3	11	153	142	-6	2	12	99	110
1	5	9	89	107	-5	3	10	209	245	1	0	11	239	196	0	3	11	162	163	-5	2	12	145	110
2	5	9	145	194	-4	3	10	292	286	2	0	11	160	148	1	3	11	182	173	-4	2	12	121	108
3	5	9	114	150	-3	3	10	88	96	3	0	11	123	122	2	3	11	83	71	-3	2	12	175	150
-8	0	10	291	298	-2	3	10	142	141	4	0	11	197	168	4	3	11	259	277	-2	2	12	169	183
-5	0	10	95	69	-1	3	10	280	313	5	0	11	350	306	0	3	11	151	159	-1	2	12	145	122
-6	0	10	312	209	0	3	10	51	35	6	0	11	234	242	3	3	11	83	99	0	2	12	157	164
-3	0	10	219	219	1	3	10	267	270	7	0	11	158	187	-6	4	11	100	92	1	2	12	269	259
-2	0	10	157	154	2	3	10	170	187	-8	1	11	153	148	-5	4	11	199	218	3	2	12	175	146
-1	0	10	619	623	4	3	10	169	175	-5	1	11	205	189	-4	4	11	245	267	6	2	12	146	162
0	0	10	122	105	5	3	10	120	131	-3	1	11	115	80	-2	4	11	128	106	-9	3	12	112	118
1	0	10	444	472	6	3	10	72	101	-2	1	11	319	288	-1	4	11	159	164	-8	3	12	129	136
2	0	10	445	417	-7	4	10	109	116	0	1	11	296	303	0	4	11	103	68	-7	3	12	84	84
3	0	10	84	73	-5	4	10	261	292	1	1	11	178	135	1	4	11	167	166	-5	3	12	136	124
4	0	10	214	183	-4	4	10	214	247	2	1	11	165	172	2	4	11	230	217	-4	3	12	230	237
5	0	10	247	232	-5	4	10	178	166	3	1	11	122	119	3	4	11	160	146	-3	3	12	292	289
-10	1	10	99	119	-2	4	10	231	276	4	1	11	157	165	-7	5	11	128	138	-2	3	12	129	123
-5	1	10	310	325	-1	4	10	161	201	5	1	11	165	196	-3	5	11	153	157	0	3	12	94	91
-6	1	10	100	83	0	4	10	149	115	-7	2	11	115	116	-2	5	11	98	63	1	3	12	177	163
-3	1	10	317	262	2	4	10	369	409	-6	2	11	126	98	-10	0	12	101	76	2	3	12	292	312
-2	1	10	174	171	3	4	10	90	103	-5	2	11	263	245	-8	0	12	131	99	3	3	12	173	157
-1	1	10	137	109	4	4	10	160	145	-4	2	11	147	132	-6	0	12	145	148	5	3	12	110	117
0	1	10	174	166	6	4	10	104	123	-3	2	11	193	197	-5	0	12	201	197	6	3	12	82	83
1	1	10	450	458	7	4	10	68	58	-2	2	11	190	234	-4	0	12	106	73	7	3	12	61	56
2	1	10	263	271	-3	5	10	137	79	-1	2	11	180	160	-2	0	12	384	366	-5	4	12	262	233
3	1	10	150	157	-2	5	10	129	146	0	2	11	260	249	1	0	12	315	290	-4	4	12	110	109
4	1	10	224	229	-1	5	10	83	109	1	2	11	314	299	2	0	12	155	146	-3	4	12	85	70
5	1	10	161	160	0	5	10	102	100	2	2	11	342	278	5	0	12	236	206	-2	4	12	76	78
-5	2	10	269	270	3	5	10	93	132	3	2	11	228	198	6	0	12	211	213	-1	4	12	153	142
-6	2	10	197	158	-3	0	11	285	269	4	2	11	249	237	7	0	12	119	125	0	4	12	208	197
-3	2	10	120	127	-6	0	11	172	130	-9	3	11	114	105	-4	1	12	233	210	1	4	12	132	153
-2	2	10	150	148	-5	0	11	191	147	-7	3	11	103	110	-2	1	12	322	293	2	4	12	136	129
-1	2	10	250	258	-4	0	11	112	96	-6	3	11	114	129	-1	1	12	207	192	6	4	12	165	152
0	2	10	122	125	-3	0	11	75	79	-5	3	11	119	138	0	1	12	192	202	5	4	12	79	74
1	2	10	179	171	-2	0	11	132	99	-4	3	11	96	112	1	1	12	241	204	-6	5	12	136	128
-7	3	10	50	62	-1	0	11	312	325	-3	3	11	126	125	2	1	12	195	166	-1	5	12	104	64

OBSERVED AND CALCULATED STRUCTURE FACTORS FOR CARE P2(1)

PAGE 6

H	K	L	10FO	10FC	H	K	L	10FO	10FC	H	K	L	10FO	10FC	H	K	L	10FO	10FC					
-7	0	13	235	220	-5	3	13	217	221	4	1	14	157	154	1	0	15	270	243	2	4	15	90	92
-6	0	13	420	454	-6	3	13	235	242	-8	2	14	207	180	2	0	15	171	157	4	4	15	96	103
-5	0	13	262	255	-3	3	13	234	231	-5	2	14	188	160	3	0	15	179	190	-5	5	15	68	80
-3	0	13	194	175	-7	3	13	152	127	-4	2	14	223	176	7	0	15	159	167	-4	5	15	135	150
-2	0	13	517	510	-1	3	13	203	189	-3	2	14	171	123	-5	1	15	192	183	0	5	15	134	198
-1	0	13	205	176	1	3	13	143	145	-2	2	14	206	177	-3	1	15	207	193	-5	1	16	297	246
0	0	13	92	55	1	3	13	206	212	-1	2	14	157	123	-2	1	15	147	148	-3	1	16	150	158
1	0	13	173	165	2	3	13	100	105	2	2	14	424	420	-1	1	15	110	125	-2	1	16	160	166
2	0	13	134	126	3	3	13	134	152	3	2	14	294	304	0	1	15	140	133	-1	0	16	265	266
3	0	13	96	101	7	3	13	76	93	-8	3	14	80	99	1	1	15	229	209	0	0	16	337	324
4	0	13	144	151	-5	4	13	159	151	-5	3	14	134	138	2	1	15	131	139	1	0	16	129	124
5	0	13	173	171	-6	4	13	145	136	-4	3	14	204	209	3	1	15	149	151	3	1	16	105	111
-7	1	13	97	91	-1	4	13	131	127	-3	3	14	121	123	4	1	15	142	159	7	1	16	87	105
-6	1	13	133	125	0	4	13	278	265	-2	3	14	130	139	-7	2	15	124	120	-2	1	16	88	108
-5	1	13	135	130	1	4	13	124	124	-1	3	14	166	175	-6	2	15	207	168	-5	1	16	199	193
-4	1	13	201	192	2	4	13	99	86	0	3	14	133	132	-5	2	15	150	157	-2	1	16	179	181
-3	1	13	166	166	4	4	13	133	143	1	3	14	100	101	-4	2	15	191	152	-1	1	16	130	127
-2	1	13	173	147	-5	5	13	110	81	2	3	14	132	169	-2	2	15	117	73	0	1	16	172	160
-1	1	13	204	195	-1	5	13	115	126	3	3	14	180	136	-1	2	15	143	103	2	1	16	226	246
0	1	13	240	223	-5	0	14	92	86	4	3	14	120	121	2	2	15	217	210	7	1	16	139	190
1	1	13	261	255	-4	0	14	224	190	6	3	14	84	113	-7	3	15	92	74	-4	2	16	169	120
2	1	13	150	151	-3	1	14	131	101	-6	4	14	102	115	-6	3	15	181	187	-2	2	16	201	217
3	1	13	306	307	-2	0	14	165	144	-4	4	14	214	182	-5	3	15	97	97	0	2	16	145	154
5	1	13	147	146	-1	1	14	228	211	-3	4	14	85	88	-4	3	15	143	154	-6	3	16	91	108
-9	2	13	81	73	1	0	14	138	160	-2	4	14	134	134	-3	3	15	165	167	-6	3	16	144	153
-6	2	13	127	125	3	0	14	210	193	-1	4	14	86	77	-2	3	15	320	311	-4	3	16	152	148
-4	2	13	126	134	-7	1	14	170	167	0	4	14	106	95	0	3	15	141	136	-3	3	16	219	198
-3	2	13	159	141	-6	1	14	204	185	1	4	14	197	181	1	3	15	107	105	-2	3	16	207	219
-2	2	13	123	99	-5	1	14	191	189	4	4	14	73	86	2	3	15	92	101	-1	3	16	134	160
1	2	13	143	112	-4	1	14	181	175	-1	5	14	140	154	3	3	15	160	186	0	3	16	139	125
2	2	13	204	223	-3	1	14	204	188	-6	0	15	104	112	4	3	15	174	199	1	3	16	212	204
4	2	13	130	134	-2	1	14	179	163	-5	0	15	213	193	-4	4	15	169	188	3	3	16	101	126
6	2	13	129	120	-1	1	14	92	100	-3	0	15	175	192	-2	4	15	95	78	-6	4	16	98	104
-8	3	13	116	139	0	1	14	162	152	-2	0	15	161	129	-1	4	15	145	153	-1	4	16	86	97
-7	3	13	94	81	1	1	14	284	312	-1	0	15	270	277	0	4	15	71	98	1	4	16	137	140
-6	3	13	157	162	2	1	14	124	132	0	0	15	337	312	1	4	15	165	189	4	4	16	108	108

OBSERVED AND CALCULATED STRUCTURE FACTORS FOR CARF P2(1)

PAGE 7

H	K	L	10FO	10FC	H	K	L	10FO	10FC	H	K	L	10FO	10FC	H	K	L	10FO	10FC	H	K	L	10FO	10FC
-1	5	16	81	136	0	3	17	113	150	1	2	18	103	153	-2	3	19	106	120	-5	1	21	131	160
-9	0	17	80	68	1	3	17	135	153	3	2	18	155	146	-1	3	19	127	149	-6	2	21	155	126
-6	0	17	173	153	3	3	17	60	86	-6	3	18	60	113	0	3	19	95	109	1	2	21	106	145
-4	0	17	252	249	4	3	17	136	184	-5	3	18	91	106	2	3	19	100	112	-5	3	21	89	109
-3	0	17	107	106	5	3	17	71	62	-2	3	18	204	203	3	3	19	87	107	-2	3	21	90	93
-2	0	17	304	312	-1	4	17	99	101	-1	3	18	136	148	-5	0	20	112	117	-1	3	21	79	100
-1	0	17	87	62	0	4	17	147	143	0	3	18	162	179	-4	0	20	174	155	1	3	21	96	109
0	0	17	195	165	3	4	17	93	90	1	3	18	80	110	-3	0	20	146	159	2	3	21	96	116
2	0	17	120	142	4	4	17	131	141	2	3	18	116	129	-2	0	20	217	217	3	3	21	62	62
3	0	17	297	324	-5	0	18	137	150	4	3	18	131	164	0	0	20	189	149	-3	0	22	213	222
4	0	17	193	234	-6	0	18	122	122	-6	4	18	71	73	4	0	20	138	146	0	1	22	120	150
-5	1	17	270	282	-3	0	18	112	111	-3	4	18	121	124	0	1	20	147	196	-4	3	22	90	113
-2	1	17	171	153	-2	0	18	150	150	-1	4	18	112	104	3	1	20	172	90	-2	3	22	79	93
2	1	17	135	156	-1	0	18	152	154	-2	5	18	81	122	4	2	20	107	119	1	3	22	87	123
-6	2	17	123	128	1	0	18	264	277	-7	0	19	151	150	-6	3	20	66	78	-3	0	23	161	215
-4	2	17	235	170	3	0	18	230	250	3	0	19	137	136	-5	3	20	80	102	-2	0	23	122	133
0	2	17	143	154	-6	1	18	120	142	4	0	19	111	157	-3	3	20	136	172	-3	3	23	80	108
1	2	17	141	176	-5	1	18	182	163	0	1	19	172	228	-1	3	20	109	123	-2	0	24	133	150
-8	3	17	43	57	-1	1	18	145	151	-5	2	19	113	109	2	3	20	48	83	-5	2	24	87	90
-7	3	17	70	68	-3	2	18	93	73	0	2	19	167	162	4	3	20	55	94	-3	3	24	66	86
-5	3	17	73	67	-5	2	18	93	101	1	2	19	190	192	2	4	20	87	98	-1	3	24	72	84
-4	3	17	99	68	-4	2	18	121	126	-6	3	19	82	107	0	0	21	122	120	-5	3	25	98	112
-2	3	17	192	169	-1	2	18	150	152	-4	3	19	65	80	3	0	21	131	141	-4	0	25	70	105
-1	3	17	149	163	0	2	18	174	153	-3	3	19	97	83										

REFERENCES

1. M.J. BUERGER, "Crystal Structure Analysis", Wiley, 1960
2. E.W. NUFFIELD, "X-ray Diffraction Methods", Wiley, 1966
3. M.F.C. LADD and R.A. PALMER, "Structure Determination by X-ray Crystallography", Plenum Press, 1977
4. M.M. WOOLFSON, "An Introduction to X-ray Crystallography", Cambridge University Press, 1970
5. G.H. STOUT and L.H. JENSEN, "X-ray Structure Determination", Macmillan, 1968
6. 'International Tables for X-ray Crystallography', Vols. I - IV (Vol I, 3rd ed., 1969, Vol II, 2nd ed., 1967, Vol. III, 2nd ed., 1968)
7. M.L. GOLDBERGER and K.M. WATSON, "Collision Theory", John Wiley and Sons, New York, 1964
8. R.G. NEWTON, "Scattering of Waves and Particles", McGraw-Hill Book Company, New York, 1966
9. W.L. BRAGG, Proc. Cambridge Phil. Soc., 1913. 17, 43 .
10. E.R. HOWELLS, D.C. PHILLIPS and D. ROGERS (1950), Acta Cryst. 3, 210
11. I. WALLER, Zeit. f. Physik, 1923, 17, 398
12. P. DEBYE, Verh. d. Deutsch. Phys. Ges., 1913, 15, 678, 738, 857
13. A.J.C. WILSON, 1942, Nature, 150, 151
14. A.L. PATTERSON, 1935, Z. Krist. m A90, 517
15. D. HARKER and J.S. KASPER (1948) Acta Cryst. 1,70
16. D. SAYRE (1952), Acta Cryst. 5, 60
17. W. COCHRAN (1952), Acta Cryst. 5, 65
18. W.H. ZACHARIASEN (1952) Acta Cryst. 5, 68
19. W. COCHRAN (1955), Acta Cryst. 8, 473
20. G. GERMAIN, P. MAIN and M.M. WOOLFSON, a - Acta Cryst., B24, 91 (1968) b - Acta Cryst., A27, 368-276 (1971)
21. C. SHELDRIK, Program for Crystal Structure Determination, 1976, University of Cambridge
22. H. HAUPTMAN and J. KARLE (1956) Acta Cryst., 9, 45-55
23. J. KARLE and H. HAUPTMAN (1956) Acta Cryst., 9, 635-651
24. I.L. KARLE and J. KARLE, Acta Cryst., 17, 835-841 (1964)
25. I.L. KARLE and J. KARLE, Acta Cryst., 21, 860-868 (1966)

26. U. D. SHENOY, 1975, Benzodiazocines: Rearrangement Reactions of Benzodiazepines; a thesis presented for the degree of Doctor of Philosophy in the University of London, Ch. 3., 24-174
27. G. SEYBOLD, U. JERSAK and R. GOMPPER, Angew Chem. Internat. Edit. Vol 12, (1973) No. 10, 847
28. R. J. GIRVEN, 1977, X-ray Structural Studies of Antibiotic Materials; a thesis presented for the degree of Doctor of Philosophy (CNA) Ch 1, 9
29. F. J. PETRACEK, Chemistry of Psychopharmacological Agents, Principles of Psychopharmacology; CLARK, W. G. and Del GIUDICE, J. Chapter 13, Academic Press, 1970
30. BRANDT, A., BASSIGNANI, L. and Re L. (1976a) Tetrahedron Letters No. 44, pp 3975-3978
31. BRANDT, A., BASSIGNANI, L. and Re L. (1976b) Tetrahedron Letters No. 44, pp. 3979-3982
32. BACHI, M. D. and VAYA, J. (1977) Tetrahedron Letters No. 25, pp 2209-2212
33. HAUPTMAN, H., 'The Structure Invariants and Seminvariants', Copies of Lecture Notes: N.A.T.O. Advanced Study Institute under the auspices of the "Ettore Majorana" Centre for Scientific Culture, Erice, Sicily, March 25 - April 6, 1974, Ch. B
34. M. O. BOLES and R. J. GIRVEN (1976a) Acta Cryst., B32, 2279-2284
35. M. O. BOLES and R. J. GIRVEN (1976b) 'Crystalline Forms of Ampicillin', paper presented at 3rd European Crystallography Meeting, Zurich, September 1976
36. S. ABRAHAMSSON, DOROTHY CROWFOOT HODGKIN and E. N. MASLEN (1963) Biochem J. 86, 514-535
37. K. J. WATSON (unpublished)
38. D. CROWFOOT, C. W. BUNN, B. W. ROGERS-LOW and A. TURNER-JONES (1949) 'The Chemistry of Penicillin', Princeton University Press, pp 367-381
39. G. J. PITT (1952) Acta Cryst., 5, 770-775
40. M. O. BOLES, R. J. GIRVEN and P. A. C. GANE (1978) Acta Cryst., B 34, 461-466
41. M. N. G. JAMES, D. HALL and D. C. HODGKIN (1968) Nature (London), 220, 168-170
42. D. C. HODGKIN and E. N. MASLEN (1961) Biochem. J. 79 393-402
43. R. D. DIAMOND (1963) D. Phil Thesis: Univ. of Oxford
44. R. M. SWEET and L. F. DAHL (1970) J. Amer. Chem. Soc., 92 5489-5507

45. V. KALYANI and D. C. HODGKIN (1970) personal communication to R. M. Sweet
46. G. L. SIMON and L. F. DAHL (1970) personal communication to R. M. Sweet
47. I. CSÖREGH and T. B. PALM (1976) Acta Cryst., (1977) B33, 2169-2174 I. CSÖREGH and T. B. PALM (1976) Chem. Comm.
48. M. O. BOLES, R. J. GIVEN and P.A.C. GANE (1977) paper presented at the 4th European Crystallography Meeting, Oxford, August 1977
49. P. BLANPAIN and F. DURANT (1977) Acta. Cryst., B33 580-582
50. P. BLANPAIN and F. DURANT (1976) Cryst. Struct. Comm. 5, 83-88
51. J. D. ROBERTS (1959) 'Nuclear Magnetic Resonance, Applications to Organic Chemistry'. McGraw-Hill Book Company, Inc.
52. A. CARRINGTON and A. D. McLACHLAN (1967) 'Introduction to Magnetic Resonance'. Harper and Row, Inc.
53. C. E. JOHNSON and F. A. BOVEY (1958). J. chem. Phys. 29, 1012
54. E. L. ELIEL (1962) 'Stereochemistry of Carbon Compounds' McGraw-Hill Book Company, Inc.
55. J. MARCH (1968). 'Advanced Organic Chemistry: Reactions, Mechanisms and Structure'. McGraw-Hill Book Company, Inc.
56. J. B. STENLAKE, G. C. WOOD, H. C. MITAL and SHEENA STEWART (1972) Analyst 97, 639-643
57. D. B. BOYD, CHIN-YAH YEH and F. S. RICHARDSON (1976) Journal of the American Chemical Society/98:20/, 6100-6106
58. F. P. DOYLE and J. H. C. NAYLER, "Advances in Drug Research", N. J. Harper and A. B. Simmonds, eds., Academic Press, London and New York, 1964, Vol 1, p. 1
59. R. BENTLEY, A.H. COOK and J. A. ELVIDGE, J. Chem. Soc., 3216 (1949)
60. KARLE, HAUPTMAN and CHRIST, Acta Cryst., 11 (1958) 757

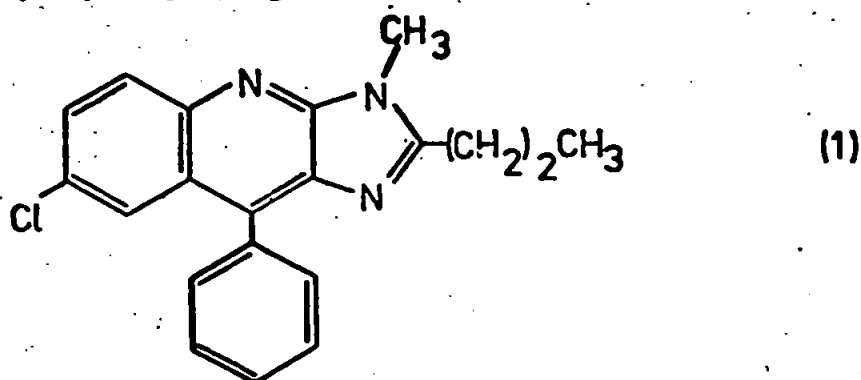
by

P.A.C. GANE

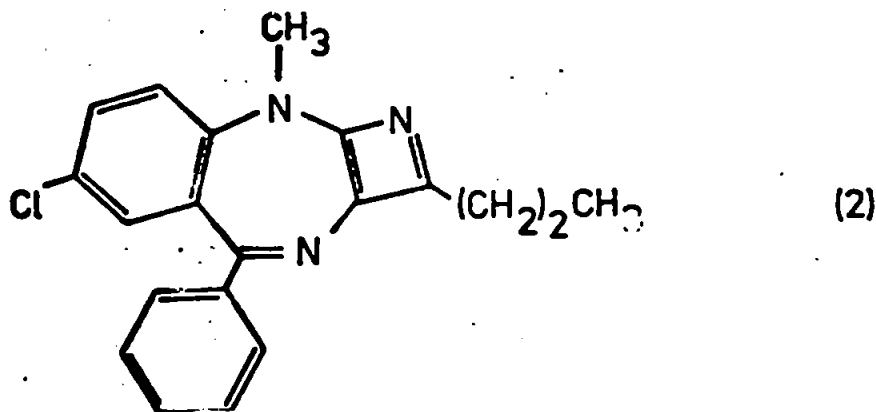
ABSTRACT OF THESIS

Effectiveness in biological chemical environments virtually defines the term 'drug' when applied to any attempt to modify that environment by the introduction of an influence in terms of a specific compound or group of compounds. Interest in the configuration of the molecules involved in such modifications led to the X-ray structure determinations, discussed in the thesis, of the following three compounds:

- (i) 7-chloro-2-methyl-5-phenyl-3-propyl[2,3-b]-imidazolyl quinoline.

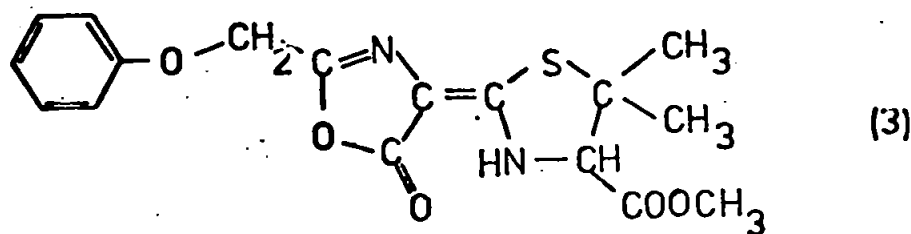


Derived from the psychoactive drug Librium, it was thought to conform to the structure:

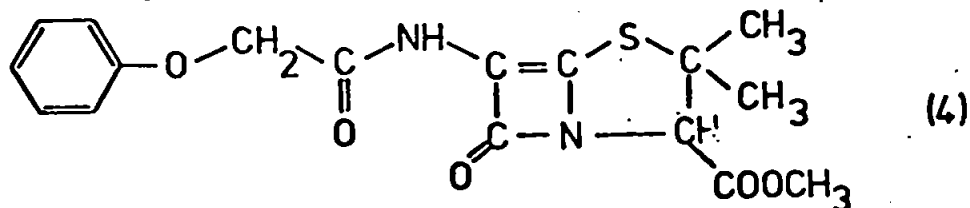


containing the highly strained 4-membered monocyclic azete system (Shenoy, a thesis submitted for the degree of Doctor of Philosophy, University of London, 1975), and suggested as one of the first examples of possible stable 4-membered azacyclobutadiene rings.

- (ii) The methyl ester of 5,5-dimethyl-2-(2-phenoxyethyl-5-oxo-1,3-oxazolin-4-ylidene)-1,3-thiazolidine-4-carboxylic acid.



$C_{17}H_{18}N_2O_5S$ was first reported by Brandt, Bassignani and Re, (1976, Tetrahedron Letters No. 44, pp 3979-3982), to have configuration (4),

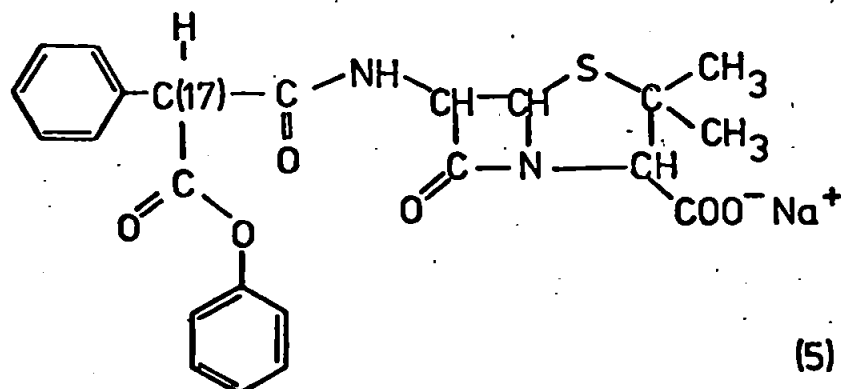


i.e. that of a novel class of DL-5,6-didehydropenicillins. Its reported weak antibacterial activity, thought to be associated with the unsaturated nature of the penicillin nucleus promoted its X-ray structure analysis.

Subsequently, Bachi and Vaya, (1977, Tetrahedron Letters No. 25, pp 2209-2212), suggested the configuration (3) which has been confirmed by the structure determination.

A comparison of the proposed derivations of (3) and (4) is made, and the conformation of the unconstrained thiazolidine ring is discussed in comparison with the constraining effect of adjacent β lactams in the nuclei of known penicillin structures.

(iii) The phenyl ester of carbenicillin (carfecillin).



The crystal structure is used to facilitate a comparison of the configurations of both the penicillin nucleus and the side-chain substituents of C(17) with other penicillin derivatives of known crystal structure.

The conformation in aqueous solution about C(17) is reflected in the modification of H^1 n.m.r. signals from the β lactam protons for the methyl and ethyl esters of carbenicillin between the two epimers. A similar effect is noted for the two diastereoisomers of amino-hydroxybenzyl penicillin, amino-phenylacetamido penicillanic acid and a tyrosyl penicillin.

To evaluate a correlation between the absolute configuration and n.m.r. studies, circular dichroism spectra from penicillin compounds have been characterised and the mutarotation exhibited by the esters of carbenicillin used to describe configurational equilibria about C(17) in terms of their characteristic n.m.r. spectra.